UNIVERSITY OF SOUTHAMPTON

FACULTY OF NATURAL AND ENVIRONMENTAL SCIENCES

SCHOOL OF OCEAN AND EARTH SCIENCE

RELATIONSHIP BETWEEN WOOD DENSITY AND ULTRASOUND PROPAGATION VELOCITY:

A NON-DESTRUCTIVE EVALUATION OF WATERLOGGED ARCHAEOLOGICAL WOOD STATE OF PRESERVATION BASED ON ITS UNDERWATER ACOUSTIC PROPERTIES

Angeliki Zisi

Thesis for the degree of Doctor of Philosophy

October 2015

UNIVERSITY OF SOUTHAMPTON

ABSTRACT

FACULTY OF NATURAL AND ENVIRONMENTAL SCIENCES

SCHOOL OF OCEAN AND EARTH SCIENCE

Thesis for the degree of Doctor of Philosophy

RELATIONSHIP BETWEEN WOOD DENSITY AND ULTRASOUND PROPAGATION VELOCITY:

A NON-DESTRUCTIVE EVALUATION OF WATERLOGGED ARCHAEOLOGICAL WOOD STATE OF PRESERVATION BASED ON ITS UNDERWATER ACOUSTIC PROPERTIES

Angeliki Zisi

With current progress in marine geophysics equipment, survey and processing techniques, we can be now closer to support needs emerging after decades of maritime archaeology and conservation practice worldwide. Acoustics have been suggested as an appropriate non-intrusive method for investigating marine archaeological sites and as a proxy for degradation of submerged archaeological timbers whilst *in situ*. The present study has significantly contributed to the use of ultrasound by conservators and archaeologists in the field of Maritime Archaeology. A new scientific way has been developed to evaluate the degree of degradation of waterlogged archaeological wood, using a reliable relationship between its physical properties during degradation and its corresponding acoustical properties. For this purpose a new reliable experimental ultrasound set-up and measurement methodology were first developed, followed by initial experiments on "fresh" waterlogged wood, degraded with a new artificial degradation process simulating closely the degradation patterns of wood recovered from marine environments. These experiments led to the establishment of reliable calibration curves between wood's density and ultrasound velocity. To evaluate the efficiency of the calibration curves, waterlogged archaeological samples from the National Museum of Denmark were successfully tested with ultrasound. The technique would be invaluable for conservators working in the laboratory for assessing the state of preservation of small wooden mobile artefacts and waterlogged timbers. Further, the data produced were used to improve reflection coefficients for waterlogged archaeological wood and add on our understanding and potential of its remote acoustic characterization whilst *in situ*. On-going research will support the correlation between the laboratorial results and the real world.

Table of Contents

List of Tables

List of Figures

Declaration of Authorship

I, Angeliki Zisi,

declare that this thesis and the work presented in it are my own and has been generated by me as the result of my own original research.

RELATIONSHIP BETWEEN WOOD DENSITY AND ULTRASOUND PROPAGATION VELOCITY:

A NON-DESTRUCTIVE EVALUATION OF WATERLOGGED ARCHAEOLOGICAL WOOD STATE OF PRESERVATION BASED ON ITS UNDERWATER ACOUSTIC PROPERTIES

I confirm that:

This work was done wholly or mainly while in candidature for a research degree at this University;

Where any part of this thesis has previously been submitted for a degree or any other qualification at this University or any other institution, this has been clearly stated;

Where I have consulted the published work of others, this is always clearly attributed;

Where I have quoted from the work of others, the source is always given. With the exception of such quotations, this thesis is entirely my own work;

I have acknowledged all main sources of help;

Where the thesis is based on work done by myself jointly with others, I have made clear exactly what was done by others and what I have contributed myself;

All the parts of this work that have been published are listed in the List of Publication section

Signed:

Date: 3/6/2016

List of Publications

Zisi, A., Dix, J.K., & Best, A. (2013). Ultrasonic direct transmission for estimating the state of preservation of waterlogged archaeological wood. In Proceedings of the 12th ICOM-CC WOAM Conference, Istanbul 2013, in press.

Acknowledgements

I would like to express my sincere gratitude and appreciation to my supervisor **Justin Dix** for engaging himself from the beginning to the last day of this research and for making its completion smooth by funding the last year of the project. I thank him for putting faith in me on a topic that was of great interest to me and for being generous and supportive throughout this long run. Thank you.

Sincere gratitude goes to two special people whose expertise, inexhaustible assistance and motivation, collegiality and humour, majorly contributed to the success of this study. **Jeremy Sothcott**, principal experimental officer in rock physics, NERC, for generously imparting me his precious knowledge on the use of the ultrasonic equipment and the theory behind it, when there was none till then, and for his engagement with my research. And **Kelvin Aylett**, mechanical technician, UoS, for his genuine interest and enthusiasm to help students, finding the best possible solutions, and for kindly opening his workshop and entrusting me with the use of the best equipment to work on endless hours and hours of drilling wooden blocks. Dear Sirs, words can never be enough to thank you.

I am highly indebted to the collaborators of this project, the National Museum of Denmark for kindly providing the archaeological material used in this study. Special gratitude goes to **David Gregory,** senior scientist at the NMD for his engagement with the project since day one and for successfully orchestrating this collaboration. I am personally thankful to **Anne Marie Eriksen** for her precious time and assistance during my short visits to the Museum, and also for her contribution to the project by preparing archaeological wood samples for shipment to Southampton together with accompanying documentation. A kind thank you to the rest of personnel working at the Museum, for making my stay welcoming. It was a pleasure to work with all of you.

I am thoroughly grateful to the following people for facilitating my work and providing me their kind help, technical support, and smiles, **Prof Ian Croudace**, **Angus Best**, **Eleni Anagnostou, Stephen Hayward**, **Neil Jenkinson**, **Graham Blythe**, **Bob and John**, **Suzanne MacLachlan**, **Mat Cooper**, **Agnes Michalik**, **John Gittins**, **Dan Hill**, **Amelia Astley**, **Kelvin Amalokwu**, **Mario Espozito**, **Moira MacLean**, **Jonathan Williams** and **Hugh Baldwin**. Special thanks go to **Kevin Saw** Head of Mechanical Engineering (OTEG) and **Rob Brown** for their invaluable collaboration on the 3D documentation of the archaeological wood samples with the Faro equipment, together with **David Owsianka** and

the rest of the OTE group, National Oceanography Centre. I am also grateful to **Robert Greenbank** from FARO Technologies for his time and help in the use of the Faro Edge and Laser Line Probe. Last, many thanks go to **Soffe & Sons** sawmill, Hampshire, and especially **Michael Soffe**, for a joyful collaboration and great service, providing good quality "fresh" wood for the needs of the present work.

To **Mark Vardy** my gratitude for valuable discussions, peering part of this thesis in the early days of its writing, lovely cups of coffee and friendly support. I am also indebted to **Julian Whitewrigth** for his valuable contribution in peering section 2.2 of this thesis for its integrity.

To my fellow colleague and dearest friend, **Greg Melling**, a grand thank you for sharing your knowledge, ideas, encouragement and friendship.

To my dear old friend **Alina Fais**.

There will never be enough words to thank my beloved parents, **Maria** and **Nikiforos**, and my brother **Nikos**, for their unending love and support, especially through the four years of my doctorate studies, some of them very difficult for our family. I am eternally yours.

My deepest appreciation and gratitude goes to **Thor Hayton** for his excellent artistic technical assistance and general feedback, and for his instrumental support, encouragement and motivation in completing this work. It would not have been the same without you.

The work is a product of three years funding (2011 – 2014) by the **Greek's State Scholarship Foundation (IKY)**, awarded to the candidate after succeeding in national written exams, and a year funding (2014 - 2015) by the **Associate Prof Justin Dix**, Head of the Geology and Geophysics Research Group, University of Southampton (UoS).

To my teacher,
Dr P.K. Kavvouras

"...when you put your ear at one end of a beam of any length whatever,
the sound even of a graver tapping on the other end can be heard,
since it follows the longitudinal channels.
By this method one can detect whether the wood is twisted and broken up by knots...."
Pliny, *Natural History* 16.184-192

(In *Greek and Roman Technology: A sourcebook*, by J.W. Humphrey,
J.P. Oleson, and A.N. Sherwood, 1998, p.338)

Chapter 1

Introduction

1.1 Rationale

Estimating the preservation state of waterlogged archaeological wood is vital for an Archaeological Conservator in order to design the appropriate treatment scheme. So far a number of destructive or near non-destructive techniques are assisting conservators in this procedure. Yet, minimum intervention is a fundamental conservation principle, because intervention can limit the research potential of archaeological artefacts. Non-destructive tools which will move the science in this direction are imperative both on the laboratory desk of the conservator, especially considering condition assessment of delicate and small artefacts (Papathoma et al., 2016); and if possible, also at larger scales such as wooden hulls, in the field. There has been a call for more research into enriching our knowledge upon preservation of underwater cultural heritage whilst *in situ* in its present burial environment, using reliable, robust and where possible, non-intrusive methods and tools (UNESCO, 2001) and specifically for the submerged wooden cultural heritage (ICOMOS, 2006; European Commission, 2014). Sites in this category can thereafter be assessed, monitored and managed using techniques specifically developed to match the archaeological underwater environment and conservation ethics until excavation becomes necessary and required resources available (Cederlund, 2004; Manders, 2009; Al-Hamdani et al., 2011; Björdal et al., 2012; Gregory et al., 2014; Matthiesen, 2015).

When faced with the question of whether or not to recover a wooden hull and its contents, of the chief parameters to consider is the assessment of its preservation state. This will draw conservators and archaeologists to tailor the best possible strategy for lifting such finds and complicated structures, and even more importantly, the extent to which conservation methodologies and engagement of dedicated hosting facilities can be predesigned. Yet, with wooden hulls either laying *in situ*, awaiting for the next excavation season or for a better future to be secured, investigation and development of methods to monitor and mitigate

their deterioration has to become a priority to safeguard it insofar as is feasible (Gregory et al., 2012).

With current progress in marine geophysics equipment and survey techniques (Plets et al., 2009; Plets et al., 2011; Mueller et al., 2013; Papatheodorou et al., 2014; Bruno et al., 2015) and processing techniques (Vardy, 2015), we can be now closer to support needs emerging after decades of maritime archaeology and conservation practice worldwide. Acoustics were suggested as an appropriate non-intrusive method for investigating marine archaeological sites by Quinn et al. (1997) and since has been further explored (Singh et al., 2000; Wunderlich et al., 2005; Bull et al., 2005; Schock, 2008; Vardy et al., 2008; Plets et al., 2008; Vardy et al., 2011). Emanating from this, quite recently acoustics was suggested as a proxy for degradation of submerged archaeological timbers by Arnott et al. (2005). Preliminary work by Arnott et al., demonstrated the potential of an ultrasonic transmission technique for use on waterlogged archaeological wood, placing the base for its use *in situ*.

The present research aims in advancing this method by reviewing and readdressing particular challenges highlighted by this past work. More specific, an enhanced method is developed to evaluate the degree of degradation of waterlogged wood, using a reliable relationship between wood's physical properties during artificial degradation and its corresponding acoustical properties, followed by successful tests on a range of archaeological wooden samples. Experiments are performed on "fresh" waterlogged wood artificially degraded, for the establishment of an empirical relationship between wood density and ultrasound propagation velocity. The efficiency of this relationship is evaluated using 'real' waterlogged archaeological wood samples provided by the National Museum of Denmark, for ultrasound testing in the laboratory.

Further analysis of the data produced is run in order to improve reflection coefficients for waterlogged archaeological wood, and add on our understanding of its remote acoustic characterization whilst *in situ*.

1.2 Value of archaeological material

From Palaeolithic time wood has been one of the basic raw materials for human beings providing them warmth and fuel to cook their food. Fire is regarded as a great step forward to the development of the civilisation; without fire the use of metals would have been almost confined to copper (Meiggs, 1982: 3). With the advance of civilisation, grew the demand in wood, and the need for constructing more roads and bridges was raised. Wood

was associated with the word *material,* namely wood for building purposes or in making articles, and was the staple of armies and fleets. Wood's determinant role in the formation of history, economy, science and politics has been widely recognised for a long time (Albion, 1926; Lane, 1965; Meiggs, 1982). Many aspects of the timber economy and shipbuilding techniques are reflected on a hull's timbers as is their wood species, quality, shape, size and geographical origin (Creasman, 2010). Preferences on timber species for use in ancient shipbuilding were driven by the wood species physical characteristics, while resistance to shipworm and related marine borers were also well considered (Steinmayer & MacIntosh Turfa, 1996). In other instances shipwrights had to adjust their sizing and shaping techniques of the raw material to match the available routes and means of transportation (Creasman & Doyle, 2010). Although superficial on timbers, tool marks, assembly, and construction marks are the key elements for reconstructing ancient tool kits and whole hulls (Hirte in Crumlin-Pedersen, 1997: 152; Pomey, 2000; Ward, 2000; Maragoudaki & Kavvouras, 2012). Unique information carried by wood is also brought into the present with dendrochronology. The science creates and expands tree-ring chronological sequences (Kuniholm, 2001), adding fixed points for archaeologists for dating finds (Bonde & Christensen, 1993), as well as reconstructing the paleoclimate, and enhancing our knowledge of the forestry practice in ancient times (Kassio, 1982).

Plentiful behavioural, cultural and scientific information can be extracted from archaeological wood deposited with ship timbers through time. It is part of the conservator's responsibility to preserve this valuable information and deliver it for public display and scientific research.

1.3 Work significance

1.3.1 Preservation *in situ*

Twenty-five years after Peterson's (1990) recommendations on the criteria for deciding upon the most appropriate conservation treatment for archaeological waterlogged wood, the rationale still remains the same (Gregory et al., 2011). Presently, and acknowledging that responsibility over the conservation of an artefact arises upon its discovery *in situ*, of the most important issues to consider is the total time needed to complete an archaeological project, i.e. its excavation, recovery, analysis and study of the data and artefacts, and the final report. The funding horizon of archaeological projects does not usually exceed five years. Thus, a treatment that would demand fifteen years for completion naturally raises issues of engaging new sources of funding together with qualified personnel, especially as

this task could solely be the most expensive part of the whole project, unless the artefacts to be conserved are of exceptional value.

A recent example can be seen through the case of Vrouw Maria shipwreck, an 18th century Dutch merchant ship, which sank off the Finnish coast in 1771 on her way from Amsterdam to St. Petersburg. While the wreck still lies in the seabed, there has been a debate about raising her or not (Ehanti et al., 2009). The actual raising of the ship is evaluated as technically possible and without jeopardising her integrity; nevertheless, there are a number of issues which must be clarified and secured before initiating the project. First on the list is the long term streaming of the necessary resources. The initial cost estimated for salvaging the wreck and placing her in a museum is estimated to be c. £70 million, of which the actual lifting is just a fraction (Ehanti et al., 2009). Where upon, the demand for extra money could be continuous as is in the form of a new museum for the Mary Rose or as in further air conditioning installations into the Vasa museum (Hocker, 2010), vital for the ship's stability after the completion of its conservation. All cases are long-term projects, proved to be highly binding and involving generous amount of money (see for example Chippendale, 1983). Such projects could include a risk not to compensate the investment (Al-Hamdani et al., 2011).

Still, it should be recognised that decisions cannot be based solely on financial and technological considerations (Stewart et al., 1995); experience has shown that with a proper and well prepared plan, diverse complications that emerge through conservation of waterlogged archaeological heritage should not prevent its full excavation, recovery and ultimately, placement among other objects of scientific research and public display (Kahanov, 1997: 326-327; Hoffmann, 2013: 163). It is exactly the ample data which can be retrieved through archaeological wood because of its "workability and its widespread use in human societies" that makes its excavation and study "avidly sought" (Peterson, 1990: 435).

It is the conservators' role to contribute in the decision making by offering the necessary knowledge from their perspective for the realisation of such long-term projects.

1.3.1.1 Defining state of preservation of a shipwreck

Nothing more than the original enthusiasm of the discovery of the wooden hull of a shipwreck can be reflected better than written testimonies as: "These pine timbers (…) are beautifully preserved and their structural integrity is generally excellent" (Fitzgerald, 1995: 33), or "The removal of part of the cargo of amphoras (…) revealed that the wood underneath was perfectly preserved" (Casson, 1994: 105). Yet, the words "beautiful", "excellent" and "perfectly" are rather the initial subjective estimation of the excavator, based

solely on what is visible; whether wood exists or not and whether timbers, planks and the rest of hull look to maintain their original size and expected shape. Finds of such nature not only trick the archaeologist in charge but even the conservators involved. It is indicative that before the introduction of methodical wood analyses, adopted from wood science standards (Hoffmann, 1981; Rowell & Barbour, 1990), definition of wood's state of preservation was similarly subjective: "Alas! very soft", or "still a bit hard" or "well, strong as fresh wood!" or "strong heart in a soft shell!" (Hoffmann, 1981). Inevitably excavators and conservators of today continue attributing archaeological wood with such characterisations, but certainly scientific approaches which objectively reveal its true degradation level, are applied thereafter.

With time and depending on the burial environmental conditions, waterlogged archaeological wood is disintegrating. The specific issue an archaeological conservator has to diagnose before deciding upon the right treatment is the reduction of wood's mechanical properties and dimensional stability, together with the loss of its "identity" as an artefact (Borgin et al., 1975; Grattan & Clarke, 1987; Schniewind, 1990).

Archaeological wood from wet and waterlogged environments shows increasing values of moisture content compared to living trees, while the wood tissue is in a process of chemical decomposition. Moisture content of green wood can range from about 30% to 200%, and even higher than 200% in some species (Dinwoodie, 2000; Forest Products Laboratory, 2010). Conservators routinely use wood's physical properties, the maximum moisture content (MC_{max}), a condition where all of the wood pores are completely filled with water, together with the basic density ($\rho_{o.d.}$) calculated from the wood sample oven-dry weight and volume in the water-saturated condition, for a basic estimation of the degree of degradation of wood. These methods are simple to use and do not demand special knowledge and experience to interpret (Bednar & Fengel, 1974; Hoffmann, 1981; Jensen & Gregory, 2006). For a more detailed condition assessment, a number of analytical techniques on the chemical and mechanical properties, and on wood's microstructure, can be applied further (Jagels et al., 1988; Hoffmann & Jones, 1990; Kim & Singh, 2000; Gregory & Jensen, 2006; Colombini et al., 2009; Fors et al., 2011; Macchioni et al., 2013).

Conservators distinguish three degradation states based on the amount of water in wood (de Jong, 1977; Florian, 1990), visualised in Figure 1-1:

Class III, MC_{max} < 185%, wood presents only a thin degraded surface layer.

Class II, MC_{max} = 185 - 400%, wood presents a sizeable solid core.

Class I, MC_{max} > 400%, the most deteriorated wood with no virtual core.

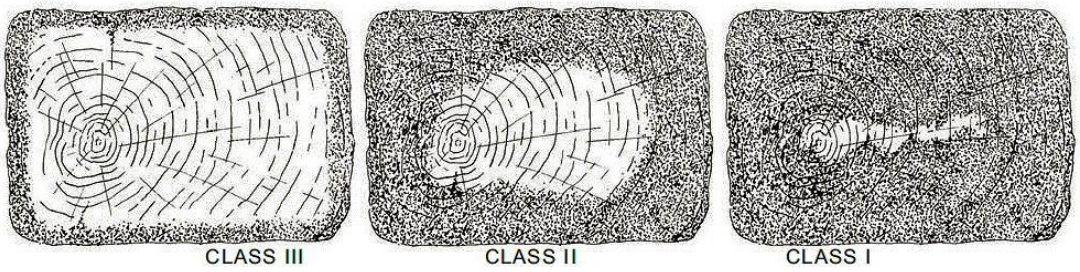

Figure 1-1 Classification for the degree of degradation of European oak (Extracted from (McConnachie et al., 2008).

While this classification is widely used by conservators today, recent study (McConacchie et al., 2008) draws attention to whether the comparison made is between like for like, since this classification was developed using exclusively European oak and assuming even distribution of the moisture content within a wood sample (de Jong, 1977). McConacchie et al. through their experiments on archaeological wood elaborate on this basis and provide a supplementary classification scheme based on maximum moisture content, this time specifically assigned to three different wood species among the ones found in the Mary Rose:

	Class A, Well preserved material dominates	Class B, Roughly equal proportions of well preserved and degraded material	Class C, Degraded material dominates
Oak	≤150%		>150%
Poplar	≤400%		>400%
Scots pine	≤250%		>250%

Although useful conclusions can be made based on maximum moisture content, especially when wood has exceptionally high water content, as of Class I or Class C, it remains an indirect way to calculate wood mass loss, as values do not count for the initial density of the wood before deterioration; hence two samples of wood with equivalent maximum moisture content can present distinctive degrees of deterioration as their initial density was different (Barbour, 1990). Being so, the basic density of the archaeological wood sample, compared to

that of "fresh" wood of the same species, is used as a reliable "bench-mark" for indicating the range of degradation of waterlogged wood (Schniewind, 1990; Jensen & Gregory, 2006).

The term Residual Basic Density (RBD %) is introduced by Macchioni (2003), calculated as the ratio between the measured density of the archaeological material and the average density of non-degraded wood from the same species, derived from the literature or measured from the available "fresh" wood samples. According to Macchioni, samples with RBD lower than 65 to 70% are considered degraded; whereas they are heavily degraded if RBD is lower than 40%. Residual density will direct the conservator towards the most appropriate conservation material and technique, which, depending on the amount of loss and size of artefact / find, can be generally divided based on the mechanism of maintaining the fabric: to those which act as bulking materials for heavily degraded wood, impregnating the cell walls and replacing the water inside the volume of pores, providing dimensional stability, as are high molecular polyethylene glycols (PEGs) (Hoffmann, 2013), sugars (Imazu & Morgos, 1997), silanols (Kavvouras et al., 2009); and to those which act as consolidants by impregnating the cell walls and forming a protective surficial layer, which provides the necessary support for wood moderately degraded, as the acetone-rosin method (McKerrel et al., 1972; Giachi et al., 2011 and Kaumarin (Hoffmann, 2013).

1.4 Evaluating density of waterlogged wood whilst *in situ*: Current options

1.4.1 Destructive and near non-destructive methods

Conventional methods which can be used for the evaluation of density derive from the scientific research on wood in forestry and wood industry, after special modification to meet the needs of cultural heritage and archaeological fabric (Unger et al., 2001). Methods can interfere in a destructive or near non-destructive way. A fast and accurate way is the destructive removal of wood cores with an increment borer, dry at 103±2°C until constant weights are reached, and determine the basic density based on the oven-dry mass and waterlogged volume of the core (Schniewind, 1990; Forest Products Laboratory, 2010). However, as the same piece of archaeological wood presents pockets with different degree of deterioration (Hoffmann & Jones, 1990; McConnachie et al., 2008), a number of representative samples should be retrieved to provide an accurate evaluation of the wood state. Another device is a penetrating tool, the Pilodyn (Clarke & Squirrel, 1985; Squirrel & Clarke, 1987; Mouzouras et al., 1990; Jordan, 2003), which leaves small diameter holes of a 0.5-3 mm in diameter on the surface of the wood. However, it is capable of measuring only

surface and sub-surface density of wood, sometimes giving qualitative and subjective results. An effect of sampling with Pilodyn in relation to wood grain orientation has been found to contribute towards this (Jordan, 2003: 71).

Pilodyn's main disadvantage is its non-direct numerical expression of wood degree of deterioration. Correlation with quantitative results has been achieved by comparing the depth of penetration of the pin with the respective densities from sampled wood cores (Gregory et al., 2007). However, depth restriction of the pin up to 40 mm limits the assessment to the immediate subsurface of the wood sample. When used underwater (Gregory et al., 2011) for the *in situ* condition assessment of the *Belgica*, a Norwegian whaler built in 1884 and sank in 1940 in Norway, it was realised that the positioning of the instrument by the diver on very degraded surficial layer caused loss of that outer layer, and penetration of the pin was executed deeper inside a better preserved wood, which led to density overestimations. Similar practical issues were noted when deployed the increment borer, to retract wooden cores (plugs) for measuring basic density, of approximately 5 mm in diameter and various lengths. This time some places were found to be impossible to penetrate with the tool or if so, were of no use after all. Another consideration noted was that, Pilodyn cannot determine the density on wood riddled with shipworms as the spring held pin can enter the hollowed tunnels (Gregory et al., 2011). It is also likely to leave out an inner undegraded part of the wood surrounding the tunnels (Jordan, 2003: 74).

Recent advances on a handheld wood density profiler based on Pilodyn's principle, were made by AKUT (2015) aiming for its use both above and under water for measuring and monitoring the degradation of wood. The tool comprises of a steel needle which can be hammered up to 120 mm in wood allowing for gradient density measurements and greater depths towards its core. On the instrument's stated advances are its objective measuring irrelevant to wood's principal plane, depth of measurement, wood species and use by a single diver, while the 3 mm diameter needle does not disrupt the structural integrity of the wood.

A non-destructive but indirect way for estimating and monitoring wood degradation whilst *in situ*, is the placement of a sufficient number of sacrificial wood samples from "fresh" wood of the same species as the ones of the wreck, if known, within the same underwater context. Determined by the current taphonomy of the shipwreck and the information one ones to gain, these 'guinea pigs' can be left exposed to the water column or / and buried in different depths. The samples act as a proxy of the degradation rate of the archaeological wood after its discovery, following a sample recovery scheme of specified intervals when

density, moisture content, chemical and mechanical properties or other aspects can be re-evaluated (Gregory, 1998; Richards et al., 2009; Veth et al., 2013). An assessment of the state of preservation of the archaeological wood itself at the moment of discovery, by retracting wood samples, might be necessary first.

Pilodyn even though giving estimations of the deterioration of timbers, is the only tool so far adopted and employed underwater, underlining the challenges for a conservator to assess the preservation state directly on archaeological wood whilst *in situ* and without interfering with its structure.

1.4.2 Non-destructive

The need for non-destructive handling is common ground between archaeological science, forestry science and the forest products industry. As defined by the forestry community, non-destructive evaluation is the science of identifying the physical and mechanical properties of the material in question without altering its final application capacity, while using the information to draw decisions for its management (Ross, 2015).

Bjurhager (2011) used X-ray to determine the cellulose crystallinity and microfibril angle of archaeological oak wood sample from the warship *Vasa,* as part of on-going efforts of its carers to estimate the residual strength of the ship after its conservation. Further, X-ray technology has been calibrated and used for evaluating wood density and material properties of the ship's timbers at current display in the museum (Kruglowa et al., 2010; Kruglowa, 2012; Lechner, 2013). It can be suggested that X-rays could be a useful tool for estimating the residual density of archaeological wood and imaging of its internal condition for e.g. extent of Teredo attack whilst underwater. Greenawald et al. (1996) demonstrated the use of an enclosed X-ray backscatter tomography scanner in the underwater environment in shallow waters, for locating damage on a naval sonar dome. The acquired signal can be directly imaged to map the density of the material as a function of position. It was possible to acquire images which gave weak indicative information about the damage, and further optimisation of the underwater system is suggested to overcome effects from the water between the surface under inspection and the scanner. Recently, General Electric has been developing a prototype underwater X-ray submersible machine for detecting signs of corrosion of pipelines, which sit on deep ocean floors (General Electric, 2014). In terms of non-destructive applicability *in situ* and in an underwater environment, acoustic methods are the only option so far where considerably work has been done in tandem with the research advances on geophysical exploration technologies of the seabed where shipwrecks lie, as mentioned above.

1.4.2.1 Ultrasound propagation in wood

Due to wood's anisotropic nature the Forestry and Forest Products Industry has been investing for many decades in ultrasound, as an appropriate non-destructive tool to examine standing trees for presence of decay or classify and grade timber, wood products and wood composites, and detect their biological degradation. Studies with ultrasound are also centred for optimising kiln drying procedures of lumber while controlling changes in wood moisture content.

Ultrasound waves for testing are produced by piezoelectric transducers which convert the electrical energy to mechanical vibration imparting a wave into wood, which then is converted back to electrical signal. Transducers are commonly designed to work on a centred frequency ranging from 20 kHz up to 1-2 MHz (Senalik et al., 2014). For wood the most favourable centre frequency range is commonly between 20 kHz and 500 kHz because of the high attenuation in wood as frequency increases (McDonald, 1978; Wilcox, 1988; Rajeshwar et al., 1997; Tanasoiu et al., 2002; Hasenstab & Ostreloh, 2009; Beall, 2002; Bucur, 2011; Senalik et al., 2014). Ultrasonic inspection can be executed using various modes (Bray & Stanley, 1997: 103), of which through transmission, is regarded as the most appropriate for lumber grading (Rajeshwar et al., 1997) and easiest to operate for measuring the velocity of propagation of the ultrasonic wave (Bucur & Kazemi-Najafi, 2011). Also called direct transmission method, it utilises two transducers in line, the transmitter and the receiver, either in direct contact or not with the face of the sample under test, always using a coupling medium to provide no loss / scattering of the signal's energy between the transducers and the wood (Gonçalves et al., 2011).

Wood's unusual acoustical properties are capable of characterising a timber as clear or flawed based on changes on the speed of sound propagating through the timber, together with sound attenuation. Hence, sound travelling times are fast in healthy and high quality timber but differentiate significantly in decayed and low quality timber. For example, Wilcox (1988) measured linear reductions of ultrasound velocity with advancing mass losses up to more than 30% in decayed fir, approximately from 2000 m/s from "fresh" to 1000 m/s the most degraded. Nicolotti et al. (2003) note velocities between 600 and 1200 m/s corresponding to decayed areas of standing trees (*Platanus hybrid* Brot.), while zones with higher velocity 1200 and more than 2000 m/s, to "fresh" areas. Knots, flaws, decay and abnormalities will dissipate the energy of the sound affecting its attenuation amplitudes (McDonald et al., 1969; McDonald, 1978; Sandoz, 1989; Ross et al., 1998; Schafer, 2000; Kawamoto & Williams, 2002; Wang et al., 2004; Bucur, 1995; 2006; 2011). Ultrasound in wood is also a function of the modulus of elasticity (MOE) and modulus of rupture (MOR)

used to estimate elastic properties of wood with applications in the field and on logs (Huang et al., 2003). Instead of applying a direct stress on the object of interest, the method is based on the object's resonant vibration from a flexural, torsional or ultrasonic excitation (Dinwoodie, 2000; Bucur, 2006).

It has been shown in simulation experiments (Kazemi-Najafi et al., 2009) that ultrasound propagation velocity can identify the extent of internal rot in standing trees. More specifically, a significant linear gradual decrease of the ultrasound velocity (approximately from 1700 m/s to 800 m/s) corresponding to an increasing ratio of internal decay to healthy wood was established, and was attributed to the direct dependency of the speed of sound to wood density and elastic modulus, and their reduction due to decay. Kazemi-Najafi and co-workers (2009: fig. 10) agree with the concept by Wang et al. (2004: fig. 1) in order to explain the drop in speed of wave propagation in their experiments, that the wave is driven to go around the hole created from the decay, resulting in longer travelling paths and velocity reductions with the latter's advance. Similar observations were reported by Secco et al. (2012) who explained the wave path diversion as the preference of sound to travel through matter (wood) rather than empty space (presence of decay) (Figure 1-2).

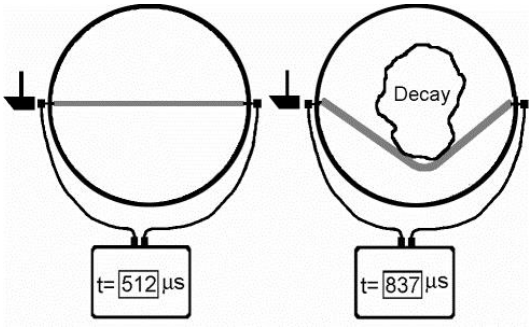

Figure 1-2 The speed of ultrasound drops in the presence of decay in standing trees as the sound gets transmitted through wood (Extracted from Wang et al., 2004: fig.1).

Dix et al. (2001) used ultrasound direct transmission method inside a water bath to test "fresh" water-saturated oak wood specimens, reproducing the waterlogged state of archaeological wood from shipwrecks. Aim was to define the reflection coefficient of waterlogged wood whilst *in situ*, where reflection coefficient is the acoustic signature characteristic of a material under specific surrounding conditions. Reflection coefficient is commonly used to identify boundaries and buried geological features / objects during seabed surveys (Kearey & Brooks, 1991; Quinn et al., 1997). Ultrasound propagation velocity

measurements using longitudinal waves[1] (Leighton, 2007: fig.1) at a resonant frequency of 500 kHz were recorded in all three principal wood axes, namely the longitudinal, radial and tangential, of specimens measuring 100 X 100 X 10 mm, specifically produced so that the shortest dimension was any of the three principal directions through which the measurement was taken. Additionally, three samples deriving from an archaeological waterlogged timber from the 17th century "Wreck 5" in Copenhagen were cut in respect to the three wood axes and used for comparison reasons. Compared to velocity measurements of air-dried oak (12% moisture content), results by Dix and co-workers showed reduction of the velocity of the oak in a water-saturated state for all wood principal directions, albeit the tangential velocity didn't show this consistency compared to the longitudinal and radial velocities. Taking under consideration the small sample size and no mention of number of repetitions, values through the archaeological samples, although seemingly of the same density as those from "fresh" wood, gave higher longitudinal velocity and lower radial and tangential velocities, underlying the effect of other parameters like degradation in archaeological waterlogged wood, which influence sound propagation, besides the apparent water content, whose effect on ultrasound propagation velocity will be discussed in section 2.5.3.

This last aspect was the basis of Arnott's work (2004) who investigated the changes of ultrasound propagation properties with changing preservation state of waterlogged wood from "fresh" towards more degraded situations, as met in archaeological wood from marine environments. A new ultrasonic through transmission technique was developed and used on "fresh" waterlogged oak and pine samples degraded by biological means. Experiments were held in a water bath using a centred frequency of 1 MHz and longitudinal waves. All three principal wood axes were studied conducting measurements through a thickness of 15mm per axis. Due to high data variability experienced, the study was not able to produce accurate quantitative results; but it was able to demonstrate a general tendency of velocity reductions with increasing wood degradation for both species. The study concluded that progression of the method will allow more accurate detection and mapping of buried sites and monitoring of the degradation state of wood whilst *in situ* (Arnott, 2004).

Ultrasound was recently used by Salmi et al. (2009) for the non-destructive evaluation of the preservation condition of the *Vrouw Maria* shipwreck timbers. Small test cubes, cut out from pine and oak samples recovered from the shipwreck, were ultrasonically tested in the

[1] Longitudinal or compressional waves or p-waves, in which particles are displaced parallel to the direction of motion of the wave.

laboratory using both a through transmission and a reflection technique. The later also called pulse-echo method, utilizes one transducer for both sending and receiving the ultrasound signal; here the sound travels twice through the test-sample thickness and is possible to locate, define and visualise internal defects (Stößel, 2004; Hasenstab & Osterloh, 2009, Bucur & Kazemi-Najafi, 2011). No calculated velocities are given, but the test determined the dynamic stiffness modulus of the degraded archaeological wood and compared it with that of "fresh" wood.

For these experiments a 300 kHz pair of transducers was used for testing the longitudinal direction of the oak, whereas 1.25 and 4 MHz pairs were used for testing the radial and tangential pine directions with the through transmission technique. The reflection technique was used for imaging and calculating the extent in mm of the degraded surface of a pine sample while being immersed in water, with 2 MHz linear array transducer. The authors suggest that the increase in the reflection amplitude of the sound through the degraded surface of the pine mirrors its reduced homogeneity, and the opposite for its intact layer. It is also proposed that the thickness of this degraded layer can be approximated to about 1-4 mm. Results on the stiffness modulus from the oak samples revealed a decrease of the shipwreck's stiffness nearly to the half of that of "fresh" oak, whereas pine's degraded surface appeared to have lost 60% of its stiffness modulus in the radial direction and around 50% in the tangential direction, when compared to that of the intact part of the archaeological sample. The stiffness reduction was attributed to soft-rot. Samples were cut from a 50 cm long pine and a 10 cm long oak sample; there is no mention upon the thickness, numbers and repetitions of the cubic samples used.

Bader et al. (2013) used ultrasound wave propagation for investigating the residual dynamic stiffness of the Oseberg ship[2] as relocation plans were considered. Samples measuring 60 X 15 X 4 mm (longitudinal X radial X tangential) deriving from stored untreated archaeological oak wood from the ship, were dried from a waterlogged condition, to a moisture content of approximately 8% aiming for the same conditions of those on the display hall. Ultrasound tests were performed on all three principal wood axes with through transmission technique in air, using a pair of transducers emitting longitudinal waves with frequencies between 50 – 500 kHz. Results are shown for the 100 kHz. The transducers were placed in direct contact with the sample, and honey was used as coupling medium. Elastic stiffness was calculated as the product of the samples' density and the

[2] A Viking Age ship which was buried in 834 AD, discovered in 1904 and is currently displayed in the Viking Ship Museum in Oslo.

square of the ultrasound propagation velocity. Considering that the study is based on a very small number of archaeological replicates, and there is no mention for number of "fresh" wood replicates and measurement repetitions for all samples, comparison of the results from the archaeological wood with those of "fresh" wood showed a much higher reduction of stiffness along the grain than across it. Specifically radial stiffness was found to be even slightly higher than that for "fresh" wood and the opposite for the tangential stiffness.

Riggio et al. (2014) also ran ultrasound tests on a range of oak and pine "fresh" and archaeological waterlogged wood, but after air drying to moisture content of about 12%. The aim was to understand the mechanical changes wood undergoes through a process of long (800 – 400 years) and short (8 years) term of waterlogging, also encouraged by natural degradation. The through transmission method with the transducers in direct contact using dry pressure coupling, at a frequency of 77 kHz, was applied on samples originally measuring 150 X 10 X 10 mm (longitudinal X radial X tangential). Correlations between wood density and ultrasound velocity and modulus of elasticity are given for directions across the wood grain. Although an extent of samples and repetitions was carried on, there is note of inaccuracy both in density measurements of the archaeological samples and the ultrasound velocity, because of severity of deformation and volume reduction that the archaeological samples underwent after the uncontrolled air conditioning, effectively due to loss or corrosion of wood structural elements. The acoustic requirement of a sample's flatness and perpendicularity to the principal propagation directions (Bucur, 1995), could not be fulfilled because of the samples' surface depressions and distortion. Additionally, the effect of the water in the wood was not accounted for at this study after all, when it is well known that moisture content of wood has great potential to change wood properties and affect ultrasonic results when wood is in an air-dried condition (Senalik et al., 2014). Or else, when wood dries below the Fiber Saturation Point (FSP, average 30% moisture content), which is the point wood cannot absorb any more water in its cell walls, and free water begins to accumulate in the cell cavities (empty voids) (Forest Products Laboratory, 2010). Efforts to confine wood's natural variability expressed by the relatively high variability (coefficient of variation[3] between 5-6%) in the density values of the "fresh" wood used, was also noted to not amend the result. Here, the challenge of precise measuring of the volume of air dried archaeological fragile wooden artefacts can benefit from a cheap device developed by Kavvouras & Fotopoulou (2006).

[3] A statistical measure of the dispersion of data points in a data series around the mean. It represents the ratio of the standard deviation to the mean and can be also expressed as a percentage.

From the above studies on the use of ultrasound to evaluate waterlogged archaeological wood, Arnott (2004) did a systematic study, keeping the wood under test in a waterlogged condition. The rest of the approaches, if not tested in a very small scale, they ultrasonically test archaeological wood that has been dried from its waterlogged condition to a moisture content which is no longer representative of its nature whilst underwater. It is the aim of the present research to build on the work done by Arnott and extend the knowledge on the use of ultrasound for estimating the state of preservation of waterlogged archaeological wood whilst *in situ*.

1.5 Research aims

In association with the initial work done by Arnott (2004), the present research keeps the same basic concept with the past work. That is to investigate how changes in the structure and the physical properties of wood affect the sound propagation, and specifically the ultrasound propagation velocity, advancing wood degradation. Of the commonalities between the two researches is, the use of a laboratory ultrasonic transmission method in combination with compressional ultrasound waves, and the use of "fresh" wood subjected to a controlled deterioration and ultrasound measuring, to investigate the acoustical properties as the wood deterioration progresses. It is emphasized here that investigating wood compressional wave properties directly on archaeological material without first controlling over experimental variables which can influence the results, would lead to dubious scientific conclusions. Additionally, there are no data on ultrasound propagation velocity of waterlogged archaeological wood existing in the literature as yet.

Of the main problems encountered by Arnott when working with "fresh" wood, was that of the natural variability of wood observed within her control wood test-pieces which led to high variability of the ultrasonic parameters measured. Although systematic relationships between degradation and ultrasonic properties in waterlogged wood could be deduced through statistical analysis, the quantification of the relationships remained. Results also showed that a natural degradation approach of the "fresh" wood, comprising two suites of experiments, one was exposure of "fresh" wood to shipworm by deploying wood test-pieces in the sea for a certain period of time, and the second was exposure of wood test-pieces to brown rot fungi in the laboratory, did not allow control over the number of degradation steps which were aimed to be produced. There is note of irretrievably lost data because of the severity of degradation that the wood possessed during the experiments making ultrasound testing impossible after a point. More specific, for the macro-deterioration

experiments the studied density range was approximately between 530-350 g/cm^3 for oak and 420-240 g/cm^3 for pine, and for the micro-deteriorated experiments the density range was between 540-375 g/cm^3 for oak and 440-385 g/cm^3 for pine. Differences in severity of degradation between test-pieces degraded under same conditions and changes in the structure resulting from degradation were also noted, complicating the interpretation of the results, whilst the experimental reproducibility of the same degradation conditions can be disputed.

Using biological means to degrade "fresh" wood for studying specific properties of archaeological wood is a common practice in Conservation science when testing the efficiency of new conservation materials and conservation techniques (Peacock, 1996; Fors et al., 2008; Preston et al., 2014). Yet, the advantage of working with 'real' degraded material caused in this case a loss of control over experimental variables and material to work with. Taking a step towards our understanding of ultrasound propagation in waterlogged archaeological wood, Arnott's main focus was the development of a robust and reliable ultrasound transmission method for testing specifically waterlogged archaeological wood, when there was not one until then. This gave little time for consideration of the most suitable characteristics of the wood test-pieces used as controls, if *in situ* applications are the objective. Retrospectively, it is regarded that the size of the control test-pieces was small and incomparable to that expected to be insonified at an archaeological underwater site.

Furthermore, recent geophysical study on the state of preservation of the wooden remains of Henry the V's flagship, the *Grace Dieu* (set sail in 1420), highlighted some practical issues as experienced in the field (Plets et al., 2008). Given the way a shipwreck is encountered on the seabed and with the current geophysical technology, it is rather overoptimistic to aim for ultrasound insonification directions on-axis with favoured wood axes, these are the longitudinal, radial and tangential axes, studied earlier by Arnott (2004). On the contrary, ideally ultrasound must be able to give reliable readings when insonifying towards the timbers of a ship irrespective of the orientation of their wood structural characteristics in relevance to the insonification axis. It would be also of great value if ultrasound can be universally useful given the variety of wood species used in ancient shipbuilding, and considering that ultrasound velocities in "fresh" wood can be distinctive among wood species (McDonald, 1978; Bucur, 1995).

As mentioned above, research on the use of ultrasound on waterlogged wood of cultural interest, has so far been focused on testing "fresh" wood after special treatment. Little study has used actual archaeological wood in a waterlogged state or without altering this

condition. Yet, research on a diagnostic tool such as ultrasound, can benefit by calibrating against the material of interest, and investigate any limitations to the approach as set by the archaeological material itself.

The present study aims to advance the past work by setting the following targets:

i. Develop a new experimental methodology which focuses on the special characteristics of the material in question both as a wood and as an artefact.
ii. Design a new artificial wood degradation process which ensures control over experimental variables and reproducibility.
iii. Study of off-axis ultrasound propagation in waterlogged wood.
iv. Establish a reliable empirical relationship between wood density and ultrasound propagation velocity for wood showing different states of degradation.
v. Assess the established relationship by using 'real' archaeological wood samples from waterlogged archaeological excavations.

1.6 Chapter outline

A literature review is given in Chapter 2 about the nature of waterlogged archaeological wood studied both as a material and as an artefact. The probe begins by defining wood in the archaeological context, i.e. as a building material for ships through the centuries. Next, ship wrecking processes and information on the environmental and other factors affecting wood's preservation / degradation within its present underwater burial environment are discussed. Basic knowledge on "fresh" wood as a structure and natural material follows, together with a description of its degradation in the marine environment. An investigation is further given on the acoustic properties of waterlogged archaeological wood. The information gathered is used to design and test an appropriate experimental methodology for assessing waterlogged archaeological wood state of preservation with the use of ultrasound, dealt with in Chapters 3 and 4. Chapter 3 is centred on the development of a new ultrasound set-up and testing methodology in the laboratory, evaluated and calibrated for the specific needs of waterlogged wood. This established, Chapter 4 introduces a new artificial degradation procedure for wood simulating closely the degradation occurrence in the marine environment. A number of artificially degraded "fresh" wood steps aiming to gradually downgrade wood's density, are produced, each one followed by ultrasound measurement of the wood. The aim is to establish the relationship between wood density and ultrasound propagation velocity. The relationship produced is assessed in Chapter 5, using archaeological material provided by the National Museum of Denmark. The

conclusions drawn from the present research results are presented in the final Chapter 6, together with an overarching discussion and implications of the work in the fields of conservation and maritime archaeology.

Chapter 2

Marine Waterlogged Archaeological Wood and its Nature

2.1 Introduction

Wood is termed as waterlogged when the whole tissue, all cell walls and cavities (Figure 2-1), are filled, or near filled with water (Barbour, 1990). In the Conservation community the term waterlogged for wood of archaeological interest also contains the connotation of the weakening of wood's structure through its chronic deterioration (Christensen, 1970: 10). Wood preservation is favoured in waterlogged environments due to the absence of oxygen which impedes the action of organisms responsible for its deterioration (Blanchette, 2000). Nevertheless, being an organic material, wood preserved in a waterlogged state for centuries undergoes weathering and degradation of its physical, chemical and mechanical properties in a rate and extent relative to its species, burial environment, processing and usage before burial. Long term, water displaces lost structural components of wood and keeps the residual wood mass in a swollen and seemingly good preservation state, retaining the initial figure and shape for many hundreds, even thousands of years (Blanchette, 2000). Yet, a microscopic analysis would reveal the extent of wood disintegration, and reduction of its dimensional stability and "identity" as an artefact if let dry without care, which can lead to extensive shrinking, warping and collapsing. Figure 2-2 shows an example of poor preservation state of waterlogged archaeological wood, suffering advanced cell wall degradation from bacteria action.

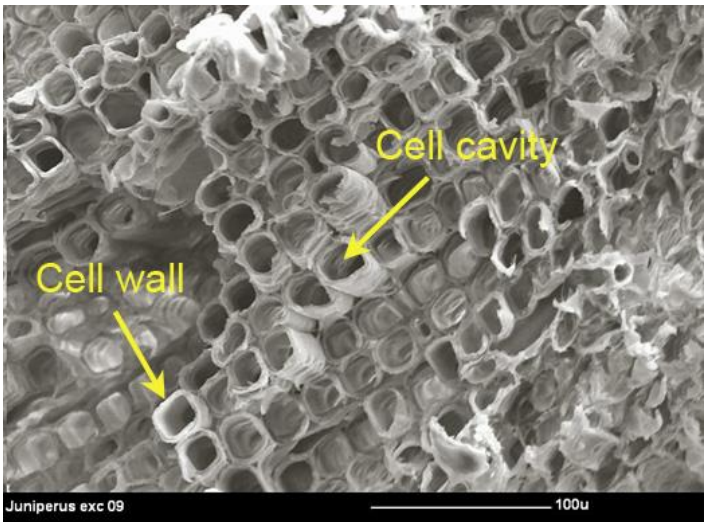

Figure 2-1 Cell structure of "fresh" juniper wood; healthy cell walls and cell cavities can be distinguished. Bar =100μm (photo courtesy of P.K. Kavvouras, modified).

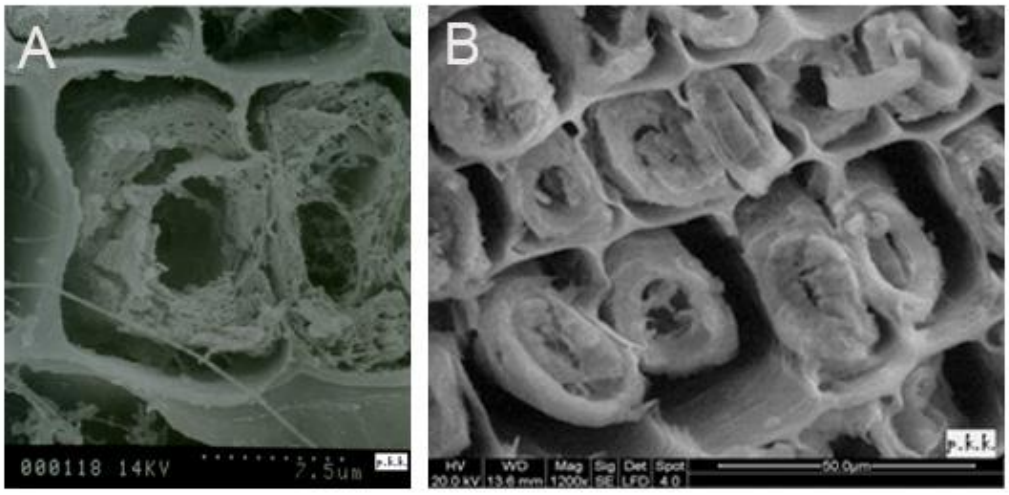

Figure 2-2 Bacterial degradation in wood from a Neolithic settlement in Greece (5500 BC). A: The residual cell walls are porous and contain minute holes B: Secondary wall separation. SEM images, bar = 7.5μm in A, and 50μm in B. (photo courtesy of P.K. Kavvouras).

To start probing the use of ultrasound propagation velocity to deduce the preservation state of waterlogged archaeological wood, whilst lying *in situ*, some questions need to be asked beforehand. Issues to consider begin from the simple question: What is there left from a wooden shipwreck to assess with ultrasound? Investigation in wrecking processes, how a wreck is encountered on the seabed, and the characteristics of the surrounding marine environment is vital to an initial definition of the preservation state of the wood based on known literature. This information will lead to a proper experimental design of the artificial degradation procedure of "fresh" wood simulating closely the real case. Knowledge over wood species commonly used in ancient times will define the selection of the preferential

experimental material to work with, whereas information of traditional shipbuilding techniques and timber dimensions will also indicate certain specifications of the ultrasound tools and methodological design to properly assess it. For example, it is known that the depth of sound penetration into a material is frequency dependent, thus the thicknesses of the material under study must be specified. Moreover, timber conversion techniques, how timber was produced from trees by practicing specific cuts, will determine the shape of the control test-pieces, as well as the orientation of wood's anatomical features and preferred insonification wood axes.

2.2 Shipbuilding

2.2.1 Wood for shipbuilding

The present study is focused on wood species used in hull construction, chiefly planks, frames and keels, because statistically these components are the most likely to be preserved. It is clear that hulls were adapted to the timber and wood species locally available (Steffy, 1994: 100; Guibal & Pomey, 2003; Crumlin-Pedersen, 2004: 48).

Certain trees were being selected for their mechanical quality and their durableness from ancient times (Pulak, 1998; Guibal & Pomey, 2003) to more recent (Albion, 1926). Light and flexible enough to be shaped, fir (*Abies sp.*) was used for building triremes as speed was the primary requisite in Mediterranean naval warfare. Pine (*Pinus sp.*) would be used as an alternative although heavier but more readily available (Steinmayer & MacIntosh Turfa, 1996). For merchantmen strength was more important than speed as they had to spend long period of time at sea; such ships were made of pine as it is more resistant to decay (Theophrastus in Meiggs, 1982: 118). Pliny remarks the resistance of pine and cypress (*Cupressus sp.*) to rot and wood worms (Humphrey et al., 1998: 341). Pine has been consistently mentioned in Greek and Latin literature as one of the best woods for shipbuilding, and found as the most common planking material of today known shipwrecks in Greek, Roman, and early Byzantine times (Fitzgerald, 1995). Pomey (in Fitzgerald, 1995: 94) refers to Roman poets' Vergil and Ovid scripts, to remark that as pine was so broadly used in those days, the poets substituted the word for that of a ship. Hard and durable oak (*Quercus sp.*) was used for frames and joineries like tenons, tenon pegs, or for false keels and mast stems, while it is the preferred species for the construction of ships in the Atlantic Europe and Baltic regions from the Bronze Age onwards (Casson, 1994; Steffy, 1994; McGrail, 2001). Pine framing has been found on ships such as the Tantura B (beginning of 9th century) and Bozburun (874 AD) while both had oak keels, and oak planks the later;

Agay A (10th century) had all planks and frames made from black pine (*Pinus nigra*) (Pomey et al., 2012). Oak and pine dominate in the finds from the Viking Age (eleventh and twelfth centuries) generally, with ash (*Fraxinus sp.*), lime (*Tilia sp.*), alder (*Alnus sp.*), birch (*Betula sp.*) and beech (*Fagus sp.*) encountered in some cases (Crumlin-Pedersen, 2004: 48).

The number of different wood species selected for a ship's structural components and their diversity can give information about the quality or complexity of the structure. A homogeneous hull build using a small assemblage of tree species can speak of the quality of the construction, whereas a larger one, of its complexity. A wide range of tree species can also signify supplying problems and resource stresses (reuse of timbers), or repairs (Goodburn, 1997; Guibal & Pomey, 2003). Additionally, species homogeneity of the timbers used for the planking, in combination with a frame variety, seen in shipwrecks dating coarsely between second century BC and fourth century AD, revealed their building tradition, which in this case was shell-first constructions (Guibal & Pomey, 2003). In earlier times there were numerous ships with only one or two timber types used, but by the 19th century, the serviceability of different species for different parts of a ship were recognised and used; elm (*Ulmus sp.*) below the waterline, oak for the sides, pine for the decks (Whitewright, 2015, pers. comm., 12 August). There could be as many as seven or eight different species deliberately used in a ship in different areas, which would transfuse high quality to the construction (Whitewright, 2011). Additionally, archaeological evidence from the Graeco-Roman and Roman era shows a species preference based on the hull size and ergonomics (Fitzgerald, 1995: 131-132). More than 50% of the planking in ships of this period dating from the fifth century BC to the seventh century AC is made out of pine, whereas more than 40% have oak framing (Fitzgerald, 1995: Table 1).

Table 2-1 comprises a selection of excavated shipwrecks spanning in time more than 3,500 years, from the Earlier Bronze Age in Britain till the Age of Global Seafaring of the sixteenth and seventeenth century in Europe, following the time period classification for wooden ship building by Steffy (1994). Certainly the list of shipwrecks in Table 2-1 is not claimed to be exhaustive. The selection criteria are further set chiefly on the basis of wood species dominating in hull constructions as documented above, which are oak and pine species, and of well appreciated and widely known examples representing different building techniques and type of vessels. Then their appeal as wreck formations and their current state is noted, i.e. whether recovered / conserved / reburied, as examples to elaborate on how estimating the preservation state of the hulls with ultrasound could have had been or can be applied in the future. Listed under each shipwreck is information about its identity

followed by some of its main hull components such as the keel, planks and frames, and their characteristics, namely dimensions and wood species. Note for thickness, see 'sided' dimension and for width see 'molded' dimension, as given in Figure 2-9.

Table 2-1 Selective summary of hull construction details of vessels from the Ancient World till the Age of Global Seafaring.

					Hull construction details						
					Keel		Planks		Frames		Reference
	Name of Shipwreck / Location	Date	Present state	Shipbuilding Technique	Dimensions	Wood Species	Dimensions	Wood Species	Dimensions	Wood Species	
Ancient World	Ferriby 1/ Humber River, North Ferriby, Yorkshire	1880-1680 cal BC	In National Maritime Museum, Greenwich Conserved?	Sewn-plank boat			central strake 14 cm thick 65 cm max. width side bottom planks c.7 cm thick	oak (*Quercus sp.)*			Steffy, 1994 Van de Noort et al., 2014 McGrail, 2014
	Uluburun / Grand Cape', Uluburun, SW Turkey	c.1300 BC	Conserved?	Shell-first pegged with mortise-and-tenon joints	27.5 cm sided 22 cm molded	cedar (*Cedrus libani*)	c.6 - 6,5 cm thick 17 and 27 cm wide	cedar (*Cedrus libani)*	? (widely spaced)		Steffy, 1994 Pulak, 1998 Pulak, 2008
	Bon-Porté I / Saint Tropez, southern coast France	550 - 525 BC	?	Sewn-plank boat planks aligned with treenails rather than tenons, lashed seams	6.4 cm sided 9.6 cm molded	pine (*Pinus sp.)*	2 cm thick	?	12 cm sided 14 cm molded spaced as much as a meter apart	conifer	Rieu et al., 1980 Steffy, 1994 Polzer, 2009

	Table 2-1 continue				Hull construction details						
					Keel		Planks		Frames		Reference
	Name of Shipwreck	Date	Present state	Shipbuilding Technique	Dimensions	Wood Species	Dimensions	Wood Species	Dimensions	Wood Species	
Ancient World	Ma'agan Mikhael / Kibbutz Ma'agan Mikhael, S Haifa, Israel	c. 400 BC	Conserved (two step PEG E 400 and PEG E 3350) In display	Shell-first planks fastened with mortise-and-tenon joints locked with tapered pegs sewing in extremities	10.5 cm sided 16 cm molded	pine (*Pinus brutia*) [false-keel is oak (*Quercus pubescens/Q. petrae*)]	3 - 5 cm thick 11.2 - 30.5 cm wide (mostly 20 cm)	pine (*Pinus brutia*)	widely spaced 75 cm centre-to-centre	pine (*Pinus brutia*)	Kahanov,1997 Kahanov,1998 Steffy, 1994 Liphschitz, 2012
	Kyrenia / Kyrenia, north coast Cyprus near the harbour town of Kyrenia	c. 300 BC	Conserved (PEG 4000) In display	Shell-first planks held together with pegged mortise-and-tenon joints	12.20 cm sided 20.3 cm molded	pine (*Pinus halepensis?*)	c. 4 cm thick	pine (*Pinus halepensis?*)	floor timbers were 9 cm sided 9 cm molded spaced 25 cm centre-to-centre half-frames were 8.5 cm sided 8.5 cm molded	pine (*Pinus halepensis?*)	Katzev,1980 Steffy, 1985 Steffy, 1994

	Table 2-1 continue				Hull construction details						
					Keel		Planks		Frames		Reference
	Name of Shipwreck / Location	Date	Present state	Shipbuilding Technique	Dimensions	Wood Species	Dimensions	Wood Species	Dimensions	Wood Species	
Ancient World	Madrague de Giens / East of Toulon, France	c. 70 BC	*in situ* Reburied in sand	Shell-first planks held together with pegged mortise-and-tenon joints double-planked	35-by-40 cm	elm	6 cm thick inner planking 4 cm thick outer planking	elm inner planking fir outer planking	half-frames c.10.5 cm molded	elm	Tchernia, 1987 Steffy, 1994 Pomey, 2004
	Caesarea / Caesarea, NW of the Hellenistic quay in Area J, between Haifa and Tel Aviv, Israel	100 AC	*in situ*?	Shell-first pegged with mortise-and-tenon joints			9 - 9.4 cm thick	pine	floor timbers were 15.5 - 26 cm molded 14- 18 cm sided half-frames were 14 - 20 molded 16.5 - 22 cm sided spaced 9 cm centre-to-centre	pine	Fitzgerald, 1995
	Blackfriars / Blackfriars Bridge, London, United Kingdom	200 AD	Museum of London?	Skeleton-first lacks edge joinery (mortise-and-tenon joints)			5 - 7.5 cm thick	oak	floor timbers 30 cm sided and 21.5 cm molded	oak	Steffy, 1994

	Table 2-1 continue				Hull construction details						
					Keel		Planks		Frames		Reference
	Name of Shipwreck / Location	Date	Present state	Shipbuilding Technique	Dimensions	Wood Species	Dimensions	Wood Species	Dimensions	Wood Species	
Medieval World	Dor D 2001/1 / Dor (Tantura) Lagoon, south of Haifa, Israel	end of 500 AD - beginning of 600 AD	Under conservation ?	Skeleton-first	11 cm sided 16 cm molded (false keel was 11-13 cm wide and 5-9 cm thick)	Cypress (*Cypressus sempervirens*) [false keel was oak (*Quercus coccifera*)]	2.5 - 3 cm thick (average) 10 to 17 cm wide	Cypress (*Cypressus sempervirens*)	floor timbers averaged 8 cm sided and 12 cm molded futtocks averaged 8.5 cm sided and 9 cm molded half-frames averaged 8 mm sided and 10 cm molded average room and space was 24 cm	beech (Fagus orientalis) pine (*Pinus brutia*) oak (*Quercus cerris* and *Q. coccifera*) elm (*Ulmus campestris*) other angiosperms *(Tamarix* and *Ziziphus spina christi*)	Mor & Kahanov, 2006 Kahanov & Mor, 2014
	Yassi Ada / Yassi Ada, Turkey	625 AD	?	Mixed construction (transition) Unpegged mortise-and-tenon, in lower section, widely spaced	22 cm sided 35.5 cm molded	Cypress	3.5 cm thick 13 - 21 cm wide	pine	14 X 14 cm room and space was 30 - 35 cm	elm	Steffy, 1994 Mor & Kahanov, 2006

	Table 2-1 continue				Hull construction details						
					Keel		Planks		Frames		Reference
	Name of Shipwreck / Location	Date	Present state	Shipbuilding Technique	Dimensions	Wood Species	Dimensions	Wood Species	Dimensions	Wood Species	
Medieval World	Skuldelev 1 / Peberrenden, north of Roskilde, Denmark	1000 -1050 AD	Conserved (PEG 4000) In display	Nordic clinker	6- 14 cm sided 16 cm molded amidships	oak	lowest strakes 2.8 - 3.4 cm thick at their centres tapering at their edges	Pine (*Pinus sylvestris*)	10 - 15 cm sided 11 - 12 cm molded (30 cm at bow and stern) widely spaced c. 1m	oak	Steffy, 1994 Crumlin-Pedersen, 1997 McGrail, 1998
	Doel 1 / Doel, Antwerp Harbour, Flanders, Belgium	1325/1326 AD	In water containers Awaiting conservation	Cog	13 X 33 cm (keelson is 30 cm sided and 23 cm molded)	European oak (*Quercus rodur* or *Q. petraea*)	bottom planks c.5.1 cm max ave. thickness and c. 40 cm max ave. width lapstrake planks c. 4.5 cm max ave. thickness and c. 38 cm max ave. width ceiling planks c. 3.5-4 cm thick and 30-35 cm wide	European oak (*Quercus rodur* or *Q. petraea*)	through-beams c. 26.5 cm average sided and 25 cm molded	European oak (*Quercus rodur* or *Q. petraea*)	Steffy, 1994 Crumlin-Pedersen, 2000 Vermeersch & Haneca, 2015

Table 2-1 continue				Hull construction details						
				Keel		Planks		Frames		Reference
Name of Shipwreck	Date	Present state	Shipbuilding Technique	Dimensions	Wood Species	Dimensions	Wood Species	Dimensions	Wood Species	
Molasses Reef / SW edge of Caicos Bank near French Cay, Turks and Caicos Islands, Caribbean Sea	early 1600 AD	Conserved In display	Caravela			averaged 4.5 cm thick	white oak *(Quercus* sp.)	c. 16 cm sided c. 16 cm molded room-and-space was 32.5 cm	white oak *(Quercus* sp.)	Oertling, 1989 Steffy, 1994
Mary Rose / Solent, England	sank 1545 AD	Under drying process after impregnation with PEG (two-step PEG 200 and PEG 2000) In display	Carrack	32 to 40 cm wide	elm and oak	outer planking 10 cm thick inner planking (ceiling planks and stringers) 6 - 8 cm thick 7. 5 - 50 cm wide orlok deck planks 2.5 cm thick main deck planks c. 7 cm thick maximum 50 cm wide upper deck planks average 4.5 cm thick	oak (castle planking is coniferous) (orlok deck beams are moslty of elm)	floor timbers 20 cm thick 25 - 50 cm wide spaced 30 - 50 cm	oak	Marsden, 2003 Preston et al., 2014

Age of Global Seafaring

Age of Global Seafaring	**Table 2-1 continue**				Hull construction details						Reference
					Keel		Planks		Frames		
	Name of Shipwreck / Location	Date	Present state	Shipbuilding Technique	Dimensions	Wood Species	Dimensions	Wood Species	Dimensions	Wood Species	
	Red Bay (San Juan) / Red Bay, Strait of Belle Isle, Labrador, Canada	sank 1565 AD	*in situ* reburied (protected, monitored and in a stable conservation environment) (covered in silt / sand and man-made materials - tarpaulin)	Galleon or Nao		beech	hull planks 4.5 - 5.5 cm thick 33 -38 cm wide castle and deck planks 3 -3.5 cm thick 19 cm wide	white oak	floor timbers 19 cm squared spaced 35 - 36 cm centre-to-centre futtocks 19 - 20 cm at the floor to about 14 cm square at the upper deck	white oak	Steffy, 1994 Loewen, 1998 Grenier, 1998 UNESCO, 2012
	Vasa / Strömmen, Stockholm, Sweden	sank 1628	Conserved (PEG 600, 800, 1500 and 4000) In display	Galleon	c. 59 X 59 cm	oak (*Quercus sp. possibly robur?*)	c. 10 cm thick ceiling planks c.11 cm	oak (*Quercus sp. possibly robur?*)	floor timber c. 38 cm molded	oak (*Quercus sp. possibly robur?*)	Fors, 2005 Cederlund & Hocker, 2006 Håfors, 2001 Hocker et al. 2012
	Dartmouth / Sound of Mull, Scotland	sank 1690	Stored in laboratory Awaiting conservation?	Frigate of fifth-rate		elm	6.3 - 7.6 thick	elm	25 cm sided, 20 cm molded c. 30.5 cm spaced from centres	oak	Martin, 1978 Steffy, 1994 Skinner et al., 2005

2.2.2 Shipbuilding traditions and timber conversion techniques

There are two ways to build a wooden boat. Putting up a strong skeleton of keel and frames, to which a casing of planks is then fixed, called *skeleton-first* construction. And second and preceding, the *shell-first* construction in which a shell (the assembly of planking) plays the structural role, while the frames (skeleton) have only a secondary, reinforcing role (Pomey, 2004). A diagnostic feature of shell-first hulls is the type of fastening the planks. Three different systems are recognised: two of them share the way planks are set together, which is edge to edge, but differentiate in the means of fastening; either they are sewn together, as practiced in Old Kingdom Egypt if not earlier, or stapled or nailed together, or joined together with mortise-and-tenons. This was done by Greek, Roman and Phoenician shipwrights, but different from the Egyptians, a complete set of frames was here installed inside the shell. The third way of fastening planks was common practice in northern Europe (used by the Vikings, and in England up to the time of Henry VIII, and in Scandinavia until this century), where a plank overlaps the one below it and is secured with pegs or nails or rivets, constructing the so-called clinker-built boat (Casson, 1994: 30-31).

Archaeological evidence shows that by the mid first millennium AD a transition from shell-first to skeleton-first shipbuilding technique, which possibly emerged on the second half of the second century AD in the Mediterranean (Casson, 1994: 35; Pomey et al., 2012), was now emerging (Mor & Kahanov, 2006). This trend may well have been afoot in NW Europe at the same time (Pomey et al., 2012). This transition, driven from social, economic, geographical and environmental impacts in Ancient Mediterranean (Pomey et al., 2012), was marked by a gradual decrease of the shell's strength in favour of a less elaborative and cheaper construction by placing the importance to the inserted frame (Steffy, 1994: 85). However, both shipbuilding techniques as well as mixed combinations of the two, co-exist during this transition, and a linear model of development as proposed by Steffy twenty years ago, can no longer be of use under new archaeological evidence (Pomey et al., 2012). As Steffy remarks, changes in mortise-and-tenon joinery follow in accord with this transition. Their less contribution into a hull's erection and strength can be seen on so far excavated shipwrecks, through a gradual increase in their spacing within planks on ships until their elimination (Figure 2-3). Metal nailed planks appeared in the place of mortise-and-tenons during the transition period and replaced them in the skeleton-first constructions (Steffy, 1994; Pomey et al., 2012). At the same time, the evolution of the framing-system and the appearance of wooden structural components, which add strength along the symmetry axis of a hull, account for this transition (Pomey et al., 2012).

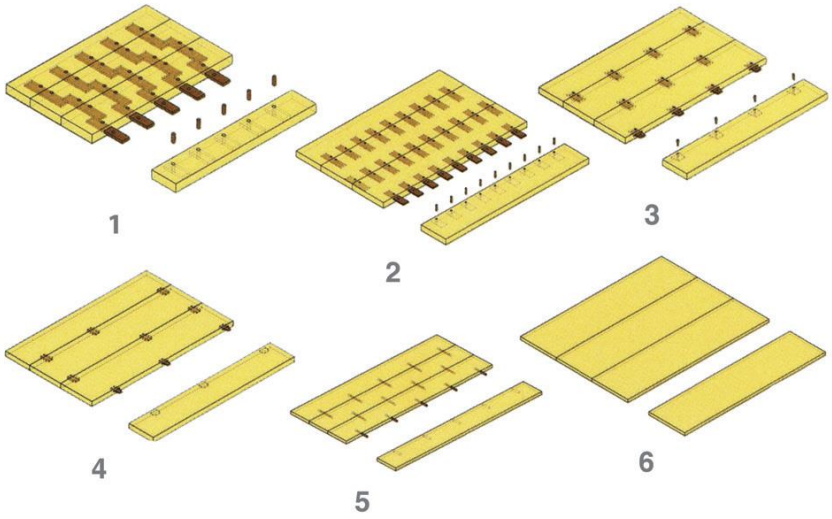

Figure 2-3 Shipbuilding transition theory based on the evolution of planking edge-fastening: 1. Uluburun (c.1325 BC); 2. Kyrenia (c.300 BC); 3. Yassıada 2 (4th AD); 4. Yassıada 1, 7th AD); 5. Yenikapı 14, c.900 AD; 6. Serçe Limanı (c.1025 AD) Extracted from Pomey et al., 2012: fig. 90).

Timber conversion

Special care was given to wood characteristics when selecting trees for building boats. Straight-grained and free of knots wood for planks, keels and keelsons, in what seems to have been in a 'green' (unseasoned) condition, was to be of particular preference in north-west Europe (McGrail, 2014: 8-9; Haneca & Daly, 2014: 97). Green wood is "fresh" wood recently felled and holds high moisture content; shipbuilders preferred it because it takes less effort to shape it compared to seasoned wood. Moreover, heartwood was highly appreciated and predominantly used for its enhanced mechanical properties and reduced susceptibility to deterioration, while sapwood was largely avoided (McGrail, 1998: 28).

Planks would be derived from logs using two main conversion methods: orienting the plank's wide surface parallel to the wood rays (*radial grain*) or tangent to the wood growth rings (*tangential grain*) (Figure 2-4). Hence, considering ultrasound insonification directions aiming on the surface of hull components as planks, then in Figure 2-4, planks A provide tangential travel paths, B radial amid the plank's width, and tangential from that point and moving towards its ends, C radial, and D insonification directions in an angle with the growth rings between 30° to 60°. Type D plank called *rift sawn*, or 'neutral-grain' by McGrail (1998: 30-31, fig.4.4), presents some of the qualities of an A plank. Lumber with growth rings at angles of 0° to 30° to the wide surface is called *quarter sawn*, and lumber with angles of 60° to 90° to the wide surface is called *flat sawn* or *plain sawn*. The use of quarter sawn lumber in shipbuilding has the advantages, in relation to flat sawn, of lower

shrinking and swelling in width, less cupping, surface checking and splitting but the cost is much higher (Bureau of Ships - Department of the Navy, 1983: 62). It also minimises the occurrence of knots (McGrail, 1976: 242-243). Knots were especially avoided in clinker planks (Crumlin-Pedersen, 2004: 49), while during the Naval War of the Revolution in the eighteenth century, one rotten knothole could be the cause of rejection of a single tree destined for a ship's mast (Coggins, 2002: 47).

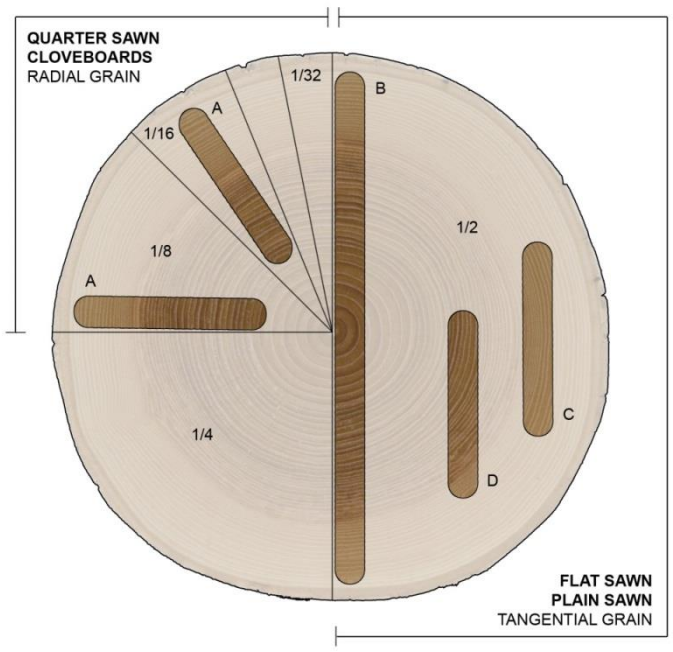

Figure 2-4 Timber conversion into quarter sawn and flat or plain sawn planks (Adapted from Crumlin-Pedersen, 2004: fig. 4.18 and McGrail, 1998: fig.4.4)

Before the broad use of pitsaws and sawmills from the later Middle Ages onwards, which allowed timber conversions in a variety of ways (McGrail, 2014: 11), oak planks were produced by radially splitting large straight-grained oak logs using mauls and wedges and continuously halving into halves, quarters, eights and so on, called *cloveboards* (Figure 2-4, A). Respectively, Pliny in his Natural History (77-79 AC) notes that "There are fibers and veins in the flesh of some trees (...) Veins are present in wood that is easily split." (Humphrey et al., 1998: 338). It could be deduced that with the terms *fibres* and *veins* Pliny refers to wood's narrow and broad rays respectively, which are clearly visible in hardwood but not softwood species, while especially in the presence of broad veins, a very typical characteristic of oak wood, these allow easy radial splits. It cannot be certain here if Pliny refers to timber conversions or that he is just featuring the natural tendency of trees such as oak to radially split when drying. Medieval Nordic boats and ships were made this way, where good quality oak was on hand. For clinker planks and frames to be robust and light at

the same time, the grain of the wood was closely matching with the shape of the hull component so that the radial grain was in parallel with the widest plank edge (Crumlin-Pedersen, 2004: 54). The notably enhanced mechanical properties of the hulls using the minimum of human effort was recognised by dexterous builders who would practice the plank radial splitting technique even in times of sawing popularity, as evidenced on the oak planking of Henry the V's flagship, the Grace-Dieu (1418) (McGrail, 1993; Clarke et al., 1993).

Tangential wood or flat sawn wood was the common cut for oak planks from prehistoric times, and for ships with a planking of pine in medieval times (McGrail, 2014: 9; Crumlin-Pedersen, 2004: 48). Such a cut would allow for maximum plank width especially nearer to the log's pith (centre), (Figure 2-4, B). Such orientations are seen for example in the Ferriby oak sewn-plank (Earlier Bronze Age) (McGrail, 1998), the pine planks of Pabuç Burnu (570-560 BC) (Polzer, 2009), the oak planks of Skuldelev 3 boat (c. 1040 AD) (Crumlin-Pedersen, 2004), the Mary Rose elm deck planks (Mardsen, 2003) and the Molasses Reef oak planks (sixteenth century) (Oertling, 1989).

Most likely emerging from the flat-bottomed plank-built boat tradition of West Germany and Low Countries, the thirteenth century trading vessel, the cog, was not pointed for the expensive and high quality woods, but instead got tailored to the pit-saw method (Greenhill, 1976; Crumlin-Pedersen, 2004: 49). Here, plank strength was compensated by increasing the plank's thickness. Pit-sawing and see-sawing (Goodburn, 1997: fig. 6) leads to flat sawn cuts. The aim was to first optimise the yield and maximum width of the planks, while the quality of the planks would follow. In Figure 2-5 the utmost of the planks is tangentially oriented. The remaining central part which includes the tree's pith can be then used for the hull's beams and keels (for example see documentations by Steffy (1994), and Adams (2013); these components give ultrasound insonification paths parallel to the rays.

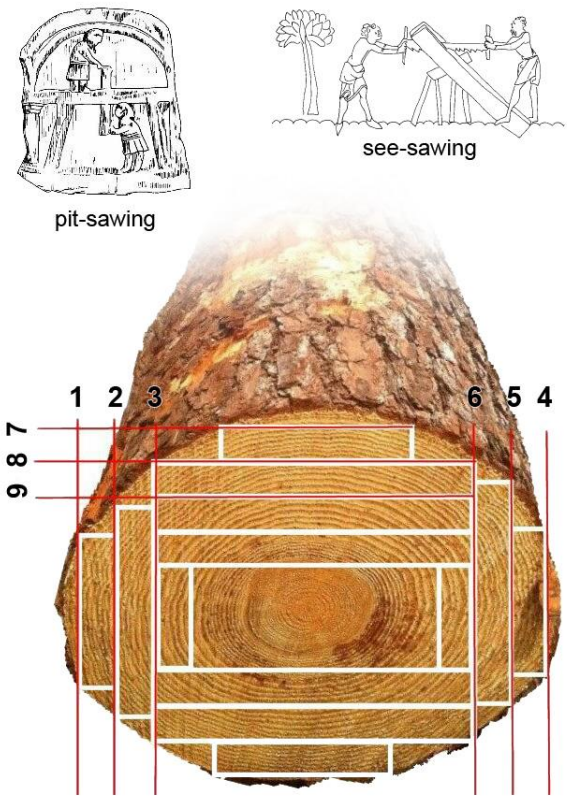

Figure 2-5 Flat sawn cuts leading to wide tangentially oriented planks and high yield (Sawing images on the top extracted from Goodburn, 1997: fig.6).

The meticulous study of the oak (*Quercus robur* or *Q. petraea*) planking of the Doel 1 cog (1325/26 AD construction date) (Haneca & Daly, 2014) confirms the preference of shipwrights towards wider plain sawn planks and especially those including part of the pith (Figure 2-4, B). These type of planks account for 71% of the hull's total planking, whereas orientations of the rift sawn or 'neutral-grain' (Figure 2-4, D), account for 17%. Another interesting aspect noted is that planks which were used as repairs, were deliberately all deriving from radially split oak logs (Vermeersch & Haneca, 2015: Table 5), as it was well known that such orientations would secure a qualitative repair and in an affordable cost because of a limited use.

From all the above archaeological evidence, it can be concluded that the majority of the wood axes expected to be insonified with ultrasound, are the radial (flat sawn) or the tangential (quarter sawn) wood axes, at least when referring to hulls' planks and beams from across different periods in archaeological time. On the other hand, it is rather unlikely to get insonifications along the grain of a log, or else the longitudinal growth axis.

From Table 2-1 it follows that hull components' thickness has indicatively ranged in time for planks between 2 cm to 14 cm, for frames between 8 cm and 22 cm, and for the keel 6 cm to 59 cm, averaging approximately at 5 cm, 19 cm and 14 cm respectively, and at 10 cm all included. Hence for experimenting, a test-piece from "fresh" wood of a 10 cm thickness could be an acceptable average representative of main hull components. Certainly, keel dimensions are by far the largest compared to those of planks and less of frames, yet planks and frames outnumber the keel within a hull, and thus have bigger significance.

2.3 Wreck formation: Prospects of wood hull preservation

In order to describe wreck formation the terminology employed by Parker (1981) is adopted here: where '*shipwreck*' is defined the remains of a wrecked ship and contents, while '*wreck*' is the site where a ship has been badly damaged or destroyed, or is the event of such damage or destruction; a '*site*' is a place investigated by archaeologists.

For assessing a site under the sea, it is the investigator's primary task to compile all the information given by the physical landscape which now hosts the cultural remains. But unlike static land monuments where the local environmental parameters and geomorphology called for the monument's location, the wrecking of a ship in its current place, if not an act of scuttling, was never premeditated. Where sat underwater, it can only show little resistance to a prevailing active and complex environmental system, which constantly transforms it under its impact (Muckelroy, 1977 & 1978: 175). The understanding of the dynamic seabed deposits in sites of interest is required for determining the formation and preservation potential of wreck assemblages (Parker, 1995).

When maritime archaeology was in its germination, rationalization of sites appeared impossible (Frost, 1962) as indeed variables associated with wreck formation and shipwreck preservation, are plenty and diverse. From the archaeological perspective, variables as are the purpose a ship was intended for, whether a light merchant or a heavy war ship, the type of wood it was built in, vicinity with other of the wreck materials that can affect the organic preservation (Pulak, 2008), as well as the reason of its sinking, whether intact or broken, the surface it hit, was that rock, sand, mud, or any combination of those, and finally, the speed the shipwreck was encapsulated by anoxic sediments or encrustations of marine biota, all would play a role on the preservation of organic material, as is wood. Ideally, a shipwreck laying in deep waters and covered to such an extent that it would be less pronounced to hinder the natural flow of sediment across the seabed, it would allow the wreck to

equilibrate with the environment and remain stable even for centuries (Frost, 1962; Dumas, 1972). But, already since those early times, efforts for simplifying complex wrecking events through *systematic observation* - an originality accredited to Christian Thomsen's (1788 – 1865) after establishing the Three-age System[4] of relative chronology in the hands of archaeological science - was now being explored for unravelling natural and cultural wrecking processes (Clarke, 1968).

Since then, the increase in the number of sites surveyed and identified, and their systematic excavation and study, together with multidisciplinary scientific research, have excelled the necessary knowledge to justify the various modes of operation involved in wrecking formation and wood preservation (Nesteroff, 1972; Caston, 1979; O'Shea, 2002; Quinn, 2006; McNinch et al., 2006; Gregory et al., 2012). As opposed to the past, it is now acknowledged that wreck sites can appear to have reached equilibrium with the surrounding environment only upon moment of discovery, because in fact they never stop interacting with the dynamic natural environment, either by exchanging material (sediment, water, organics and inorganics) or by energy (wave, tidal, storm), until reach of final disintegration (Gregory, 1995; Quinn, 2006).

Material Input

To start probing the prospects of wood preservation under the impact of these surroundings, the maximum of a wooden hull expected to remain after wrecking is first contingent on the reason of the accident itself. Muckelroy (1978: 166) distinguishes two extreme circumstances: one is the vessel which fell intact, and was dragged to the bottom by a combination of ballast, contents and inflowing water, causing everything trapped between decks to sit on the seabed and if lucky, get buried over time and preserved. Tomalin et al. (2000: 21) note respectively that where *Pomone's* (wrecked 1811) organic materials did survive it was because they were pinned to the seabed under the ship's heavy armaments. Likewise, the well stowed cargoes of amphorae carriers sink with the hull to the seabed, and upon discovery although the upper works are scattered around, the lower layers of the cargo are still *in situ*, promoting shelter to the underlying portions of the original wooden hull (Figure 2-6) (Dumas, 1972: 30; Muckelroy, 1978: 166; van Doorninck, 1981). The other extreme is a shattered vessel having just experienced a catastrophe on the sea surface, dropped all its heavy items, whereas the buoyant ones, as pieces of wood, floated away, or if

[4] The periodization of human prehistory into three consecutive time periods, named for their respective tool-making technologies: the Stone Age, the Bronze Age and the Iron Age.

waterlogged, sank as well. The 14th century BC *Uluburun* wreck could broadly fit this category as part of the ship, if not most of it, did go down with the cargo still on as evidenced by the latter's layout on the steep rocky slope. After tacking on a rocky point of 'Grant Cape', either under the influence of winds or a captain's fateful manoeuver, she went down leaving a large number of copper and tin ingots, *pithoi*, stone anchors, amphorae and the rest of an ample and diverse cargo scattered over the cape's slope. However, only a few percent of original structure survived, including part of her keel and adjacent timbers (Pulak, 1998). It can be assumed that wood either drifted away after smashing to bits on the cliff's face or perished after exposure to the sea water column, as the morphology of the area did not allow her entombment. Between those two extremities lie unexhausted wrecking cases which can only be dissected separately (O'Shea, 2002).

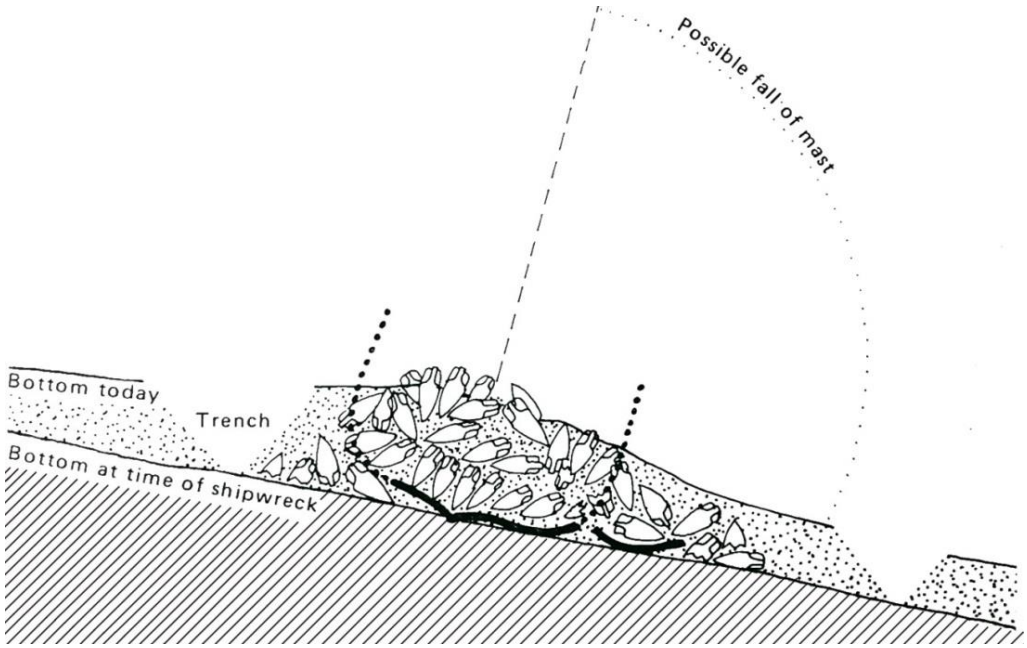

Figure 2-6 Transverse section of hypothetical amphorae wreck showing wooden hull preservation potential under the cargo layers (Dumas, 1972: 31).

Variables influencing wreck formation

It appears that from the moment of wrecking, and potentially at any time after that, the physical processes (waves, currents, storms and tides) interacting with the seabed's morphology and sediment's characteristics, are the weighing factors dictating a shipwreck's integrity as a unit (Ward et al., 1999; Quinn, 2006; Wilkens & Richardson, 2007). Actions to monitor the frequency of occurrence and force of such dynamic regimes around sites of interest towards preventing or mitigating their impact on a shipwreck if so needed, are indispensable and possible to make, although can sometimes seem of little assistance when

an unpredicted incidence, as an intense storm or a tsunami takes place at a moment in time, capable of a profound re-arrangement of the underwater scenery (Wheeler, 2002). In the aftermath of the physical processes, and once lodged underwater, it is the moment of the biological and chemical processes to activate and interact with the wrecked ship (Ward et al., 1999).

Respectively, personal experience led Dumas (1972: 30) to note that a wooden hull will partially cave in the sea bottom, by itself or under the weight of its cargo once the wood becomes waterlogged. In the meantime, 'scouring', a phenomenon taking place around the base of a marine structure introduced to the seabed, due to an increase in flow velocity and turbulent intensity around it, takes effect. It is driven by the sediment's oscillatory motion caused by waves or / and bi-directional flow due to tidal currents, leading to the sediment's erosion around the structure, here shipwreck, which shifts into the scour pit where it gets buried, encouraging preservation (Jenkins et al., 2007; Whitehouse, 1998; Quinn, 2006; Wilkens & Richardson, 2007: fig. 5). Yet, scouring is a non-linear process and artefacts or structural components which were sunk beneath the seafloor, could re-appear under the impact of the hydrodynamic environment, jeopardising the integrity of the underlying shipwreck (Ward et al, 1999; Quinn, 2006; Astley et al., 2014).

Interaction is also anthropogenic. Port and coastal installations can periodically expose wreck sites as their existence disturbs the flow regime of the local natural phenomena, as are currents and wave motion. Fitzgerald (1995: 7) characteristically mentions that because of the human intervention on the surroundings close to the *Caesarea* wreck site (1st century AC), the wreck could either get uncovered or buried beneath a meter of sand within a period of just 48 hours, swaying its oxic / anoxic conditions and hence, preservation. An act of human vandalism, the explosion of two homemade bombs on the *Molasses Reef* wreck (early 16th century) just before its second excavation phase, caused serious damaging of artefacts and cut off hull timbers which were subjected to the destructive effect of the tides and waves, but luckily were not perished for ever (Oertling, 1989). Scattering and damage of shipwreck sites by fishing practice (e.g. see *Mary Rose* site, in Marsden, 2003: 69), especially of those sites yet to be discovered, is another obnoxious human disruption of their preservation state that calls for action (Brennan, 2011). So does the effect of other human activities. Some are driven by contemporary technological advances in underwater robotics and equipment now accessible to the general public, and can encourage inappropriate archaeological practice such as treasure hunting; and others are powered by human's unrestrained want for more development and exploitation of the ocean floors. All add up to

variables undermining the existence of the underwater cultural heritage and its emergence (Adams, 2007).

Environmental parameters affecting wood hull preservation

A wooden shipwreck that will make it to the sea bottom, will interact with it both physically, chiefly as a source of scouring, and chemically, as a source of new organic material for feeding living organisms. It will also introduce corrosion products to the sediment. With time the shipwreck will transform into a fragment of the intrinsic geological configuration and its physical affect will fade (Ferrari & Adams, 1990). Still, its presence will call, or not, for biological activity, as although safely buried from the top side, it can be yet undermined from below. The likelihood of this, its extent and rate, as well as the type of micro and macro-organisms and marine flora active, will be determined by the local environmental characteristics, the burial depth and the material input (as defined above). The yield and diversity of marine life can in fact be used as an index for the preservation potential of the shipwreck (O'Shea, 2002: 214). A thorough insight into the site characteristics impacting the survival of historic waterlogged wood is given by Jordan in his review (2001). Parameters as water level, pH, dissolved oxygen content, redox potential and concentrations of chemical elements of a site should be evaluated (Gregory & Jensen, 2006).

A classification of marine environments based on the relationship of biozones to land, sea bottom, depth and light is here presented, originating from Hedgpeth's *Treatise on Maritime Ecology and Paleoecology* (1957: 18, 22) and later adopted by Florian (1987: fig.1-9) (Figure 2-7). Based on the biozone's characteristics as are type of seabed, the seabed movement forced by waves and currents, the sunlight, water temperatures and salinity fluctuations, it is easier now to single out the physical, chemical, geological and biological characteristics of the environment surrounding and interacting with a site. It is expected that a shipwreck lying in the abyssal zones will be subjected to a different deteriorating environment compared to a wreck in the intertidal and neritic zones. Depth seems to inversely influence the variability of the deterioration of a wreck within the same zone across the geographical map, with that of the abyssal being the most constant (Hedgpeth, 1957; Florian, 1987). Still, wreck preservation appears to be chiefly determined by the sea bottom composition, rather than the depth it is encountered at (Van Doorninck, 1981).

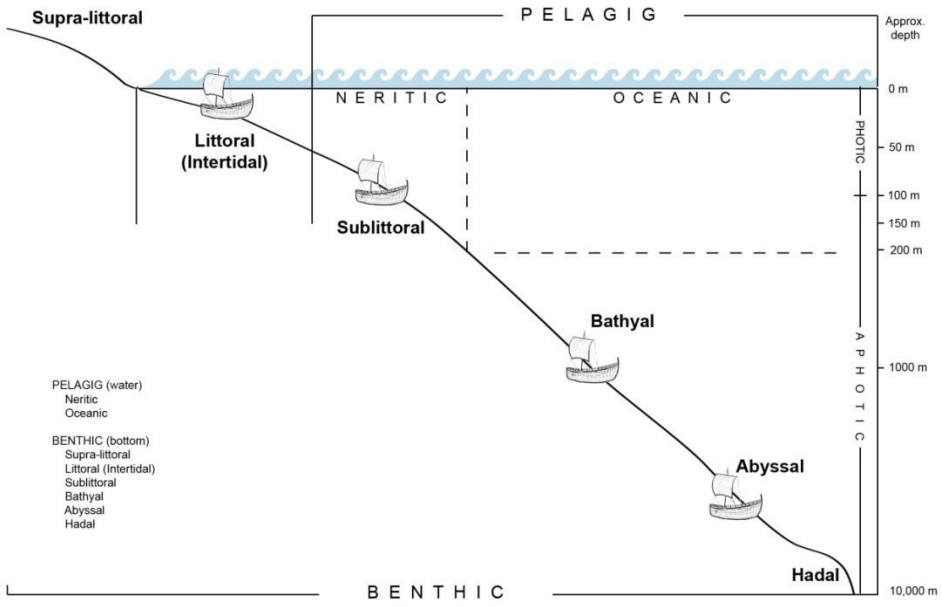

Figure 2-7 Possible shipwreck positions in relation to marine environments biozones (Adapted from Hedgpeth, 1957: fig.1 and Florian, 1987: fig.1-9).

Within the wreck, the possibility of a ship's timbers to be preserved and to what extend depends on the micro-environment or else the wood / marine environment interface, as this defines the speed of deterioration (Björdal & Nilsson, 2008). Two conditions play a chief role, the interface affiliation and the chemical environment (Florian, 1987). Generally two different boundaries of timbers and the environment can be met, timbers either exposed in the open seawater column or within the seabed (Gregory et al., 2012). Theoretically the part of the wooden ship meeting the sediment is the one preserved in a good condition, favoured by the fairly anoxic conditions promoted in close relation to sediment type and inclusions (e.g. organic matter), and environmental conditions (Jordan, 2003). Analysis of the silt/clay sediment from around the Kolding cog shipwreck, Kolding Fjord, Denmark, showed that anoxic conditions were prevalent at a depth only 6 mm below the sediment / water interface (Jordan, 2003). Jordan suggests that wood degradation from microbial activity is more likely related to the exposition of wood's end-grain surface[5] rather than depth of anoxia in the sediment. This suggestion could be supported by the fact that, colonisation of wood by erosion and tunnelling bacteria starts through wood's rays, and by soft-rot fungi through rays and vessels (pores) (Björdal, 2012).

[5] The transverse section or cross-section of a tree stem. Wood rays and wood pores (vessels) can be distinguished on this section (Forest Products Laboratory, 2010).

Since the early past, it has been systematically observed that well preserved wood generally belongs to the hull's bottom (Dumas, 1972), or as given elsewhere, it is the primarily portions of the hull below the waterline that remain on a site (Van Doorninck, 1981), which is actually the most informative concerning overall design and construction (Steffy, 1994). O'Shea (2002: 220) adds that in most cases the bilge and keel assembly is firmly embedded in the sea bottom because constructionally it is of the heaviest parts of a hull, which get heavier due to the fact that most of the time it is fully submerged in the water, and hence become of the most waterlogged whilst seagoing. Riley (1988) observes that ships typically "sink to the waterline" when they come to rest upright in a floor of sand. But there is also a chance that a section of either side of a tilted vessel will be found; it can be here expected that the wood can be in a worse preservation condition compared to the bottom's wood, as the sides would have been exposed for a longer time in the water column, before collapsing in the sand (Dumas, 1972). Frost (1963: 180, fig.37) describes that the waterlogged hull sides open or split due to their overweight and drop, and the softened hull now reshapes following the curvature of the subject layer where it comes to rest.

To exemplify the above theories on wreck formation and wood state of preservation, three fully excavated, conserved and studied shipwrecks are selected here to represent three different prototype wrecks. These are the Kyrenia, Mary Rose and Vasa. The first two wrecks could be classified as fairly common situations encountered in underwater archaeological records, as part of their hull was already perished upon discovery; but differentiate in burial location, as one was discovered in the warm, bright and high saline Mediterranean waters and the other in North Europe, with prevailing low temperatures, salinity and darkness. As such, the degradation environment acting upon them is different. As is also their resistance to it, given that they are built from different wood species, pine and oak respectively; while pine is considered as more resistant to decay, severity of degradation cannot be solely based on wood species, but the wide diversity of conditions under which the wood was exposed, has to be considered (Schniewind, 1990). The third wreck is a rather rare one since the entire ship was preserved intact. Yet, anticipation for more ships like the later, lie with deep water archaeology, which promises to give a plethora of undisturbed and high-resolution assemblages (Adams, 2007: 49).

Their presentation aims to assist in a first visualisation of quite familiar wreck scenarios under the eyes of a non-intrusive tool, for assessing the state of preservation of their wooden members. Wood can be found directly exposed into the water column or hidden under piles of amphorae and / or layers of sediments. It is encouraging that it could still be detected remotely using marine geo-acoustic techniques, due to the contrast in density and

sound velocity between the wood and surrounding environment (Mindell & Bingham, 2001; Plets et al., 2009). Together with this, the type of the ship, how much of its original structure was discovered and to what preservation condition it was, are presented. A reconsideration of these prototypes under the light of the experimental conclusions of the present study, is given in the final discussion, in Chapter 6.

Prototype wrecks

i. Kyrenia (4th BC)

The first case is an amphorae vessel. The fourth century BC, the *Kyrenia*, was a small merchant ship sank off north of Cyprus towards the end of its century. Her journey was ended most likely after a pirate attack, as supported by a number of spearheads found beneath the hull, some bent from impact (Katzev, 1981). Kyrenia's wooden hull was preserved at the port side from the keel to above the waterline, and slightly less so on her starboard side. It is known that she had a rather tranquil descent to a depth of 30 m where she gently sat on a flat, muddy sand seabed (Green et al., 1967), with a heel of about 15 degrees on her port bottom (Steffy, 1985: 72). At that position she got gradually well buried under the muddy sand, as only a number of a hundred amphorae covering just about an area of 3 X 5 m was visible at the moment of her discovery (Figure 2-8) (Green et al., 1967). Yet, further beneath 60% of the hull area and more than 75% of her representative timbers would be found preserved in a very good condition as noted, rewarding maritime archaeology with valuable historical information (Steffy, 1985).

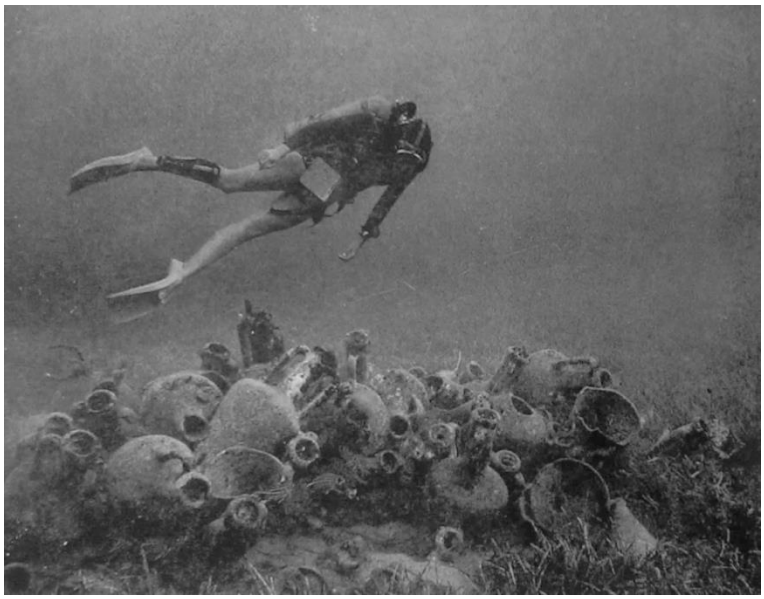

Figure 2-8 The Kyrenia wreck: the top of the 'iceberg' (Photo: Pennsylvania University Museum, National Geographic Society, Extracted from Katzev (2005).

However, there was time before that, that in the ideal salty, warm and bright Mediterranean waters, the exposed hull became a rich feeding ground for the shipworm Teredo as revealed by a pronounced action of the shipworm in the keel's cross-section (Figure 2-9) (Katzev, 1980: 418). Notes on a weak preservation state of the wood, which was so pliable upon salvage that it was decided to take apart the hull and lift it in sections (Katzev, 1970), was later verified by its chemical analysis which showed a very significant reduction of the wood's cellulose (Katzev, 1980). The US Forest Products Laboratory which ran the analyses, also advised the archaeological team that the wood had high inorganic inclusions (*ibid.*: 418), i.e. was in a process of fossilisation (Castro & Roig, 2007). This probably confused the excavators as the wood was very soft; yet high inorganic content does not necessarily mean a visible increase of wood's hardness (e.g. Giachi et al. 2003), here because of the critical reduction of the crystalline cellulose amount. But it surely exhibits an increase of its weight with a phenomenal increase of its density. In the absence of residual density level records, it can be deduced that Kyrenia's wood had lost most of its wood mass and was highly degraded, most likely classified as Class I (section 1.3.1.1), given the high molecular PEG which was used to conserve it (Table 2.1).

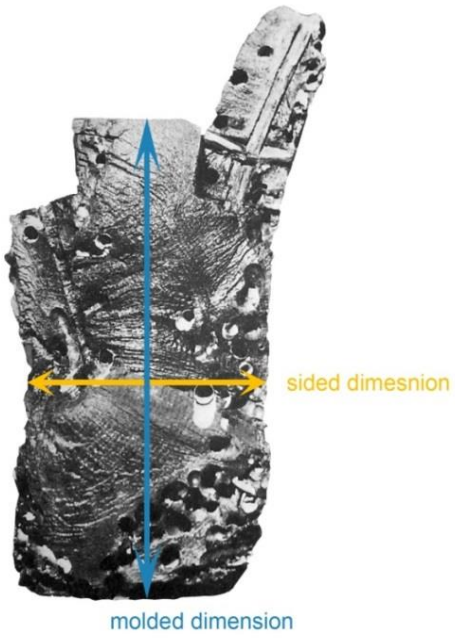

Figure 2-9 Shipworm Teredo infestation apparent on the cross-section of a broken piece from Kyrenia's keel and piece of the garboard (Modified from Katzev, 1980: fig.1). Keel was sawn and hewn from a single log of *Aleppo pine*, sided 13 cm at the top and 10 cm at the bottom, and molded an average of 20.3 cm (Steffy, 1994: 43).

ii. Mary Rose (sank 1545)

The second shipwreck is Henry VIII's Vice Flagship, the *Mary Rose*. The ship had a sudden end in 1545 in the Solent estuary off Portsmouth, for a reason which under new light comes to an agreement with the contemporary statements that the ship critically destabilised after a bad turn in calm shallow waters and sank swiftly together with her broken pieces (Bell et al., 2009). From her systematic excavation beginning 1971, it was found that the vessel had settled in the silt seabed on her starboard side, at an angle of heel of 60 degrees (Rule, 1983: 67), which now became the ship's bottom (Bell et al., 2009).

The Mary Rose excavation diaries reveal a detailed rationalisation and recording of her wreck formation (Mardsen, 2003; Jones, 2003). In 1545 the ship weighed down into the upper sediment layer and rapidly buried herself on a featureless bed of mud and hard clay, assisted by the scouring action of the tides below the surface; that this could be a reason for the unsuccessful attempts to raise her immediately after her sinking (Marsden, 2003: 77, 83). Proud of the seabed, she acted both as a protective shelter and a trap to the incoming sediments flow, so that the organic objects inboard were quickly protected from biological and erosive actions, according with the fact that the influence of scouring on site formation is intense towards the beginning of the wrecking process (Figure 2-10, A) (Quinn, 2006). With time, as the standing hull was giving way coming in line with the sea floor, the scouring action ceased and sediments started to accumulate in the scour ditches (Figure 2-10, B). By the end of the sixteen century she was completely buried (Figure 2-10, C).

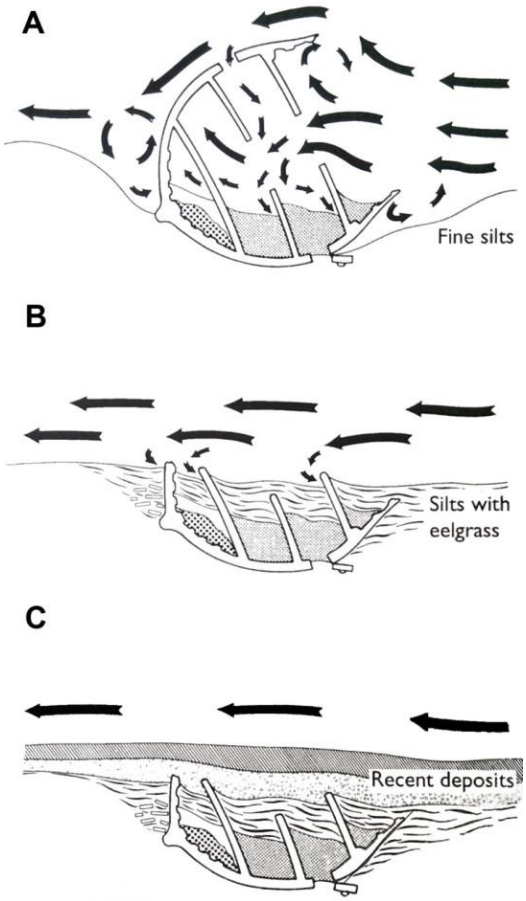

Figure 2-10 Wreck formation of the Mary Rose shipwreck (Extracted and modified from Mardsen, 2003: fig. 9.6).

The parts exposed to the water column inevitably suffered from mechanical abrasion and biological attack, and were all perished by the early nineteen century. However, the buried part of the ship's hull and artefacts were preserved under the deposition of soft and organically rich sediments, which promoted anoxic conditions. Differential erosion was identified on timbers which were found to be worn away on one side more than the other, evidencing their exposure prior to collapse (Mardsen, 2003: 84). The top of the frames were more exposed and badly eroded by abrasive action of the silt bearing currents (Jones, 2003: 22), yet the planking found more than a meter beneath, although at the top thin and distorted, were in excellent condition further below (Mardsen, 2003: 34). Weakening of the *Mary Rose* timbers was further addressed to the action of biological organisms as bacteria, soft rot fungi, actinomycetes and wood boring animals.

Predominantly the ship's oak and pine timbers preserved an inner relatively sound wood core, adjacent to a transition zone of moderately decayed wood surrounded by decayed or heavily decayed wood (Squirrell & Clarke, 1987; Mardsen, 2003), a pattern very commonly confronted in wood recovered from marine environments (Christensen, 1970; de Jong, 1977). For conserving Mary Rose's hull, a two-step impregnation regime with PEG of molecular

weights 200 and 2000 was adopted. With the low molecular weight PEG it is possible to reach the inner and healthier core of waterlogged wood, while the high molecular weight PEG follows, as suitable to support the more heavily degraded outer layers. The two-step process was established by Hoffmann (1986) for treating waterlogged timbers holding several distinct qualities at the same time, as those of Mary Rose.

iii. Vasa (sank 1628)

The third shipwreck is the warship *Vasa* in Sweden. She might not have had the chance to make history in battle as Gustav Adolph's flagship, but she has been certainly flagged as the first inspiring in a series of many maritime projects, which came into realisation after hers, successfully bridging maritime archaeology with the inquisitive interest of the general public (Hocker, 2006: 473). She sunk intact on her maiden voyage within the Stockholm harbour, the reasons to be found in construction faults (Hocker, 2006: 44, 58).

Vasa is one of the most extensively preserved seventeenth century shipwrecks (Steffy, 1994: 149), for several reasons, the first being that she never suffered from wear and tear, but was quickly stationed in the aquatic vitrine. She came to a rest in an upright position, and got partially embedded in the clay, yet not so deep to knock the underlying bedrock (Figure 2-11) (Hocker, 2006: 65). This arrangement should have assisted in the lower decks better preservation than the upper ones, as deduced from the different molecular weights of PEG (polyethylene glycol) used as the conservation material; PEG 600 and 1500 for the lower decks, and PEG 4000 for the upper decks and outside hull (Fors, 2005: 29). Every deck was found to be covered by a favourable layer for wood preservation of up to one meter or more, of organic-rich mud with some clay and silt (Hocker & Wendel, 2006: 150). Loose articles or structures that were once held in place with iron nails and bolts, were now found preserved under the built-up muddy sediment.

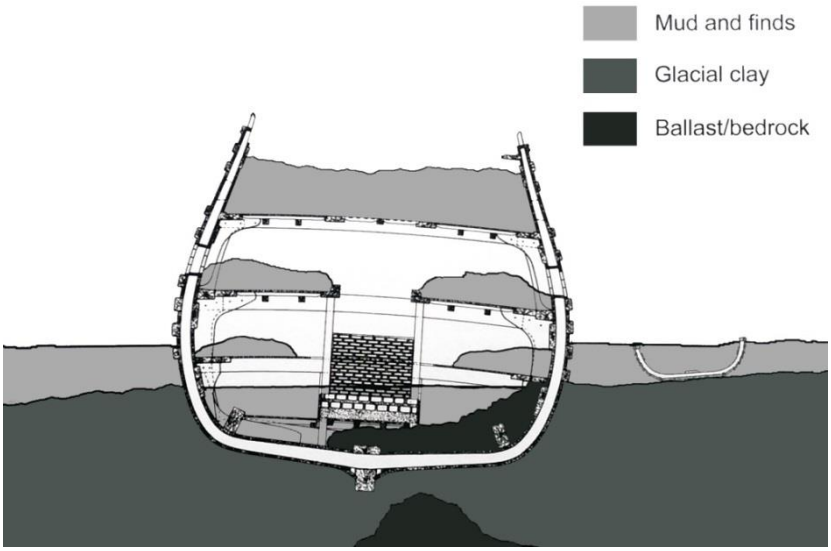

Figure 2-11 Sediment stratigraphy of Vasa *in situ* (Extracted from Hocker, 2006: fig.2.5).

The surrounding chemical environment, a combination of toxic waste material from human activity and local physical and chemical characteristics of the underwater environment, acted as a passive preservative for the wooden structures. A combination of low oxygen, high hydrogen sulfide, low below 0.5% salinity (in the open ocean salinity is typically between 3.5-3.7%), and the cold and dark waters of Stockholm's harbour inhibited the manifestation of any oxygen-dependent living organisms, like Teredo or gribbles and marine flora, except sulphate reducing bacteria and erosion bacteria (Hocker, 2006: 66; Fors, 2005). Oak timbers were found to have a rather healthy interior core as opposed to an exterior degraded wood layer, rarely exciding 15mm in thickness. This external decayed layer was susceptible to a combinational action of sediment and water constant flow and local currents which rasped it off with time.

Ironically, for such a considerable volume of preserved ship, it is rather the 'invisible' chemical content within its timbers, placed by the bacteria using up the sulphur compound of the surrounding water, which is now challenging her integrity following her conservation (Sandström et al., 2002; Ljungdahl, 2006; Lechner et al., 2013).

2.4 Character of marine waterlogged archaeological wood

2.4.1 Disintegration due to physical, biological and chemical processes

Water inside waterlogged wood protects it both as a barrier from the attack of organisms, and as an oxygen expeller together with overlying sediment (Hedges et al., 1985). The macroscopic structure of wood can appear unusually unchanged (Borgin et al., 1975) if actions by different biotic and abiotic forms of deterioration have not caused distinctive changes within wood cells.

The exposed wood is susceptible to the attack of aerobic marine organisms, the marine borers. The organisms belong to two distinct groups, Molluscs (Teredo, Bankia, Martesia, Nausitropia) and the Crustaceans (Limnoria, Sphraeroma, Chelura) (Tsoumis, 1968). The amount of infestation depends on factors like the species of the organism, temperature, salinity and dissolved oxygen content in the seawater, as well as symbiotic presence of fungi and species of wood (Tsoumis, 1968); although a later study showed no discrimination between species of wood as long as the larvae had a fair ease of access to the wood surfaces (Santhakumaran, 1970; Gregory, 1998).

Looking virtually intact, inside waterlogged wood can be a network of tunnels made by organisms with very little wood substance remaining (Björdal & Nilsson, 2008). The tunnels are dug by bivalve molluscs like Teredo species or by Pholad and the holes burrowed by crustaceans like Limnoria. The damage is either vertically or horizontally to the grains (Jones, 2003). The larvae shipworm Teredo requires at least 12‰ salinity and temperatures between 15°C and 25°C to develop; temperatures of 30°C or below freezing are lethal for the organism. The organism is restricted to 200 m depth (Florian, 1987). After free swimming for a short period the larvae begins excavation in the wood with a 1 – 3 mm diameter hole and can extend its tunnel along the grain not more than 25mm in diameter, preferentially attacking the earlywood (Steinmayer & MacIntosh Turfa, 1996). While progressing through the wood, the Teredo may line its borings with a characteristic thin layer of calcite less than 1 mm (Heise et al., 2011). As an adult it has a length between 305-700 mm and a 12 mm width (Teredo navalis) or 1.50-1.80 m length and 22 mm width (Bankia setacca) (Keeney & Pollio, 1984). However, the length of the tunnels depends on the extent of the attack; when the attack is extensive the tunnels become crowded and their length and diameter may be limited (Lopez-Anido et al., 2004). The only visual signs of external damage are the small openings in the wood made by the larval stage of the shipworm. Pholads are more restricted

in their occurrence than the shipworm; their tunnels are approximately 5-10 mm in diameter and range in depth from 3-8 times the length of their shell.

Crustacean have a length between 3-6 mm (Limnoria or gribbles) while their width varies from 1/3 to 1/2 of their length. They excavate long narrow tunnels 1-2 mm in diameter, with regular spaced respiration holes to the wood's surface, and rarely moving deeper than 12 mm from the wood surface. In softwoods they preferentially bore into earlywood leaving the latewood irregularly perforated resulting in characteristic concentric zones. Gribbles are limited by 18-15‰ salinity and to 530 m in depth (Florian, 1987). Underwater tide currents and the act of Limnoria remove superficial degraded surface layers allowing borers to penetrate deeper into wood, while the exposed calcite tubes left by Teredo break and fill with sediment (Jones, 2003; Heise et al., 2011).

The accumulation of sediment on the wreck transforms it into a geological formation sitting on the seabed with low impact on the environment (Ward et al., 1999) and protected from further deterioration, reaching a stable equilibrium with the surrounding burial conditions (Pearson, 1987). Nevertheless, deterioration can be present even under the "protection" of the underlying sediment. Wood is most likely going through high degradation of its chemical composition due to the action of micro-organisms (Björdal, 2012), found on the wreck itself and from the surrounding material, regulated by the level of oxygen in relevance to sediment depth, levels of organic particulate material and water saturation (Ponnamperuma, 1972; Björdal et al., 2000). Timbers above seabed and within the first tens of centimetres beneath it can be attacked by soft-rot fungi (SR) (*Ascomycetes* and *Fungi imperfecti*) and tunnelling (TB) bacteria, with their action lowering as moving to near-anaerobic levels. Erosion bacteria (EB) can be present at this dysoxic layer also; however it's within the near-anaerobic layer they solely dominate (Björdal & Nilsson, 2008; Kretschmar et al., 2008). Erosion bacteria vary in size between 1-8 μm in length and 0.5-0.9 μm in diameter and aim for the cellulose rich parts of the wood, while they are unable to degrade the lignin, in contrast with tunnelling bacteria which are capable of weakening the integrity of the whole cell wall (Björdal, 2012). Decay from soft-rot and bacteria starts at the wood surface and moves inwards, leaving a uniform soft and spongy wood layer of a few millimetres and depending on the wood species under attack. The fragmentation of polysaccharides to hydrolysable monomers by the bacteria and fungi leads to further degradation of wood's constituents i.e. cellulose, and lignin in the end (Fengel, 1991). At a sediment depth greater than 50 cm from the sea floor, any biological activity on wood seems to be inhibited (Gregory, 1998; Björdal & Nilsson, 2008), on the whole indicating that the deeper a timber is buried in the sediment the best preserved it will be. It is also

suggested that the larger the timber the slower is its decay; bacterial action can be present even after 1200 years (Björdal & Nilsson, 2008). The primary mechanism of degradation caused by the action of the bacteria is that the wood loses its mass, which creates cavities subsequently occupied by water i.e. the maximum water content increases (Kim & Singh 2000). Moreover and in a lesser extent, hydrolysis takes place, which initially is limited to extracts and hemicelluloses.

Nonbiological chemical deterioration is noted to affect the physical and chemical properties of wood even in absence of any biological attack (Blanchette et al., 1994; Jurgens et al., 2009), but abiotic deterioration is probably not the primary degradation mechanism for most archaeological wood (Hedges, 1990).

2.4.2 Physical and mechanical properties of marine waterlogged archaeological wood

Determining the artefact's density and comparison with that of "fresh" wood of the same species is indicative of the likelihood of the wooden material to collapse during conservation (Jensen & Gregory, 2006), hence assisting in making proper decisions upon the right conservation material and procedure. A density as low as 0.1g/cm^3 corresponds to a severely degraded piece of wood, while densities around 0.4-0.5 g/cm^3 correspond to well-preserved wood (Jensen & Gregory, 2006). Archaeological oak samples in waterlogged condition ranging in age from 50 to 1600 years have been found preserving as much as 96% and as low as 20% of their density compared to recent wood values, averaging at c. 0.370 g/cm^3, with a minimum of 0.122 g/cm^3 and maximum 0.620 g/cm^3. For other species aged between 70 up to 100,000 years old, residual density values even higher than those of "fresh" wood, have been noted (between 56% - 105%), averaging at c. 0.300 g/cm^3 for pine and spruce (*Pinus sylvestris* and *Picea abies*), with a minimum of 0.220 g/cm^3 and maximum of 0.450 g/cm^3 (Schniewind, 1990: Table I and II). Such observations are to be expected as the comparison is made between individual archaeological samples to mean values of "fresh" wood, considering natural variation in wood properties as they form under unique environmental and climate conditions (Schniewind, 1990).

For defining archaeological wood mechanical properties a chemical determination of the wood structure is first useful. Carbon, hydrogen and oxygen combine to form the principal organic components of wood substance, namely *cellulose*, *helicelluloses* and *lignins*. The first two are also called carbohydrates and polysaccharides. These three principal organic components are arranged to build wood cell walls which have a crystalline structure due to the crystalline properties of cellulose, while lignins are amorphous. Cellulose accounts for

the high strength of wood, whereas hemicelluloses and lignins contribute by supporting the cellulosic skeleton and adding to the elastic and compressive strength of wood. If any of these three components is reduced or removed, it destabilizes the coherence of the wood structure and decreases drastically its strength (Tsoumis, 1968).

Responsible for the wood's cell wall decomposition are several types of microorganism (section 2.4.1) aiming primarily for the nutritious polysaccharides and in some cases lignins too. In waterlogged wood, deterioration starts from its most hydrophilic and more readily hydrolysable component of the cell wall, the hemicelluloses, followed by the less hydrophilic cellulose and last, the most stable and more hydrophobic lignins (Schniewind, 1990). Thorough analysis of waterlogged wood samples from open ocean sediment deposits spanning in age from 25,000 to 2500 years (Hedges et al., 1985) revealed this selective degradation sequence of wood's structural components during burial.

Severely deteriorated wood has lost its strength because of reductions of the crystal structure in the remaining cellulose. Cell walls can turn thin and weak and become prone to shrinkage and collapse. Mass loss might occur, but not detected if replaced by minerals, typical of deteriorated archaeological waterlogged wood (Hedges, 1990: fig.10). Careful study of the mechanical properties of buried archaeological waterlogged wood in the literature (Schniewind, 1990: Table 5) indicates a broad reduction of wood's compression strength parallel to the grain, static bending and stiffness (modulus of rupture and modulus of elasticity). It was also observed that strength losses are not directly proportional to mass losses and degradation of the quality of the remaining substance also takes place. Increases in the plasticity of deteriorated cell walls (Jagels et al., 1988) have been suggested as a possible explanation of high values of impact bending strength matched with low stiffness values (Schniewind, 1990).

2.5 Acoustic properties of waterlogged archaeological wood

To address the research objectives, this study's working hypothesis was whether classifying the preservation state of waterlogged archaeological wood, would be possible *in situ* having the minimum knowledge over a shipwreck, as is wood species and position on the seabed. The present research will focus its interest in studying a hardwood (*Quercus sp.*) and a softwood (*Pinus sp.*) trees for two reasons, the first being that these trees and wood species have been used commonly in ancient shipbuilding as explained in section 2.3. A second reason is that they are significantly different as far as structure and density are concerned,

as it is well known that considerable variations in structure exist within the two wood classes, the hardwoods or broadleaved trees and the softwoods or conifer trees (Bureau of Ships - Department of the Navy, 1983).

Table 2-2 presents a number of ultrasound studies on "fresh" and archaeological oak and pine wood. Velocities through the three principal wood axes, as well as a few examples on off-axis insonifications (V_{RT}), are given, together with the moisture content and frequency they were taken at. Literature in forestry science for ultrasound velocities on wood holding moisture content well above the FSP, as met in archaeological wood, is limited; mainly because above the FSP transmission time remains largely unaffected by the moisture content (Ross & Hunt, 2000).

Table 2-2 Ultrasound velocities in "fresh" and archaeological oak and pine wood from literature.

				Ultrasound propagation velocity (m/s)			
Reference	Species	Moisture content (%)*	Frequency (kHz)	$V_{longitudinal}$	V_{radial}	$V_{tangential}$	V_{RT}**
Fresh							
McDonald, 1978	Eastern White Pine	d	150-200?	4350	2470	1550	
	Ponderosa Pine	g	150-200?	4390	1620	1460	
	Red Oak	g	150-200?	4110	2040	1790	
Sakai et al., 1987	Pine	12	1000-4000	5380	2440	2100	
Bucur, 1995	Oak	12	1000	5071	2148	1538	
	Pine	12	1000	5000	2100	1200	
Quinn et al, 1997	Oak	12	?	3120	1960	1230	
	Scots Pine	12	?	6010	1480	1000	
Karsulovic et al., 2000	Pine	10	500	5952	2079	1690	
Dix et al., 2001	Oak	s	500	2882	1668	1528	
Arnott, 2004	Oak	wg	800	3846	2435	2235	
	Pine	wg	800	4084	1781	1724	
Kabir et al., 1997***	Rubber wood	75.2	45		1620	1125	1300
	Rubber wood	14.6	45		2060	1500	1690
Ringger et al., 2003	Spruce	8	20-350		2000	1700	1500
Archaeological							
Dix et al., 2001	Oak	wg	500	3564	1527	1383	
Bader et al., 2013****	Oak	8	100	4248	2285	1510	

** d = dry (unspecified), g = green (unspecified), s = saturated (unspecified), wg = waterlogged, for oak MC_{maxL}=133%, MC_{maxR} =123%, MC_{maxT} =128%, and for pine, MC_{maxL} =183%, MC_{maxR} =160%, MC_{maxT} =149%.*
*** At an angle of 45°between the direction tangent to the annual ring and insonification direction.*
**** Approximate values.*
***** Average.*

It is clear from Table 2-2 that $V_L >> V_R > V_T$ for both wood species and irrespective of moisture content. Above the FSP and for "fresh" wood, oak longitudinal velocities have been found to hold values between approximately 3100 m/s to 5100 m/s, the radial between 1960 m/s to 2150 m/s and tangential, 1230 m/s to 1540 m/s. For pine, values fall between 4350 m/s to 6000 m/s, 1500 m/s to 2500 m/s and 1000 m/s to 2100 m/s, respectively. Below the FSP, velocity values generally vary around the ranges for dried wood, for both wood species. It is difficult to see clear trends, due to data variation.

Ultrasound velocities on Table 2-2 can be characterised as a typical set of values for oak and pine families, which are the interest of the present study. Velocity variation between studies is expected to be influenced by the control of wood's natural variability during test-sample preparation, wood's density, proportions of earlywood and latewood, annual ring curvature, and frequency (Bucur, 2006). Bucur & Feeney (1992) using horse chestnut at 12% MC, observed that V_R, V_T and V_{RT} are insensitive to frequencies higher than 250 kHz and up to 1500 kHz. On the contrary, V_L is strongly influenced by frequency, showing an increase in velocity from 100 kHz to 250 kHz, and from that point, a steady but smaller increase up to 1500 kHz. Horse chestnut, even being wood, is regarded as a substrate of very high homogeneous anatomy for studying acoustics on wood; thus results from other species can be compared against it, Respectively, Arnott et al. (2002) also demonstrated the frequency independence of radial and tangential velocities, and not that for longitudinal, using waterlogged "fresh" oak and for a frequency range between 300 – 1000 kHz. This agreement between the two studies, promotes the velocity independence of frequency for the two main wood axes of interest of the present study, the radial and tangential axes, and for moisture contents either below or above the FSP. This can potentially allow putting aside the frequency variable from the ultrasound propagation velocity in waterlogged wood. This would be rather useful considering that marine geophysical surveying tools may operate at frequency ranges between a few kHz up to few hundreds; for example, 1.5-13 kHz (Plets et al., 2009), 100 kHz, 500 kHz and 3.5 kHz (Papatheodorou et al., 2014).

Investigation on wood structure, anatomical elements and physical properties, leading to ultrasound velocity variations within a tree and among different wood species in "fresh" wood, together with knowledge upon the effect of wood orientation on ultrasound when aiming at angles in between the three principal wood axes, is first necessary.

2.5.1 Influence of structure and density

The anisotropic nature of wood is a challenging feature when the acoustical properties of the material are studied in relation to its structure (Bucur, 1988). Ultrasonic waves are mechanical waves and their speed of travel involves the physical properties and elastic constants of the material through which they are propagating (Feeney & Chivers, 2001). The physical properties of the cellular wall, density, modulus of elasticity etc., and the shape and size of the wood fibers or other elements affect the transmitted ultrasonic field. Each structural element acts independently as an elementary resonator (Bucur, 1995). Unlike solid homogeneous materials which have a constant acoustic velocity, wood's natural anisotropy is induced by the specific deposition of anatomical elements during the life of a tree, affected by environmental, meteorological and genetic factors (Tsoumis, 1968).

On a transverse or cross-section (RT plane) of a stem, three parts can be distinguished: the *pith* at the centre, the *wood* (*xylem*) in the middle and the *bark* at the outer part (Figure 2-12). Wood and bark are produced from a tissue called *cambium*, which exists between the two parts, visible only under microscope. Stem growth in diameter is seen through the superposition of relatively easy to discriminate concentric layers, called *growth rings* or *annual rings*. Growth rings can be distinguished because of differences in *earlywood* and *latewood*. Light-coloured earlywood is the wood which develops during the beginning of the growing session, when the growing rate is faster, and is defined by thin-walled cells and low density; dark-coloured latewood is the wood which develops at the end of the growing session and is defined by almost solid thick-walled cells and greater density. An additional feature can be identified, that of an inner dark portion forming around the pith and expanding gradually, called *heartwood*, and a peripheral lighter one, called *sapwood* (Figure 2-12).

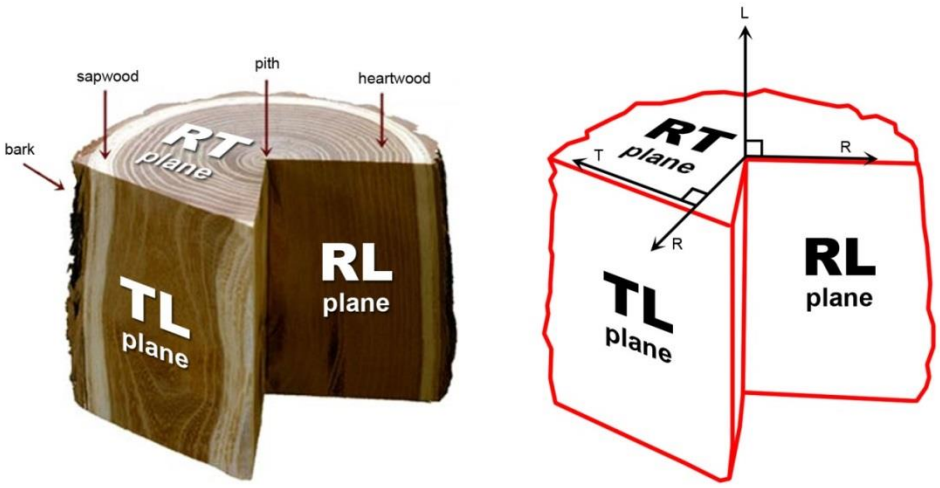

Figure 2-12 A sector of coniferous stem showing planes in wood: RL is parallel to the R and L axes, TL is parallel to the T and L axes and RT is parallel to the R and T axes; also given the pith, heartwood and sapwood, growth rings with light coloured earlywood and dark-coloured latewood; rays are invisible macroscopically in conifers (Adopted from http://www.woodanatomy.ch).

Heartwood is the result of the progressive transformation of sapwood into dead tissue, which is wood that has stopped participating in the translocation and storage of food, and provides only mechanical support, as opposed to the still serving sapwood. The formation of heartwood is a natural aging process and is associated with aspiration of bordered pits and formation of tyloses, which affect heartwood's permeability to fluids; and with deposition of extractives, which protects the wood from decay. More specific, pits are discontinuities in the secondary wall serving as passages between neighbouring cells and have two essential components, the *pit cavity* and the *pit membrane*. Pit aspiration is a phenomenon taking place when the pit membrane moves across the pit cavity from the central position and seals off one of the pit apertures, thus preventing the water flow through that pit (Phillips, 1933). Softwoods are statistically more prone to pit aspiration as bordered pits are typical features of the tracheids, which are the bulk cell type comprising more than 90% of softwoods' volume. Hardwoods bulk cell type is the fibres, which contribute only to a limited extend to fluid movement. Furthermore, tyloses can be described as hairlike ingrowths which can develop in the empty space of adjoining cells and act in a similar way as to pit aspiration (Figure 2-13).

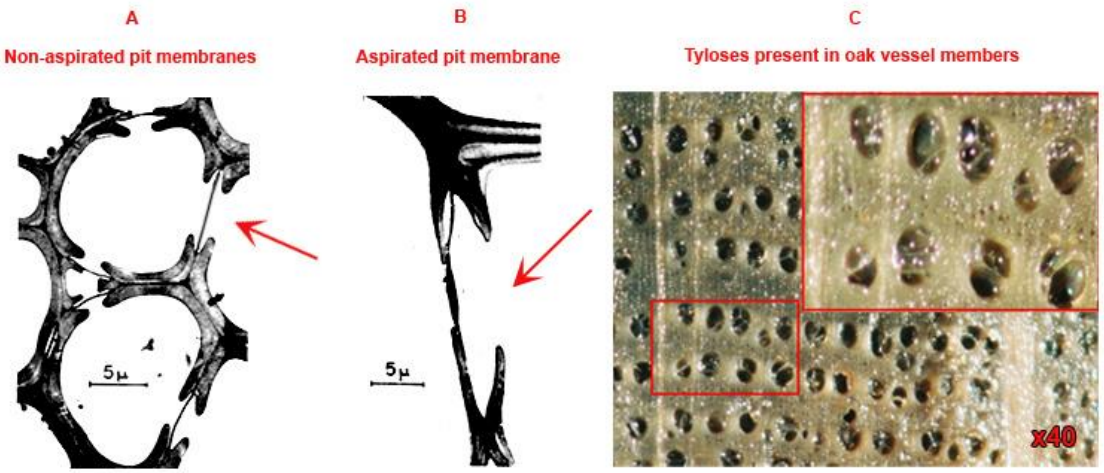

Figure 2-13 Factors influencing liquid transport in wood and so, waterlogging process. A: An aspirated membrane of a bordered pit in softwood (*Sequoia sp.*). B) Bordered pits in a hardwood (*Quercus sp.*) (Extracted and modified from Tsoumis (1968: fig. 5,12), C: tyloses inside oak's vessel elements (pores), seen as a nearly transparent membrane (photo courtesy P.K.Kavvouras).

All woods have *rays* which on a transverse surface appear as lines extending in the general direction from pith to bark. Rays differentiate in width, especially within wood genus. They are more readily visible in broadleaved trees than in conifer trees even with naked eye. So is the presence of *pores* or *vessels*, a hallmark of broadleaved trees; based on their distribution as seen on the transverse surface, two main classifications exist: the *ring-porous*, such as oak, elm and ash, in which the pores of earlywood are noticeably larger and arranged in a ring, and the *diffuse-porous*, such as maple and beech, where the pores are of the same size and uniformly distributed within a growth ring (Tsoumis, 1968).

One of the main elements that distinguish broadleaved from conifer trees is the presence of distinct rays (Forest Products Laboratory, 2010). Especially oak consists of many rays broad and conspicuous, while narrow rays are also present; pine has indistinguishable rays. Ray cells have their longest axis radially oriented which allows faster ultrasonic wave traveling (Sakai et al., 1987; Kabir et al., 1997). Compared to pine, oak has more ray cells per surface area (Barkas, 1941: 545, Table II; Fengel & Wegener, 1989: 12). Figure 2-14 illustrates the microstructural difference between oak and pine as faced by the acoustical wave travelling through; a richer tubular structure in the presence of both narrow and broad oak rays, in the radial insonification direction allows faster travelling times compared to pine. Such an acoustical conducting structure does not exist in the tangential direction; hence travelling times are much slower here for either wood species (Bucur, 1988). The longitudinal orientation of fibers or tracheids is partially disturbed by "horizontal tubes", or medullary

rays, forming highways for sound to travel attributing the longitudinal direction by far the fastest wood direction irrespective of wood species (Bucur, 1995). Note, Figure 2-14 is out of scale for representation purposes, yet individual cell elements depicted are of the order of less than 1 mm in real.

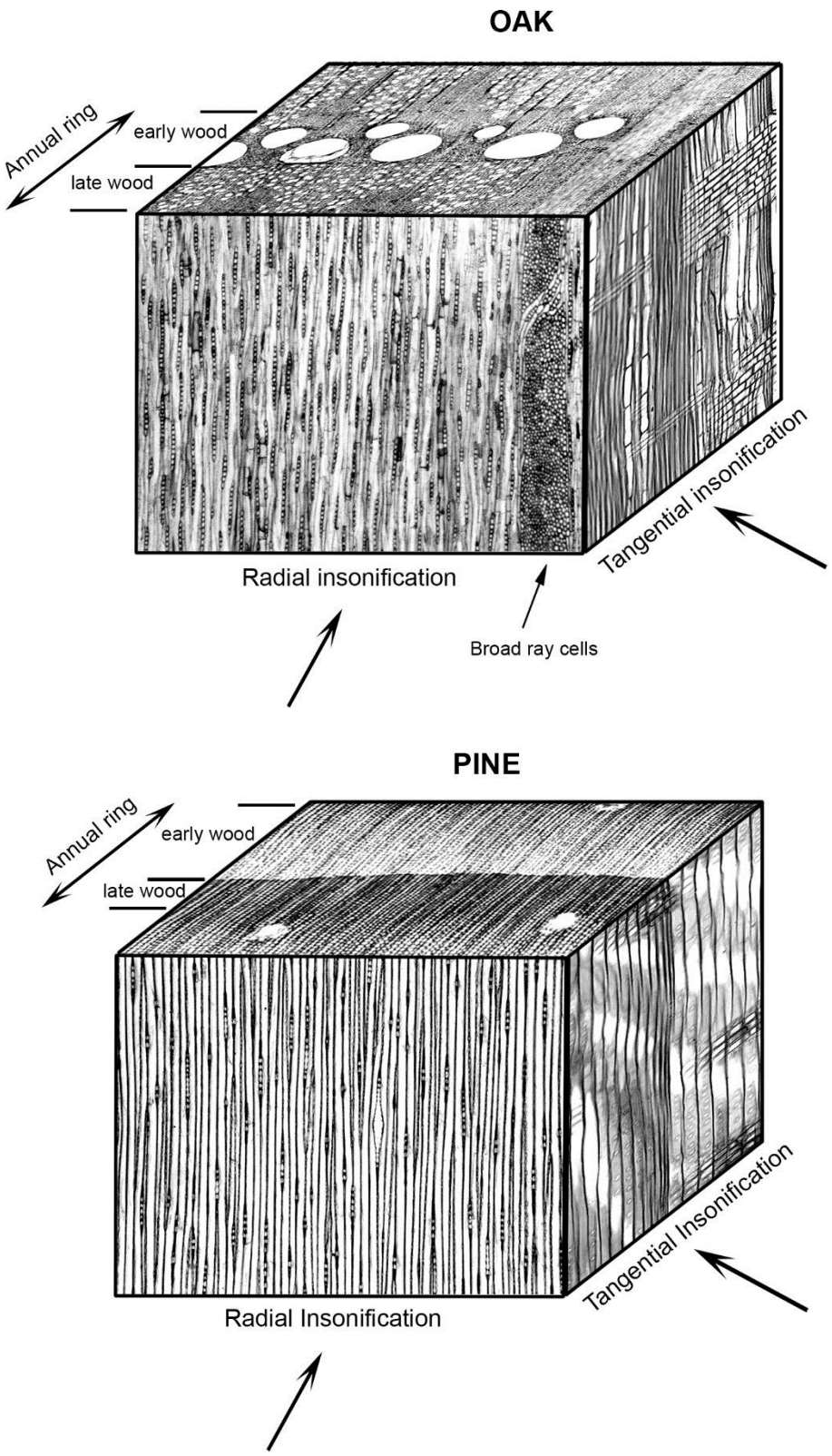

Figure 2-14 Orthrographic representations of ultrasound insonification of ring-porous oak (*Quercus petraea*) and pine (*Pinus Sylvestris*) microstructure per principal wood axis. Not in scale. (Synthesis from photos courtesy of P.K Kavvouras).

The relative proportions of the types of wood cells define its density and strength properties. The range in density of "fresh" timber is from 0.12 g/cm³ to 1,2 g/cm³, when mean density value at 12% moisture content is 0.725 g/cm³ for oak and 0.515 g/cm³ for pine (Dinwoodie, 2000: fig. 3.1). Density is presented as the best prediction of timber strength; the higher the density the higher the stiffness and various strength properties (Dinwoodie, 2000). Density variations observed within annual rings comprised of denser latewood and less dense earlywood are responsible for velocity variation within wood species (Feeney et al., 1998). There is higher lignin in radial than in the tangential walls (Tsoumis, 1968), higher lignin in softwoods than in hardwoods, and more cellulose and hemicellulose mass in hardwoods than in softwoods (Dinwoodie, 2000). Velocities through the principal tree growth axis for "fresh" oak and pine are given in the summary Table 2-2.

2.5.2 Influence of insonification angle in relation to tree growth axes

Given the way a wreck has sat on the seabed and its present position, remote sensing of the wooden timbers must ideally be able to take measurements 'shooting' towards any direction in relation to the three principal wood axes, longitudinal (L), radial (R) and tangential (T), as noted in section 1.5. For this reason, the present study adds off-axis insonifications of wood, in order to investigate ultrasound propagation of timbers in the transverse plane (RT). In a transverse plane, the wave propagation path shifts from a radial towards a tangential direction. This can be pictured in respect of sawn angle as a flat sawn cut (Figure 2-4, B-D).

It has been observed (Forest Products Laboratory, 2010) that in static tests, the modulus of elasticity, and the compression and tension strength of wood perpendicular to grain, shows a kind of threshold at 45° orientation of the growth ring with respect to the direction of stress. If 90° represents a "clear" radial stress and 0° a "clear" tangential stress, then some species show 40% to 60% lower properties at 45° orientation; For those species with lower properties at 45° ring orientation, properties tend to be about equal at 0° and 90° orientations. For species with about equal properties at 0° and 45° orientations, properties tend to be higher at the 90° orientation (Forest Products Laboratory, 2010: 5-31). McDonald (1978) using the through transmission technique, demonstrated that the sound velocities recorded in rotation from a longitudinal to a radial direction and from a longitudinal to a tangential direction, continually decreased. However, the velocities obtained from moving from a radial to a tangential direction on the transverse plane, give a parabolic-type of relationship, showing a trough about halfway through the rotation (Figure 2-15). This acoustical anisotropic performance of wood is related to its anatomical structure with respect to the sound propagation direction.

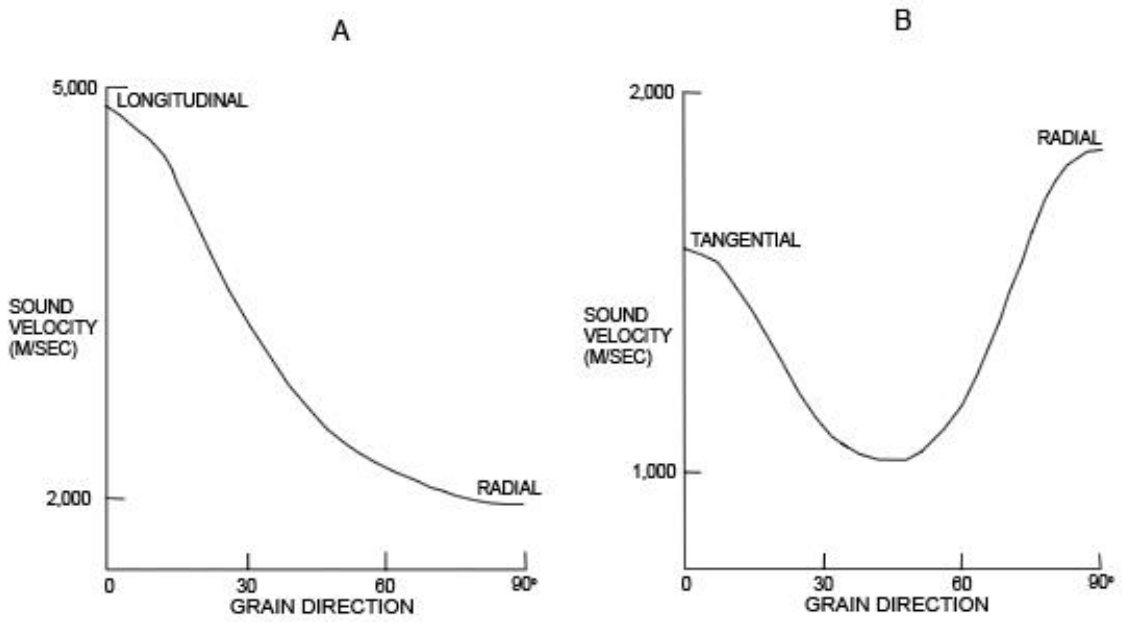

Figure 2-15 A, change in ultrasound propagation velocity from L to R wood axis, B, from T to R wood axis (McDonald, 1978: fig.7 and 8).

Although data for off-axis ultrasound velocities for oak and pine were not found in the literature, the examples given in Table 2-2 for rubber wood (diffuse-porous hardwood) and spruce (softwood), show the V_{RT} behaviour being either the slowest compared to V_R and V_T, or that the velocity drops continuously while moving from radial to tangential insonifications.

It is well established that $V_{RT} < V_T < V_R$ for hardwoods and oak (McDonald, 1978; McIntyre & Woodhouse, 1986; Bucur et al., 2002; Sebastian et al., 2014) with this rating not being necessarily the norm as within the broader families of hardwoods and softwoods, species show individual behaviours when rotating from R to T axis (Ringger et al., 2003; Garab et al., 2010). According to Price (1929), the strains in the RT direction involve distortion of the cross section of the longitudinal cells (fibers in hardwoods and tracheids in softwoods) as opposed to the R direction where the strains are parallel to the long dimension of the longitudinal cells, and as such, the lowest elasticity is obtained for both soft and hardwoods. Respectively, McIntyre & Woodhouse (1986) note large shearing motions between the growth rings during the propagation of mechanical ultrasound waves, which lead to reduced velocities and effective reduced wood elasticity in the RT plane.

Forestry studies interest on wood's elasticity out of the principal axes derives from understanding strength of panel products on transverse loading. They use specimens whose face is cut to give insonification directions with varying growth ring angles. These can be

increment angles, for example of 15°, between 0° and 90° each of which represent either the radial or the tangential axis (Kabir, 2001; Garab et al., 2010). However, purpose of the present work is not to study the angular dependency of ultrasound propagation, but that of density in wood with 'neutral' grain (Figure 2-4, D). Experimentation with 'neutral' grain wood aims to simulate insonification towards the timbers of a ship irrespective of the orientation of their wood structural characteristics in relevance to the insonification axis.

2.5.3 Influence of moisture content

Waterlogged archaeological wood has moisture content well above the Fiber Saturation Point which corresponds to approximately 30% moisture content (section 1.4.2.1). Wood physical and mechanical properties, such as wave speed and attenuation, are strongly related to the amount of water included (Senalik et al., 2014); above the FSP, the physical and mechanical properties of wood do not change as a function of moisture content (Forest Products Laboratory, 2010). In Figure 2-16, moisture content has more significant effect on ultrasonic velocity for pine below the FSP than above it, as does for other wood species (Sakai et al., 1990). However, when free water exists in the cell cavities (MC≥30%), the controlling factor for ultrasonic scattering becomes wood's porosity (Bucur, 2006). Extant literature states that the speed of sound propagating through "fresh" wood decreases with increasing moisture content (Beall, 2002; Oliveira et al., 2005; Calegari et al., 2011; Dundar et al., 2013), while the decrease is proportional to the influence that moisture content has on the modulus of elasticity and wood density (Dinwoodie, 2000; Forest Products Laboratory, 2010).

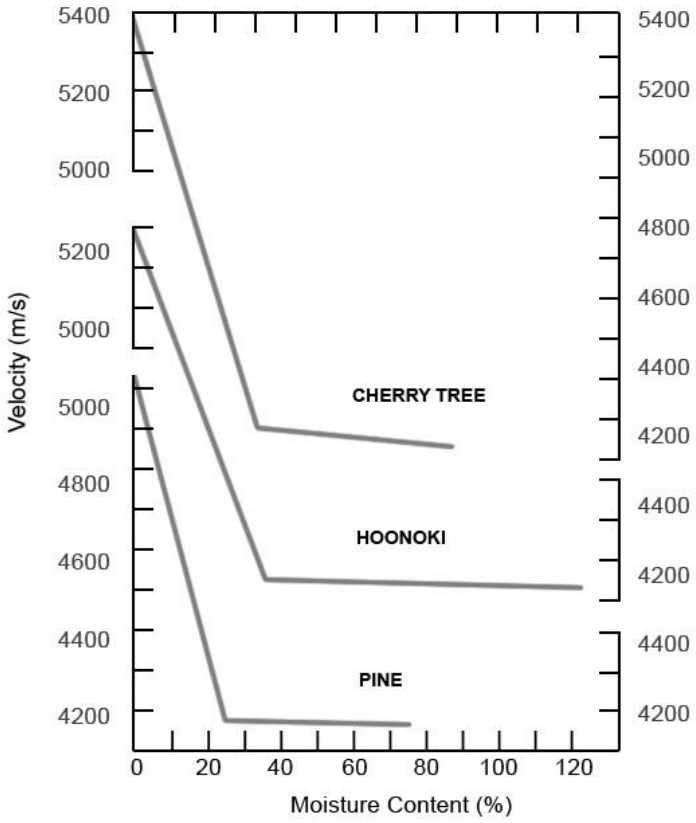

Figure 2-16 Effect of wood's moisture content on ultrasound velocity in relevance to FSP (at 1MHz) (Modified on data by Sakai et al., 1990: fig.3).

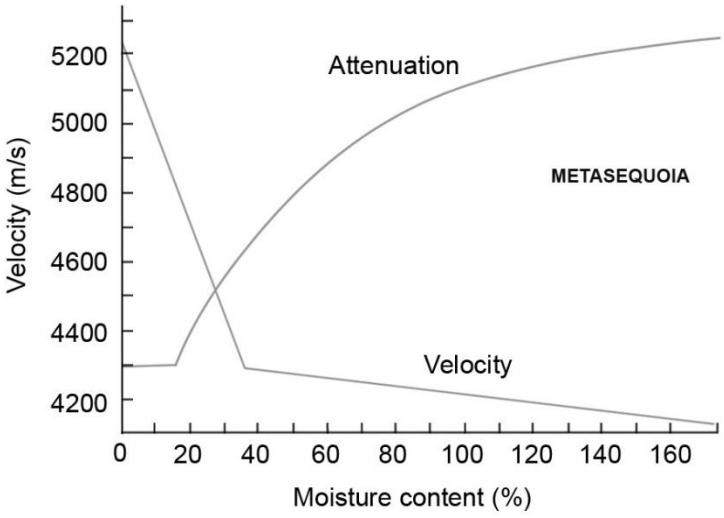

Figure 2-17 Ultrasound velocity and attenuation with increasing moisture content in Metasequoia (at 1 MHz) (Modified on data by Sakai et al., 1990: fig.6).

The moisture changes the ultrasound velocity through two parameters: one is the intrinsic effect on the stiffness constant and the other is the density. The free water is also expected to contribute to the ultrasound velocity through increasing attenuation and corresponding velocity drops (Kabir et al., 1997) (Figure 2-17). More specific, according to Sakai et al. (1990) in "fresh" wood with MC above the FSP, significant acoustic loss takes place due to alternating vibrations between wood cell walls and free water triggered by the ultrasound propagation. Respectively, Wang & Chuang (2000) elaborate on this phenomenon and note that as free water molecules are not strongly attached to the wood cell walls, they do not vibrate simultaneously with the latter, as there can be a mismatch with each of the components (wood and free water) resonant frequency which entails a reduction of the velocity. Moreover, Shukla & Prakash (1990) agree that in saturated media the velocity reduction ties in with increasing porosity. It can be expected that this behaviour of ultrasound propagation velocity will be present when testing waterlogged archaeological wood, which has undergone reduction of its density, or else its porosity has increased, and now holds high levels of free water inside its lumina.

2.6 Chapter conclusions

For achieving the research aims set in section 1.5, the present study consults the literature of maritime archaeology in order to define the material of interest from an archaeological point of view. Based on the literature review, it is decided to experiment with oak and pine wood species. Favourable insonification axes are going to be the Radial and Tangential axes. Wood with 'neutral grain', presenting angles 30-60° between the direction tangent to the annual rings and the insonification direction, is going to be used for investigating ultrasound propagation velocity for off-axis insonifications. Test-piece thickness of 10 cm is found to be a representable average thickness of an ancient hull's main components, namely planks, frames and keel.

Furthermore, ultrasound propagation velocity is expected to be influenced by the structural difference between wood species, here oak and pine, as seen through difference in density, cell composition and arrangement in the tissue. Archaeological waterlogged wood has undergone reduction of its density, loss of its principal organic components, whilst larger amounts of free water are now occupying its cell walls and increased porous system. All the above are expected to influence ultrasound propagation, by reducing its strength and elasticity, and further, the ultrasound velocity, compared to that of "fresh" wood. The

information given in this Chapter about wood structure is going to be readdressed in the following sections, where appropriate.

Chapter 3

Evaluation and Calibration of Experimental Ultrasound Set-up

3.1 Introduction

The primary objective of the present research is to develop a new experimental methodology using ultrasound centred on the special characteristics of the material under investigation both as a wood and as an artefact. The second objective flows from the first and aims to optimising the experimental set-up with the available equipment.

This research considers that the reliability, sensitivity and repeatability of the experimental ultrasound set-up will be seriously affected by:

- **Selection of Wood Sample**
- The quality and initial moisture content of the "fresh" wood sample which will be used for the production of the control test-pieces.
- **Test-piece production**
- The control test-pieces' geometry, considering:
    a. Dimensions (thickness) of wooden ship hull structural components as reflected in the archaeological records,
    b. Anisotropy of wood permeability to liquids,
    c. Sound beam characteristics.
- The control test-pieces' cutting orientation, considering:
    a. Timber conversion techniques based on archaeological evidence.
    b. A test-piece shape that would guarantee both "clear" radial and "clear" tangential insonification paths on the same test-piece with the same anatomical characteristics.
- The transmitter's acoustic frequency for insonification.
- **Waterlogging procedure**

- The waterlogging degree of the control test-pieces.
- **Equipment and Method**
- The rigidity of transducer and test-piece supporting frame.
- The selection of the most suitable material for calibrating the set-up.

In order to evaluate the new system, three test samples with known velocities (standards), brass, Perspex and polyethylene, are used for calibrating the system at first. Next, seven control test-pieces produced from "fresh" oak wood are ultrasonically tested after applying a special waterlogging procedure. All measurements are held within an immersion tank having the transducers deep in tap water facing each other, and the test-piece aligned in between them. The sensitivity of the method is tested by insonifying all three anatomical directions of the wood, longitudinally, along the grain, (V_L), radially, parallel to the rays (V_R) and tangentially, tangent to the growth rings (V_T).

3.2 Wood test-piece preparation

3.2.1 Selection of the appropriate wood sample

A quarter sawn timber measuring approximately 1300 X 100 X 100 mm (Longitudinal x Radial x Tangential) deriving from the heartwood of a mature oak tree recently felled from the New Forest, Hampshire, was acquired from a local sawmill. The wood species is identified as Sessile oak (*Quercus petraea*) (Figure 3-1), on the basis of cross sectional anatomical features, i.e. ring porous, latewood pores arranged in radial flame like bands; rays many, broad and conspicuous; latewood pores numerous, very small and not distinct, using wood identification keys (Kavvouras, 2004). Oak wood is selected following its abundant use throughout the history of shipbuilding covering a wide geographical area of preference by local shipwrights as evidenced by the archaeological records of ancient ships, as presented in section 2.2.1 and Table 2-1. Based on the same evidence, a *Quercus* species is selected. Heartwood was the preferred part of the timber used by boatbuilders over time (section 2.2.2). A quarter sawn cut will allow "clear" radial and tangential ultrasound insonifications (Figure 2-4).

Figure 3-1 Identification of wood sample. Low magnification photograph (X4) from Sessile oak (*Quercus petrae*) cross section.

In order to reduce the inherent variability of wood due to its heterogeneous and anisotropic nature, the selected sample fulfils the requirements of the so-called in wood science *clear* wood, used for determining fundamental mechanical properties. Clear straight-grained wood is wood where the fibers run parallel to the growth axis, and has no knots, shakes, checks, reaction wood, wood-boring insect or wood rotting fungi attacks, spiral grain, false growth rings, growth ring width variation, and pitch pockets (McDonald, 1978; Forest Products Laboratory, 2010). It is well established that these natural growth characteristics and biological attacks affect the mechanical properties of wood (Kretschmann, 2010: 5-26), and as a consequence, the sound propagation due to changes in density and /or elastic properties (McDonald et al., 1969; McDonald, 1978; Berndt et al., 1999; Kawamoto & Williams, 2002; Kabir et al., 2002; Wang et al., 2004; Forest Products Laboratory, 2010; Bucur, 2011).

Moreover, the wood sample is in an unseasoned, *green* state. This permits a faster and more complete waterlogging of the wood test-pieces for three reasons. First, because green wood holds more pathways, known as *pits*, still open for water (sap) diffusion, in contrast to air or kiln dried wood, where these pathways begin to close up due to surface tension forces affecting the *pit membrane* (Tsoumis, 1968). The phenomenon is more apparent in the heartwood (Comstock & Côté, 1968). Second, green wood is free of drying-induced defects which would scatter the signal energy and affect the sound speed (Berndt et al., 1999). Third, green wood is already in possession of high moisture content (≥ 30%), a good starting point for a complete and faster waterlogging of the control test-pieces. In some cases moisture content of "fresh" wood can be higher than 200% (Dinwoodie, 2000, Forest Products Laboratory, 2010).

3.2.2 Production of test-pieces

Consistent with the research's target for control over wood's natural variability, experimental reproducibility, and overall, ability to understand which parameters affect the ultrasound propagation velocity of waterlogged wood, the following approach is taken.

First, in section 2.2.2 it was concluded that 100 mm can be an acceptable average thickness representative of main hull components, based on the respective literature. Moreover, as matters their shape, rectangular and/or square cross-sections are encountered. In accord with these, the wood sample was sawed with a band saw into twenty cubic blocks with nominal dimensions 80 X 80 X 50 mm (R X T X L). This is a considerably larger test-piece compared to the test-pieces used by Arnott (2004), measuring 15 mm per insonification plane. At the same time, a larger test-piece compensates for the error in the measurement which is multiple in a small sized one. In other words, the between replicate measurements variation, because of wood structural variability, tends to decrease as the test-piece size increases, i.e. occurrence of structural defects, growth ring width, latewood proportion and ray width variation (Bucur, 1995). The radial and tangential dimensions are set to 80 mm to eliminate the curvature of the growth rings due to the geometry of the tree stem, and thus provide "clear" radial and tangential orientations. Moreover, taking into account that permeability in wood is directionally dependent, the longitudinal dimension is set shorter than the rest so to enhance the water absorption along the grain. More specific, it is known that permeability in hardwoods is controlled by the vessel elements (Figure 3-1, where pores see vessel elements), the main cell type of hardwoods, aligned parallel to the axial direction, while tangential flow is low and radial rather poor (Dinwoodie, 2000; Forest Product Laboratory, 2010). This will minimise the time of the waterlogging procedure, as long duration can be expected (Smith, 1954). This differentiation of the longitudinal dimension to that of the radial and tangential dimensions is acceptable, as this study's main focus, is these two wood growth axis (section 2.2.2). In consequence of the test-pieces cutting, it is possible to derive all three velocities, along and across the grain, from the same wooden block with the same anatomical characteristics. In contrast, Arnott (2004) in her experiments used different test-pieces to represent each wood axis, thus results can't be absolute comparable. In addition, the variability attributed to the likely inherent difference between test-piece–to–test-piece physical and mechanical characteristics, was as such introduced to the readings. It is well established that wood sample properties vary with sampling position in tree trunk (height, diameter) tree age etc. (Kazemi-Najafi et al., 2009; Pereira et al., 2014). The use of the same test-piece for measuring both radial and tangential

ultrasound propagation velocity seems to serve the aim of between replicate measurements variability reduction.

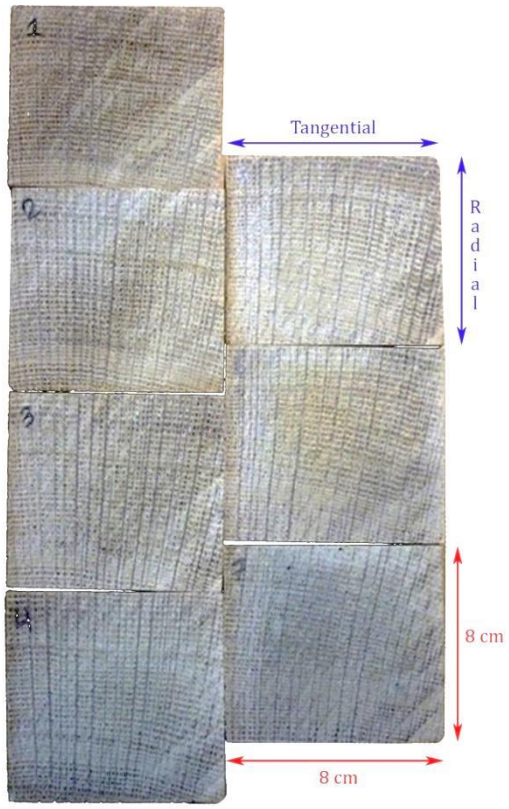

Figure 3-2 The oak wood test-pieces for the ultrasound propagation testing as seen in cross section. Oak's thick rays can be easily distinguished with naked eye.

All wood surfaces were sanded on a disc sander to remove sawing splinters. The green weights of all blocks were taken to the nearest 0.01 g and their dimensions to the nearest 0.01 mm. The average of twelve measuring points per plane (L = height, R = thickness, T = width) was used to calculate the blocks' volume. From those twenty blocks, seven blocks were separated for the ultrasound propagation tests (Figure 3-2). Another five blocks were used for measuring moisture content (MC) and basic density ($\rho_{o.d.}$) as follows:

$$MC = \frac{Ww - Wo.d.}{Wo.d.} \times 100 \qquad (3.1)$$

Where, *MC* is the moisture content of wood (%), *Ww* is the wet weight of wood (here green) and *Wo.d.* is the weight of wood after oven drying at 105°C for 24h[6].

$$\rho_{o.d.} = \frac{Wo.d.}{Vw} \quad (3.2)$$

Where, $\rho_{o.d.}$ is wood's dry density, *Wo.d.* is the weight of wood after oven-drying at 105°C for 24h, and *Vw* is the wet volume of wood (here green). The wood sample had a mean green moisture content of 77 ± 7.7% and a mean basic density of 0.549 ± 0.006 g/cm^3 (Table 3-1).

Table 3-1 Physical properties of the test-pieces used to characterise the wood sample.

Oak Test-piece	Basic Density (g/cm^3)	MC (%)
O1	0.556	76
O2	0.541	79
O3	0.545	77
O4	0.548	88
O5	0.556	67

As seen in Table 3-1, the wood chosen is in a fair moist state. A variation in wood's green moisture content is expected due to inherent variation (Forest Products Laboratory, 2010) and is of minor importance here as the wood will be further subjected to the waterlogging procedure; however, the close to 1% variation in density marks a good set of replicas showing an acceptable structural homogeneity among them.

3.2.3 Geometry of the radiation field – Phenomena affecting wave propagation in wood

Prior to the main ultrasound testing, pilot experimentation with waterlogged "fresh" wood oak proved that the 1 MHz central frequency used by Arnott (2004) for transmitting and receiving the signal, was so high for the present study's thicker wood test-pieces, that it was not possible to receive an interpretable read out of the signal. This can be attributed to the attenuation of the signal's energy during propagation and the frequency (Kearey & Brooks, 1991), as well as the fact that wood structure acts as a filter anyway (Bucur, 1995), all reasons

[6] Constant weight.

contribute to the reduction of the amount of the output pulse energy finally reaching the receiver. This can be further explained if a transmitted sound pulse is seen as a spherical shell with an expanding radius *r,* and its intensity is:

$$I = \frac{E}{4\pi r^2} \tag{3.3}$$

Then along the ray path the pulse's strength will decrease. Added to this is the fact that higher frequency waves attenuate more rapidly than lower frequency waves as a function of time or distance (Buckingham, 2000).

Given this, it was decided to reduce the frequency level. A broadband pulse nominal at 500 kHz eliminated the problem, as a signal through the 80 mm thick oak test-pieces could be now read out clearly. But additional influential phenomena regarding the way sound waves propagate in a material have to be also considered in order to avoid interference leading to erroneous calculation of the ultrasound properties of the material under test. The phenomena are related to sample preparation and acoustic beam characteristics (Bucur, 1995), and count for the appropriateness of the test-piece size and the equipment arrangement, as described below.

3.2.3.1 Wavelengths passing through wood

Wavelength is the distance between two successive peaks of a wave travelling in space and is inversely proportional to the frequency of the wave:

$$\lambda = \frac{V}{f} \tag{3.4}$$

Where, λ is the wavelength of the acoustic beam, V is the velocity of the sound in the transmitting medium and f is the beam's frequency. For pure compressional waves to occur in solids, the minimum dimension in all directions must be greater than a wavelength (Cremer & Heckl, 1973) or differently, >2λ (Bucur, 1995). Based on velocities received during the pilot ultrasound propagation tests using nominal frequency at 500 kHz, a number of more than five wavelengths along the grain and near twenty across the grain were measured. These correspond to long propagation times of the ultrasonic signal in wood and leads to high measurement accuracy (Bucur, 1995). The selected test-piece size in this work advances propagation times received by Arnott (2004), where wavelengths passing through wood were four in the radial and tangential directions and just one in the longitudinal direction, based on her comparable velocities received at 500 kHz.

3.2.3.2 Near / far field

As the acoustic beam travels outwards from the surface of a transducer, it gradually spreads out exhibiting two distinctive zones; first the near-field, adjacent to the transducer's face, followed on by the far-field. According to Huygens's Principal, all points of a wave front may be regarded as new sources of wavelets that expand in every direction. As individual wave patterns interact, the peaks and troughs from adjacent sources interfere resulting to constructive and destructive superposition and consequently, complex pressure amplitude characteristics (Bushberg et al., 2012: 474, 493). The near-field is the region where this interference is pronounced, while the phenomenon surpasses its critical point for destructive interference to occur, in the far-field (Medwin & Clay, 1998: 31) (Figure 3-3). Hence, all acoustic measurements are executed with the test-piece placed in the far-field allowing plane sound waves propagation and good lateral resolution (Kearey & Brooks, 1991).

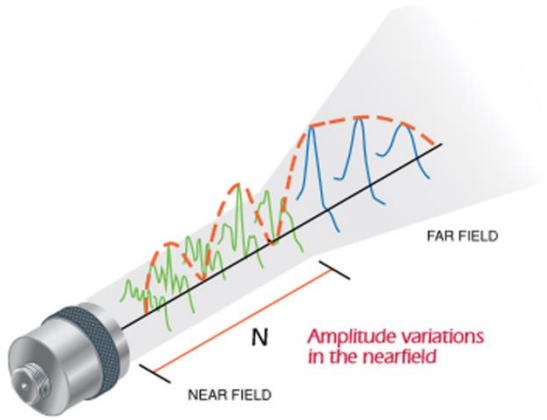

Figure 3-3 Definition of near-field / far field for a single element transducer as are the ones used in the experiments (Extracted from Olympus, 2012).

The distance to the far-field, or else transition distance (in reference to the change from one zone to the other), is determined by the diameter of the transducer and the wavelength of the sound beam according to the relation:

$$D = \frac{\alpha^2}{\lambda} \tag{3.5}$$

Where D is the distance from the transmitter, a is the radius of the transducer and λ is the wavelength of the beam. The greater the sound's source the larger the near-field zone. Modifying Equation 3.5 by substituting the wavelength of the beam by Equation 3.4, then:

$$D = \frac{\alpha^2 f}{V} \tag{3.6}$$

Thus, the length of the near-field is proportional to the frequency of the source. So, the distance to the far-field where the test-piece can securely be placed for ultrasound testing, is calculated using the maximum frequency of the broadband transducers. To define the frequency range a Fast Fourier Transform test was run on the signal produced by the 500 kHz set of transducers while sending a spike to pass through an aluminium standard with the transducers in direct contact with it. The bandwidth had a lower 3db cut-off frequency f_1 = 355 kHz and an upper 3dB cut-off frequency f_2 = 667 kHz measured at the highest peak of the received signal. At -3dB the power of the signal is more than 50% of the maximum hence is more significant to use. Using the average velocity from consecutive measurements taken through the tap water alone in the immersion tank[7], calculated to be 1474 m/s, the distance to the far-field was found to be 73 mm. Thus, throughout the experiments all samples were placed in between the transducers with their front face in a distance of 90 mm from the front face of the transmitter; therefore well into the far-field.

3.2.3.3 Beam divergence – Edge effects

It is important that the test-pieces' insonification surfaces are large enough to not allow the beam's diameter extent of spread to coincide with their edges, as that would result to the beam getting reflected and refracted (Figure 3-4). The maximum dimension of the test-piece that edge effects can affect the ultrasound measurements is calculated by measuring first the angle of the beam leaving the transmitter θ_T:

$$\theta_T = \sin^{-1}\left(0.48\frac{\lambda}{a}\right) \tag{3.7}$$

Where, λ is the wavelength in the tap water inside the immersion tank used for the ultrasound experiment for which a velocity of 1474 m/s was measured at 500 kHz, and α is the transmitter radius (0.0127 m) (Best, 1992). This angle was found to be 6.4°. The maximum test-piece dimensions where beam edge effects can affect the measurements are then calculated using:

[7] Tap water temperature in the immersion tank was kept at 18°C ±2°C using an aquarium heater.

$$d = r \tan \theta_T + \alpha \tag{3.8}$$

Where, d is the beam's diameter touching the test-piece surface, α is the transmitter's radius and r is the distance from the transmitter face to the rear face of the test-piece (Arnott, 2004). As R = T = 80 mm, and including a distance of 90 mm, d is calculated to be 32.6 mm. Any dimension above this will prevent from the phenomenon occurrence and as such supports the choice of the test-pieces' size.

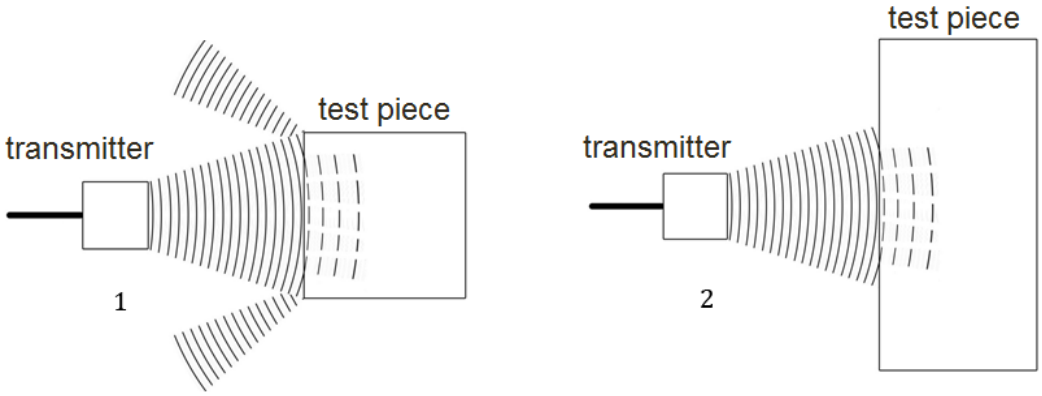

Figure 3-4 Reflection and refraction of sound beam due to side wall effects, 1. To avoid energy loss the test-piece had a dimension larger that the beam's diameter touching its surface, 2.

3.2.4 Test-piece waterlogging procedure

Arnott (2004) notes that another reason which led to the high data variability could be an incomplete waterlogging of the wood test-pieces used as controls for the experiments, as trapped air bubbles could have scattered both the incident and transmitted energy. It is important to secure a successful waterlogging of the wood otherwise the definition of the relationship between wood's density and sound speed will be uncertain. In addition, the air-free condition of waterlogged wood has a better impedance match of wood cell wall and water and should scatter less than a three-phase system (wood-water-air) because of the stronger scattering of the signal in wood and air (Berndt et al., 1999).

For the present study, a special impregnation chamber was built for the needs of the waterlogging procedure, also sufficiently large to hold a big number of wood test-pieces at one time. The procedure is adapted from Choong & Tesoro (1989). More specific, the "fresh" wood test-pieces are placed inside the impregnation chamber with their cross section facing the lid of the chamber, and separated with small footings. This configuration assists the expulsion of air bubbles from the wood's structure while a vacuum is applied from the top

of the chamber later on. The chamber with the test-pieces is evacuated of air for 60 minutes, followed by an introduction of carbon dioxide. The gas runs constantly under a slight pressure into the chamber for one hour, in order to replace the air in the wood. At 20°C air is less soluble in water (0.1511 x 10^4 mole fraction) compared to carbon dioxide (7.023 x 10^4 mole fraction) (Wilhelm et al., 1977: 226, 230). A subsequent vacuum is then applied on the test-pieces for another 60 minutes and de-aerated tap water is slowly introduced (Figure 3-5). Thereafter, a vacuum is applied periodically for 48h following a cycle of 15 minutes on - 15 minutes off with the use of a time switch, until no air bubbles can be seen. Special care is given during vacuum applications due to the possibility of rupturing the pit membranes (Usta, 2005), thus cutting off the flow pathways to water. A vacuum pressure of 20 kPa is used initially (Matsumura et al., 1999; Zimmermann et al., 2006), which gradually increases (up to 70kPa), determined by the presence or not of bubble exhalation.

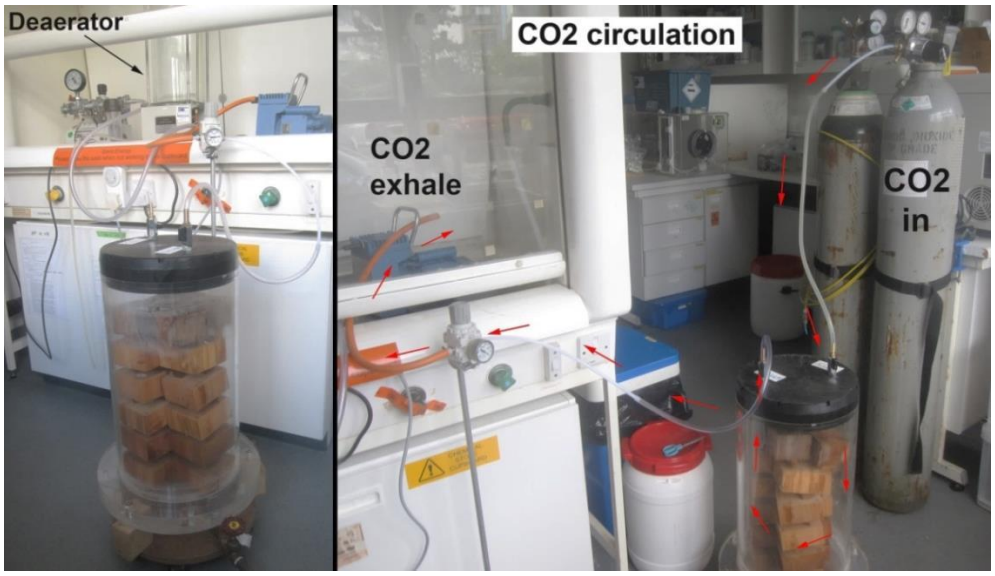

Figure 3-5 Right-hand side: Feeling the under vacuum impregnation chamber containing the wood test-pieces, with gas CO_2. The gas was continuously fed into the chamber under a slight pressure. Left-hand side: Preparing de-aerated tap water to introduce into the impregnation chamber.

After this procedure the test-pieces remain immersed in the impregnation chamber. The waterlogging is considered as complete when the weights of the test-pieces reach a constant after repetitive weighs. To verify the waterlogging efficiency, a basic laboratory technique is used comprising a 0.6lt pressure vessel coupled to a Virax 50 bar hydraulic pump (Figure 3-6) (Sothcott, 2013, pers. comm., 8 February). The test-piece is sealed inside the vessel filled with water and a pressure of 5 bar is applied; a non-drop in pressure level inside the vessel after 5 min is indicative of the waterlogging success.

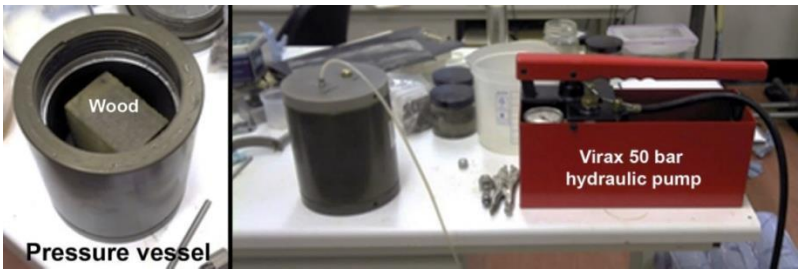

Figure 3-6 Testing waterlogging efficiency using a pressure chamber and a hydraulic pump.

The test-pieces were used for the ultrasonic testing after a total of 149 days of immersion in tap water. By then they had gained 23% of their original weight in water. The maximum moisture content (MC_{max}) at that stage is calculated using (3.1), but this requires oven-drying the test-pieces to retrieve the $W_{o.d.}$, effectively destroying them. Instead, the oven-dry density measured from the five wooden blocks destroyed to derive the physical properties of the wood sample, is used, together with the V_w for each of the seven test-pieces (3.2). It is well known that the volume of wood remains unchanged above FSP (Forest Products Laboratory, 2010). The maximum moisture content of the seven test-pieces after the completion of the waterlogging procedure is found to be approximately 120% (±3%) on average.

3.3 Equipment

All ultrasonic tests are performed within a reinforced polyethylene tank specifically built and used by Arnott (2004). Two horizontal aluminium rods are now added for securing the stability of the frame structure, aiming for a higher precision to the measurements (Figure 3-7). A special clamp was also designed and built to hold the wooden test-pieces during the insonification. The support system is capable of being tilted and rotated to allow good alignment of the test-pieces' surfaces to the transducers' axis.

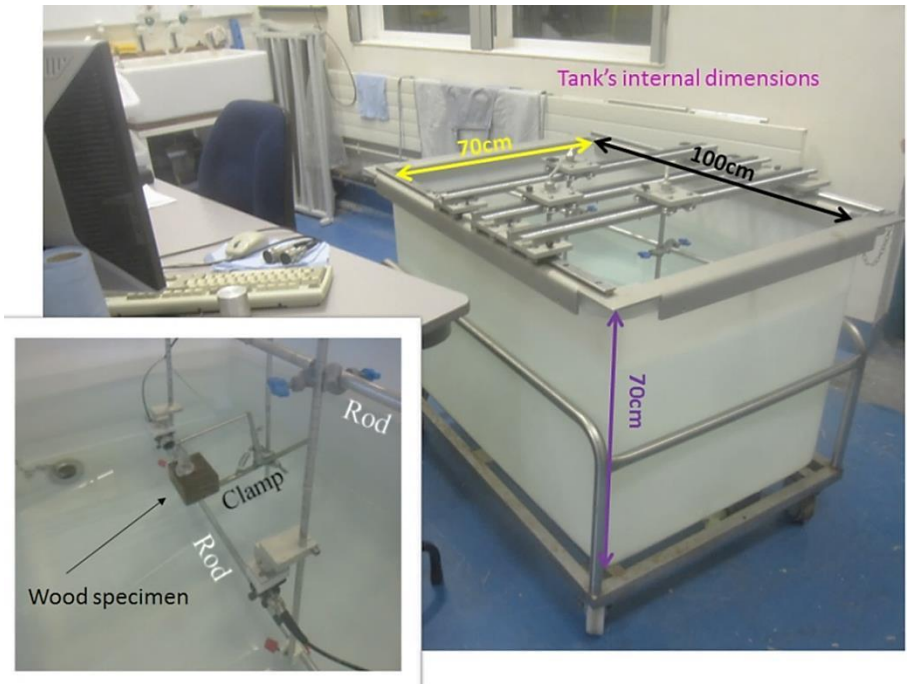

Figure 3-7 The immersion tank and the insonification set-up underwater.

The water between the transducers acts as a very good couplant needed to propagate the sound energy through the wood, as the similarity of the acoustic impendences of water and wood result in a small reflection of sound at the wood/water boundaries (McDonald, 1978). Aluminium rods of various lengths (from 330 to 30 mm), measured to the nearest 0.001 mm, were built and are used for keeping the right distances between the transducers or for placing the test-pieces to the far-field, during the experiments. To set the distance between the transducers a number of velocity trial measurements through water only were conducted, each time resetting the travelling path. Accounting for the size of the test-pieces, the distance to the far-field, the usable tank's space, and the consistency in water velocity measurements, the distance between the transducers is set to 330 mm. This distance is checked / reset each time a test series is to be made using the respective aluminium rod. It is noted that for maintenance reasons, the transducers are removed from the water at the end of a day's tank measurements and are let to dry off till the following.

A pair of heavily damped, longitudinal wave transducers (Panametrics Model V301) with a dominant frequency of 500 kHz and an active element with a radius of 0.0127mm, coupled with a pulse generator (Panametrics Model 500PR) for creating and transmitting the sound, are used. Longitudinal or compressional waves or Primary *P*-waves (particle trajectory in the direction of the wave travel) are chosen in agreement with Arnott (2004) and since such waves are more adaptable in the underwater environment (Kearey & Brooks, 1991). The transducers are driven to produce broadband signal containing a range of frequencies. The

high-pass filter on the pulse generator is set to 'out' otherwise this would cut-out the useful lower frequencies used for the ultrasound tests. The higher frequencies are also naturally cut out by the large thickness of the test-pieces, allowing dominant frequencies in the level of about 100 – 200 kHz to be tracked, agreeing with Beall (2002). For displaying the received signal a LeCroy 9314CL Digital Storage Oscilloscope (DSO) is used. The equipment associated with the experiment is given in Figure 3-8.

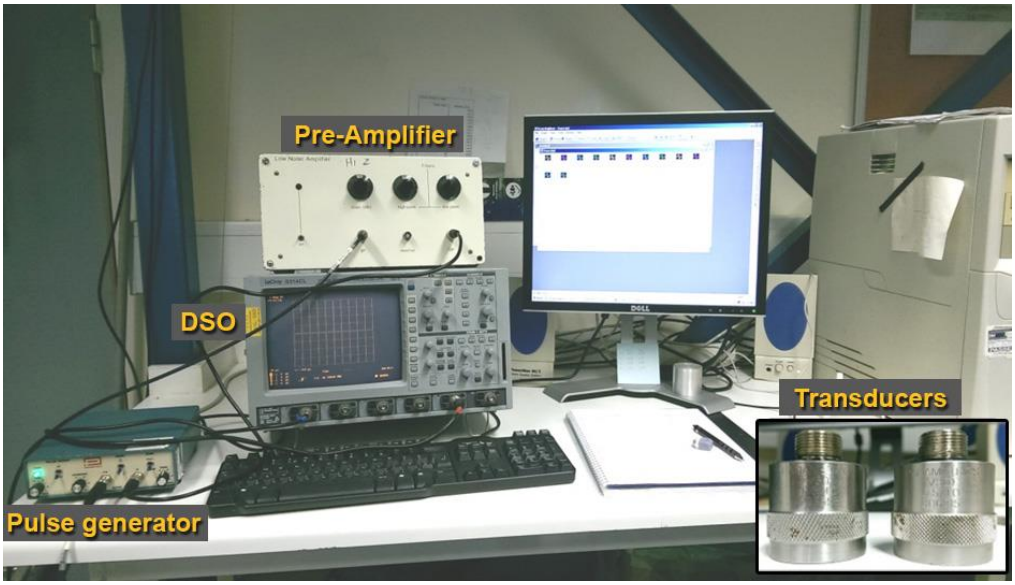

Figure 3-8 Electrical hardware used for the ultrasound experiments.

Before each measurement the system is calibrated using three standard reference materials. The materials chosen for calibrating are brass, Perspex and polyethylene with respect to reference wood velocities (Kollmann, 1968; McDonald, 1978; Bucur, 1995; Arnott, 2004) and standards available. Results together with that for tap water are given in Table 3-2. Any difference in the velocities for the three standards compared to the literature should be assigned to the possible difference in density of the standards used, as higher densities give higher velocities (Kaye & Laby, 1986).

Table 3-2 Ultrasound velocities through tap water alone in the immersion tank and through the standard reference materials used for testing and calibrating the experimental ultrasound set-up.

Calibration materials							
	Present study					Reference	
	Velocity (m/s)	STD	CoV (%)	Repetitions	Density calculated (g/cm^3)	Velocity (m/s)	Density (g/cm^3)
Tap Water	1474	2	0.14	6			
Brass	4363	64	1.47	6	8.475	4373[a]	8.520
Perspex	2776	5	0.18	6	1.188	2700[b]	1.180
Polyethylene	2240	4	0.18	6	0.938	2080-2460[b]	0.930 – 0.970 0.910 – 0.940

[a] Kaye & Laby, 1986; [b] Olympus, 2013

3.4 Method

A 110 V pulse of approximately 0.5 μs duration produced by the pulse generator is used to excite the transmitting transducer creating a longitudinal wave travelling through the water and wood, and then captured by the receiving transducer held in line with the transmitter. At the same time another pulse (AC 500mV 1MΩ), is sent by the generator to the DSO, in order to trigger the recording of the signal by synchronising the two pieces of equipment. After propagating through water and wood, the received signal is sent first to a pre-amplifier (custom built), before being amplified for a second time by the pulse generator (Figure 3-9). The total voltage gain is between 39.1dB and 41.6dB for the water and standards, and 59.2dB for the wood. Through the pulse generator the reinforced signal is passed through to the DSO and is finally displayed on the oscilloscope's screen (Figure 3-10). The sampling rate is to 100 MS/s (or 1,000,000,000 Hz) securing no loss of information during the conversion of the analogue signal to digital[8]. By use of the delayed sweep feature the signal is sum-averaged by 512 times, giving a high signal-to-noise ratio.

The time-of-flight (TOF) (Senalik et al., 2015: 23), is the time it takes a sound wave to travel through a medium, is extracted from the received signal by manually picking the first-break of the transmitted signal on the oscilloscope. Sommerfeld (in Brillouin, 1960) defines the first-break or else, onset time, as the time at which the energy of the signal is first seen to arrive, expressed as an obvious change in its behaviour. Trials were also made by picking

[8] Perfect reconstruction of a signal is possible when the sampling frequency is greater than twice the maximum frequency of the signal being sampled. Here the f_{max} = 667 kHz, thus any sampling rate above 1,334,000 Hz would fulfil the requirement (Kearey & Brooks, 1991).

the first-peak of the signal as a more readily identifiable characteristic. Yet, one advantage of using the onset time is that it is less influenced by the dispersion-dependent waveform modification, like a peak is. Onset travel times may then be more consistent than those that rely in the picking of some later waveform feature likely to be influenced by dispersion (Molyneux & Schmitt, 1999). Where dispersion, are waves of different wavelengths of a pulse traveling at different phase speeds because of the elastic moduli and density of the material (Kearey & Brooks, 1991); and because of the absorption of the wave energy by the material during propagation, the scattering due to inhomogeneities in the structure, and the geometry of the sample under test (Bucur, 1995). Phase speed refers to the speed of the *phase velocity*, one of many a *group velocity* like the one deriving from a broadband signal consists of, due to the presence of a range of frequencies in the signal. Including the high signal-to-noise ratio before the first arrival (Figure 3-10) it is also easy to determine the first-break throughout the measurements (Coppens & Mari, 1995). Results on ultrasound measuring of the standard reference materials and their small variation (Table 3-2), give strength to the decision of using the first-break to determine velocity through the wood.

The TOF of the signal through the water and the wood is marked down to the nearest 0.001 μs. The ultrasound velocity of the test-pieces is subsequently calculated applying:

$$V = \frac{h}{\left(\delta t + \frac{h}{V_W}\right)} \tag{3.9}$$

Where, V is the longitudinal wave velocity through the test-piece (m/s), h is the test-pieces's thickness (m), δt is the time through the water and test-piece minus the time through the water only (s) and Vw is the velocity through the water only (m/s) (Blitz & Simpson, 1996: 95). For all TOF, the delay in transit time between the transmitter and the receiver when in direct contact, due to construction parameters (found to be 1.645μs after repetitive measurements), is subtracted from the received time. The waveform of each recorded signal together with its respective data, are consequently saved in a computer using ScopeExplorer software (Teledyne LeCroy©).

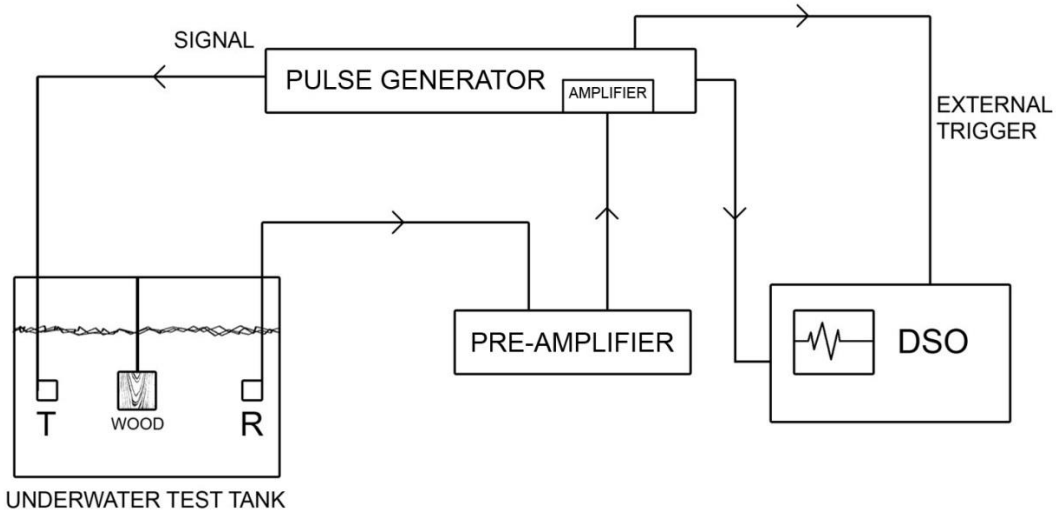

Figure 3-9 Schematic presentation of the experiment's equipment arrangement for use with the immersed ultrasound through transmission technique.

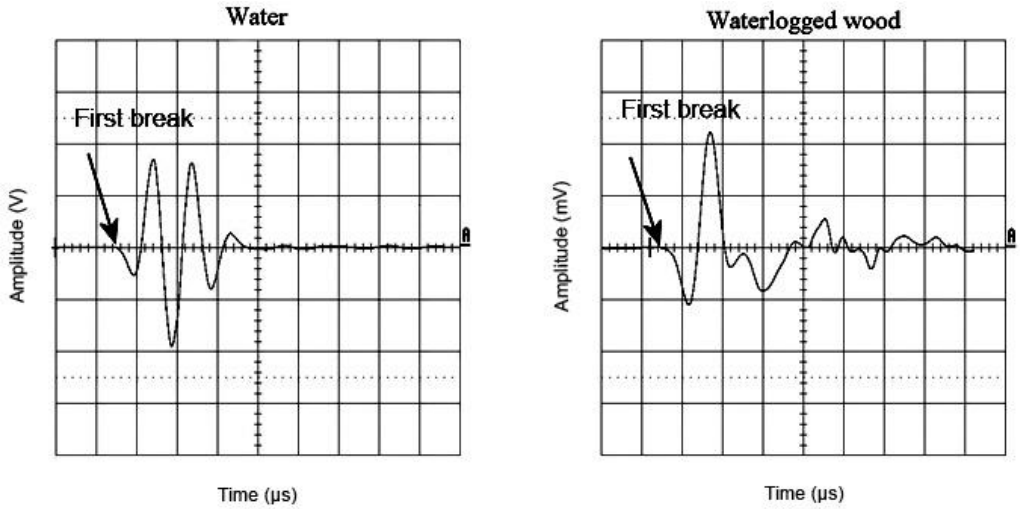

Figure 3-10 Two characteristic signals one through water (left) and one through the longitudinal plane of a waterlogged oak wood test-piece (right).

Three insonification regions of interest (ROI)[9] per wood plane are defined on a test-piece: one targeting the centre of each plane, and then one to the left and one to the right of the centre (Figure 3-11). Six repetitive sets of ultrasound propagation velocity measurements were executed insonifying the centre of each principal axis (L, R and T) of the seven waterlogged wood test-pieces. To increase the spatial sampling as proposed by Berndt et al.

[9] (ROI, Laugier, 2004).

(1999) the sixth set included the insonification of the regions left and right of the centre. The aim is to test whether the selection of the wood sample and the procedure chosen to prepare the test-pieces, were capable to exclude from the readings any effects of wood spatial inhomogeneity induced by its anatomical structure. Some overlapping between the three insonification regions is expected given the beam's diameter (33 mm) and the plane's thickness (80 mm), however, the beam's nature is to emphasize the central properties of the area it is insonifying (Berndt et al., 1999).

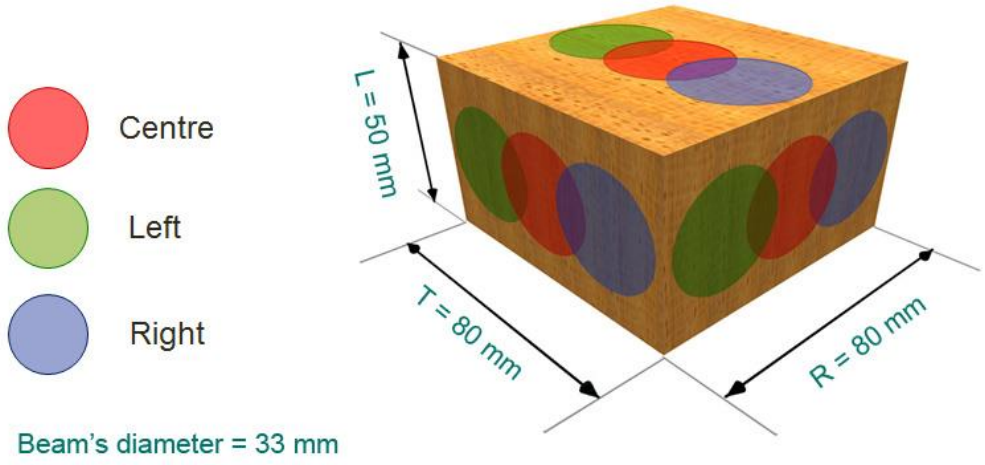

Figure 3-11 Definition of insonification regions of interest (ROI) on a wood test-piece.

3.4.1 Propagation of uncertainty

A number of arithmetic operations were performed in order to calculate the uncertainty in the velocity calculation, or else its *experimental error*. It is accepted that no *systematic error*, caused by possible flaws in the equipment or the design of the experiment was present, as that would have reflected in the measurements during the continuous calibration procedures. Hence focus was on the estimation of the *random error* associated with the uncontrolled variables in the velocity calculations (Harris, 2003). Error propagation was performed on Equation 3-10 for all velocity measurements (calibration material, water, and wood all directions) using 1% as time measurement 'accuracy' (Bucur, 1995), and $\pm 254 \cdot 10^{-4}$ mm (Mitutoyo digital calliper) as distance precision for keeping the distance between transducers and for measuring the thickness of test-pieces, measurements. Uncertainties were added in quadrature based on Harris (2003) formulas, after simplifying the equation so that the variable *h* appeared only once:

$$e\%V = \frac{1}{\left(\frac{\delta t}{h} + \frac{1}{V_W}\right)} \quad (3.10)$$

In this study the experimental error associated with the velocity was calculated to be 0.34% for the brass standard, 0.36% for the V_L, 0.71% for the V_R, 0.77% for the V_T at 67% confidence intervals. Arnott (2004) calculated 1.5% experimental error, but because this was significantly smaller compared to the high data variability, she used 95% confidence interval for her measurements.

In the current study velocity values are presented together with their coefficient of variation, the dimensionless measurement of the variability relative to the mean, and expressed as a percentage (CoV%); this being the most common approach among wood science community making possible comparisons across different wood properties and studies (Bucur, 2006).

Moreover, where given, the strength of a relationship between two variables is measured by the coefficient of determination, symbolised by r^2 if the regression involves only one independent variable, and by R^2 if it involves more than one (Freese, 1964). The coefficient of determination represents the percentage of the data that is the closest to the line of best fit. Basically, it is the square of the correlation coefficient or *Pearson correlation*, *r*, as well used in literature, e.g. if $r = 0.94$, then $r^2 = 0.88$.

The coefficient can vary from 0 to -1 and from 0 to +1, where -1 represents a perfect positive relationship, 0 a no relationship, and +1 a perfect positive relationship. For defining the in between magnitudes of a relationship, the classification by Dancey & Reidy (2004) is used: strong (±0.9 to ±0.7), moderate (±0.6 to ±0.4), and weak (±0.3 to ±0.1).

3.5 Results

3.5.1 Reliability of the measuring system

The ultrasound velocities measured along the three principal axes of the waterlogged oak wood test-pieces are presented in Table 3-3. An Independent-Samples T-test using SPSS statistical programme was run to compare the velocity means received from all three regions of interest. There was no statistically significant difference between the means, which supports our considerations of the material selection and test-piece preparation as

set in section 3.1. It also proves that the ultrasound beam was not subjected to edge effects. The averaged velocities from all ROI were calculated to be 4103 m/s (± 143 m/s) for the longitudinal direction, 2061 m/s (± 40 m/s) for the radial, followed by the tangential, 1922 m/s (± 21 m/s). The results confirmed the anisotropic behaviour of wood presenting the characteristic pattern $V_L >> V_R > V_T$. The dispersion of measurements, expressed by the coefficient of variation for all three wood axes V_L=3.48%, V_R=1.96% and V_T=1.07%, is close, or even lower than the range given by Bucur (1995) for relative velocity measurements in air-dried beech, Douglas fir and spruce, 3.7% - 7% for V_L, 5.39% - 7% for V_T, 8% for V_R, and for saturated spruce, 6% V_L and V_T, and 10% V_R. Oliveira & Sales (2006) notes coefficients of variation between 4.0% and 8.6% for the longitudinal velocities of tropical woods at 12% MC. However, especially for the radial and tangential velocities of our immediate interest, the coefficient of variation in the present study is the lowest noted. Actually, velocity variability in the tangential direction is nearly equal to that of the calculated experimental error (less than 1%). Although it is nearly double in the radial direction, it can be suggested that the methodology is capable to distinguish changes in "fresh" wood, as those induced by degradation, which are not strictly influenced by its biological nature as a highly variable material. The higher radial variability compared to the tangential one, can be attributed to the coexistence of broad and narrow xylem rays in some hardwoods as is oak here, the broader rays being faster sound conductors than the narrower ones (Spycher et al., 2008). All the above are in favour of the establishment of a reliable and accurate performance of the system built and the measurement technique. Based on our choices it was possible to control wood's natural variability and acquire consistent velocity measurements.

Velocity values agree with those of McDonald (1978) for green Red Oak (Table 2-3) for all wood axes but V_T which is faster here. Compared to Dix et al. (2001) saturated oak, velocities are higher in all insonification directions. Compared to velocities by Bucur (1995) for oak at 12% MC, there is a drop in velocity of the waterlogged oak test-pieces for both V_L and V_R, but not for V_T. The velocity under dry conditions is expected to be higher than in humid conditions (Bucur, 1995; Oliveira et al., 2005). Moreover, as noted in section 2.5.3, velocity variation between studies can be influenced by the importance given to controlling wood's natural variability when preparing test-samples, wood's density, proportions of earlywood and latewood, annual ring curvature, coupling of the transducer to the sample, and frequency (Bucur, 2006).

Table 3-3 Ultrasound propagation velocities at 500 kHz nominal frequency, per wood axis of the waterlogged oak test-pieces, MC_{max}≈120% and basic density 0.549g/cm³. Arnott's oak at 500 kHz, MC_{max}= 114% and basic density 0.547g/cm³.

	Ultrasound propagation velocity (m/s) Oak		
	Longitudinal	Radial	Tangential
All ROI			
Mean	4103	2061	1922
STD	143	40	21
Replicas	7	7	7
Number of measurements	56	56	56
CoV (%)	3.48	1.96	1.07
Centre			
Mean	4094	2056	1921
STD	144	37	22
Replicas	7	7	7
Number of measurements	42	42	42
CoV (%)	3.52	1.80	1.14
Arnott (2004)			
Mean	6327	1841	1598
STD	2718	54	172
Replicas	10	10	10
Number of measurements	10	10	10
CoV (%)	42.96	2.93	10.76

In addition, a re-analysis was performed on Arnott's (2004) data using the respective ultrasound velocities from waterlogged "fresh" oak received at 500 kHz together with its physical properties. Despite the agreement on the physical properties of the waterlogged wood used in the present study and by Arnott (MC_{max} was 114%, ± 8; $\rho_{o.d.}$ was 0.547 g/cm³, ± 0.029, n=30), there are noteworthy differences in the velocities received and their variability. By far the most outstanding difference is that of the very high longitudinal velocity, measured to be 6327 ± 2718 m/s, ranging from 3609 m/s up to 9045 m/s. By contrast, radial and tangential velocities are lower than those calculated during current experiments, values being 1841 ± 54 m/s and 1598 ± 172 m/s respectively. The variability in these velocities is more reasonable compared to the longitudinal, possibly due to a larger number of wavelengths which seem to have passed through the radial and tangential test-pieces (section 3.2.3.1). Further, Arnott's coefficients of variance were 42.96% for the

longitudinal velocity, 2.93% for the radial and 10.76% for the tangential velocities. Except from that of the radial velocity, coefficient of variance is much higher than in the present study and the literature, with that of the longitudinal being extreme. It could be derived that since the oak wood material used in the two separate studies shows to have the same density and moisture content, the hypothesis that the waterlogging of the past test-pieces was insufficient, and hence that being the reason of high data variability, is probably unlikely. It is rather factors related to test-piece preparation, as those of initial moisture content, early- and latewood proportions, annual ring curvature, as explained in the introduction of this Chapter. Additionally, a reason introducing errors to velocity measurements can derive from misalignment of the transducers and the test-piece, especially for relative high frequencies (Bucur, 1995). The present study has enhanced the stability of the transducers and test-piece supporting frame on the initial holding system by Arnott (2004).

3.6 Chapter conclusions

This initial experimental phase achieved to improve the work done by Arnott (2004), by establishing a new ultrasound measuring system for waterlogged wood using the immersion, through transmission technique. The novelty derives from giving the emphasis to wood both as a material and as an artefact. Dimensions and cutting orientations of a hull's wooden components as seen in the archaeological records have been taken into account. It was possible to confirm key wood structural controls on velocity measurements, and it was possible to lower the coefficient of variance and derive absolute, consistent and repeatable results with good accuracy. The following conclusions can be highlighted:

1. The characteristic anisotropic behaviour of wood $V_L >> V_R > V_T$, is here verified. Velocities through waterlogged oak with $MC_{max} \approx 120\%$ and basic density 0.549 g/cm^3, are: V_L = 4103 m/s (±143 m/s), V_R = 2061 m/s (±40 m/s), and V_T = 1922 m/s (±21 m/s).
2. Coefficient of variation in ultrasound principal axial velocities as seen in the literature, and more specific for wood above the FSP, has been narrowed with the new methodological approach presented here. The following factors have been found to control this:

i. Wood's quality and initial moisture content
ii. An enhanced waterlogging procedure
iii. A relative large test-piece size (80 X 80 X 50 mm, R x T x L)
iv. Elimination of annual ring curvature
v. Even spaced earlywood and latewood layers
vi. Deriving all three principal velocities through the same test-piece
vii. Frequency (nominal 500 kHz) and sound beam characteristics
viii. Rigidity of the supporting frame holding transducers and test-piece in good alignment
ix. A suitable calibration material.

3. Consistent velocity measurements have been received both within a test-piece (insonification through three different regions per axis) and between test-pieces, using seven replicates and multiple repetitions of each measurement.

4. Radial and Tangential velocity variability is respectively, nearly double and nearly equal to that of the experimental error (<1%).

It is suggested that the new experimental methodology is sensitive for use on wood in order to distinguish and measure different levels of wood degradation as encountered in the marine archaeological environment. The next experimental phase of the study is to use the new ultrasonic set-up to establish the empirical relationship between wood's density and ultrasound propagation velocity, progressing wood deterioration.

Chapter 4

Establishment of Wood Density – Ultrasound Propagation Velocity Relationship

4.1 Introduction

Having established a reliable ultrasonic set-up for testing waterlogged wood in the laboratory, the next research aim is to design a new artificial wood degradation procedure. The procedure has to closely simulate the degradation of archaeological wood using means which are both controllable and reproducible so to overcome past issues highlighted by Arnott's work (section 1.5).

The drawbacks of using biological means for degrading "fresh" wood in the work by Arnott, was a loss over the number of degradation steps produced at the end, while aiming for a specific density range could not be pre-set. The density change advancing the time the wood test-pieces were subjected to biological degradation, showed various trends. A general trend for wood degraded by shipworms was either minor density drop-offs of 1% to 6% or rises of 1% to 12%, followed by rapid drop-offs of 23% to 50%. For wood degraded by fungi, density showed in most cases rapid drop-offs from 0% straight to 18% or 32% and in a few drop-offs from 0% straight to 13%, followed by further drop-offs of 19% to 38%, as compared to the undegraded wood density. The reason for observing densities rises when the opposite would be expected is explained by the fact that, the set of test-pieces used for measuring ultrasound properties at each degradation phase, from zero degradation up to the last set of degraded test-pieces, was a new set at each time. The set possessed different initial densities. Thus, starting points were constantly different leading to the observed density fluctuations. At the end, a number of three or four wood macro-degradation / density levels (depending on wood species used) and two for the wood micro-degradation / density levels (for both wood species) were obtained.

In light of this, for the establishment of a reliable empirical relationship between waterlogged wood density and ultrasound propagation velocity, the present study decided to perform ultrasonic measurements on waterlogged freshly cut wood test-pieces artificially degraded. A new wood degradation methodology is developed to simulate the gradual loss of wood mass and hence porosity increase and density decrease, resulting from the activity of wood decay organisms (section 2.4.1). The objective is to produce a sufficient number of wood deterioration levels, pairing mechanical and chemical means of controlled and reproducible deterioration in the laboratory. This study creates a set of increasing degradation levels by gradually removing wood mass from the test-pieces by drilling holes along the grain (longitudinal axis). The total number of degradation levels which can be achieved, are prefixed, as the initial density (zero degradation) is known, together with the volume of each test-piece and the diameter of the drill-bit used to remove wood mass; thus the remaining density after each degradation step can be derived beforehand. It is emphasized that the same test-pieces used for measuring ultrasound properties at a non-degraded state, are the same subjected to the stepwise degradation, so that one can observe the change in ultrasound propagation velocity for the same wood test-piece constantly throughout the whole degradation procedure. This will minimize variability in the observations and enhance interpretation of the results.

Hence, with this mechanical approach it is possible to plan in advance the density levels one wants to study. The rate of density loss will be also consistent, which permits a better understanding of ultrasound as it propagates through degraded wood, based on sequential and close by observations, instead of rapid drop-offs. In the present work, setting as starting point the density of the wood in fresh condition, and taking into account the wood species used, the test-pieces size, and drilling designs, it was derived that the density levels which would be achieved by mechanical means, is representative of well-preserved wood to beginning of moderately degraded wood, based on conservators' classifications of wood deterioration (Jensen & Gregory, 2006). This is represented by approximately 20% loss of its original density.

Yet, waterlogged archaeological wood can be found in a severe degradation state, showing even more than 80% density loss compared to that of fresh counterparts (Fengel, 1991; Babiński et al., 2014). For this reason, the mechanical treatment is followed by a chemical application, aiming to further the material loss and reach towards lower wood density levels. The exact density level that would be reached via the chemical treatment could not be known in advance as it is affected by wood species and test piece microstructure; however, the applied procedure is well controlled and reproducible. Ultimately, every

drilling step or chemical application represents an increasing degradation or porosity / decreasing density level where ultrasound propagation velocities are obtained.

With the new methodological approach the present study aims to give more confidence on the correlation between ultrasound propagation velocity and wood density during degradation. To achieve this, first the sensitivity of the experimental set-up as designed and tested in Chapter 3, and the reproducibility of tests are evaluated through:

- The study of the effect of number of drilled holes, representing rotting wood mass loss on ultrasound propagation velocity;
- The study of hole diameter on ultrasound propagation velocity.

The choice of insonification directions is based on log orientation during timber conversion into hull components, as described in section 2.2.2. "Fresh" quarter sawn timber is used for achieving at the same time on the same test-piece, both radial (RL plane[10]) and tangential (TL plane) ultrasound insonification directions (on-axis). Flat sawn timber (Figure 2-4, D) is used for off-axis insonification on the RT plane. Hence a new set of test-pieces is specifically produced, where the growth rings meet the face of the test-piece at a nominal angle of 45°, as in Figure 4-1, B. Given that the tangential axis is perpendicular to the radial axis, in Figure 4-1 ultrasound travels through position A parallel to the wood rays (0° angle) and gives "clear" radial velocities; through B it is at a nominal angle of 45° to the wood rays and gives off-axis velocities; and through C it is perpendicular to the wood rays (90° angle) and gives "clear" tangential velocities.

[10] The first index is for propagation direction, the second for polarization (Bucur, 1995)

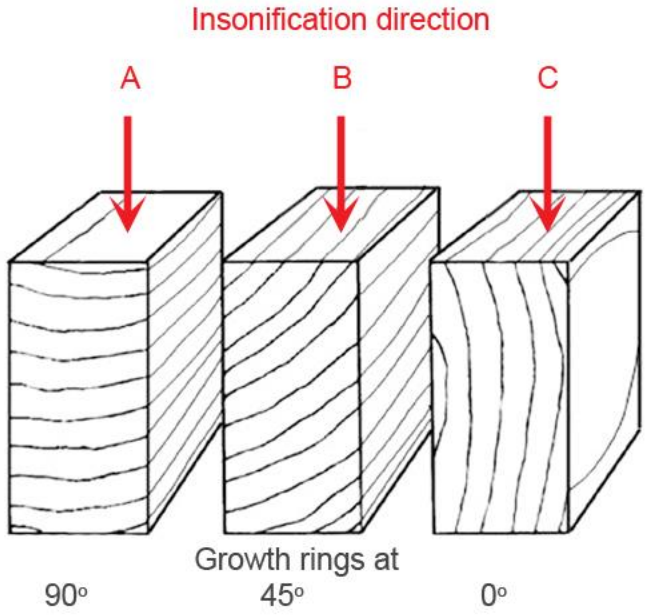

Figure 4-1 Direction of ultrasound in relation to direction of growth rings: 90°, 45°, and 0° (Modified from Forest Products Laboratory, 2010: fig. 5-6).

The experimental variables used for the establishment of the wood density – ultrasound propagation velocity relationship are:

- **Wood structure**. Oak and pine wood species are selected complying with ancient shipbuilding practices as established in section 2.2.1, and because they are significantly different as far as structure and density are concerned, as presented in section 2.5.1.

- **Insonification in relation to Radial and Tangential tree growth axes**.
  - On-axis
    - On radial axis
    - On tangential axis
  - Off-axis, within RT plane

4.1.1 Test-piece preparation

The wood selected for these experiments derives from the New Forest in Hampshire and fulfils the requirements of *clear* straight-grained wood and green moisture content, as described in section 3.2.1. Wood samples used for the manufacture of test-pieces came from the outer heartwood region of Sessile Oak (*Quercus petraea*) and the sapwood of Scots Pine

(*Pinus sylvestris*), complying with the species evidenced in the archaeological records, as well as local availability. The sapwood of pine was chosen because the phenomenon of pit aspiration is more frequent in the heartwood of softwoods than that of hardwoods (section 2.5.1) and thus fluid transportation is still active in the living sapwood and will allow a more efficient waterlogging of the test-pieces. Secondly, even when reaching maturity, pine has a smaller diameter than oak (White, 1998), so in order to avoid pronounced growth ring curvature, sampling has to be carried towards the outer perimeter of the log, where growth ring curvature decreases. The above characteristic is of great importance for the test-pieces used in on-axis insonification experiments, i.e. to have "clear" radial or tangential insonifications.

Two oak and pine quarter sawn beams, and one oak flat sawn, were further sawn each in fifteen test-pieces measuring 80 X 80 X 50 mm (Radial x Tangential x Longitudinal). Their dimensions, weights and volumes were measured as described in section 3.2.2. Density and moisture content of the wood samples in green condition were calculated before the waterlogging procedure using four blocks per wood sample, with the rest of the test-pieces subjected to the waterlogging procedure as applied in section 3.2.4. Moisture contents before and after waterlogging, and basic densities of the wood samples, are given in Table 4-1. It is mentioned that the oak test-pieces used for evaluating the experimental set-up in Chapter 3, are re-used here. For coherence reasons their physical properties are also given in Table 4-1, under heading *Oak Tree 1*.

Table 4-1 Density and moisture content (green and maximum) of the wood samples used for the artificial degradation.

Wood Species: Oak (*Quercus petraea*)								
Tree 1, quarter sawn			Tree 2, quarter sawn			Tree 3, flat sawn		
MC_{green} (%)	MC_{max} (%)	Basic Density (g/cm^3)	MC_{green} (%)	MC_{max} (%)	Basic Density (g/cm^3)	MC_{green} (%)	MC_{max} (%)	Basic Density (g/cm^3)
77	120	0.549	97	108	0.567	89	96	0.559
[8]*	[3]	[0.006]	[2]	[1]	[0.005]	[10]	[2]	[0.008]
(5)	(7)	(5)	(4)	(5)	(4)	(4)	(4)	(4)
{10}	{3}	{1}	{2}	{1}	{1}	{11}	{2}	{1}

Wood Species: Pine (*Pinus sylvestris*)		
Tree 1, quarter sawn		
MC_{green} (%)	MC_{max} (%)	Basic Density (g/cm^3)
138	170	0.426
[10]	[3]	[0.007]
(4)	(5)	(4)
{7}	{2}	{2}

*[std], (replicas), {CoV%}

Table 4-1, shows that wood's inherent moisture content variability whilst in green state, drops after the waterlogging procedure, as wood cavities are now filled with water. The higher moisture content of pine in green state is expected, as the sample derives from the sapwood of the tree (Forest Products Laboratory, 2010). The low coefficient of variation of wood's density for both oak and pine wood samples, 1-2%, proves that the wood structure between replicates of the same timber, e.g. annual ring width, earlywood - latewood proportion, ray width variation, is homogeneous, justifying a good group of replicates and hence, a control over the error introduced to the readings after repetitive measurements due to natural wood variability.

The outline of the experimental design of this research phase is given below:

Oak Tree 1 log (quarter sawn): the group consists of the same oak test-pieces used in Chapter 3. This group is now subdivided and used to study:

1) Whether drilling holes to simulate decay mass loss, is capable of affecting ultrasound propagation velocity. To accomplish this, holes of 2mm diameter are drilled in steps on the test-pieces of the first subgroup.

2) The effect of hole diameter on ultrasound propagation velocity. For this study, the second test-piece subgroup is drilled with 10mm diameter holes, simulating the boring

tunnels of the *Teredo* macro deterioration (see section 2.4.1). Results from the two subgroups are then compared to explore the dependency of the ultrasound propagation velocity on hole diameter.

Oak Tree 2 log (quarter sawn): the group consists of the on-axis insonification test-pieces, cut at a nominal angle of 90° of the growth rings to the test-piece surface, providing "clear" radial and tangential insonifications on the same test-piece. The group is used to study:

1) The effect of insonification direction in relation to Radial and Tangential tree growth axes.

Together with the ***Pine Tree 1 log (quarter sawn)*** group consisting of on-axis insonification test-pieces, the two groups are used to study:

2) The influence of wood structure and wood density on ultrasound propagation velocity.

A chemical treatment (described in detail in 4.1.2.3) is applied to all oak and pine test-pieces deriving from *Oak Tree 2 log* and *Pine Tree log 1*. The chemical treatment is applied in two steps, aiming to remove more wood substance and achieve lower density levels, as noted above.

Oak Tree 3 log (flat sawn): the group consists of the off-axis insonification test-pieces, cut at a nominal angle of 45° of the growth rings to the test-piece surface. The group is used to study:

1) The effect of insonification direction in relation to Radial and Tangential tree growth axes (in tandem with *Oak Tree 2 log* test-pieces' results).

As will be explained in section 4.2.1.2, after the initial experimentation with the 2mm diameter holes it was decided to increase the width of the drill bit. Therefore test-pieces from Oak Tree 2 and 3 logs, and Pine Tree 1 log, are drilled with 3mm diameter holes. Investigation regarding the effect of hole diameter on ultrasound propagation relationship, this time using the data from the drilled oak test-pieces with 3mm diameter holes, is additionally given with the ones from 2 and 10mm diameter holes.

Table 4-2 Experimental outline for the artificial degradation of waterlogged "fresh" wood (*1st treatment, **2nd treatment).

Wood Species: Oak (*Quercus petraea*)

Tree 1, quarter sawn (insonification on-axis)					Tree 2, quarter sawn (insonification on-axis)					Tree 3, flat sawn (insonification off-axis)				
Hole Diameter (mm)	Replicas	Number of Holes	Basic Density (g/cm³)	Loss in Density (%)	Hole Diameter (mm)	Replicas	Number of Holes	Basic Density (g/cm³)	Loss in Density (%)	Hole Diameter (mm)	Replicas	Number of Holes	Basic Density (g/cm³)	Loss in Density (%)
-	5	0	0.549	0	-	5	0	0.567	0	-	5	0	0.559	0
2	2	99	0.518	6	3	5	64	0.527	7	3	5	64	0.520	7
2	2	183	0.492	10	3	5	112	0.496	12	3	5	112	0.491	12
2	2	250	0.471	14	3	5	144	0.476	16	3	5	144	0.472	16
2	2	302	0.455	17	3	5	162	0.465	18	3	5	162	0.461	17
2	2	357	0.437	20	3+NaOH*	5	162	0.348	39					
10	3	12	0.444	19	3+NaOH**	2	162	0.305	46					
10	3	20	0.374	32										
10	3	25	0.331	40										

Wood Species: Pine (*Pinus sylvestris*)

Tree 1, quarter sawn (insonification on-axis)				
Hole Diameter (mm)	Replicas	Number of Holes	Basic Density (g/cm³)	Loss in Density (%)
-	5	0	0.426	0
3	5	64	0.395	7
3	5	112	0.372	13
3	5	144	0.357	16
3	5	162	0.348	18
3+NaOH*	5	162	0.310	27
3+NaOH**	2	162	0.292	31

4.1.2 Artificial degradation

The present study introduces a new wood degradation simulation concept as it faces a different degradation layout in archaeological wood, than the forestry community has to deal with, as pointed in section 1.4.2.1. This work has to consider a reverse wood deterioration occurrence, from the outside towards the inside (Figure 1-1), as well as the presence of free water filling the gaps in the waterlogged wood, instead of air in the green wood of standing trees. One may assume that this time the ultrasound beam will not avoid the denser than air water (ρ = 1g/cm^3) contained in wood's vacant spaces, while a reduction in the velocity of ultrasound propagation, progressing the wood mass removal (decay), can be here ascribed rather to correspondingly increasing levels of ultrasound attenuation (section 2.5.3), than longer travelling times (Figure 1-2).

The experimental approach to simulate wood mass loss, and consequently density reduction, is to gradually remove wood mass from the wood test-pieces via drilling holes. A 2 mm diameter hole is selected as being practically the nearest possible diameter to simulate the minute, of the order of tens of a millimetre cavities, caused by fungi and bacteria attack within the cell wall (section 2.4.1). At the same time, a 2 mm diameter hole simulates the tunnelling widths of the Teredo when it begins its excavation in the wood as a larva, and the perforation size of 1-2 mm of the wood's surface due to the action of Limnoria, which leaves regular spaced respiration holes on its surface (section 2.4.1). Also, with a small diameter hole it is possible to fit more holes per test-piece volume, thus create a greater number of degradation levels, enough to study the suitability of the degradation methodology. Drilling is executed along the grain (longitudinal growth axis). It initiates at the perimeter of a wood test-piece and progressively moves inwards to its centre, in accord with the degradation occurrence in archaeological wood. Each drilling / degradation step involves drilling two parallel rows of holes along the edges of a test-piece. This is followed by ultrasound propagation velocity measurements to test the loss of mass resulting from the drilling. This procedure carries on until the whole area of the test-piece transverse surface (RT plane) is filled with holes corresponding to maximum degradation via drilling.

The array of holes is designed to follow the geometry shown in Figure 4-2. Spacing between holes and rows takes under consideration the utilization of the total test-piece transverse surface, the diameter of the preferred hole, and securing the minimum gap between holes so to avoid their convergence or breakage during drilling. For the 2mm diameter holes, the distance between the centres of holes is set to 5 mm, and the distance between successive rows to 2.5 mm. For the 3mm diameter holes these distances are set to 8 mm and 4 mm

respectively, and for the 10mm diameter holes, to 18 mm and 9 mm respectively. It is noted that for the 10mm diameter holes only one row of holes is drilled at a time.

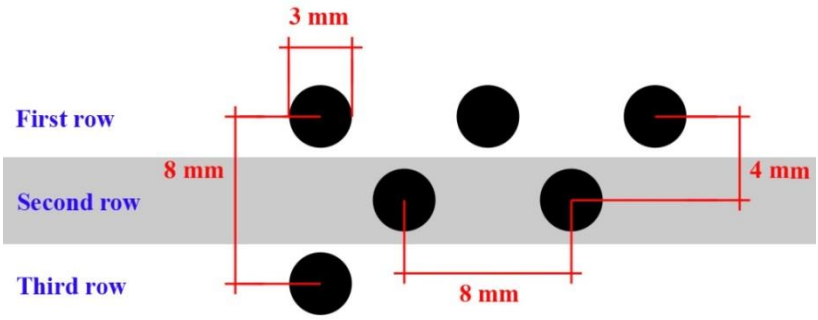

Figure 4-2 Geometry of the hole array drilled for a controlled simulation of wood mass loss; spacing for 3 mm diameter holes.

Obviously, the approach turns the longitudinal direction useless to further ultrasound testing; however, as explained in section 2.2.2, it is the surface across the grain of the timber which is most likely to be accessed by ultrasound in practice, due to timber conversion techniques in ancient shipbuilding. Hence, it is intentionally excluded from testing hereafter.

4.1.2.1 Drilling procedure

Drilling trials revealed the difficulty in drilling through the rather large thickness of the test-pieces, which were also in a waterlogged state, while wood's structure, e.g. the existence of wide rays in oak and in lesser extent the growth ring boundaries in both oak and pine, tended to impose on the propagation of the drill bit, sometimes causing a diversion from the vertical, especially when using the 2mm drill bit. After many tests trying to refine and standardize the drilling technique in order to achieve reproducible results, the following drilling procedure was established.

A variable speed Bridgeport Shipley Turret Milling Machine fitted with D.R.O. (Direct Read Out), is used. A large parallel jaw vice is mounted on the table of the machine to wedge the wood test-piece while drilling (Figure 4-3). The vice ensures constant distance of holes from outside of the test-piece. This is obtained by using ground stock parallels and a D.T.I. (Digital Test Indicator). At first zero datum is set on one of the test-piece's corners. After that and for each degradation step zero datum is set to be the last hole drilled in the previous session. At the start of drilling each hole a manually held stop is used to ensure that the drill does not wander on first entry. At this initial entry point drilling is manual. Drilling is carried out using the woodpecker process, i.e. drilling under feed for 5-10 mm,

disengage and clear swarf / saw dust from drill flutes, keeping on cycles until complete hole is drilled.

Figure 4-3 Drilling wood test-piece with a Bridgeport Turret Machine.

Custom grounded 2mm and 3mm in diameter brad point drill bits suited for hardwoods and softwoods are used, combining two flute lengths to drill each hole. The short series brad point drill bit is used to drill the first approximately 30mm of the hole, followed by the long series brad point drill bit which drills the hole throughout the 50mm thickness of the test-piece. For the 10mm diameter holes a forstner bit is used to drill throughout the test-piece thickness in one go. Distances between the holes' centres and between rows are kept accurate by using the D.R.O. A set of representative images of degradation steps created using a 3mm and a 10mm bit on quarter sawn oak test-pieces are given in Figures 4-4 and 4-5 respectively.

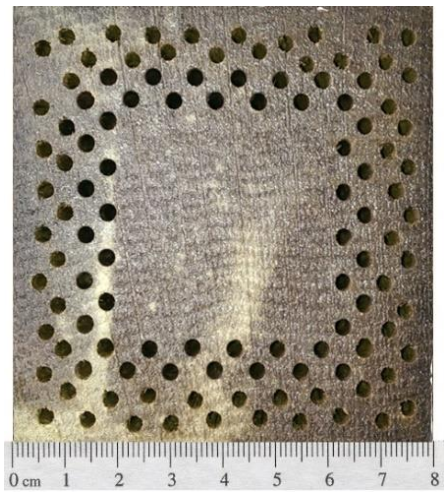

Figure 4-4 Oak test-piece transverse surface drilled with 3 mm diameter holes, at 2nd drilling step representing 12% loss in density.

Figure 4-5 Oak test-piece transverse surface drilled with 10 mm diameter holes, at 1st drilling step representing 19% loss in density.

4.1.2.2 Calculating wood density after drilling

In order to determine the basic density ($\rho_{o.d.}$) achieved after each drilling session the remaining wood mass ($W_{o.d.}$) has to be defined first. This has to be computed indirectly as oven-drying the test-pieces is not an option, given that the same test-pieces have to be further drilled and ultrasonically tested. First, the total volume removed per drilling session is calculated:

$$V_{out} = \pi r^2 h \, x \, n_{holes} \tag{4.1}$$

The volume out combined with the known density ($\rho_{o.d.}$) for each wood species (Table 4-1), will give the mass ($W_{o.d.}$) removed from each drilling session and for each test-piece, using (3.2), where V_w is the waterlogged volume of each test-piece. Consequently the remaining wood mass for each test-piece can be calculated from the initial known mass, and used for calculating the basic density reached after each drilling session (3.2.). It is mentioned that alternatively, the weights of the test-pieces after each drilling could be also used by subtracting them from the original undegraded waterlogged weight, which would be then converted into $W_{o.d.}$. However, it was observed that in practice, excess water would still be attached to the walls of the drilled holes due to capillary forces, even though rigorously shaken (as only the weight of the wood without that of the water in the holes is the purpose

here), which was adding uncertainty to the reading, especially as the tossing and wiping procedure of the drilled test-pieces could not be identical for all of them.

4.1.2.3 Chemical treatment with alkali

Marine archaeological wood is buried in an alkaline environment. Currently seawater pH is averaging at a level of pH 8.0, the higher values measured at the surface with low CO_2 concentration due to photosynthesis (Millero, 2006 and 2007). Wood encountered in closed waters can be subjected to high pH levels, fluctuating between 8.2 to 8.9 during the day, or to low pH values and proportional to temperature, if lying close to upwelling waters in equatorial regions (Millero, 2006: 266), or if lying at the sediment interface in oxygen depleted local areas, responsible for the yielding of hydrogen sulfide (H_2S), which can reduce the pH to 7.0 (Florian, 1987). Near a depth of 1000 m, pH can be as low as 7.5 with a possibility to increase in very deep waters under certain circumstances (Millero, 2006).

Even if wood is exposed to constant environmental conditions (Borgin et al., 1975), inevitably some abiotic deterioration of wood takes place after all (Blanchette et al., 1994). The aim set here is to design a chemical procedure which will accelerate the deterioration of wood in the laboratory through the use of alkali.

As noted in section 2.4.2 chemical deterioration in waterlogged wood shows a selective deterioration sequence summarised in order of the less resistant to decomposition as hemicellulose < α -cellulose < lignin. This chemical mechanism of wood alteration and deterioration has been noted for its resemblance to alkali treatment of wood (Parameswaran, 1981; Blanchette et al., 1991).

Wangaard (1966) subjected hardwood and softwood beams to alkali degradation (sodium hydroxide, NaOH), after a pre-soaking treatment with water, aiming to determine their residual strength. A considerable effect of the alkali on the cell-wall causing swelling, significant decreasing of the hemicellulose content, degradation and alteration of the carbohydrate network and decrease in lignin content, were noted leading to low strength retention. Mirahmadi et al. (2010) treated spruce and birch wood species after grounding, with 7% w/w sodium hydroxide for 2h at different temperatures from -15 to 100°C and ambient pressure. Significant reduction of the hemicelluloses content is noted for both species, and more for the birch, while the higher reductions derived from higher treatment temperatures (about 20% reduction for birch as opposed to 7% for the spruce at 100°C). At the same time, the cellulose's crystallinity decreased. Very limited or no destruction of the lignin occurred. The acid-insoluble lignin could not be significantly removed from the wood

components of the spruce, but was reduced the maximum by approximately 5% in birch at 100°C. Acid-soluble lignins were not affected by the treatments.

Considering the above, the effect of alkaline treatment on the control wood test-pieces, will be twofold: destruction of the wood cell wall integrity, and removal of its chemical components, ultimately leading to the desired density reduction and effect on the ultrasound propagation velocity.

This work follows the procedure suggested by Wangaard (1966), who used wooden beams of large size (12,7 mm X 12,7 mm X 228,6 mm). All fully pre-drilled with 3mm diameter holes, oak and pine waterlogged test-pieces are used, ensuing the efficient diffusion of the alkali in the whole wood mass. Additionally, as seen in Figure 4-2, the wood thickness around drilled holes is between 4 to 8 mm, which is regarded small enough to be attacked (Panthapulakkal & Sain, 2013). All test-pieces are immersed in 10% w/w NaOH solution at 50°C for 96 hours. Subsequently, the test-pieces are rinsed with tap water for one week to eliminate the chemicals (rinsing solution pH 7). All test-pieces are then ultrasonically tested. Two replicates from each wood species are used to determine the density reached after the chemical treatment and one per species for SEM (Scanning Electron Microscopy) analysis of their microstructure appearance after the alkaline attack. The remaining two test-pieces per wood species are treated for a second time with the sodium hydroxide following the same procedure. After its completion and ultrasound testing, the test-pieces are cut in halves; one from each test-piece is used to define the density per wood species after the degradation, and the one left for SEM analysis of their microstructure after the second treatment. For the determination of the wood density the test-pieces are oven-dried at 105°C till constant weight is reached (3.1). MC_{max} is also determined as supplementary information of the degradation severity (3.2).

4.1.3 Ultrasound testing

Ultrasound testing after each artificial degradation step is conducted following the methodology described in section 3.4. After each drilling session, the test-pieces are immersed back into water inside a desiccator, and a 70kPa vacuum is applied following a cycle of 15 minutes on - 15 minutes off, for 24h. By the end of this procedure no air bubbles are seen coming from the wood or the drilled holes. The test-pieces are then ultrasonically tested. Special care is given so that the test-pieces are kept continuously fully submerged in water during transportation from the vacuum chamber inside the water test tank, so that no water can be drained from the drilled holes and replaced by air, as this can affect the ultrasound measurements.

As in section 3.4, ultrasound testing of each test-piece includes measuring ultrasound propagation velocity in three different regions of interest (ROI) per wood plane (Figure 3-11), executing three repetitions of each measurement (i.e. n = nine measurements per wood plane X number of replicas). The velocities received from all three ROI for each drilling / degradation step, are group averaged to give the one velocity representative of that density level of the test-piece as a whole.

4.2 Results

4.2.1 Evaluation of the drilling procedure

The primary aim of this experimental step is to test the ability of the artificial degradation via drilling holes, on affecting the ultrasound propagation velocity in increasingly deteriorating waterlogged wood test-pieces. The experimental set-up adequacy to capture any ultrasound propagation changes is evaluated at the same time. For this purpose the effect of number of holes drilled on the wood test-pieces and that of hole diameter on ultrasound propagation velocity are considered.

4.2.1.1 Study of the effect of number of holes drilled

The simulation of wood mass loss, and hence density reduction, by gradually drilling holes in wood test-pieces, is studied by drilling holes of 2mm in diameter in oak (Table 4-2). A small diameter hole allows, among other specific experimental conditions explained in section 4.1.1, to create a sufficient number of steps to study the response of the ultrasound propagation velocity on a stepwise increase of number of holes in the wood test-pieces.

The results from this procedure are presented in Figure 4-6. Ultrasound propagation velocity is plotted against number of holes in this instance, as the purpose here is to first test the effectiveness of the drilling procedure in wood as a technique to cause velocity changes.

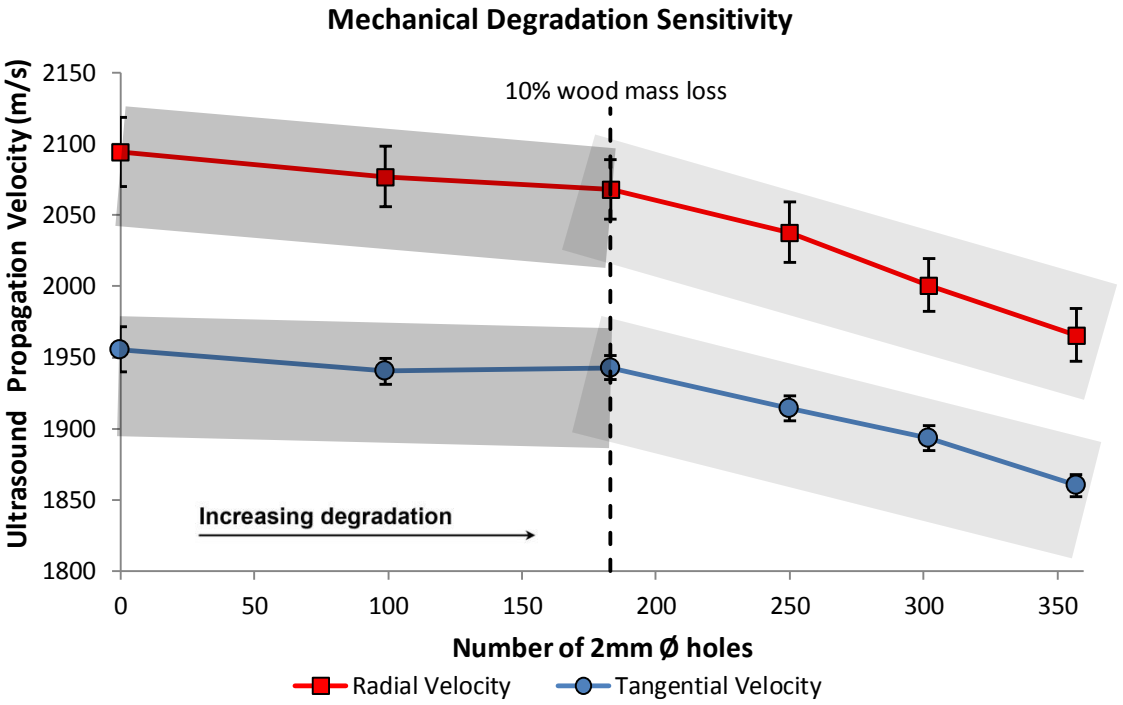

Figure 4-6 Ultrasound velocity drop progressing hole drilling on oak waterlogged test-pieces. Error bars is STD.

The gradual increase of the total number of holes, after what appears to be a threshold at approximately 180 holes which corresponds to 10% mass loss (see Table 4-2), causes a constant drop of the ultrasound propagation velocity, for both Radial and Tangential axes. The extent of velocity drop is 6% in the radial and 5% in the tangential direction. The experimental set-up proves sensitive to measure this change in ultrasound propagation velocity. Apart from this performance, is it also capable of detecting deterioration when wood shows little mass loss. (Keeney & Pollio, 1984), found no consistent correlation of low frequency ultrasound velocity, for frequencies likely to be between 24 kHz and 200 kHz, when mass loss from most likely, saturated wood, was less than 25%. In the present study the respective wood loss reaches the maximum of 20% of its initial mass corresponding to 357 holes (Table 4-2), and it is detectable as a change in ultrasound propagation velocity. Ultrasonic wave velocity may be able to detect low wood weight losses even below 10% using frequencies between 37 - 500 kHz with the through-transmission method (Wilcox, 1988). Nicolotti et al., (2003) detected decay in standing trees corresponding to 15% wood mass loss, using ultrasound tomography operating at 33 kHz. Moreover, the present results also show that ultrasound propagation velocity is sensitive to distinguish between the two principal wood axes, radial and tangential, throughout the drilling degradation procedure. Coefficient of variation is notably low between 0.92% - 1.16% for the radial velocities and

between 0.42% and 0.81% for the tangential velocities, expressing good test reproducibility and a reliable experimental set-up.

4.2.1.2 Study of the effect of hole diameter on ultrasound propagation

As noted in section 4.1.1, holes of 10mm in diameter are also applied in parallel with the 2mm diameter holes, aiming to explore whether ultrasound propagation shows a dependency on the drilled hole diameter. In essence, results show whether wood decay, as manifested from the activity of different wood decay organisms, influences ultrasound propagation. To explore this, the relationship between ultrasound propagation velocity and loss in wood mass received from the wood test-pieces drilled with holes of 2mm in diameter is compared with that from the oak wood test-pieces drilled with 10mm diameter holes. Yet, as mentioned in section 4.1.1, after initial experimentation with the 2mm drill bit, a wider drill bit is selected to replace it. The reason is that drilling with a 2mm drill bit proves to not be rigid enough to overcome the stresses generated by the structural inconsistency of the oak wood test-pieces. This causes wandering of the drill bit while drilling, resulting in frequent drilled hole diversions from the vertical, eventually affecting the reproducibility of the drilling procedure among replicates (Figure 4-7). In order to improve the performance of the drill bit and reproducibility of results, while upholding to the scientific conditions explained in section 4.1.1, the next smallest diameter drill bit of 3mm in diameter, is tested. The slightly thicker drill bit proves to overcome the influence of wood's anatomy, which tends to impose on the propagation path of the drill bit while moving along the longitudinal axis of the rather thick wood test-pieces (50mm) (Figure 4-8).

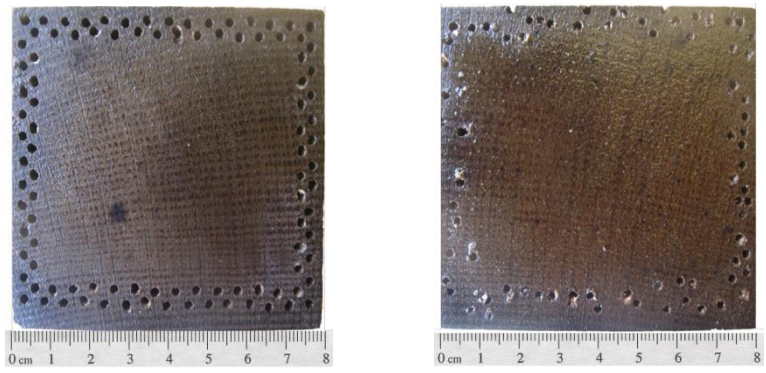

Figure 4-7 Left: 2mm Ø holes top view (drilling surface). Right: 2mm Ø holes bottom view (drill out).

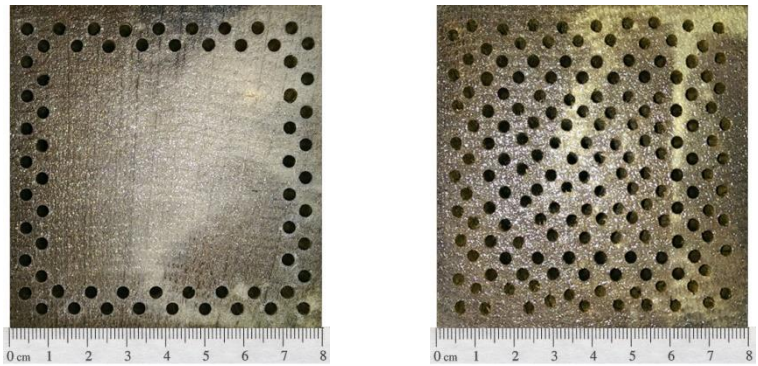

Figure 4-8 Left: 3mm Ø holes top view (drilling surface): first two rows. Right: 3mm Ø holes bottom view (drill out): after drilling completion.

Results from the effect of hole diameter on ultrasound radial and tangential propagation velocities, are given first for the 2mm versus 10mm in Figures 4-9 and 4-10, 2mm versus 3mm in Figures 4-11 and 4-12, and 3mm versus 10mm in Figures 4-13 and 4-14. As the intention is to test the degradation method, mass loss is used at this stage, this being the objective variable and most appropriate to explain the effect of the hole size on ultrasound propagation, rather than wood density. All velocity measurements received per mass loss level are plotted for all cases. Linear trendlines are drawn using all measurements per 'hole diameter' group.

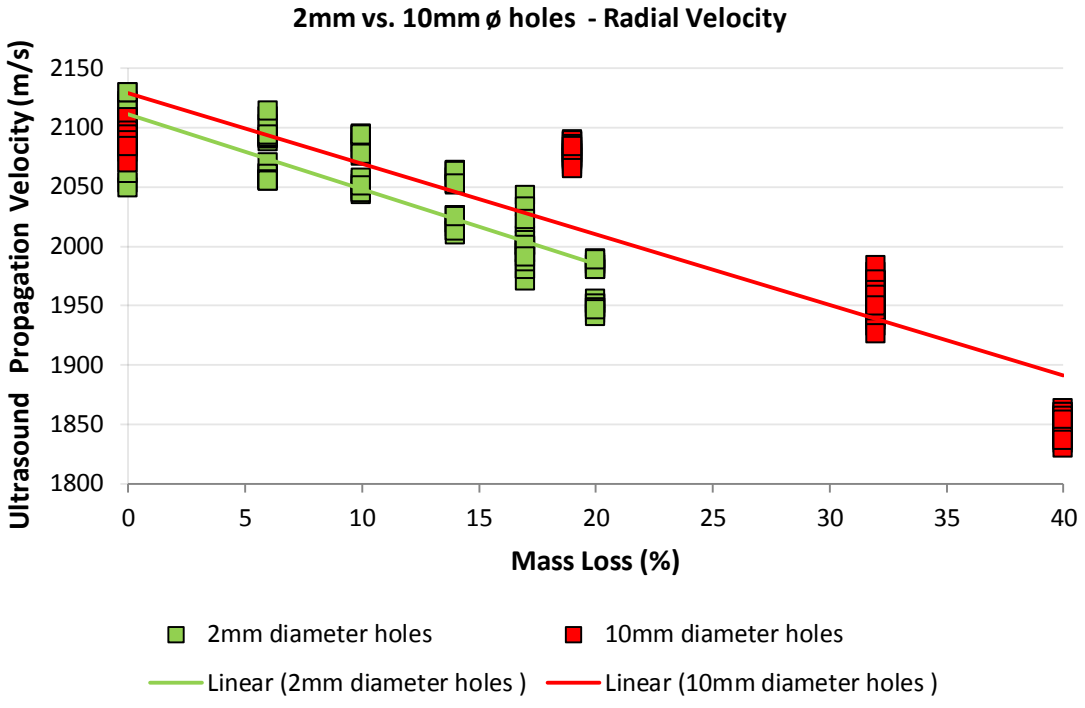

Figure 4-9 Effect of hole diameter on ultrasound propagation velocity: 2mm versus 10mm, Radial insonification (n_{2mm} = 18 and n_{10mm} = 27 measurements per mass loss level).

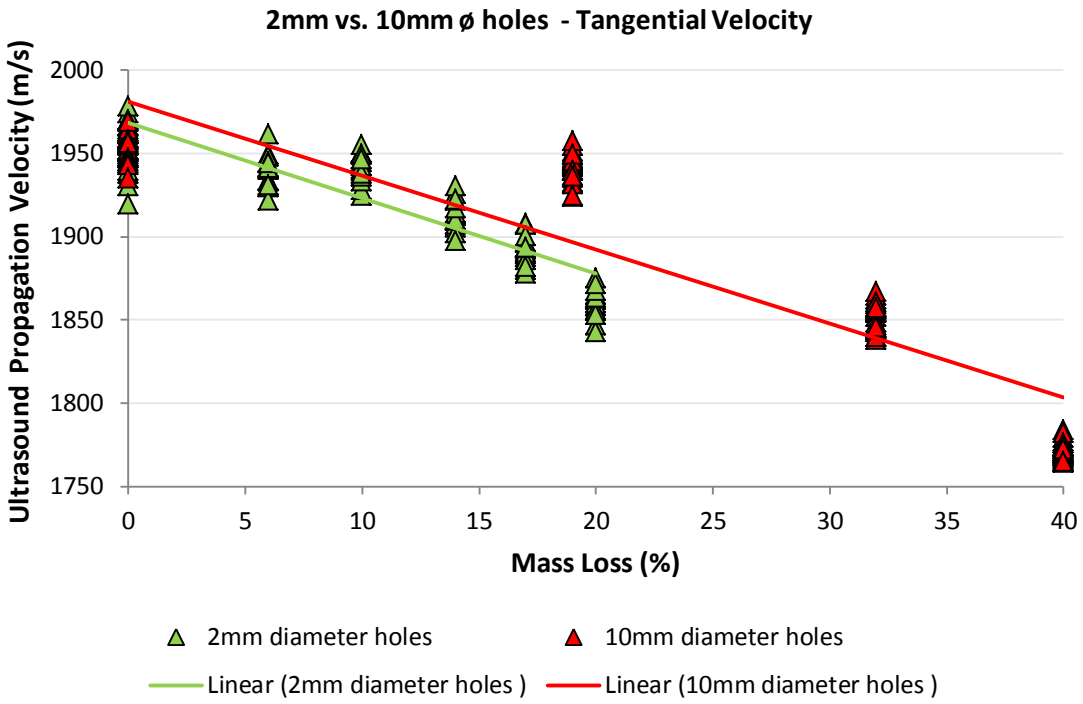

Figure 4-10 Effect of hole diameter on ultrasound propagation velocity: 2mm versus 10mm, Tangential insonification ($n_{2mm} = 18$ and $n_{10mm} = 27$ measurements per mass loss level).

In Figures 4-9 and 4-10, ultrasound propagation velocity drops with increasing number of holes irrespective of hole diameter for both radial and tangential wood axes. The extent of velocity drop from drilling 10 mm diameter holes is 12% for the radial direction and 9% for the tangential velocity. For the 2mm it is 6% and 5% respectively. Coefficient of variation for the 2mm 'hole diameter' group is between 0.92% and 1.16% for the radial velocities, and between 0.42% and 0.81% for the tangential velocities. For the 10mm 'hole diameter' group coefficient of variation is between 0.34% and 0.72% for the radial velocities, and between 0.29% and 0.45% for the tangential velocities. At the common mass loss of 19-20%, and for both wood axes, the velocity received from the 10mm drilled test-pieces is higher than the one from the 2mm drilled test-pieces. However, the two regression lines appear to travel in a similar general direction, lined in parallel with a small shift in both axial velocities. A One-Way ANCOVA test is performed in SPSS in order to study the effect of hole diameter on ultrasound propagation velocity while controlling for wood mass loss. Results show that homogeneity of regressions does statistically exist, or else the slopes from the 2mm and 10mm 'hole diameter' groups do move in the same trend, in both radial and tangential wood axes. The two groups are statistically significantly different from one another, with equality of variances of the either axial velocity not met across the two groups. The test shows that,

for both axial velocities, the influence of mass loss % has a more significant effect on the velocity than the hole diameter, and thus should be included when testing the effect of the hole diameter. More specific, mass loss can explain 79.5% of the variance in radial velocity compared to 7.4% by the hole diameter, and 80.9% of the variance in tangential velocity as opposed to 5.6% by the hole diameter. It is mentioned that the statistical test is run including all measurements taken per mass loss level and not just the average velocity at that level. Summarising, based on the statistical analysis, hole diameter doesn't seem to have a strong influence on velocity as does loss in wood mass in predicting the two principal axial velocities between 2mm and 10mm diameter holes.

In Figures 4-11 and 4-12, the results received from drilling 3mm diameter holes are given together with those from the 2mm diameter holes. Drilling with the 3mm proves equally effective in changing the ultrasound velocity which shows drops extending to 5% for the radial velocity and 3% for the tangential. Coefficient of variation was between 0.73% and 0.94% for the radial velocities and 0.73% to 1.29% for the tangential velocities. A One-Way ANCOVA test is run this time between the 2mm and 3mm 'hole diameter' groups. The One-Way ANCOVA test shows homogeneity of regressions in the case of the radial velocity (Figure 4-11), but not for the tangential velocity where slopes seem to travel unparalleled (Figure 4-12). The two groups are statistically significantly different from one another, with equality of variances of the either axial velocity not met across the two groups. Given this, mass loss % continued to be here the strongest predictor of both axial velocities with 79.2% of the variance in radial and 64.8% in the tangential velocity being explained by mass loss %, in contrast to 11.1% and 35.2% by the hole diameter, respectively.

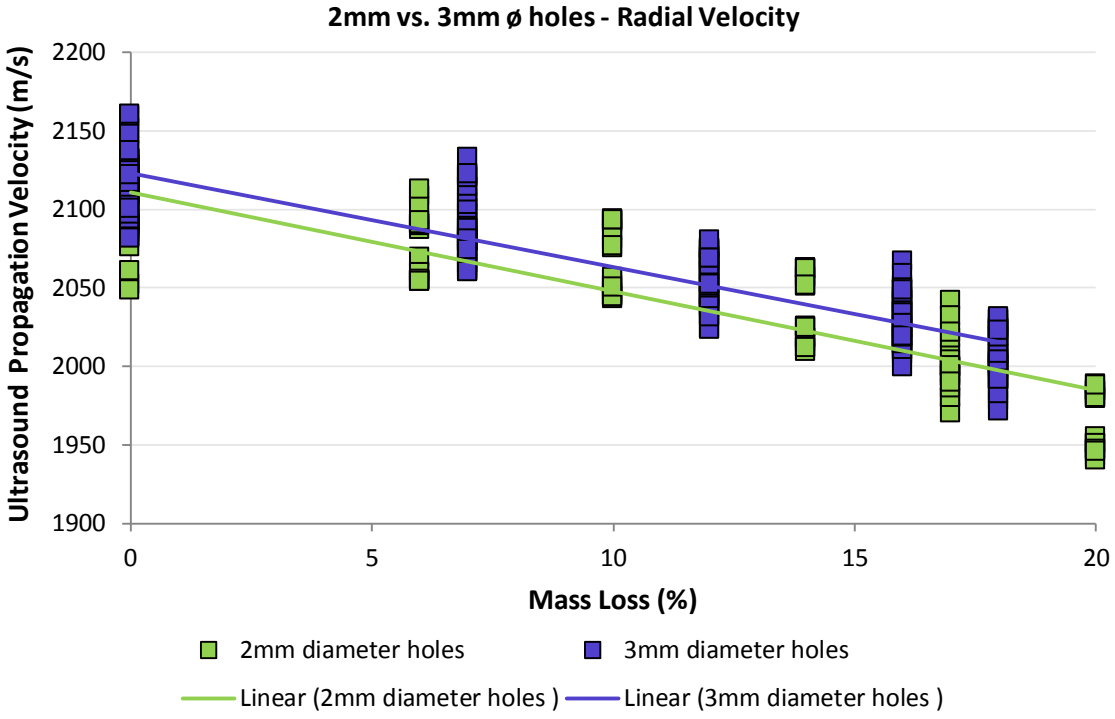

Figure 4-11 Effect of hole diameter on ultrasound propagation velocity: 2mm versus 3mm, Radial insonification ($n_{2mm} = 18$ and $n_{3mm} = 45$ measurements per mass loss level).

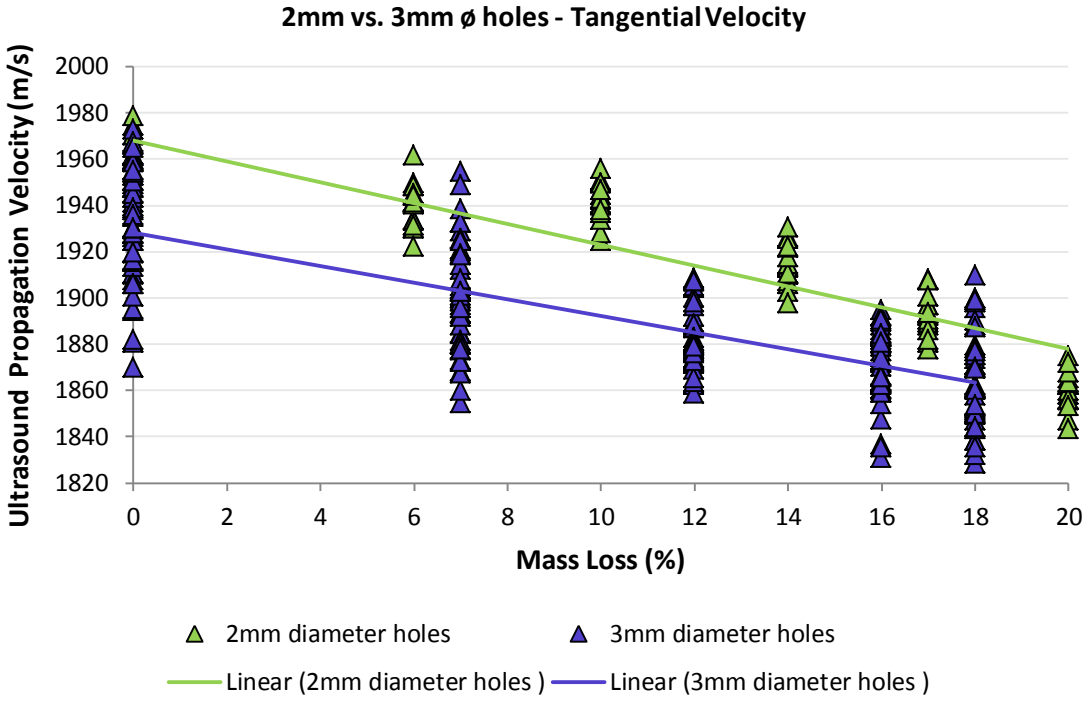

Figure 4-12 Effect of hole diameter on ultrasound propagation velocity: 2mm versus 3mm, Tangential insonification ($n_{2mm} = 18$ and $n_{3mm} = 45$ measurements per mass loss level).

To complete the study of the influence of hole diameter on the ultrasound propagation velocity, a final test is run this time between the 3mm and 10mm 'hole diameter' groups. Results show homogeneity of regressions for the radial velocity (Figure 4-13), but not for the tangential velocity (Figure 4-14). With equality of variances of either axial velocity not met across the two groups, the groups are not statistically significantly different from one another in case of the radial velocity, but are for the tangential. In accord with the previous 'hole diameter' groups comparisons, mass loss % has the strongest effect on the ultrasound propagation velocity in comparison with the hole diameter. Mass loss explains 81.2% of the variance in the radial velocity and 74.7% in the tangential velocity, while 0.8% is explained by the hole diameter in the radial and 31.3% in the tangential velocity. Here as well, the statistical test is run including all measurements taken per mass loss level.

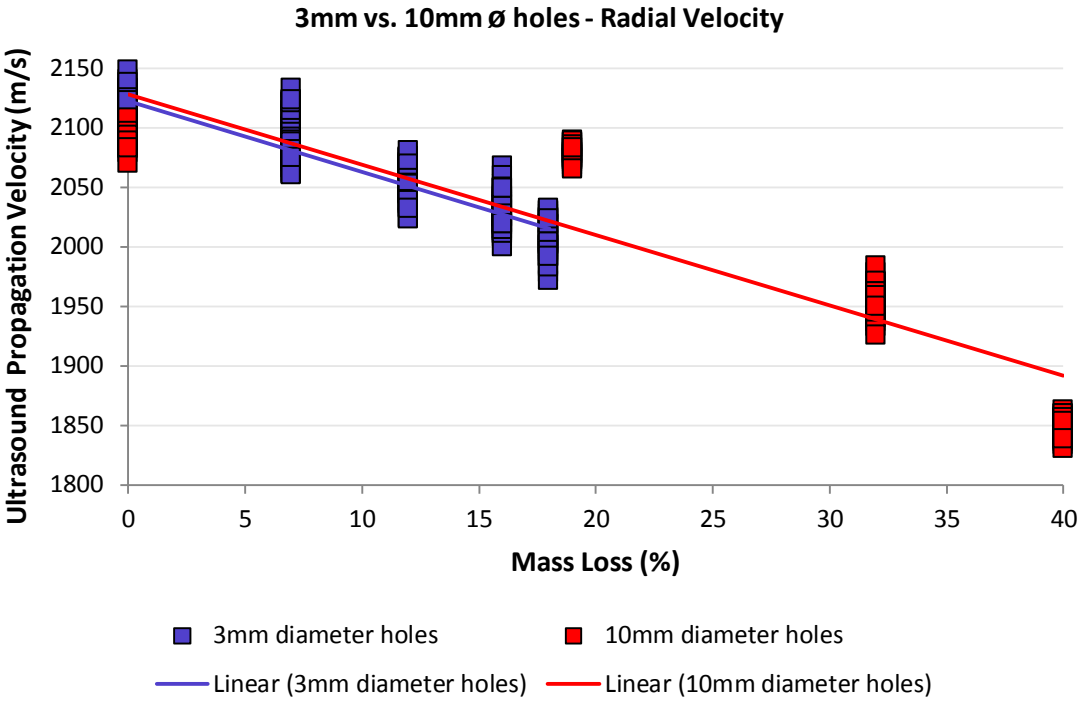

Figure 4-13 Effect of hole diameter on ultrasound propagation velocity: 3mm versus 10mm, Radial insonification ($n_{3mm} = 45$ and $n_{10mm} = 27$ measurements per mass loss level).

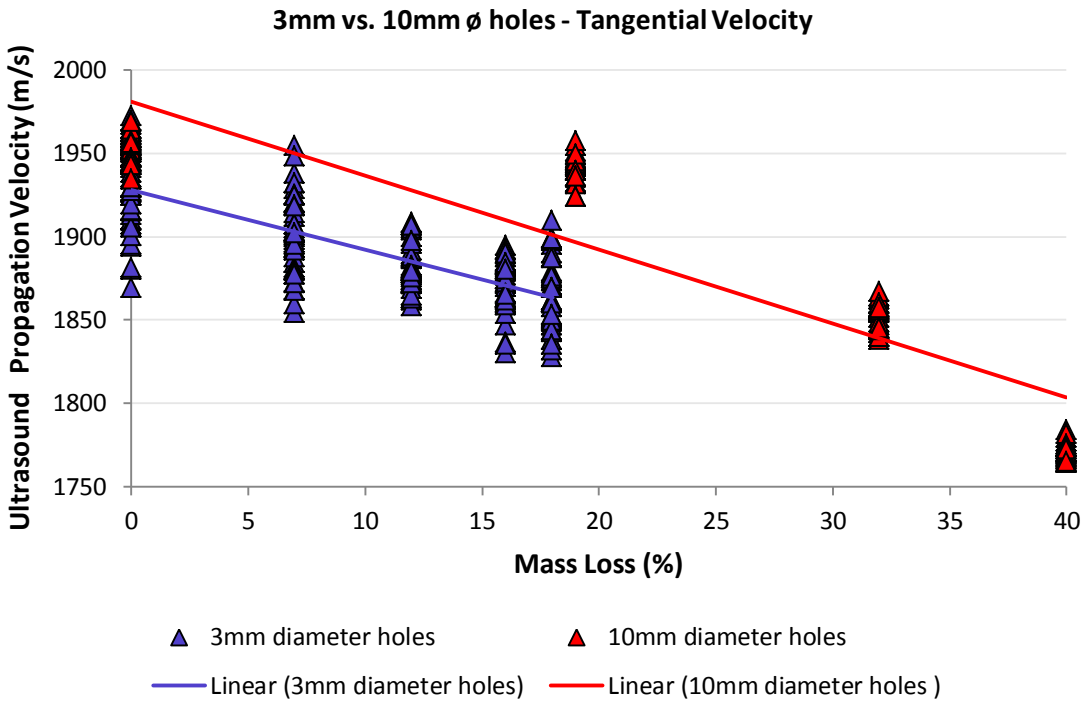

Figure 4-14 Effect of hole diameter on ultrasound propagation velocity: 3mm versus 10mm, Tangential insonification ($n_{3mm} = 45$ and $n_{10mm} = 27$ measurements per mass loss level).

Evidence from using the statistical tests, show the importance of mass loss % as a significant predictor of the ultrasound propagation velocities on radial and tangential axes, and the lesser contribution of the hole diameter to it. It is decided to adopt hereafter the 3mm diameter drill bit for the drilling degradation of the wooden test-pieces, as this diameter will improve experimental reproducibility in relation to 2mm. In addition, it has the advantage of allowing the execution of more degradation steps in contrast with the 10mm drill bit, as well as controlling for smoother wood degradation rates or else acquiring tighter data for the establishment of the relationship between ultrasound propagation velocity and wood density.

4.2.2 Wood density – Ultrasound propagation velocity relationship

4.2.2.1 Effect of wood structure (insonification on-axis)

First experimental variable of this experimental phase, for the establishment of the wood density – ultrasound propagation velocity relationship, is the influence of the wood structure on the ultrasound propagation. Oak and pine species are selected complying with ancient shipbuilding practice and because they are significantly different as far as structure and density are concerned. Quarter sawn waterlogged test-pieces are drilled with 3mm

diameter holes, followed by velocity measurements for each drilling / degradation session. Figure 4-15 show the results from this procedure.

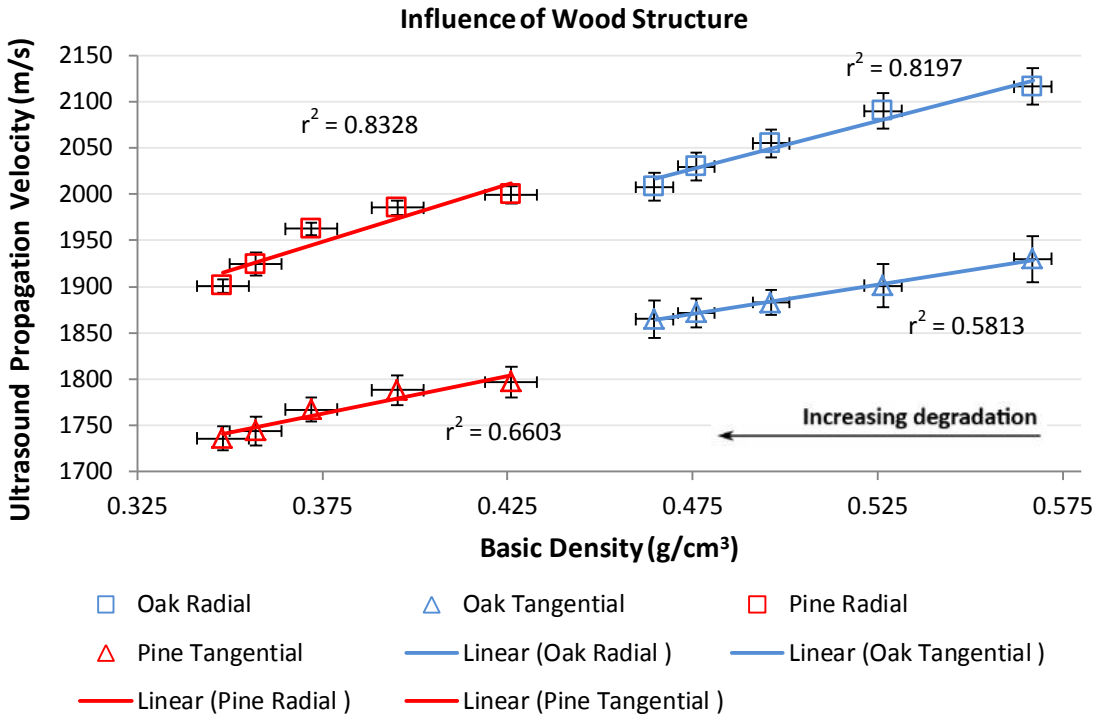

Figure 4-15 Influence of oak and pine wood on ultrasound radial and tangential propagation velocity. Error bars is STD, n = 45 measurements per density level.

From Figure 4-15 it can be observed that there is a gradual reduction of the ultrasound propagation velocity with density for both oak and pine and in both radial and tangential insonification directions. Coefficient of determination, r^2, was derived including all measurements per density level. There are moderate linear correlations for tangential velocity and wood's density (r^2 = 0.58 for oak and 0.66 for pine), and strong for radial velocity for both oak and pine wood (r^2 = 0.82 and 0.84 respectively).

For a wood density range between 0.567g/cm³ and 0.348g/cm³, ultrasound propagation velocity can distinguish between oak and pine structure throughout the degradation procedure; except the area around 2000 m/s, where the radial velocity of the last degradation step for oak and the first, non-degraded of pine, are overlapping, even though there is a density difference of approximately 0.040g/cm³. Results verify wood density influence on ultrasound velocity (Bucur, 1988) as the velocities from dense oak are constantly approximately 100m/s faster than those of the less dense pine in the radial axis and approximately 125m/s in the tangential axis (Tables 4-3 and 4-4).

Table 4-3 Radial ultrasound propagation velocities for oak and pine wood test-pieces after drilling procedure.

	Radial ultrasound propagation velocity (m/sec)									
	Oak					Pine				
Basic density (g/cm^3)	0.567	0.527	0.496	0.476	0.465	0.426	0.395	0.372	0.357	0.348
Mean	2116	2090	2055	2030	2008	1999	1985	1962	1924	1901
Maximum	2161	2133	2081	2067	2032	2018	2002	1978	1949	1921
Minimum	2082	2060	2023	2000	1972	1979	1970	1945	1904	1885
CoV (%)	0.94	0.93	0.73	0.73	0.75	0.46	0.41	0.34	0.65	0.37

Table 4-4 Tangential ultrasound propagation velocities for oak and pine wood test-pieces after drilling procedure.

	Tangential ultrasound propagation velocity (m/sec)									
	Oak					Pine				
Basic density (g/cm^3)	0.567	0.527	0.496	0.476	0.465	0.426	0.395	0.372	0.357	0.348
Mean	1930	1901	1883	1872	1865	1797	1788	1767	1744	1736
Maximum	1973	1955	1909	1895	1910	1828	1824	1789	1767	1763
Minimum	1870	1854	1858	1831	1828	1770	1763	1740	1715	1713
CoV (%)	1.29	1.24	0.73	0.82	1.09	0.93	0.91	0.72	0.91	0.77

The prevalence of oak's tangential velocity to that of pine's can be explained by the density distribution within the annual ring structure consisting of earlywood and latewood layers. Feeney & Chivers (2001: Table 1), give a set of typical values for earlywood and latewood thickness for ring porous hardwoods and softwoods, which show that for hardwoods, the early and late wood regions are typically of equal width, whereas for softwoods, the earlywood region is typically five times wider than the latewood region. These analogies are similar to the present ones that of the pine's earlywood region being three times wider than the latewood region, and that of oak's equal. The difference in thickness has theoretically a direct effect on the contribution of each layer to wood's stiffness, as it is density dependent (Kahle & Woodhouse, 1994: 1255), where a single line in the latewood region is predicted to contribute up to 80-90% of the total wood stiffness, when the same line in earlywood region could contribute 10-20 times less in overall. Correspondingly the velocities received from softwood earlywood and latewood show a greater difference than they do in hardwood (Feeney & Chivers, 2001).

Furthermore, oak shows a slightly higher variability in velocity than pine, and especially in the tangential insonification axis. Variability in radial axis is associated with the coexistence

of oak's broad and narrow xylem rays (Spycher et al., 2008). Part of the variability could potentially be laid also on the annual ring structure, where elastic behaviour and density of wood varies roughly periodically in the radial direction (Feeney et al., 2001; Feeney & Chivers, 2001). McIntyre & Woodhouse (1986: 19-20) note that the periodicity of the wood as represented by the ring structure, can produce a series of frequency "pass bands" and "stop bands", within which waves can and cannot propagate respectively, if the wavelength is close to the ring spacing. To overcome the effect, the wavelength has to be at least four times the ring spacing (*ibid.*). In the present study the ring spacing in oak is approximately 2mm whereas the wavelength is double that length, and possibly small enough to introduce variations in the radial velocity on account of the amplitude reflections from changes in the acoustic impedance from ring to ring (Feeney et al., 2001).

In the tangential axis one possible explanation for the variability is the somewhat wavy appearance of the annual rings (Figure 4-16) of the oak test-pieces, which could have disturbed in a different way the sound propagating in a straight line through the wood. For comparison, according to Spycher et al. (2008), the tangential "waves" of curly maple sycamore wood (angiosperm) (Figure 4-17) represent an extended pathway for the axial propagation of sound waves, leading to greater attenuation than in a regular structure sycamore wood.

Figure 4-16 Wavy appearance of annual rings in oak test-piece (cross section).

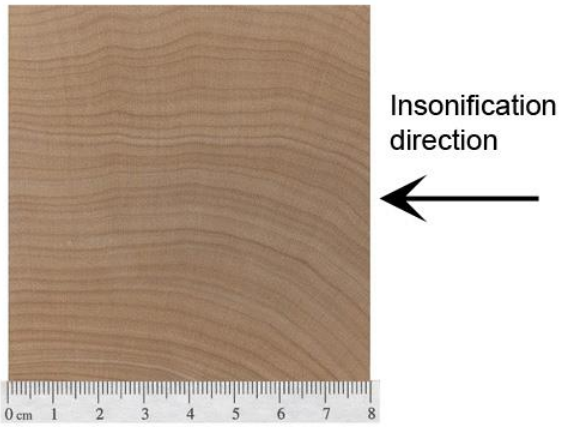

Figure 4-17 Wavy appearance of annual rings in Hard Maple (cross section).

Velocity values seem to overlap for different densities in the high to moderate density range in terms of wood degradation level, of 0.570g/cm^3 to 0.460g/cm^3. However, here coefficient of variation was between 0.73% and 0.94% for oak radial velocities, 0.73% and 1.29% for oak

tangential velocities, 0.33% and 0.65% for pine radial velocities, and between 0.72% and 0.93% for oak tangential velocities, throughout the whole degradation process. Coefficients of variation are notably lower compared to those in the literature regarding propagation velocities of ultrasonic waves in saturated clear wood, 10% for the radial and 6% for the tangential velocity (Bucur, 2005). They are also predominantly lower or about that of the experimental error, except that of oak tangential, which is slightly higher. This adds confidence to the ultrasound readings.

In Figure 4-15 pine velocities for both wood orientations show to follow the trend of oak but for lower density range. Grouping the experimental data received from both wood species, a strong fit into a linear relationship between wood density and ultrasound velocity irrespective of wood structure is noted (Figure 4-18). Coefficient of determination is very high in both axial velocities, r^2_{VR} = 0.92 and r^2_{VT}= 0.91 and significant at the 0.001 level (n = 450).

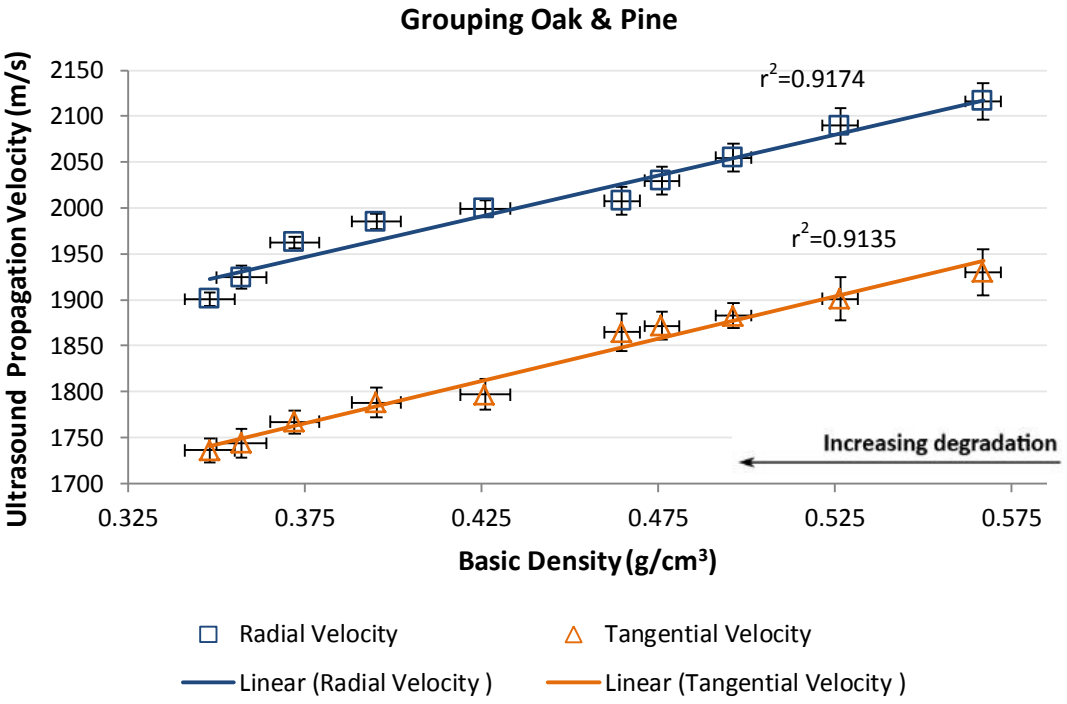

Figure 4-18 Relationship between wood density and ultrasound propagation velocity irrespective of wood structure for quarter sawn timber. Error bars is STD, n = 45 measurements per density level.

Merging oak and pine velocities in order to build the relationship between wood density and ultrasound propagation velocity, can be here endorsed. The significance of this integration is twofold; first, it adds strength to the relationship by multiplying the data points composing it and extends the density range under study irrespective of wood

structure used; and second, it proposes that estimating the state of preservation of a wooden shipwreck whilst *in situ* can be possible without being it necessary to know the source of the timbers, here oak or pine. Respectively, Jordan et al., (1998) note the influence of the annual rings' periodicity in the radial direction and the curvature of the rings in the tangential direction, on wave propagation, for it tends to obscure the species to species variation. Moreover, similarities in the behaviour of the ring-porous oak and low density softwoods in the acoustic field, have been noted by Bucur (1995). It is indicative that compared to diffuse-porous hardwoods, in the ring-porous oak the influence of the wide bundle of rays and the large diameter pore vessels, impede ultrasound propagation velocity in the tangential axis, while the same effect ensues from the ring-like arrangement of the pores for ultrasound velocity in the radial axis (Borst et al., 2012).

4.2.2.1.1 Results after alkali treatment

As reported in section 4.1.2.3, a treatment with 10% NaOH was applied twice to all fully pre-drilled oak and pine test-pieces aiming to reach lower density levels. These results are given in Table 4-5.

Table 4-5 Physical properties of waterlogged oak and pine wood after the two chemical applications with NaOH.

	NaOH			
	1st treatment		2nd treatment	
	Basic Density (g/cm^3)	MC_{max} (%)	Basic Density (g/cm^3)	MC_{max} (%)
Oak				
Mean	0.348	188	0.305	211
CoV(%)	1.84	2.83	1.65	2.73
Pine				
Mean	0.310	195	0.292	218
CoV(%)	0.14	0.56	2.22	3.02

Macroscopically all test-pieces from both wood species appeared slightly swollen after the chemical degradation as expected. Because of this, their dimensions were measured again, as in section 3.2.2, to secure accurate velocity measurements (3.9). An SEM image of an oak test-piece microstructural appearance after the treatment is given in Figure 4-19. The integrity of the cell wall has been disturbed due to the effect of the alkali on the chemical components of the wood. It is suggested that the loss of chemical components, led to the

exposure of the cellulose fibrils (Parameswaran, 1981). This is visible as a structural change on wood's surface as fibers appear to have been separated due to intra-wall failures.

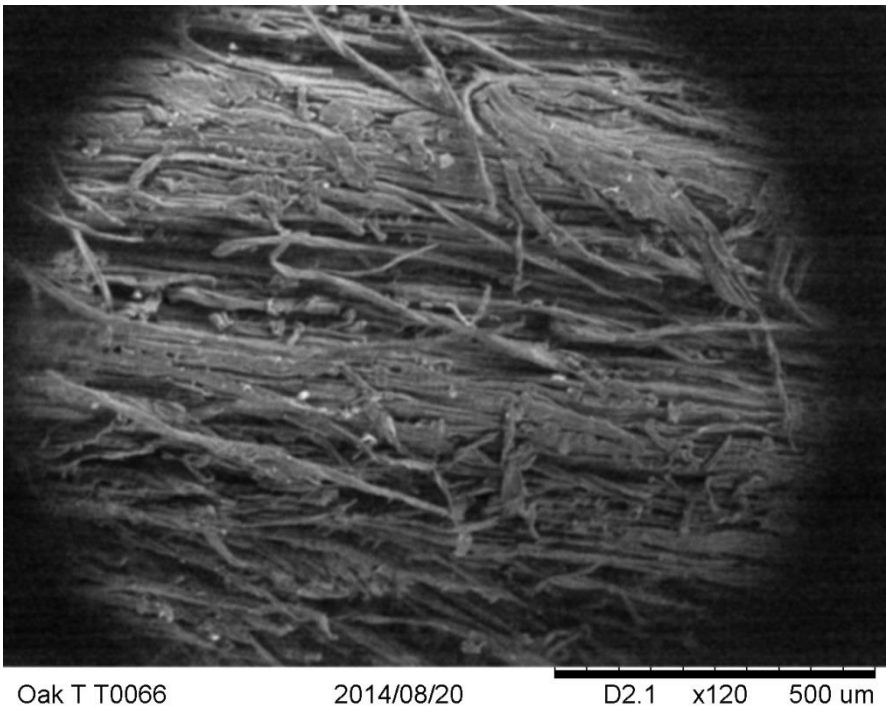

Figure 4-19 SEM image of treated oak test-piece TL plane with NaOH (first application). The integrity of the cell wall has been disturbed, visible here as loosened texture. Deposition of NaOH among fibers is also visible as scattered white crystals.

The NaOH first application caused a further density reduction from the fully pre-drilled state of the test-pieces, showing density loss of 39% for the oak and 27% for the pine compared to the "fresh" state. After the second application the test-pieces underwent an additional density loss, finally extending to 46% loss for the oak and 31% for the pine. This corresponds to RBD of 54% for the oak test-pieces and 69% for the pine test-pieces, hence both oak and pine are considered degraded with residual density less than 65-70% compared to "fresh" wood (Macchioni, 2003), after the completion of the whole artificial degradation process, mechanical and chemical. The higher resistance to alkali attack of the softwood pine as opposed to the hardwood oak (Wangaard, 1966), is here confirmed. After the first application oak retained 61% of its initial dry mass and pine 73%[11]. Respectively, Wangaard notes weight retentions of 81.5% for White oak and 86.7% for Douglas-fir, given

[11] Mass retentions were not corrected for possible retained NaOH.

here as a softwood reference as there was no pine included in his experiments. Given that the test-pieces are treated for the same period of time as in Wangaard, the differences noticed in the degree of degradation between the two studies, can be ascribed to the pre-drilled state of the test-pieces which permitted the chemical to have access throughout the whole of their volume. Additionally, the larger transverse surface area of the present test-pieces (6400 mm^2) allowed faster penetration times than in Wangaard's test-pieces (161 mm^2) (see section 3.2.2 for permeability in wood).

The ultrasound propagation velocities received from the chemically treated wood test-pieces are given in Table 4-6, and plotted in Figure 4-20 as a continuation of the velocities received after the drilling degradation.

Table 4-6 Ultrasound propagation velocities for oak and pine wood test-pieces after treatment with NaOH.

	Ultrasound Propagation Velocity (m/sec)			
	Radial		Tangential	
NaOH treatment	1st	2nd	1st	2nd
Oak				
Basic Density (g/cm^3)	0.348	0.305	0.348	0.305
Mean	1724	1691	1678	1650
Maximum	1760	1695	1701	1659
Minimum	1708	1687	1660	1641
CoV(%)	0.55	0.13	0.51	0.32
Pine				
Basic Density (g/cm^3)	0.310	0.292	0.310	0.292
Mean	1738	1701	1661	1640
Maximum	1750	1709	1684	1650
Minimum	1727	1696	1641	1629
CoV(%)	0.33	0.18	0.61	0.36

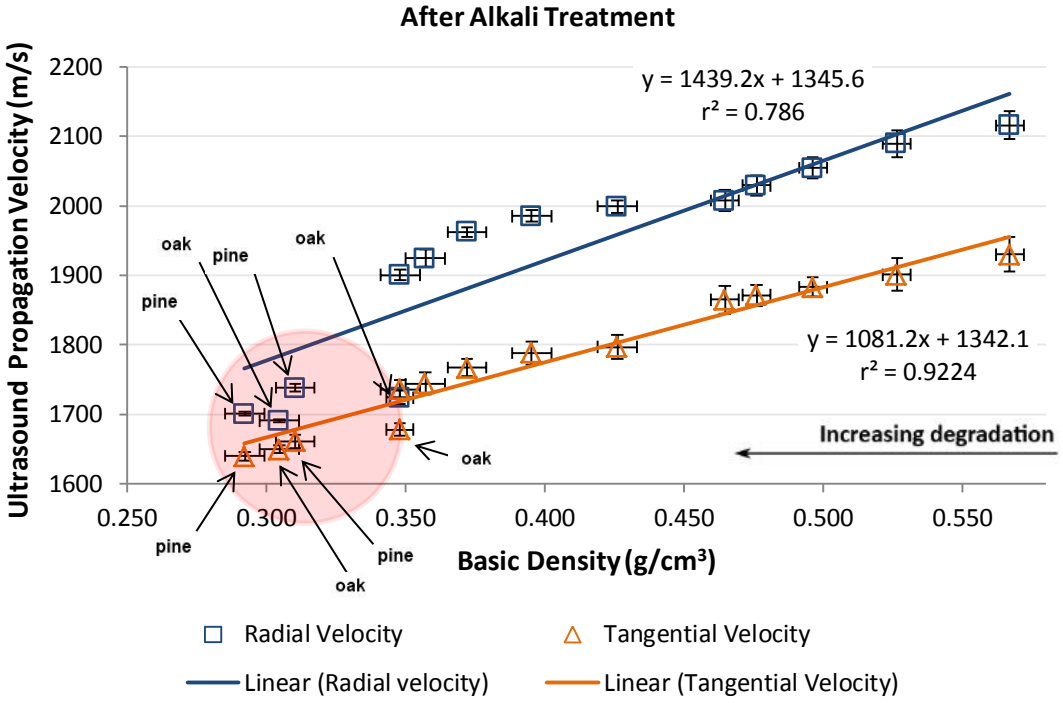

Figure 4-20 Relationship between wood density and ultrasound propagation velocity irrespective of wood structure for quarter sawn timber after the chemical treatments with NaOH (in red circle). Error bars is STD, n = 45 measurements per density level.

After the chemical treatment of the oak and pine wood test-pieces with the alkaline, a further reduction of the ultrasound velocity in both principal axes is observed. Referring to the literature in section 4.1.2.3, the use of alkali proved effective in downgrading the quality of the cell wall expressed by respective drops of wood's density and microscopic appearance. Effectively, the chemical treatment altered wood's elastic constant, seen in Figure 4-20 as a change of the velocity behaviour from that during the drilling treatment. This can be further supported in Figure 4-21 which shows the effect of the alkali treatment on the elastic properties (load/deflection) of lignum-vitae. Treatment with NaOH plasticises the wood and thus alters its sound properties. This has a direct reference to waterlogged archaeological wood degradation, where strength losses are not directly proportional to mass losses but degradation of the quality of the remaining substance also takes place (Schniewind, 1990) (section 2.4.2). It also resembles the spongy touch of degraded archaeological waterlogged wood.

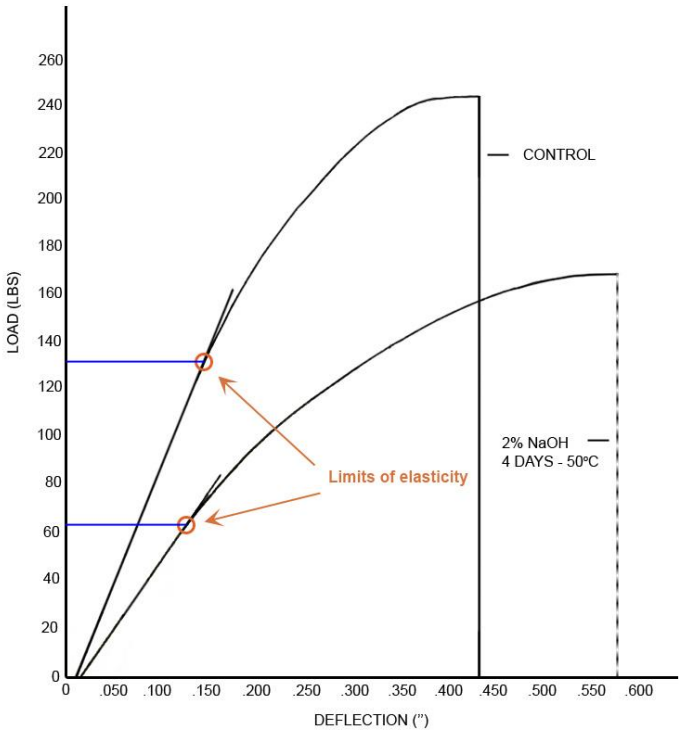

Figure 4-21 Effect of NaOH on bending properties of lignum-vitae (Extracted and modified from Wangaard, 1966: fig.3).

It is known that the ultrasound velocity is proportional to the continuity of crystalline regions in the cell wall (Oliveira et al., 2002), while cellulose is the stiffest component of the cell wall which critically affects its elastic properties (Borst et al., 2012), and hence ultrasound propagation times (Feeney & Chivers, 2001). The radial velocity for both wood species shows a greater affect by the chemical attack than the tangential oak and pine velocities which follow well the tangential regression. This can be expected as the radial direction consists of regions with larger amount of cellulosic material than the tangential (Oliveira et al., 2002) (section 2.5.1), hence is more prone to attack. The different response of the two axes to the chemical treatment is also reflected on the coefficient of determination of the slopes, that of the tangential being stronger than the radial. Both regressions are very strong, radial is r^2_{VR} = 0.79 and tangential r^2_{VT} = 0.92, and significant at the 0.001 level (n = 576).

An additional observation can be noted here. From Figures 4-18 and 4-20, there is evidence that as wood will degrade in the marine environment, it will transform to a more isotropic material. It can be expected that the influence of wood structure, characteristic to wood species, will gradually lose its effect on ultrasound propagation velocity. In Figure 4-18 it can be observed that till the application of the chemical treatment, the two axial slopes, V_R and

V_T seem to travel in parallel trends, with that of V_R constantly travelling in higher velocity range than that of the V_T. However, in Figure 4-20, after the completion of the chemical treatment, it seems that with further downgrading of the quality of the wood, the two slopes tend to meet. This is better explained in Figure 4-22, which shows that advancing the wood degradation, after both mechanical and chemical means of deterioration, the anisotropy between axial velocities across the grain tend to reduce, so in oak as in pine. At the same time so does structural differences between the two wood species.

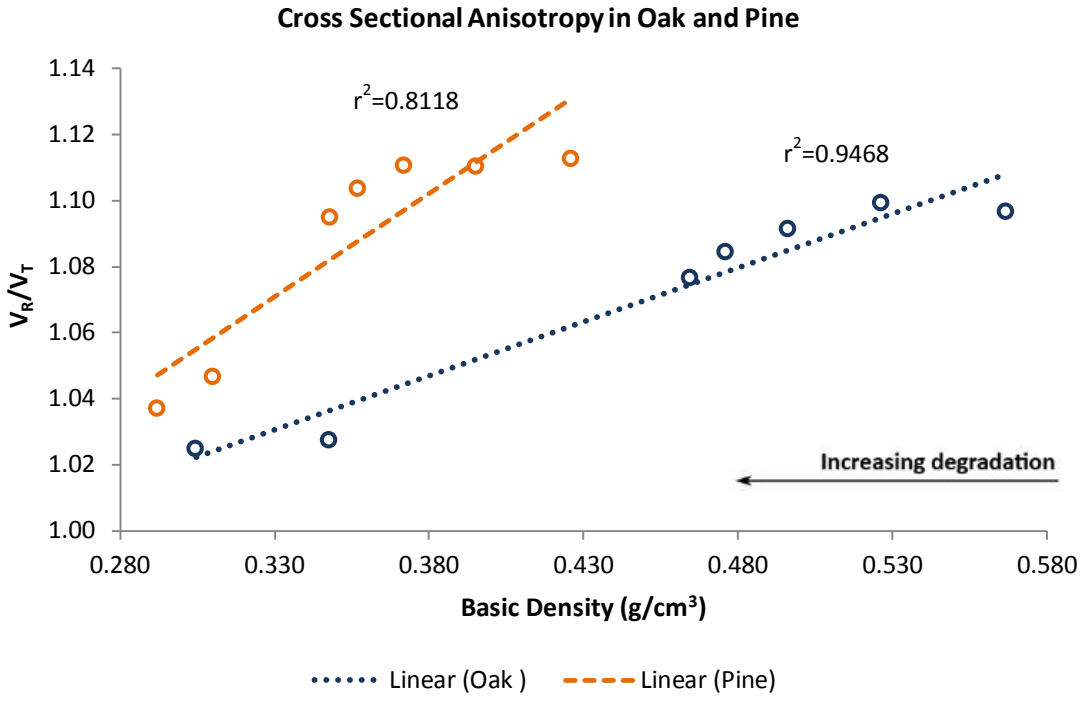

Figure 4-22 Cross sectional anisotropy in oak and pine advancing the artificial degradation.

This observation strengthens the present research's aim that, estimating the preservation state of waterlogged wood whilst *in situ*, may be possible with limited knowledge of a shipwreck's hull, for example its wood species, especially when wood is heavily degraded, holding less than 40% of its original density (classification by Macchioni, 2003).

4.2.2.2 Effect of insonification direction (on-axis/off-axis)

The second experimental variable for the establishment of the wood density – ultrasound velocity relationship, is the influence of insonification directions of ultrasound in relation to the Radial and Tangential wood axes, or else RT plane. The experiments started using oak test-pieces first. A new set of oak test-pieces is produced deriving from flat sawn timber (Table 4-2: Tree 3). In order to have comparable results between on- and off-axis

insonification ultrasound testing, the test-pieces of the new set have the same dimensions as the on-axis test-pieces, which is 80 X 80 X 50 mm (R X T X L). The cutting orientation for the off-axis test-pieces is determined by the diagonal, defined by a wood ray, of the square cross-section of a test-piece, which runs at a nominal 45° to either edge of the test-piece[12]. This is represented as an example on the cross-section of test-piece O72 in Figure 4-22. On a test-piece, two insonification sides are defined, where ultrasound measurements are taken, Side A (Figure 4-23) and Side B (Figure 4-24). With this cutting orientation, the insonification direction meets the wood ray direction at the three regions of interest per side (ROI: one at the centre of a test-piece, one to its left and one to its right), at various angles (φ'). Including all five replicates, on Side A angles average at 78° (±7°) and on Side B at 39° (±8°).

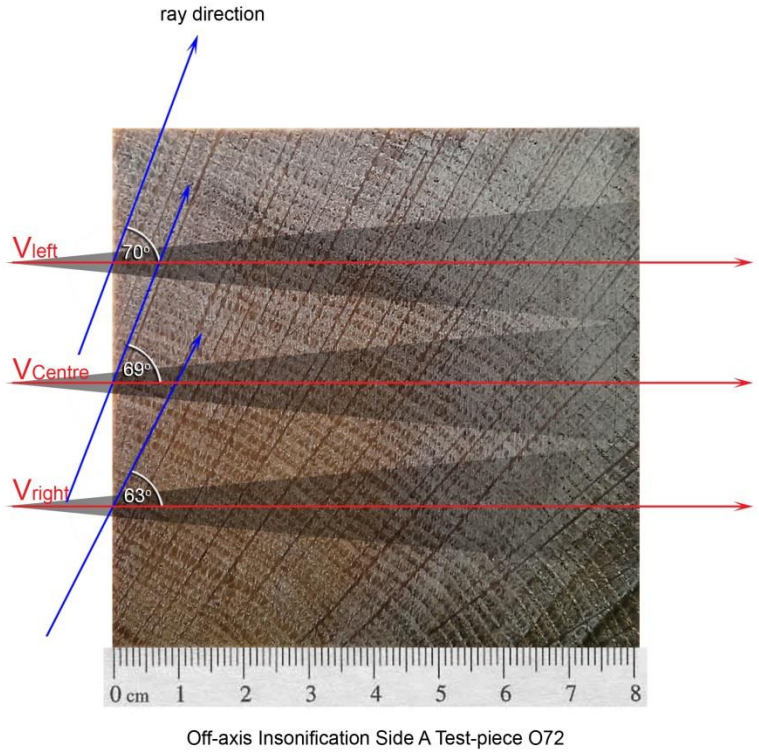

Figure 4-23 Oak flat sawn test-piece cross-section: Side A. Red arrows show the insonification direction. Blue arrows define the wood rays. Angle φ' in degrees is defined between the insonification axis per ROI and wood rays. V stands for velocity.

[12] Similar orientation is given in Figure 4-1, B for a rectangle cross-section of a piece of wood.

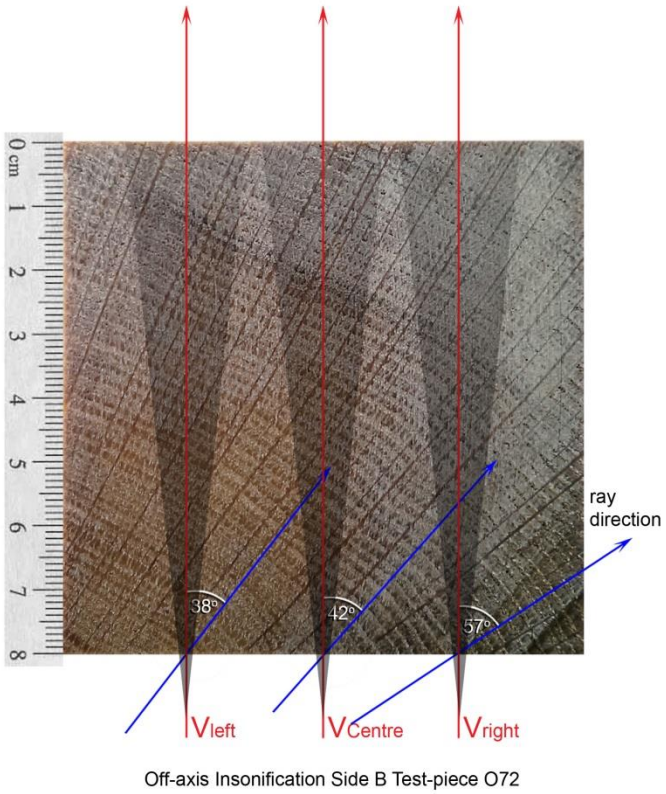

Figure 4-24 Oak flat sawn test-piece cross-section: Side B. Red arrows show the insonification direction. Blue arrows define the wood rays. Angle φ' in degrees is defined between the insonification axis per ROI and the wood rays. V stands for velocity.

As for the on-axis oak test-pieces (Table 4-2: Tree 2), the off-axis oak test-pieces are subjected to the artificial degradation by drilling sequential rows of holes of 3mm in diameter as described in section 4.1.2, followed by velocity measurements after each degradation step following the same procedures as detailed in section 4.1.3. Figure 4-25 give the results from the drilling procedure.

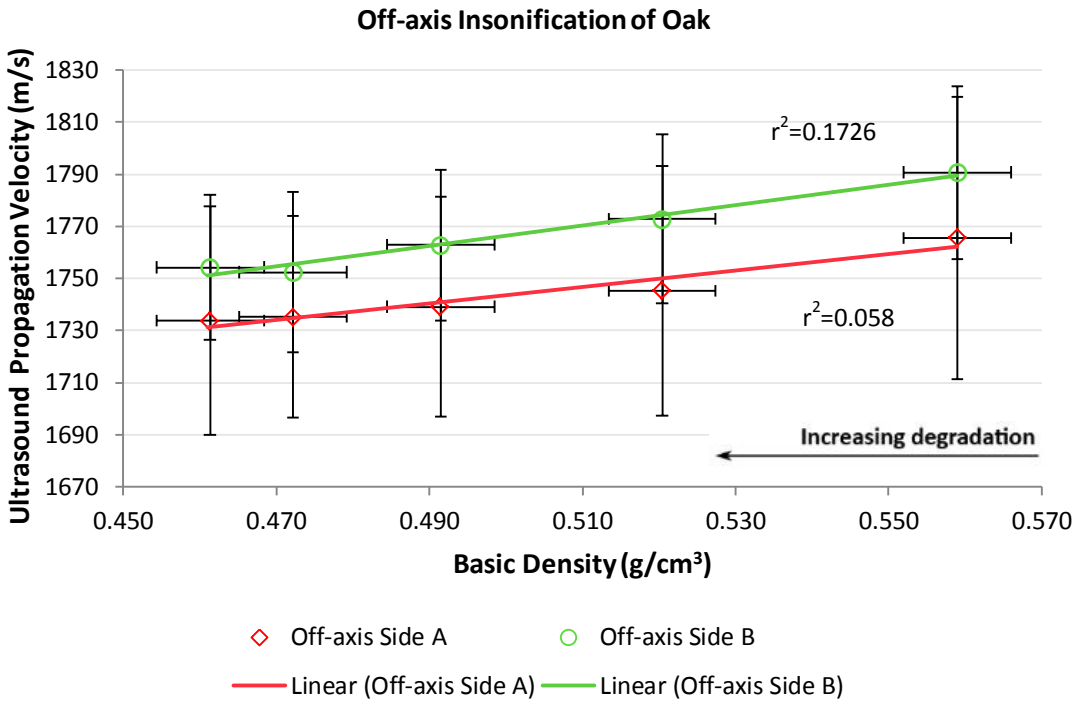

Figure 4-25 Off-axis ultrasound propagation velocities of oak test-pieces. Error bars is STD, n = 45 measurements per density level.

Compared to the oak on-axis insonification results (Figure 4-15 and Tables 4-3 and 4-4), two noticeable observations can be made from the off-axis insonification of the flat sawn oak test-pieces. Firstly, off-axis insonification gives constantly, from zero degradation and for the whole drilling degradation, lower velocity values than the on-axis insonification, even lower than the "clear" tangential, and second, yields a higher variability range of the ultrasound propagation velocity. Coefficient of variation is here even three times higher than in on-axis insonifications; it is between 2.23% and 3.07% in Side A and between 1.59% and 1.86% in Side B (Table 4-7). What is more, for both off-axis insonification sides there is little or no linear relationship established between wood density and ultrasound propagation velocity. There is a weak relationship between density and velocity for Side B, $r^2 = 0.17$, and a non-existent in Side A, $r^2 = 0.06$, significant at the 0.001 level.

Table 4-7 Off-axis ultrasound propagation velocities of oak test-pieces after drilling procedure.

	Off-axis ultrasound propagation velocity (m/sec)									
	Side A					Side B				
Basic density (g/cm^3)	0.559	0.520	0.491	0.472	0.461	0.559	0.520	0.491	0.472	0.461
Mean	1766	1745	1739	1735	1734	1791	1773	1763	1752	1754
Maximum	1894	1822	1809	1811	1834	1842	1836	1805	1800	1819
Minimum	1661	1646	1669	1659	1659	1707	1700	1704	1676	1703
CoV(%)	3.07	2.74	2.42	2.23	2.53	1.86	1.82	1.64	1.75	1.59

It is still intention to establish the relationship between wood density and off-axis ultrasound propagation velocity. The conventional theoretical model for wood is that of an "orthotropic like" solid (Bucur & Declercq, 2006; Feeney & Chivers, 2001). However, the simple orthotropic theory ignores the curvature of the growth rings (McIntyre & Woodhouse, 1986), when off-axis effects can cause inhomogeneous and complex state of stresses. Instead the assumption of polar orthotropy can offer a more detailed representation than a transversely isotropic model, as it distinguishes between the two perpendicular directions R and T (Figure 4-26) (Dahl, 2009: 21). A polar coordinate system is most representative near the centre of a tree trunk (pith), so that the growth ring curvature is obvious (ϕ), and a polar / cylindrical coordinate system can be plausible (*ibid.*).

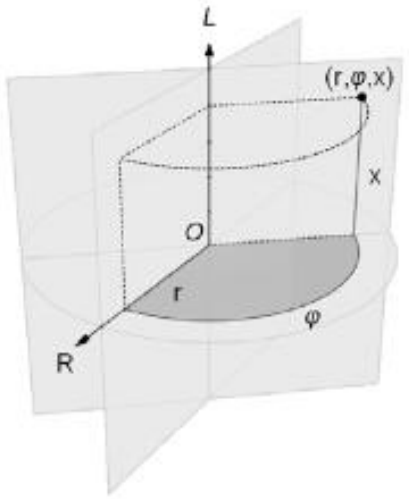

Figure 4-26 Polar coordinate system (Extracted from Dahl, 2009: fig.3-4).

Wood as a polar anisotropic material may not necessarily give the shortest travel time when considering curved paths (Aicher et al., 2001: 109). Sanabria et al. (2014) report significant route shifts of a normally incident ultrasound beam by an angle χ within wood due to the

growth ring structure. The degree of refraction is dependent on the angle φ between the insonification axis and the direction tangential to the growth rings. Note that angle φ represents in essence the same condition as the angle φ' as defined in Figures 4-23 and 4-24, between the insonification axis and the wood rays, for angle φ' is complementary to angle φ as supported by the theory of radial direction perpendicularity to the tangential direction. Sanabria et al. (2014) developed a two-dimensional Finite-Difference Time-Domain (FDTD) numerical simulation model, validated against analytical calculations, and showed that ultrasound beam deviates from the insonification direction for shifts ranging between -30° and 10°, showing a tendency to line up with the principal wood axes radial and tangential. Off-axis angle φ is changing continuously along the propagation path depending on path orientation and pith location (Aicher et al., 2001:), while longer travelling paths in wood aggregate the beam refraction phenomenon so that the wave propagation becomes progressively complicated, leading to spatial delays (Sanabria et al., 2014). However, no shifts (χ=0) are theoretically expected when insonification directions coincide with the principal R and T axes (*ibid.*). Figure 4-27 exemplifies the theoretical insonification beam shifts on oak test-piece O64 based on Sanabria et al.

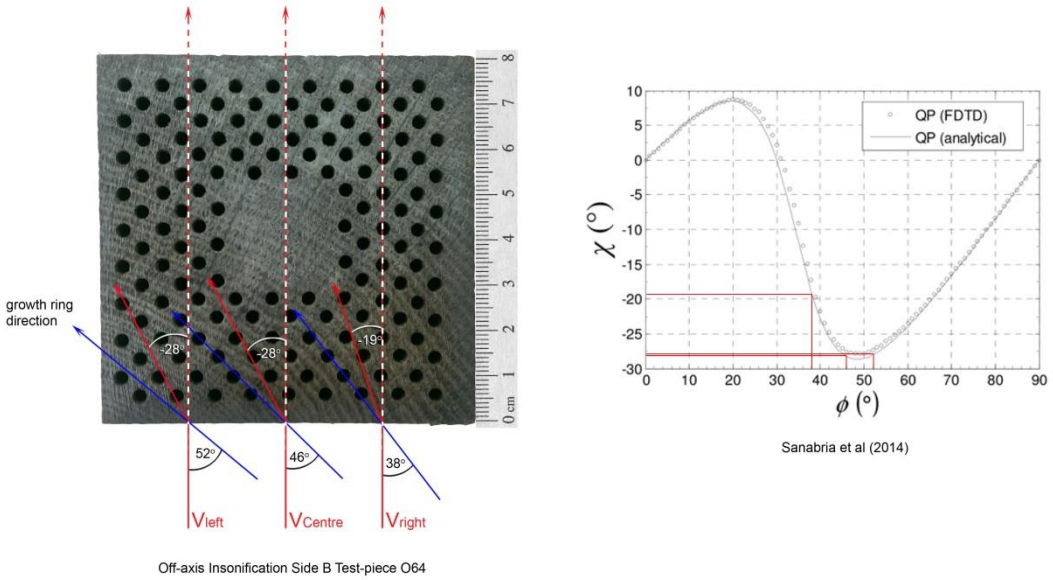

Figure 4-27 Ultrasound beam deviates from the insonification direction by a ϕ-dependent angle χ, exemplified on test-piece O64, Side B (3rd drilling step). Right hand side figure from Sanabria et al., 2014: fig.2b.

In Figure 4-27 it can be observed that the diverted insonification beams tend to travel parallel with the lines formed by the drilled holes on an off-axis test-piece. But this is a different hole arrangement compared to the on-axis insonifications, where theoretically

ultrasound wave travels in straight lines based on Sanabria et al. Hence, it is suggested that part of the propagated ultrasound wave is not affected by the same amount of holes as it is on the on-axis insonifications. As a complication, a relationship between wood density and ultrasound velocity could not be established for the off-axis insonification directions as in the on-axis.

To further investigate the existence or not of a relationship between the two variables it is decided to change the drilling procedure so that holes will be in line between successive rows. Ultimately, at the end of the drilling procedure, the hole arrangement will be seen as a shift of 45° from the on-axis final arrangement, as depicted in Figure 4-28. This should now allow comparable off-axis results with those on-axis, as the sound beam will theoretically encounter the same hole arrangement as on the on-axis insonifications (Shulka & Parkash, 1990: 85, fig.15).

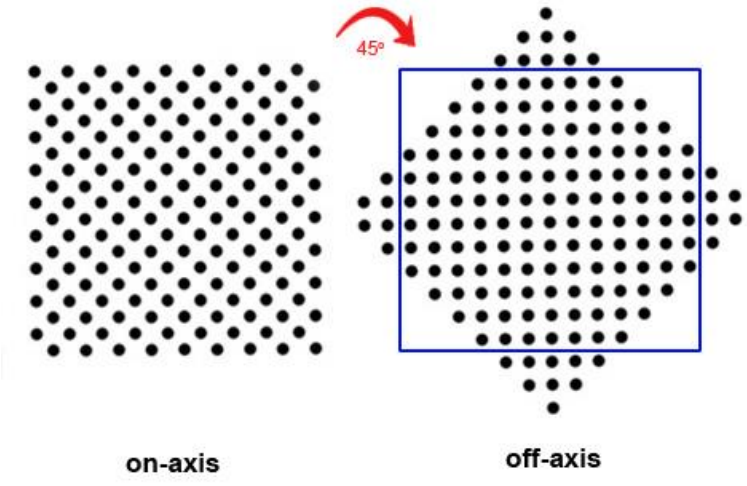

Figure 4-28 New hole arrangement after rotation by 45°.

A new set of five flat sawn waterlogged oak test-pieces are used for this new testing deriving from the same Oak Tree 3 (Table 4-1). In the new drilling array the distances between holes centres is set to 5.5 mm and the distances between rows to 9 mm. This new arrangement misses one degradation step on the advantage of creating as many as possible comparable degradation steps with the on-axis test-pieces, having the same number of holes per drilling session. Results from the new off-axis ultrasound testing are presented in Figure 4-29.

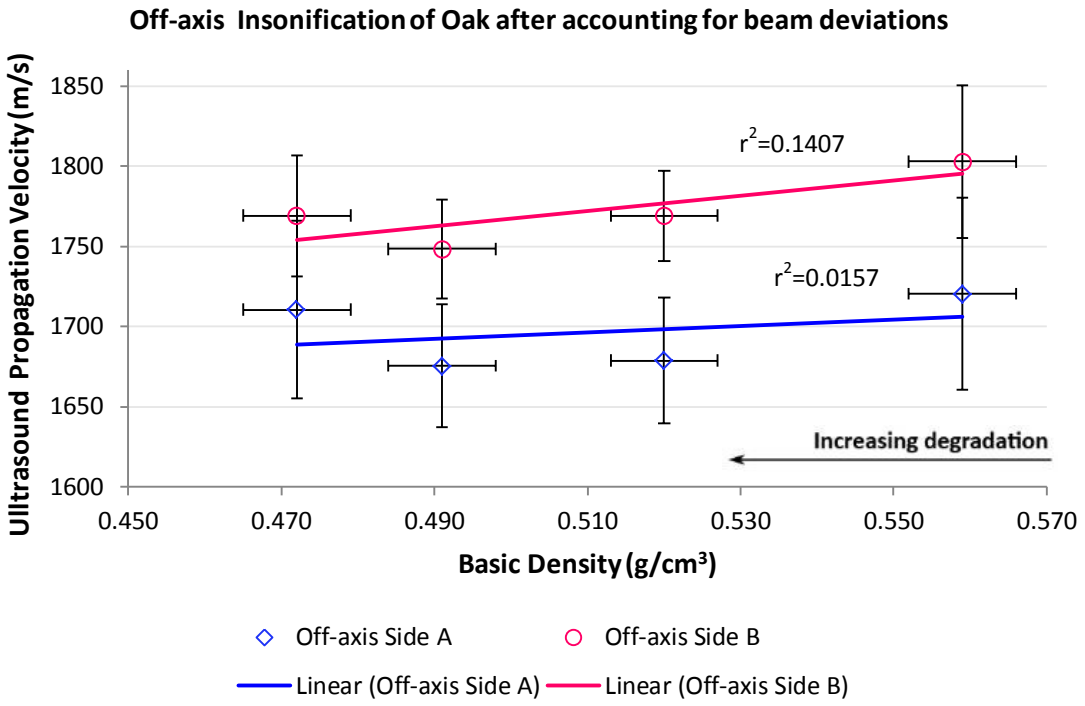

Figure 4-29 Off-axis ultrasound propagation velocities of oak test-pieces after accounting for beam deviations. Error bars is STD, n = 45 measurements per density level.

Results show that even after accounting for the beam deviation due to the growth rings curvature interference, and hence, the rearrangement of the drilled holes, no relationship between wood density and ultrasound propagation velocity at off-axis insonifications is found. As shown previously in Figure 4-25, here too a weak relationship between density and ultrasound velocity exists for Side B, r^2 = 0.14, and a non-existent for Side A, r^2 = 0.02, both significant at the 0.001 level. Coefficient of variation remains higher than in on-axis insonifications, between 2.29% and 3.48% in Side A and between 1.60% and 2.65% in Side B (Table 4-8). The higher variability of the ultrasound velocity obtained for the off-axis velocities is likely to derive from strong scattering of the beam energy at the earlywood and latewood transitions (Sanabria et al., 2014). The long travelling paths of ultrasound through the test-pieces thickness of the present study has to be also considered as the wave propagation becomes increasingly complex with longer propagation paths in wood (Sanabria et al., 2014).

Table 4-8 Off-axis ultrasound propagation velocities of oak test-pieces after accounting for beam deviations.

	Off-axis ultrasound propagation velocity (m/sec)							
	Side A				Side B			
Basic Density (g/cm³)	0.559	0.520	0.491	0.472	0.559	0.520	0.491	0.472
Mean	1720	1679	1675	1710	1803	1769	1748	1769
Maximum	1827	1761	1772	1818	1887	1835	1828	1847
Minimum	1634	1618	1616	1637	1653	1734	1706	1714
CoV (%)	3.48	2.34	2.29	3.25	2.65	1.6	1.77	2.14

Nevertheless, the variability in velocity and the failure of establishing a relationship between wood density and ultrasound propagation velocity off-axis proves the complexity of wave propagation phenomena for flat wood plates (McIntyre & Woodhouse, 1984). Figure 4-30 quotes evidently the higher variability in velocity within ROI in off-axis compared to on-axis insonifications for oak.

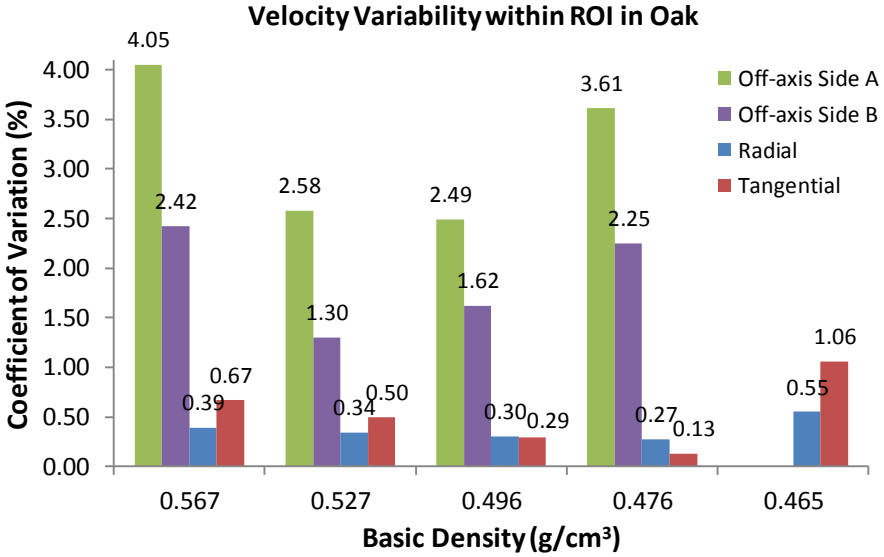

Figure 4-30 Velocity variability within ROI in quarter and flat sawn oak test-pieces.

Furthermore, the possibility that the technique itself, i.e. the drilling procedure, could have contributed to the high coefficient of variation in the off-axis velocities, was investigated. If variation in velocity had increased because of the drilling procedure, this would make it inappropriate to use as a technique. The solution was to use the relative variation in velocity (RVC) as applied by Secco et al. (2012), using Equation 4.2:

$$RVC = \left[\frac{V_{reference} - V_{measured}}{V_{reference}}\right] X\ 100 \qquad (4.2)$$

Where, $V_{reference}$ is the velocity of a test-piece at zero degradation (no holes) and $V_{measured}$ is the measured velocity in the drilled test-piece at each degradation step. The percentage of hollowness represents the amount of loss in wood mass via drilling in relation to the intact test-piece (Table 4-2: Tree 3).

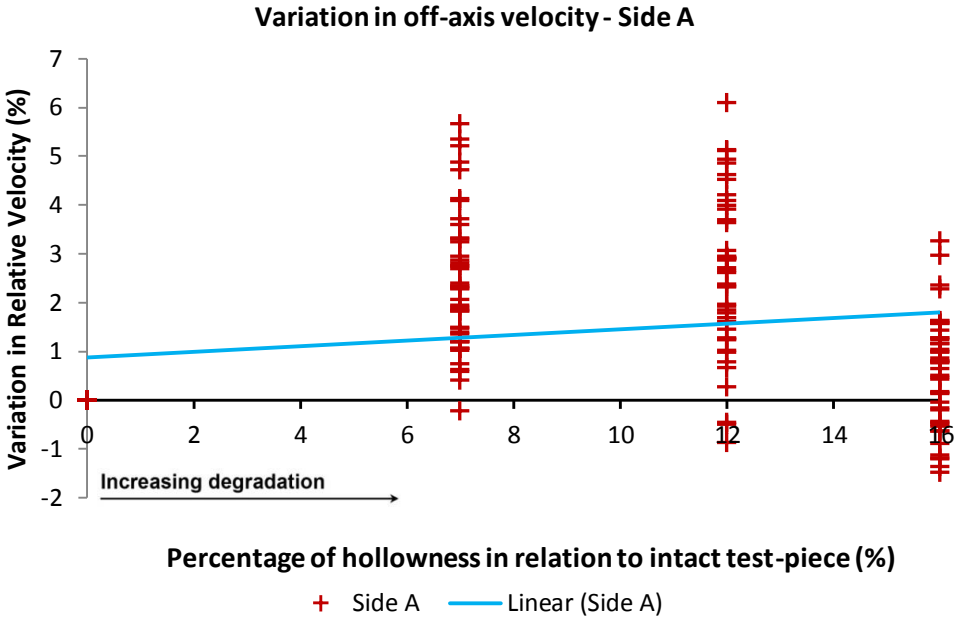

Figure 4-31 Variation in relative velocity (RVC) for off-axis Side A insonification of oak test-pieces during drilling procedure (n=45 per percentage hollowness).

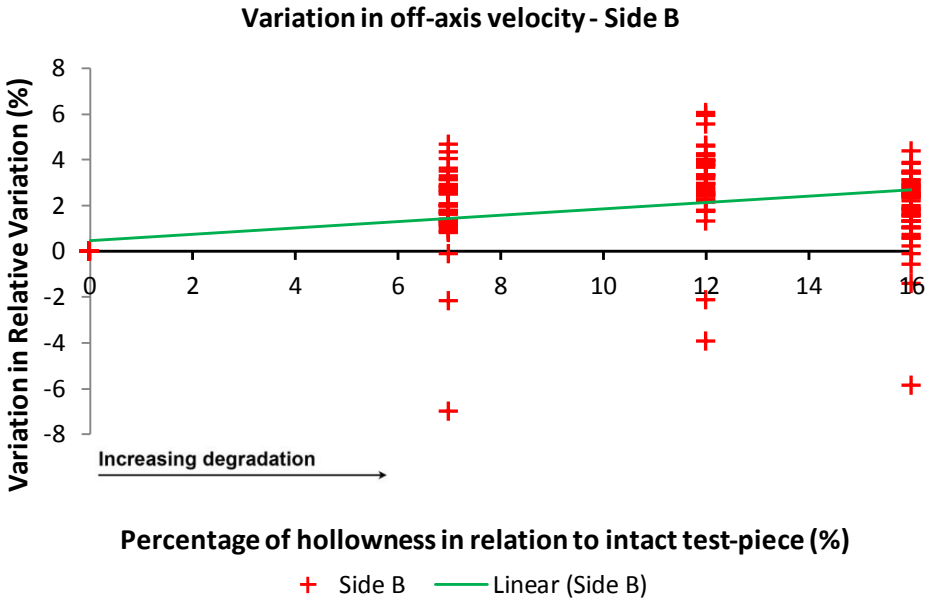

Figure 4-32 Variation in relative velocity (RVC) for off-axis Side B insonification of oak test-pieces during drilling procedure (n=45 per percentage hollowness).

Figures 4-31 and 4-32, point that the magnitude of the velocity variation is found to be irrelevant to the drilling procedure. In other words, the variation in velocity remains high although wood mass is continuously removed from the wood test-pieces. Overall, results address the dependency of the ultrasound off-axis propagation velocity on the continuous changing angle φ due to the curvature of the growth rings and the test-piece size. Although the present study was capable to receive velocities through the off-axis oak test-pieces when undegraded, it was not possible to see significant changes in ultrasound velocity for a range of densities (degradation steps) under this cutting orientation. Ultrasound propagation velocity is found to be a very weak predictor of wood density in off-axis orientations during wood degradation, as opposed to on-axis. This proved, it is found unnecessary to further run off-axis insonification experiments for pine test-pieces.

4.3 Chapter conclusions

The aim of this experimental phase was the establishment of the relationship between waterlogged wood density and ultrasound propagation velocity. The experimental variables set where the ultrasound insonification in relation to Radial and Tangential tree growth axes (on- and off-axis), as well as the wood structure, here specifically selected between oak and pine. The following conclusions can be drawn:

1. A strong relationship has been found between ultrasound propagation velocity and wood density for on-axis Radial insonification $y = 1439.2x + 1345.6$, $r^2 = 0.786$
2. A strong relationship has been found between ultrasound propagation velocity and wood density for on-axis Tangential insonification $y = 1081.2x + 1342.1$, $r^2 = 0.9224$
3. The relationship between ultrasound propagation velocity and density seems to be independent of wood anatomical features characterising hardwood or softwood species.
4. Ultrasound waves travel faster in Radial than in Tangential direction. It seems that the orientation and the abundance of radial parenchyma is a decisive factor.
5. For degraded wood (here oak and pine), with a density range between 0.567g/cm^3 (“fresh”) and 0.292 g/cm^3 (degraded), V_R ranges from 2116 m/s to 1691 m/s, and V_T ranges from 1930 m/s to 1640 m/s.
6. The relationship between ultrasound propagation and wood density shows to be stronger in the Tangential direction than in the Radial direction.

7. Advancing the degradation wood becomes more isotropic across the grain as indicated by the reduction of V_R/V_T ratio.
8. Off-axis insonification of "fresh" oak results in lower ultrasound propagation than on-axis insonification, $V_L = 2116$ m/s >> $V_T = 1930$ m/s > $V_{RT} = 1770$ m/s.
9. No significant relationship between wood density and ultrasound propagation velocity has been found in off-axis insonification. The coefficient of variation has been found to be much higher in off-axis insonification velocity measurements than on-axis. The coefficient of variation does not seem related to the test-piece hollowness or else degradation procedure.
10. The ultrasound propagation velocity is significantly affected by the insonification angle, i.e. the angle formed between wave propagation path and wood growth rings.

Chapter 5

Assessment of Wood Density – Ultrasound Propagation Velocity Relationship

5.1 Introduction

The target of the third experimental phase of the present research is the evaluation of the reliability of the relationships established in Chapter 4, between wood density and ultrasound propagation velocity, for real archaeological material. For this purpose a number of archaeological waterlogged wood samples, are provided by the National Museum of Denmark (NMD) for testing with ultrasound.

5.1.1 Sample documentation

A total of 23 waterlogged archaeological samples available from the NMD collection, are rated as appropriate for the experiments. The archaeological samples derive from both land and sea archaeological excavations in Denmark. In order to properly interpret the results from testing the archaeological wood samples, and to assess the adequacy of the relationship built from the artificial degradation of the control wood test-pieces, the rationale is to hold the same experimental variables from Chapter 4, which are:

1. Samples will chiefly derive from oak and pine wood species.
2. Wood sample's basic density has to be within the range of studied densities, i.e. between 0.567 g/cm^3 – 0.292 g/cm^3.
3. Wood samples with a thickness greater than 80mm and not less than 20mm are excluded from testing. The maximum dimension is defined by the maximum dimension of the control wood test-pieces as set and tested in previous Chapters 3 and 4, i.e. 80 X 80mm (R X T). The minimum dimension is set by the number of wavelengths passing through the wood under test,

enough to secure pure compressional wave propagation, as explained in section 3.2.3.1. The present study was able to produce reliable and reproducible results for a number of twenty wavelengths travelling across the wood grain and five along the wood grain (section 3.2.3.1). Based on this, using the highest velocities received from the radial and tangential wood axis (data from Figure 4-17), and operating at a nominal frequency of 500 kHz, the number of wavelengths passing through a 80mm thick wood sample is twenty, and through 20mm is five, hence setting the limits of samples' dimensions

4. Additionally, sample size has to fit in the water test-tank, in the space between the transducers (330mm), and comply with set experimental ultrasound testing prerequisites, as is to have adequate space to place the sample to the far field (section 3.2.3.2) and avoid edge effects (section 3.2.3.3).
5. Samples have to have a more rectangular and not cylindrical shape, following the shape of the control wood test-pieces.
6. Cut orientations will include quarter-, flat- and rift sawn, and exclude tree disks.

Table 5-1 summarises the information per selected archaeological wood sample as provided by the NMD, except that of wood species, sawn orientation, and visible type of macro-organism attack, assessed by the writer.

The majority of the samples are identified as oak (*Quercus sp.*), together with one maple (possibly *Acer campestre*, *Acer pseudoplatanus* or *Acer platanoides*) and one spruce (possibly *Picea abies*) species. The basic density of the oak species ranges between 0.531 g/cm^3 to 0.299 g/cm^3 for the most degraded. The basic density for the maple sample is 0.409 g/cm^3 and for the spruce sample it is 0.309 g/cm^3. Compared to the density of fresh wood counterparts (Bucur, 1995), oak samples indicatively show a density reduction of approximately 12 – 50%, the maple 34% and the spruce 36%. NMD calculates basic densities by using 50 mm complete sections from each wood sample (Section 3.2). The wood structure can be generally described as degraded (Macchioni, 2003). Attack from gribbles and Teredo is visible on the outer surfaces and cross-sections of a number of samples, as given in Table 5-1 (Figure 5-1). Probing the wood surface with a pin reveals that the majority of the samples present a degraded and soft outer layer of approximately 10 mm on average,

and a more solid inner core. This is visible as a discolouration of the outer part (dark colour) on the cross-section of the samples, indicatively shown here for samples S272 and S293 (Figure 5-1). On others, as in the maple sample, the pin penetrates without any resistance further inside the wood mass, signifying advanced wood degradation by the activity of microorganisms.

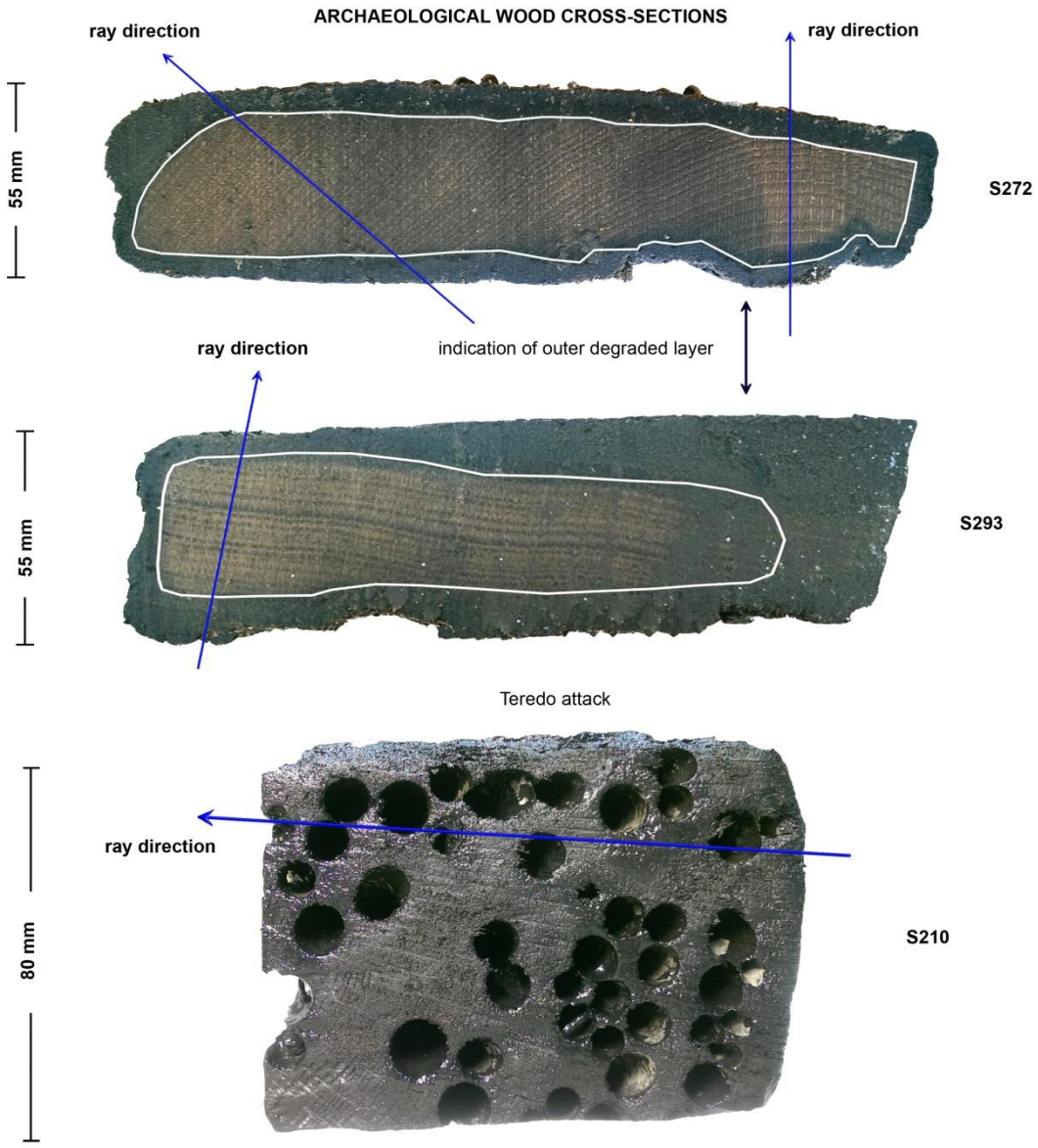

Figure 5-1 Degradation patterns on archaeological wood samples from the National Museum of Denmark, as seen in their cross-section. All three samples are identified as oak species. S272 and S293 are slices cut off with a band saw from the original sample.

Table 5-1 Summary of the origin, wood species, basic density, sawn orientation and visible macro-organism attack of the archaeological wood samples used.

Archaeological Wood Sample	Wood Species	Basic Density* (g/cm^3)	Sawn Orientation†	Origin		Macro-organism Attack
				Sampling Sites	Burial Environment	
S200	Oak	0.531	flat	-	-	Teredo (sporadic)
S289	Oak	0.467	flat	Femern Bælt	Sea	Teredo (isolated) & Gribble (heavy)
S184	Oak	0.462	flat	B&W	Land	-
S205	Oak	0.452	flat	-	-	-
S294	Oak	0.448	flat	Femern Bælt	Sea	-
S292	Oak	0.448	flat	Femern Bælt	Sea	Teredo (sporadic) & Gribble (sporadic)
S178a	Oak	0.427	quarter	Nybro, stolpe 2	Land?	-
S185	Oak	0.416	flat	Nybro	Land?	-
S226	Maple	0.409	quarter	-	-	-
S299	Oak	0.407	quarter	Femern Bælt	Sea	Gribble (isolated)
S272	Oak	0.396	flat	Femern Bælt	Sea	Gribble (isolated)
S004	Oak	0.388	flat	Nydam?	Land (fresh water)?	Gribble (heavy)
S094	Oak	0.382	flat	Nydam?	Land (fresh water)?	-
S293	Oak	0.382	quarter	Femern Bælt	Sea	Gribble (isolated)
S290	Oak	0.361	quarter	Femern Bælt	Sea	Teredo (isolated)
S211	Oak	0.352	flat	Kolling kog?	Land / beach sand (ship)?	-
S210	Oak	0.333	quarter	Kolling kog	Land / beach sand (ship)	Teredo (heavy)
S258	Oak	0.316	flat	-	-	-
S241	Oak	0.316	quarter	-	-	-
S105	Oak	0.309	flat	Nydam?	Land (fresh water)?	-
S213	Spruce	0.309	flat	Kgs. Nytorv KBM	Land	-
S096	Oak	0.299	quarter	Nydam?	Land (fresh water)?	-
S271	Oak	?	flat	Femern Bælt	Sea	Gribble (heavy)

* From NMD, † Figure 2-4

The cutting orientation of all samples is also identified at their cross-sections. In Table 5-1 the sawn orientation is derived from Figure 2-4 (section 2.2.2): with a flat sawn orientation describing a cut which includes the pith or part of it as is a 'B' board in Figure 2-4, or exclude it as a 'D' board; while a quarter sawn orientation corresponds to an 'A' or 'C' board. A 'B' board will give all types of insonification directions, i.e. radial, tangential and off-axis; a 'D' board will give off-axis; an 'A' tangential; and a 'C' radial (Figure 5-1). Sample S272 is classified to have a flat sawn orientation (Figure 2-4, D board) and can give both radial and off-axis insonifications as sound travels through its thickness. Sample S293 (Figure 2-4, D board) gives off-axis insonifications and S210 tangential insonifications (Figure 2-4 A board).

5.2 Ultrasound testing of waterlogged archaeological wood samples

5.2.1 Method

5.2.1.1 Sample thickness measurement at insonification point

For accurate velocity measurements, it is important to be able to measure sound's travelling distance through the archaeological material with a good accuracy. Given the archaeological samples' non symmetrical shape and rough surfaces, measuring the thickness at the position where the ultrasound will travel, can be problematic using conventional digital vernier callipers. It is in particular very difficult to take a measurement from the centre of wide samples as the callipers in hand were too short to reach, or could not embrace the uneven sides of the sample because of the fixed shape of the external jaws.

In order to resolve this problem this present study used a non-contact laser scanner, FARO Edge and Laser Line Probe, for 3D documentation of the archaeological waterlogged samples, provided at the National Oceanography Centre, Southampton (Figure 5-2). The scanning allows the acquisition of high resolution images, consisting of up to 3,000,000 data points contouring an individual wooden sample. Hence, it is possible to overcome the irregularity of the surfaces and be able to measure the thicknesses of the wooden samples at any position to the nearest 0.0001mm (Figure 5-3). The image is then processed using Geomagic® Control interface where it is possible to virtually cut a sample at any desired position and measure the travel path of sound through the wood sample (Figure 5-4).

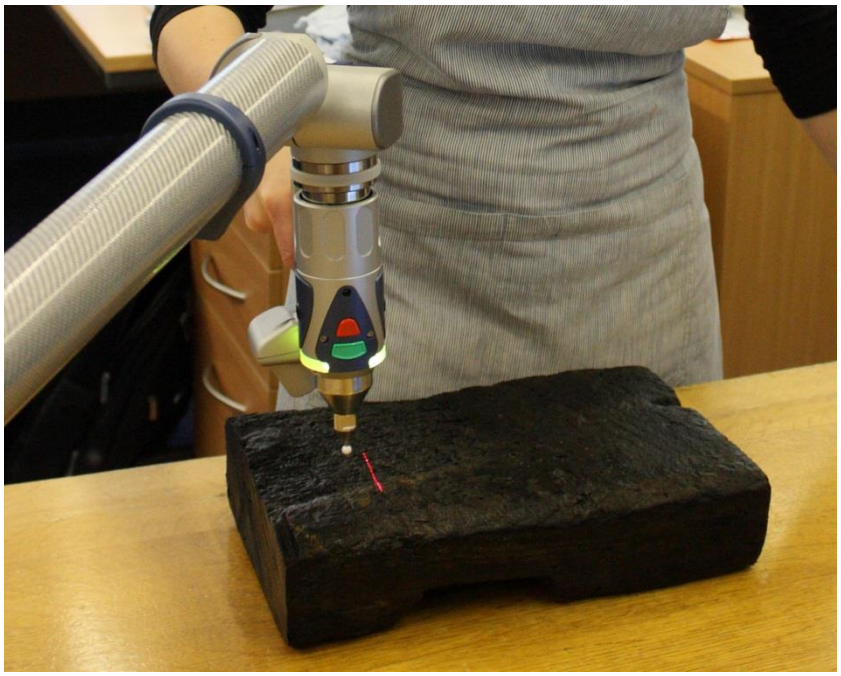

Figure 5-2 Scanning waterlogged archaeological wood with FARO Edge and the Laser Line Probe.

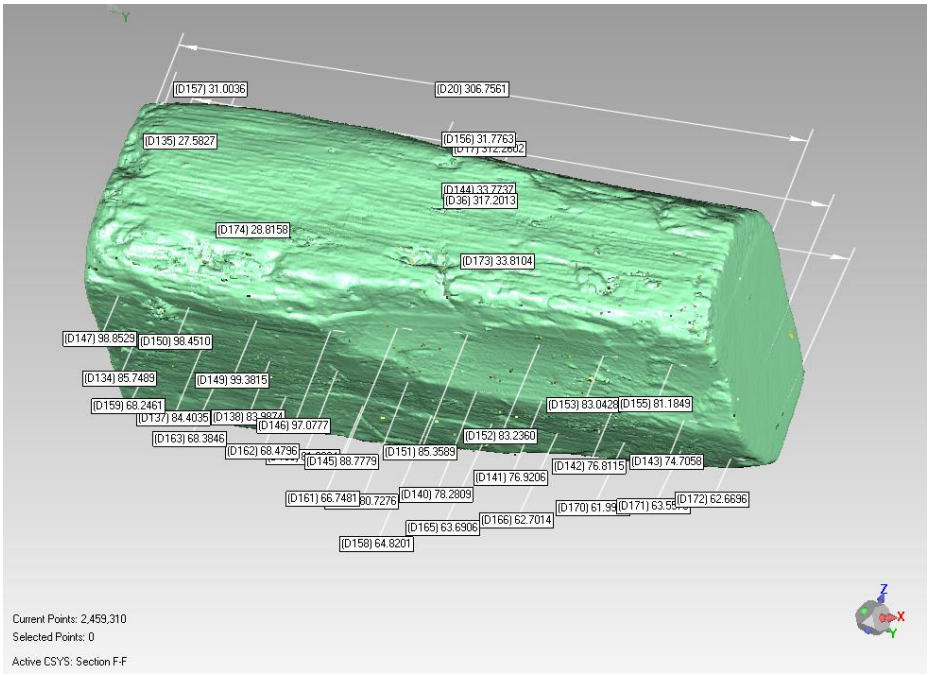

Figure 5-3 3D image documentation of archaeological sample S178a acquired with FARO Edge laser scan (dimensions shown in mm).

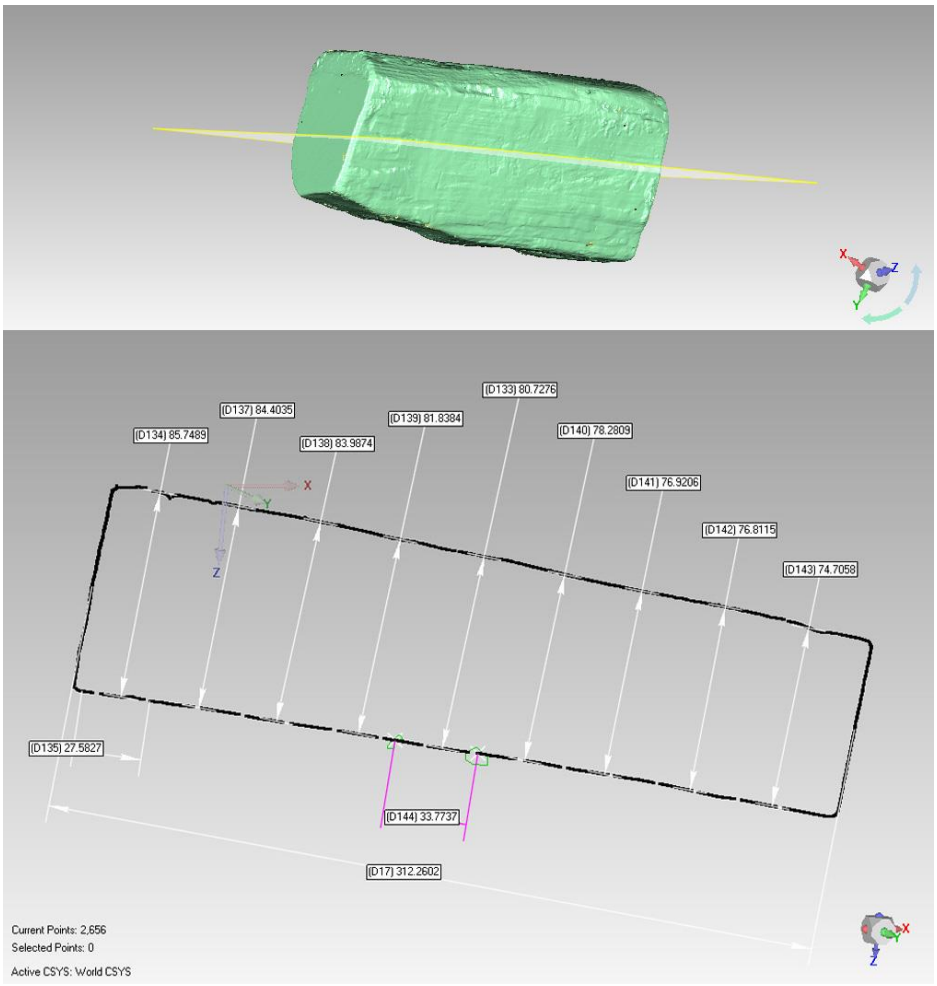

Figure 5-4 Measuring thicknesses (sound travelling paths) on a cross-section from sample S178a (dimensions shown in mm).

5.2.1.2 Ultrasound measurement

All ultrasound measurements are taken using the same set-up and settings as described in previous Chapters 3 & 4 (Figure 5-5). Before the beginning of a set of measurements on the wood samples, the system is calibrated with the use of the brass standard. Calibration measurements are carried on regularly throughout the measurement period. Pins are used to indicate the insonification positions, or regions of interest (ROI), on a wood sample, using the thickness measurements from the 3D images (Figure 5-6). Each pin is removed before the measurement is taken, although its presence is found to not affect the measurement. Repetition of measurements on three samples proved that the accuracy of the velocity measurements ranges between 0 to ± 23 m/s. Thus, each insonification position is ultrasonically tested once. Results are given in Table 5-2 for all samples.

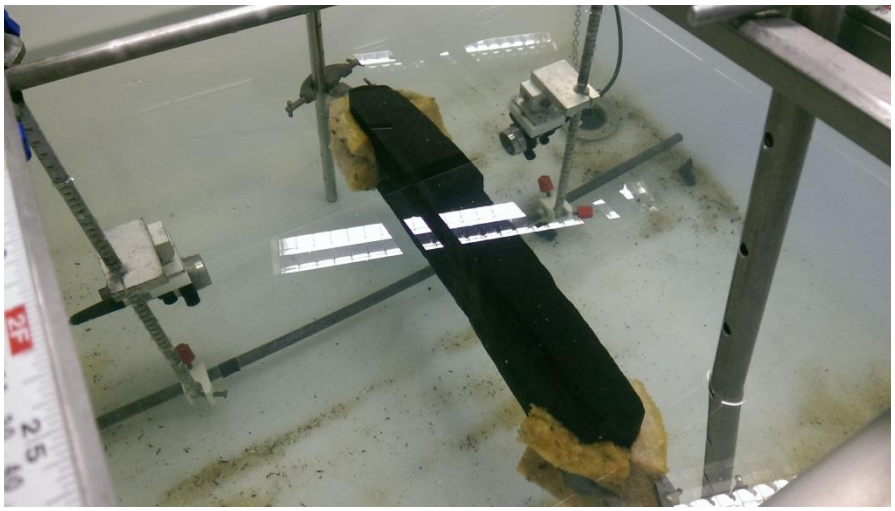

Figure 5-5 Ultrasound testing setup of archaeological wood sample in the water test tank.

Figure 5-6 Marking ROI on archaeological sample S178a using pins before ultrasound testing based on 3D documentation.

5.2.1.3 Measuring point description

As given in Table 5-1, the cutting orientations of archaeological samples include quarter and flat sawn types. Within each sample, a number of ultrasound measurements are executed on set regions of interest. The insonification positions are categorised based on the insonification in relation to Radial and Tangential tree growth axes (on- and off-axis); or else, the angle between the insonification axis and the wood rays (section 4.2.2.2). Figure 5-7 shows an exemplified flat sawn wood cross section, which features the three different orientations as met on the provided archaeological wood samples. Specifically, closer to the pith of the tree (Position 1) the insonification axis coincides with the radial axis, closer to

the outermost wood layers (Position 3) the insonification axis coincides with the tangential axis, while the area lying in between (Position 2) matches the off-axis insonifications.

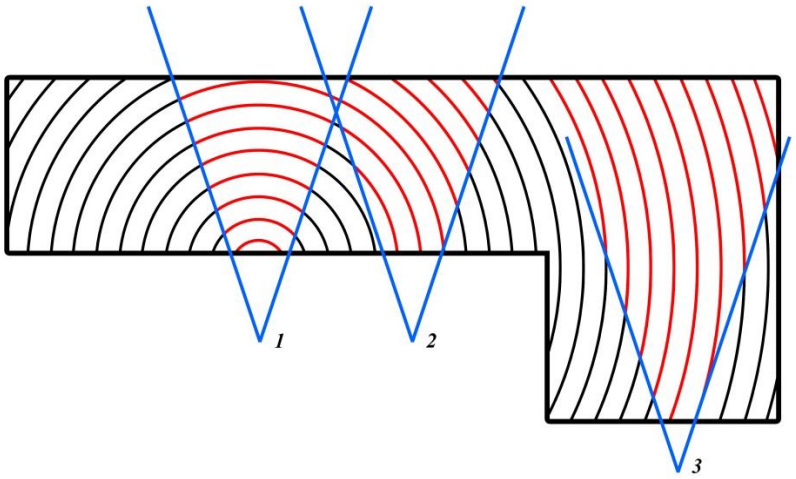

Figure 5-7 Exemplified flat sawn wood cross section. Aiming at positions 1 ("clear" radial) and 3 ("clear" tangential) represents a quarter sawn cut, while aiming at position 2 represents a rift sawn cut.

The insonification angle on a region of interest (ROI) on a sample is defined as the angle between the insonification direction and the wood ray direction, taken at the sample's insonified surface at that position (Figure 5-8 and Table 5-2). Angle measurement is executed digitally on orthotropic photographs taken from the cross-section of all samples.

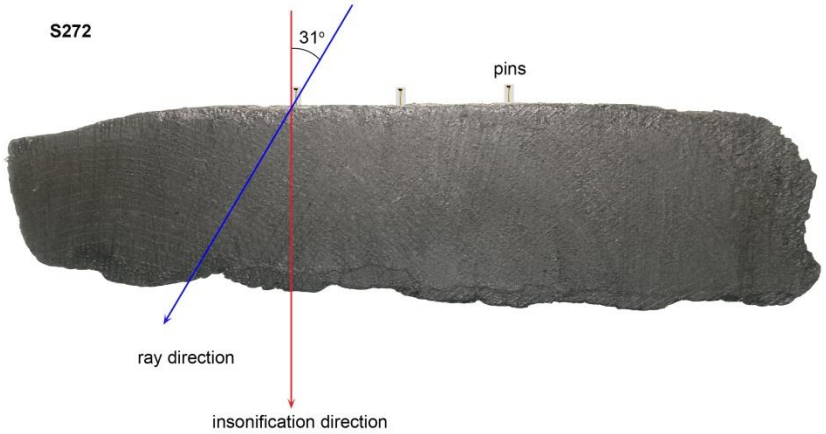

Figure 5-8 Angle between ray direction and ultrasound insonification direction measured at the sample's insonified surface at each insonification position defined by the pins, here exemplified on the cross-section of sample S272.

5.2.1.4 Density re-measurement

At this stage of the research within the controllable laboratorial conditions, it is decided to take new density measurements deriving exactly from the insonification position on the sample in order to determine accurately the relationship between the wood density of an archaeological sample and the ultrasound propagation velocity through it. The density values measured by the NMD are indicative of the level of degradation of the whole sample and are used only as indicative of the sample degradation at the moment of initial selection. For determining the degree of deterioration of the archaeological samples, the density and the MC_{max} based on the oven dry weight, are calculated. This measurement is made after the ultrasound measurements, as the sampling takes place at the same position of the insonification performance. A tree increment borer (Haglöf©) is used in order to retrieve wooden cores with a diameter of 5mm (Figure 5-9). Sampling along the radial axis, can be problematic, as the borer has a tendency to break apart the first degraded surface on entry, and before arriving to a solid wood centre. Additionally, even if the surface layer was retained, radial cores showed poor consistency along the outer degraded layer most likely because of the growth ring layering in this direction (Figure 5-10). Similar problems were encountered by Haneca & Daly (2014). These tendencies were not present in the tangential direction. Loss of the degraded outer layer would lead to underestimation of the density values, whereas lack of core integrity can lead to error in the volume measurement.

Figure 5-9 Sampling archaeological wood sample with an increment borer for density determination.

Figure 5-10 Wooden core extracted with the increment borer along the radial direction showing signs of disintegration of the archaeological wood's outer layer.

To overcome the above issues, an alternative method is used for the radial sampling. A nominal 10 X 10 mm rod, of a length equal to the sample's thickness at the position of insonification (travelling path), is extracted by cutting down the sample with the use of a band saw. This rod is now used for determining the basic density as it includes the full wood length of ultrasound's travelling path.

The, tangential cores and radial rods are weighed, and their waterlogged volume is acquired using the Archimedes method. The cores are then oven dried for 24h at 105°C. Results on the physical properties of the waterlogged archaeological samples are given in Table 5-2. At the specified ROI, the basic density of the oak samples ranges between 0.561 g/cm^3 the least degraded and 0.344 g/cm^3 the most degraded, for the maple sample it is between 0.332 to 0.318 g/cm^3, and for the spruce sample it is 0.422 g/cm^3. A difference in density values is noticed between the current determinations and the values received from NMD, with some exceptions; here density reductions are between 6-43% for oak, 48% for maple and 13% for spruce, compared to fresh counterparts. The fairly good preservation condition of the spruce sample is also verified with the pin test, sawing resistance to its entry. NMD's densities derive from 50 mm complete sections from each sample, thus quite a variation is expected due to the larger sample size. Based on the density calculations made by the present study, spatial density variability of the wood samples is found to be either in the range < +0.010 g/cm^3, or between +0.010 to +0.016 g/cm^3 (e.g. Figure 5-11) or between +0.027 to +0.044 g/cm^3 from the lowest density value recorded. This is lower than 0.050 g/cm^3 which is a fair variability considering the nature of the archaeological material, also considered when designing conservation treatments (Gregory, 2014, pers. comm., 22 August). Coefficient of variation in spatial density for the archaeological wood samples ranges between 0.91% the lowest and 9.48% the highest. This gives confidence to the relationships established in Chapter 4, where coefficient of variation for density from the artificially degraded wood test-pieces is between 1 to 2% (Table 4-1). Hence, the density values determined at the position of insonification are used to match with the respective

ultrasound propagation velocity measurements. Results also show the correspondence of the MC_{max} increasing to decreasing density. Based on the maximum moisture content ranging between 110-270%, the archaeological oak assembly comprises of samples classified both as Class III (de Jong, 1977) or Class C (McConacchie et al., 2008), where wood presents only a thin degraded surface layer, and Class II (de Jong, 1977) or Class A (McConacchie et al., 2008), where wood presents a sizeable core (section 1.3.1.1, Figure 1.1). Maple is classified as Class II (Class A) with MC_{max}=241%, and spruce as Class III (Class C) with MC_{max} = 125%.

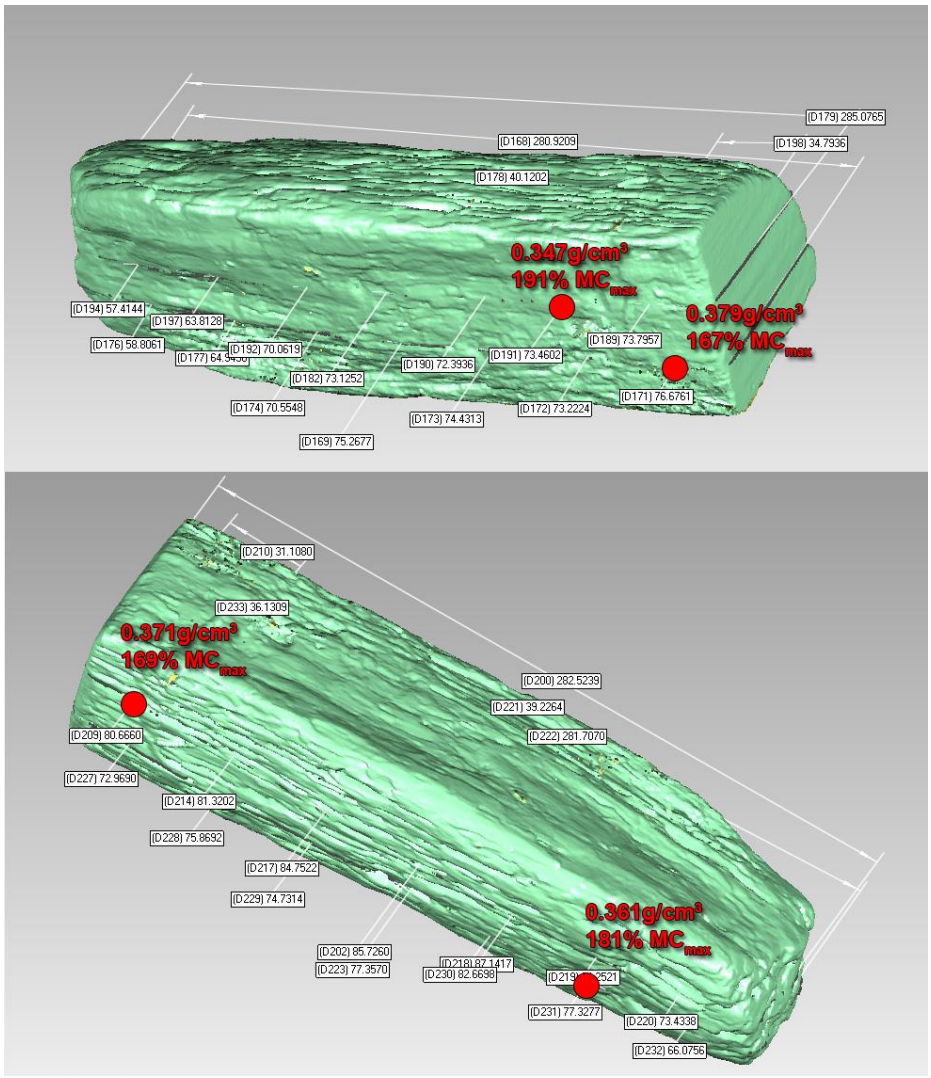

Figure 5-11 Variability in density and maximum moisture content in Sample S185.

Table 5-2 Summary of insonification angle, ultrasound propagation velocity and physical properties, measured at different insonification positions per archaeological wood sample.

Archaeological Wood Sample	Insonification Angle	Velocity (m/s)†	Basic Density (g/cm^3)	MC_{max} (%)	Macro-organism Attack
S004	30° (RT)	1989	0.520	127	Gribble (surface)
S004	40° (RT)	1888	0.525	118	Gribble (surface)
S004	75° (RT)	1907	0.491	129	Gribble (surface)
S004	75° (RT)	1960	0.470	126	Gribble (surface)
S004	0° (R)	2054	0.468	151	Gribble (surface)
S094	33° (RT)	1901	0.473	146	-
S094	51° (RT)	1949	0.464	138	-
S094	0° (R)	1963	0.520	127	-
S096	78° (RT)	1706	0.358	188	-
S096	78° (RT)	1732	0.357	180	-
S096	78° (RT)	1716	0.344	188	-
S105	36° (RT)	1816	0.359	196	-
S178a	90° (T)	1844	0.434	148	-
S178a	90° (T)	1816	0.381	174	-
S184	43° (RT)	1896	0.505	132	-
S184	43° (RT)	1918	0.480	135	-
S185	61° (RT)	1897	0.379	167	-
S185	74° (RT)	1778	0.347	191	-
S185	80° (RT)	1787	0.371	169	-
S185	85° (RT)	1872	0.361	181	-
S200	90° (T)	1950	0.535	121	Teredo (sporadic)
S205	19° (RT)	1877	0.511	131	-
S205	59° (RT)	1829	0.438	141	-
S205	59° (RT)	1829	0.433	148	-
S210	90° (T)	1624	0.390	176	Teredo (heavy)
S210	90° (T)	1692	0.349	214	Teredo (heavy)
S211	57° (RT)	1798	0.412	152	-
S211	57° (RT)	1751	0.404	154	-
S211	75° (RT)	1715	0.386	172	-
S213*	71° (RT)	1683	0.422	125	-
S226**	0° (R)	1850	0.332	235	-
S226	0° (R)	1842	0.329	235	-
S226	0° (R)	1800	0.319	248	-
S226	0° (R)	1819	0.318	247	-
S241	90° (T)	1861	0.461	147	-
S241	90° (T)	1885	0.449	144	
S241	90° (T)	1867	0.435	155	-
S241	90° (T)	1885	0.430	160	-
S241	90° (T)	1909	0.419	159	-
S271	56° (RT)	1923	0.544	110	Gribble (surface)
S271	72° (RT)	1878	0.527	117	Gribble (surface)
S271	0° (R)	1973	0.558	114	Gribble (surface)
S272	31° (RT)	1925	0.463	150	Gribble (surface)
S272	45° (RT)	1856	0.457	144	Gribble (surface)
S272	51° (RT)	1841	0.455	144	Gribble (surface)
S289	24° (RT)	1923	0.547	118	Gribble (surface)
S289	59° (RT)	1898	0.542	111	Gribble (surface)
S289	64° (RT)	1837	0.547	120	Gribble (surface)
S289	0° (R)	1938	0.561	115	Gribble (surface)

Table 5-2 Continue

Archaeological Wood Sample	Insonification Angle	Velocity (m/s)†	Basic Density (g/cm^3)	MC_{max} (%)	Macro-organism Attack
S290	90° (T)	1744	0.417	162	-
S290	90° (T)	1727	0.409	174	-
S290	90° (T)	1755	0.406	164	-
S293	13° (RT)	1768	0.348	277	-
S293	13° (RT)	1800	0.391	197	-
S294	24° (RT)	1996	0.497	137	-
S294	24° (RT)	1925	0.429	177	-
S294	0° (R)	2154	0.497	139	-
S294	0° (R)	1962	0.444	167	-
S299	0° (R)	1924	0.436	165	-
S299	0° (R)	1924	0.459	153	-
S299	0° (R)	1907	0.459	153	-

†Individual measurements, * Spruce, ** Maple

5.3 Evaluation of calibration curves

5.3.1 Insonification on-axis

In Figure 5-12 and 5-13, the results from ultrasound testing through archaeological wood are given for the Radial and Tangential insonifications respectively, and are plotted in comparison with the predictive curves presented from Chapter 4. Data derives from Table 5-2 and for the insonification positions which correspond to 0° and 90° angles between wood rays and ultrasound propagation direction; they are 13 individual measurements in total per growth axis. Results from the maple sample are included in the radial insonifications, which derive predominantly from oak samples; tangential insonifications derive only from oak samples. From Figures 5-12 and 5-13 it can be seen that results from archaeological wood fall around the predictive curves established in Chapter 4 for both on-axis insonifications and that there is an even data distribution to both sides of the curves, especially for the tangential case. Some data as those from samples S289 and S271 for the radial insonifications, and one from S210 and one from S241 for the tangential insonification, fall further out from the best fit lines derived from the artificially degraded wood. For samples S289 and S271 a likely explanation may be that the position of the ultrasound measurement includes half of the tree's pith. It is well known that the pith has a different cellular structure in comparison with the surrounding wood (Tsoumis, 1968). From a wood utilization point of view it is a defect, and the wood immediately around it often contains small checks and knots of various sizes, and may also develop shakes (Tsoumis, 1968). It is expected that these internal defects can affect velocity values (section 1.4.2.1), and may have contributed to the slower than expected ultrasound velocities received from these samples, given their high density (S289 = 0.561 g/cm^3 and S271 = 0.558

g/cm^3). There are no other insonification positions including the pith among the rest of the samples apart from these two samples. Sample S210 is the only presenting heavy attack by Teredo as seen in Figure 5-1; yet, this decay manifestation does not seem to explain the velocity deviation from the best fit line, as one out of the two measurements seem to fall very close to the best fit line. As for sample S241, three out of four measurements on the sample fall closer to the line, one being the outlier probably for reasons of the nature of the archaeological material. Special note is given to the results received from insonifying wood other than oak. Velocities received through the radial insonifications of maple archaeological wood, sit exactly on the predictive curve from the artificially deteriorated wood compromised by oak and pine. Although results from maple derive from a small data group, this result can be indicative of the appropriateness of the relationship built in Chapter 4, to estimate the preservation state of wood with ultrasound, irrespective of wood structure, or else, wood species. Maple is a diffuse-porous hardwood, with pores widely spaced and rays of varying thickness, which are macroscopically visible (Kavvouras, 2004).

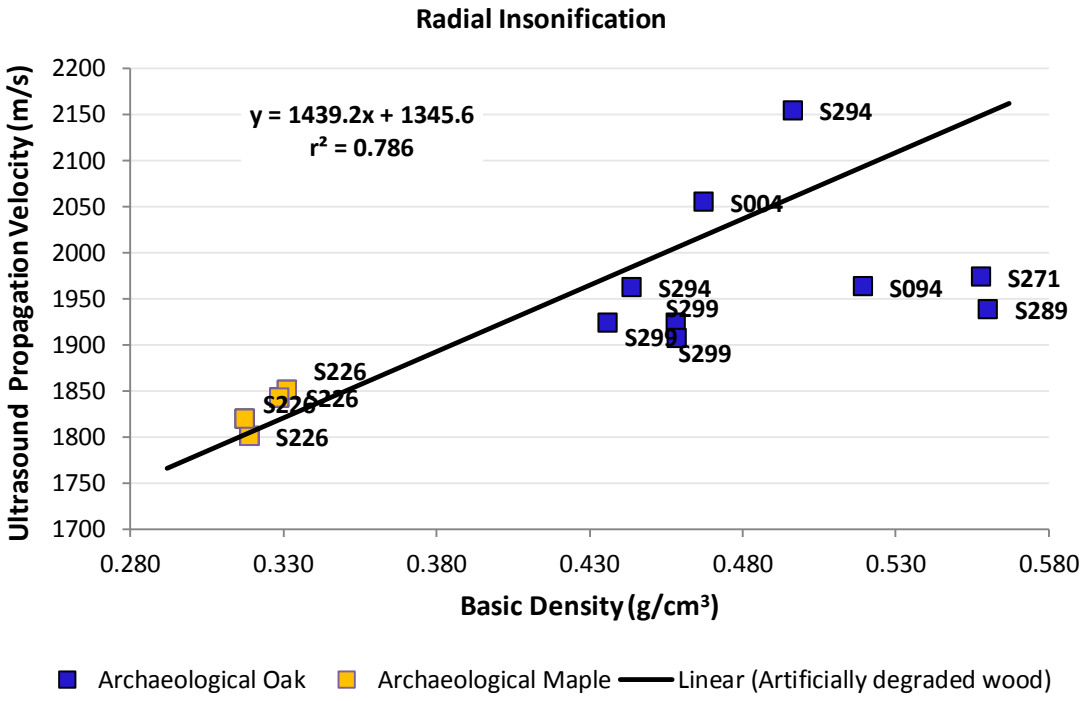

Figure 5-12 Archaeological wood against the predictive curve. Radial insonifications.

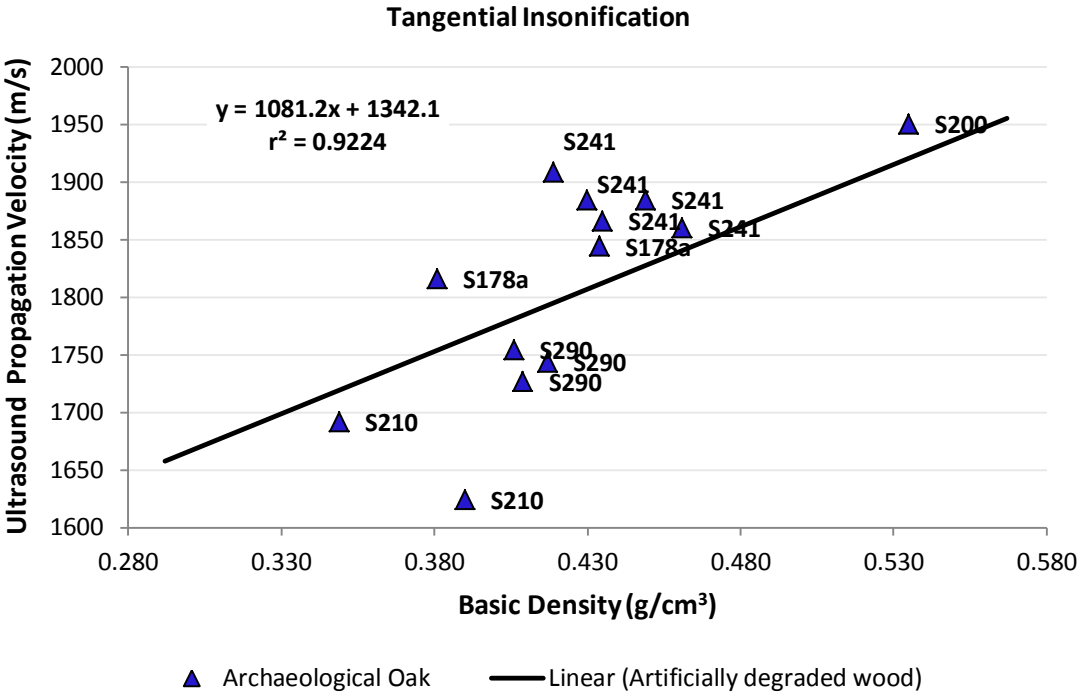

Figure 5-13 Archaeological wood against predictive curve. Tangential insonifications.

Furthermore, in order to explore how the data received from the archaeological wood compare to the ones from the artificially degraded wood, the two on-axis groups are here joined in one group representing each principal growth axis. Figures 5-14 and 5-15 give the results for the Radial and Tangential axes respectively. The grouping derives strong linear relationships between basic density and ultrasound propagation velocity for both principal wood axes. For the radial insonifications, 77.6% of the variation in the velocity is accounted by basic density, whereas for the tangential insonifications basic density can account for 91% of the variation in the velocity. Both regressions are statistically significant at the 0.001 level (n = 589 in total for each regressions; $n_{\text{artificially degraded}}$ = 576 and $n_{\text{archaeological}}$ = 13). Certainly, results from actual degraded wood are expected to show variance due to the nature of the archaeological material. However, it is noted that the addition to the results from the artificially degraded wood, those from the archaeological wood, including the outliers commented on above, does not seem to significantly affect the strength of the predicted curves. The two relationships between wood density and ultrasound propagation velocity, $y_{\text{radial}} = 1420.3\rho_{o.d} + 1352.5$ and $V_{\text{tangential}} = 1084.6\rho_{o.d} + 1340.9$ as given in Figures 5-14 and 5-15, can be used for the evaluation of flat-sawn and quarter-sawn boards respectively, under the provision that insonification angle between sound direction and wood rays, is 0° (Figure 5-14) or 90° (Figure 5-15). Hence it is possible to increase the number of observations

(n) comprising the calibration curves, this time by including real archaeological material, adding significance to the relationships.

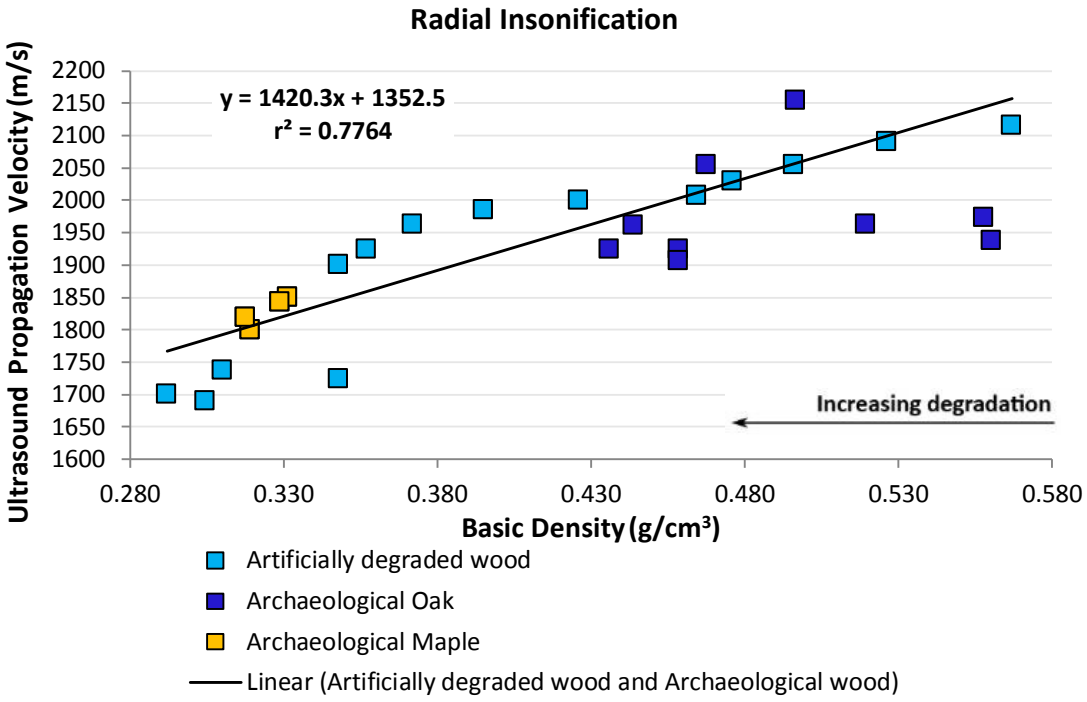

Figure 5-14 Archaeological and artificially deteriorated wood. Radial insonification.

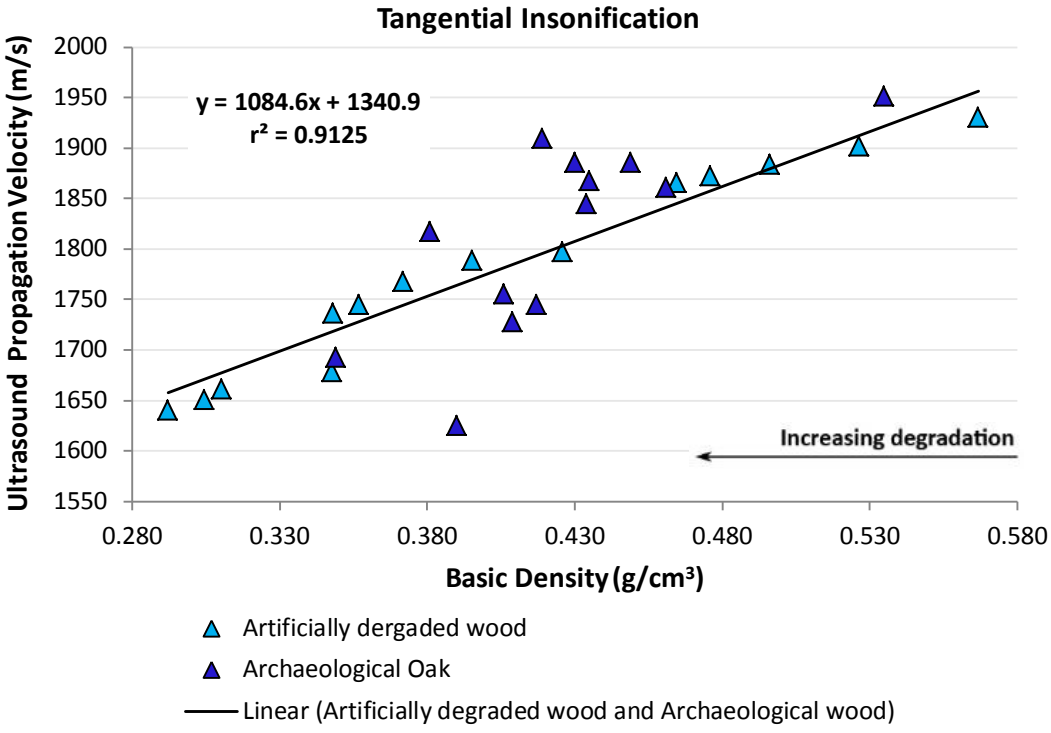

Figure 5-15 Archaeological and artificially deteriorated wood. Tangential insonification.

5.3.2 Insonification off-axis

Returning to one of the main scientific questions of the present study set in section 1.5, when in the field, it is desired to be able to receive quantitative results for insonifications towards the timbers of a ship, irrespective of the orientation of their wood structural characteristics in relevance to the sound direction. In Figure 5-16, a section of the Kyrenia's hull as drawn by Steffy (1994), gives indicative information about the cutting orientation of the planks and keel used, as visible at their cross-section. A classification is applied here, based on the angle created by the wide surface of the board and the growth rings of the tree; flat-sawn, with angles between 0-30°, rift-sawn with angles between 30-60°, and quarter-sawn, with angles between 60-90° (section 2.2.2 and Figure 2-4).

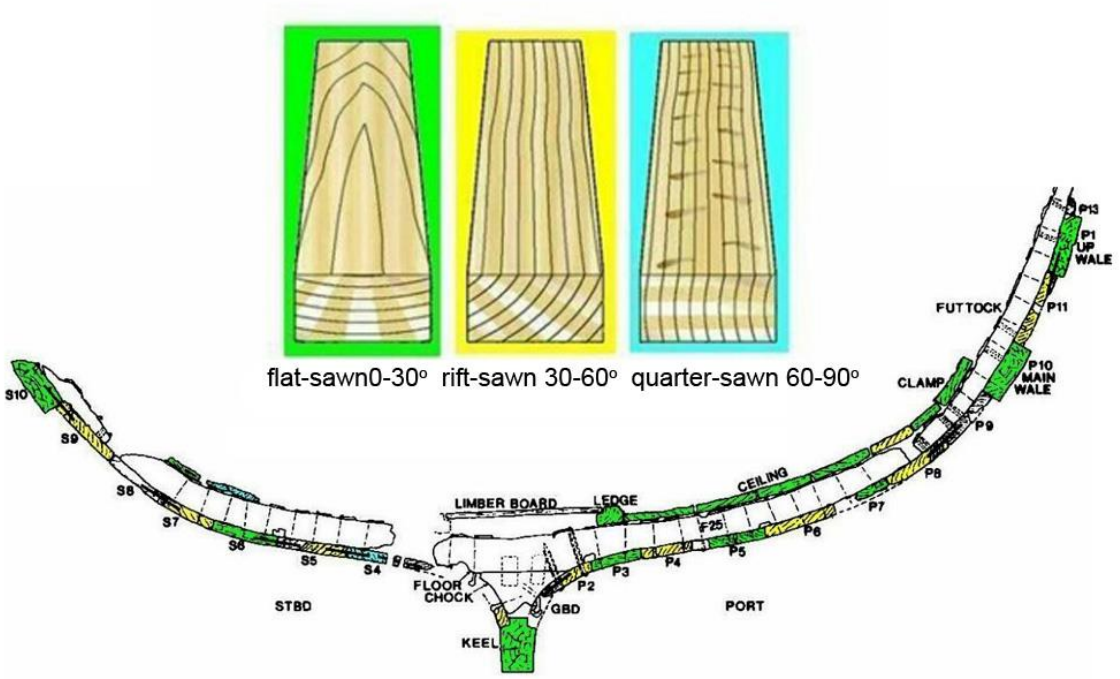

Figure 5-16 Hull section of the Kyrenia ship. Modification on a drawing by Steffy, (Steffy, 1994: fig. 3-31).

Based on this classification, the velocities received through the archaeological wood samples, deriving from insonification angles up to 30° for the radial direction, and down to 60° for the tangential direction, are now added to the initial groupings (Figures 5-14 and 5-15) of the archaeological and artificially degraded wood. Thus there are two new nominal groups, the 0-30° and the 60-90°.

Taken from Table 5-2, velocities received through insonification at angles between 13-36° are grouped with the radial velocities (0°), and the velocities at angles between 59-85°, are grouped with the tangential velocities (90°). This angle selection is based on Independent t-

test ran on SPSS, where the velocity means from the artificially degraded wood and the archaeological wood from various angles (those on-axis also included), are compared. In Table 5-3, the analysis shows that the mean velocity from the archaeological samples (0-36°), is 1914 m/s (±89 m/s), and that from the artificially degraded wood (0° or radial), is 1944 m/s (±132 m/s). There is no statistically significant difference in velocity, depending on whether the velocity derives from the archaeological wood, including insonifications through angles from 0° up to 36°, or the artificially degraded wood at an angle of 0°.

The mean velocity from the archaeological wood samples (59-90°), is 1831 m/s (±89 m/s), and that from the artificially degraded wood (90° or tangential), is 1792 m/s (±92 m/s). There is no statistically significant difference in velocity depending on whether the velocity derives from the archaeological wood, including insonifications through angles from 59° up to 90°, or the artificially degraded wood at an angle of 90°.

Table 5-3 Results from Independent t-test analysis of the mean velocities between archaeological wood samples and artificially degraded wood, for the two groups, 0-36° and 59-90°.

	Wood	N	Mean	Std. Deviation	Std. Error Mean	Levene's Test of Equality of Variances[13]	Sig. (2-tailed)
Velocity (0-36°)	Archaeological	23	1914	89	19	not assumed	.134
	Artificially degraded	576	1944	132	6		
Velocity (59-90°)	Archaeological	29	1831	89	16	.722	.224
	Artificially degraded	576	1792	92	4		

The reason why velocities received from angles bigger than the nominal 30°, i.e. up to 36° can still be grouped with those between 0-30° and derive significant agreement, as well as for the 60-90° grouping, could be supported in Figure 5-17. Karsulovic et al. (2000) studied the variation of the ultrasonic velocities on samples from pine (*Pinus radiata*) in respect to growth ring angle on wave propagation, by rotating the samples in the RT plane in increment steps of 15°. They operated at a frequency of 500 KHz and used the through transmission technique, similar to the present study. Mean velocities received through the radial axis was 2079 m/s (±152 m/s) and 1690 m/s (105 m/s) through the tangential, which are in good agreement with the respective velocities measured for pine in this study, i.e.

[13] Tests the null hypothesis that the population variances between groups are equal (called homogeneity of variance) before running the t-test. SPSS adjusts the t-test in cases where equality of variances cannot be assumed.

1999 m/s (±9 m/s) and 1797 m/s (±17 m/s) respectively. Hence, correlations between the two studies can be suggested. Karsulovic et al. (2000) established a polynomial regression between growth ring angle and ultrasound velocity (Figure 5-17). Here the growth ring angle is defined as the angle between the insonification angle and the ray direction, in accord with the present study. Two trends may be observed on this regression as highlighted in Figure 5-17, which suggest that the change in ultrasound velocity follows the same trend form approximately 0-35° and from 60-90°. No such trend is visible for velocities received between approximately 35 to 60° to the growth ring angle.

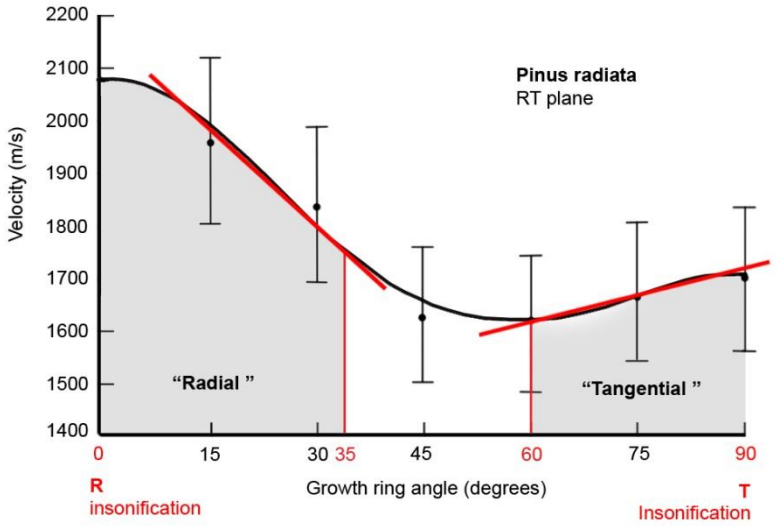

Figure 5-17 Relationship of ultrasound velocity with growth ring angle of *Pinus radiata* at the RT plane (Extracted and modified from Karsulovic et al., 2000: fig. 6).

Compared to results from the on-axis insonifications (Figure 5-14 and 5-15), the inclusion of measurements from flat-sawn boards with insonification angles ranging from 0° to 36° (Figure 5-18) results in a partial weakening of the wood density – ultrasound propagation velocity linear relationship. The same applies for quarter-sawn boards in Figure 5-19, when the insonification angle ranges from 59° to 90°. However, density can still account for 76.5% of the variation in the velocity for wood insonified in angles between 0° to 36°, and for 89.7% of the variation in the velocity for wood insonified in angles between 59° to 90°. Both linear regressions are statistically significant at the 0.001 level (n=599 and n=605, respectively, Table 5-3). Further, it is noted that a second order polynomial is found to be a stronger predictor of the two relationships, r^2=0.83 and r^2=0.92 respectively; more data from testing archaeological wood with ultrasound, can point towards a more suitable type of regression. A linear is here preferred for it is straightforward.

As observed earlier for the maple sample, Figure 5-19 includes velocity received from the spruce archaeological sample, which is a conifer tree. Velocity through spruce groups well with the velocities received from the archaeological oak and the artificially degraded oak and pine, implying that the relationships built, can be used for testing wood of different species. Spruce can be described as a homogeneous structure with gradual transition from earlywood to latewood (Kavvouras, 2004).

Last, it is highlighted that the relationships seem capable of predicting the ultrasound velocity through archaeological wood, regardless of the degradation occurrence. As given in Table 5-2, ultrasound testing included archaeological samples presenting attack from Teredo and Gribbles, while deterioration due to microbiological attack is also present through softening of the wood tissue. In section 4.2.1.2 statistical analysis tests were ran in order to study the effect of the hole diameter, simulating different types of wood degradation, on ultrasound propagation velocity. Results had generally sawn that mass loss (or density) is a stronger predictor of the ultrasound velocity than the diameter of holes. Although there were instances as for the 2mm vs. 3mm V_T and 3mm vs.10mm V_T, where the hole diameter was able to contribute by 35 and 31% respectively to predicting the velocity, which can be regarded as a noticeable contribution, in the real world the relationships built by using only 3mm diameter holes, seem here appropriate for testing archaeological wood showing various degradation types.

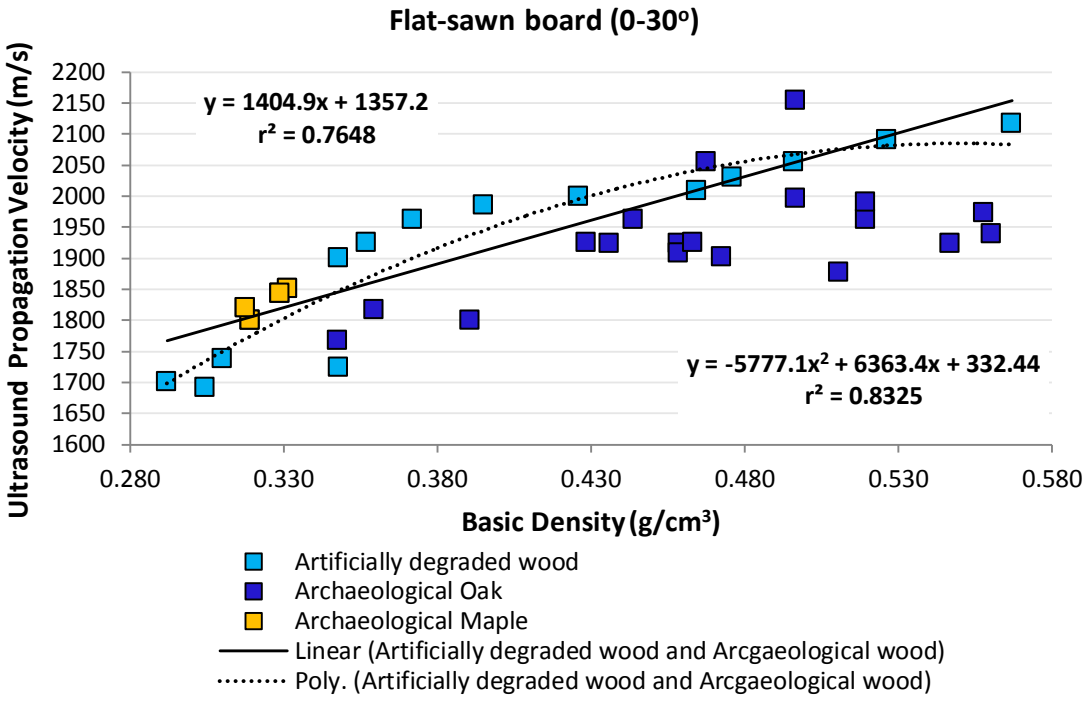

Figure 5-18 Wood density–ultrasound propagation velocity relationship for flat-sawn board.

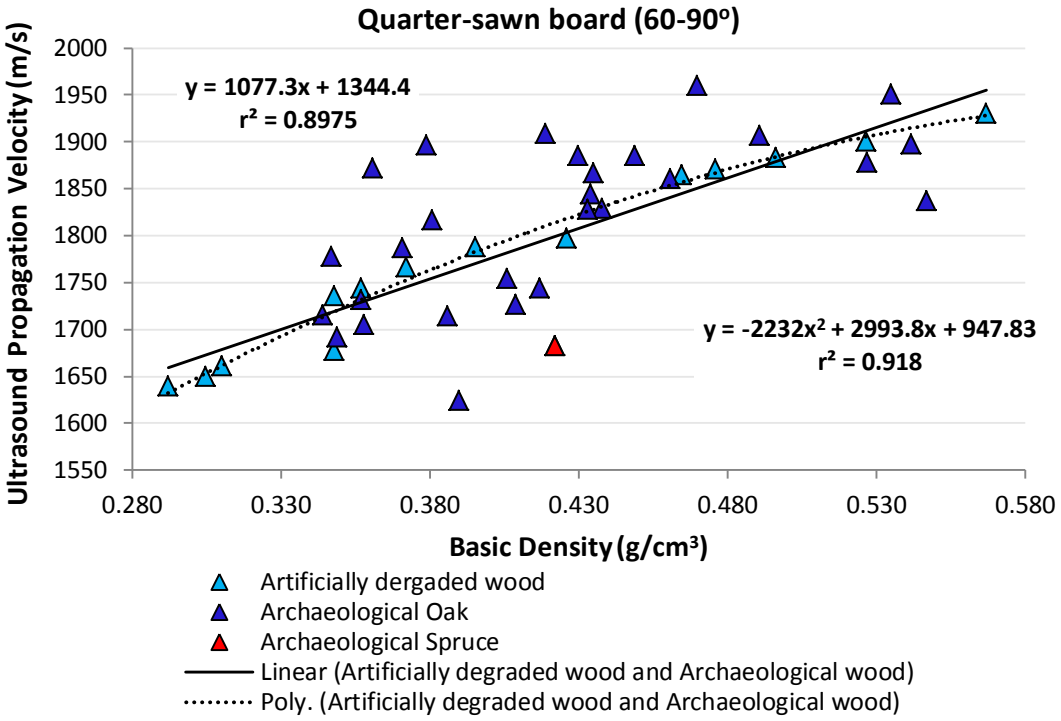

Figure 5-19 Wood density–ultrasound propagation velocity relationship for quarter-sawn board.

5.4 Chapter conclusions

Degraded archaeological wood samples, with a density range between 0.561 g/cm³ to 0.318 g/cm³, have been successfully tested with ultrasound through transmission technique, using the methodology built in Chapter 3. The relationships established in Chapter 4, have proved their appropriateness to predict the state of preservation of waterlogged archaeological wood, irrespective of type of degradation. After the inclusion of velocities taken at angles between 0° and 36°, and, 59° and 90°, the new relationships can be used for *in situ* applications. The following can be summarised:

1. A strong linear relationship has been established between wood density and ultrasound propagation velocity, which can predict Radial Velocity through waterlogged wood based on its density, $y = 1420.3x + 1352.5$, $r^2 = 0.776$.
2. A strong linear relationship has been established between wood density and ultrasound propagation velocity, which can predict Tangential Velocity through waterlogged wood based on its density, $y = 1084.6x + 1340.9$, $r^2 = 0.91$.
3. A strong linear relationship has been established between wood density and ultrasound propagation velocity, which can predict the velocity through waterlogged flat-sawn timber based on its basic density $y = 1404.9x + 1357.2$,

r^2 = 0.765. A second order polynomial seems to be a stronger predictor of the relationship, r^2 = 0.83, y = -5777.1x^2 + 6363.4x + 332.44.

4. A strong linear relationship has been established between wood density and ultrasound propagation velocity, which can predict the velocity through waterlogged quarter-sawn timber based on its basic density, y = 1077.3x + 1344.4, r^2 = 0.897. A second order polynomial seems to be a stronger predictor of the relationship, r^2 = 0.92, y = -2232x2 + 2993.8x + 947.83.
5. There is indication that the relationships can be used for estimating the preservation state of other wood species apart from oak. Here maple and spruce have been successfully tested.
6. It is possible to derive quantitative results in situ when angles between insonification direction and wood rays are between 0-30° and 60-90°.
7. Quantification of wood's state of preservation based on its density seems to be possible irrespective of degradation type, (Teredo, gribble and microbiological)
8. It was not possible to predict velocities for timbers with 'neutral grain', or else insonification at angles between 30-60° between sound direction and wood rays, due to lack of a relationship between wood density and ultrasound propagation velocity at nominal 45°, as established in Chapter 4.

Chapter 6

Discussion and Conclusions

6.1 Discussion

6.1.1 Introduction

The main aim of the present research was to improve on our knowledge on a promising non-destructive tool in the hands of Archaeological Conservators and Marine Archaeologists. The initial work by Arnott (2004) was able to derive the basic principal of ultrasonics and waterlogged wood. This study comes in to take this work to the next phase to provide a working tool with well tested relationships for estimating the state of preservation of waterlogged archaeological wood, both in the laboratory and *in situ*.

In order to accomplish this, a number of experimental stages were designed this time placing wood at the epicentre of the investigation counting in both its materialistic and archaeological attributes. The following experimental stages have been executed towards this accomplishment:

a) Development of a new reliable experimental ultrasound set-up and ultrasound measurement methodology for waterlogged wood.
b) Development of a new artificial wood degradation process simulating closely the degradation patterns of wood from marine environments.
c) Application of the ultrasound measurement methodology on 'real' archaeological wood samples from waterlogged archaeological excavations.
d) The establishment of four new empirical relationships between wood's density and ultrasound propagation velocity, to predict the degradation level of wood recovered from underwater marine burial environments.

A discussion of these stages is given in the following sections.

6.1.2 Ultrasound set-up and methodology

The new ultrasound measuring system is based on Arnott's (2004) development of an ultrasonic through transmission immersion technique for testing waterlogged wood. The novelty of the present study is adjusting the technique to test waterlogged, archaeological wood, here exemplified as the chief building material of ancient wooden ships. Based on this target, the wood species, dimensions and cutting orientation of the test-pieces used as the controls, suitable for later testing 'real' archaeological material, were defined. Consequently the operational frequency was set to 500 kHz. Action was taken to avoid consequences deriving from sound beam characteristics, i.e. edge effects, number of wavelengths traveling through the test-pieces, and safe placement of the test-piece to the beam's far field. New rigid supporting frames holding the transducers and test-piece in good alignment were constructed. Brass, Perspex and polyethylene standards were repetitively tested with the new set-up in order to evaluate and calibrate it, and assure accurate measurements through the wood. An error propagation analysis proved that the system is capable of measuring the velocities corresponding to the three main wood growth axes with an error of less than 1%. Special care was given to the design of a new robust waterlogging procedure for wood. It is important to secure a successful waterlogging of the wood otherwise the definition of the relationship between wood's density and sound speed will be uncertain. In addition, the air-free conditions of waterlogged wood allows for a better impedance match between the wood cell wall and water. Sound scattering should be here less than a three-phase system (wood-water-air) because of the stronger scattering of the signal in wood and air. This can further assist to reduction of variability in velocities. All the above considerations together with, the selection of proper wood quality, using the same test-piece to derive all three principal velocities, contributed to the success of the present study to acquire very low coefficient of variations of the ultrasound axial velocities, lower than the experimental error, or just above it, and the coefficient of variations given in the literature. Absolute, consistent and repeatable results with good accuracy were derived. The characteristic anisotropic behaviour of wood $V_L >> V_R > V_T$, was here verified. The new experimental set-up and methodology were suggested as sensitive to use on waterlogged wood where changes on ultrasound velocity could be attributed to its degradation state rather to the characteristic high natural variability of wood, a fundamental problem encountered by Arnott.

6.1.3 Artificial wood degradation process

Waterlogged wood can be generally found directly exposed into the water column or hidden under layers of sediments. Its degradation commonly involves the conjoined action

of physical, chemical and biological factors, which ultimately lead to wood's loss in mass, and hence, density reduction. It is the density, the benchmark of wood's degradation level by archaeological conservators, the reason the present study focuses on establishing a relationship between wood density and ultrasound propagation velocity.

In order to be able to apply the tool in the field, ultrasound must ideally be able to give reliable readings when insonifying towards the timbers of a wooden structure as that of a ship, irrespective of the orientation of their wood structural characteristics in relevance to the insonification axis, besides the preferred orientations identified to be the on-axis Radial and Tangential axes (section 2.2.2). As derived in section 2.2.1, it would be also of great importance if ultrasound could be universally informative given the variety of wood species used in ancient shipbuilding.

Considering this, exploiting the structural differences between broadleaved oak tree and conifer pine tree species and their ample use in ancient shipbuilding, these two wood species were used in the present study in order to explore the influence of the wood structure on ultrasound propagation velocity, bearing in mind that in "fresh" wood ultrasound velocities are characteristic of wood species. As regards the ability of ultrasound to 'read' wood irrespective of its structural alignment to the insonification axis, two sets of control test-pieces were produced: quarter sawn oak for studying on-axis insonifications with the principal growth axes, radial and tangential, and flat sawn oak test-pieces for studying off-axis insonifications in relation to these two axes.

In order to overcome Arnott's limitations of wood's degradation procedure using biological means, the present study introduced a new artificial degradation process to simulate the mechanisms of wood mass loss in a marine environment. The approach aimed to rectify reproducibility of the procedure, control over the degradation steps produced, and no loss of data due to severe degradation of the wood test-pieces from the biological activity, as experienced in the past. In contrast with the past work, the same test-pieces were used, from the beginning and throughout the degradation procedure, so to be able to receive absolute and comparable results, and reduce the variability in the measurements. A combination of a drilling process using a 3mm diameter drill bit to sequentially remove mass from the test-pieces, followed by a chemical treatment with alkali, was applied to all quarter sawn oak and pine test-pieces. The chemical treatment was not applied on the flat sawn oak test-pieces for the experimentation with this set terminated after the drilling process which showed that although this study was able to acquire velocity measurements from the off-axis test-pieces, it was unable to see changes in ultrasound propagation

velocity for a range of densities under this structural condition. In overall, a total number of six degradation steps (four from drilling and two from the chemical treatment) were executed, for the oak and pine quarter sawn test-pieces, and three for the flat sawn oak test-pieces, in addition to a "fresh", zero degradation measurement. By the end of the artificial degradation, oak test-pieces lost 46% of their original density and pine's 31%. Both groups are considered degraded with residual density less than 65-70%, when heavily degraded classes wood presenting less than 40% RBD.

The present study was successful in establishing two significant empirical calibration curves explaining the relationship between wood's density and ultrasound propagation velocity, for wood in various stages of degradation, but under the provision that insonification is executed on-axis with the two principal wood growth axes, the Radial ($y = 1420.3x + 1352.5$, $r^2 = 0.776$) and the Tangential ($y = 1084.6x + 1340.9$, $r^2 = 0.91$). Each curve is derived after the inclusion of a total of 576 velocity measurements deriving from ten control wood test-pieces, five from each species (for exact number of replicates per density level, refer to Table 4-2). In respect with the aims of this research, it was possible to derive relationships which also seem to be independent of wood anatomical features characterising hardwood or softwood species, here those of oak and pine. Additional evidence is given towards reasonable speculation that when waterlogged archaeological wood will reach high levels of degradation, i.e. wood with residual density less than 40% and classed as Class I or Class C (section 1.3.1.1), wood's structural characteristics influence on ultrasound propagation velocity will cease. In other words, wood becomes more isotropic across the grain as indicated by the reduction of V_R/V_T ratio. At the same time it also looks for the structural differences between wood species, here oak and pine. This observation agrees with conservation practice, where heavily degraded wood from different species could be treated within the same conservation tank. This result enhances the applicability of the calibration curves, as estimation of the density of waterlogged wood seems possible having no knowledge of its species origin whilst *in situ*. Nevertheless, a substantiated estimation by the archaeologists in charge of the underwater site, regarding the wood species of the wooden hull, will allow the calculation of the residual density of the wood present, based on the density of the "fresh" wood species counterpart. Hence, a first estimation of wood's preservation state can be drawn, and different preparatory scenarios of treatment / management can be designed, until more knowledge is acquired progressing the study / excavation of the site. For cases where it is difficult to run estimations as such or no excavations plans are due, the tool could still be useful for monitoring the state of preservation of the wood by comparing seasonal measurements and mark likely changes.

A step further from Arnott's work which focused on testing ultrasound propagation through the three main tree growth axes, this study explored off-axis insonifications of waterlogged wood simulating degradation in archaeological wood. The aim was to study whether the positioning of a wooden member *in situ* in relevance to the insonification axis, could be ignored. However, although velocities were received and an interrelation $V_R > V_T > V_{RT}$ was found, it was not possible to establish a significant relationship between wood's density and ultrasound propagation velocity in this case. The main reason seems to be that ultrasound propagation velocity is significantly affected by the insonification angle, i.e. the angle formed between wave propagation path and wood growth rings which brings in high velocity variability. This seems to pose a constraint to the use of the tool for *in situ* applications.

Yet, testing recovered material in the conservation laboratory, where it is easy to identify the tree growth axes and align the transducers so to receive on-axis velocities, is possible. Conservators should be able to use the through transmission immersion method developed in this study in order to estimate the density of the wood material they are called for treating. Ultrasound will enable them to 'sample' or else take as many non-destructive velocity measurements as desired in order to evaluate the residual density (RBD) following wood species identification. Ultrasound will travel through the whole thickness of a wooden piece / object and will be able to show possible spatial variability in wood's density and signify areas of different preservation. With the through transmission technique, the conservator will receive an average estimation of the area the sound travelled through. If further knowledge is desired, for example the extent of the outer degradation layer, then other ultrasonic techniques can be suggested as is the pulse-echo technique (see section 1.4.2.1). Arguably ultrasound calls for the acquisition of special equipment and the conservator's training before use; but it is certainly an attractive alternative especially for cases where any interaction with the object is confined by conservation ethics and practices.

6.1.4 Ultrasound on 'real' archaeological wood samples

Research on a diagnostic tool as ultrasound, can benefit by calibrating against the material of interest, and investigate any limitations to the approach as set by the archaeological material itself. To the best knowledge of the author, it is the first time ultrasound velocities are given for a range of archaeological wood whilst in a waterlogged state, and moreover, correlated with their residual density. The present study collaborated with the National Museum of Denmark, which provided the archaeological material for assessing the calibration curves built using the artificial degraded wood. Wood samples tested with ultrasound using the set-up and methodology developed in this study, comprised chiefly of

oak species, one maple and one spruce. The material derived from both sea and land excavations, while all three main types of degradation were present (Table 5-2), i.e. Teredo, gribbles and micro-activity (fungi and/or bacteria).

To be able to use the calibration curves, a classification of the ultrasound insonification positions defined on the archaeological samples was made based on the angle between the insonification axis and the wood ray direction at that position. Insonification positions with an angle equal to 0° were appointed as radial (R), with an angle equal to 90° as tangential (T), and with any angle in between the two principal axes, as off-axis (RT) (Table 5-2). The velocity measurements used to assess the Radial and Tangential calibration curves were those deriving from R and T angles. A total of thirteen individual velocity measurements per insonification axis were eligible for use. Bearing in mind the nature of the material of interest, at a first glance results from the archaeological wood were encouraging of the suitability of the two curves in relating ultrasound with archaeological wood's basic density, as data were plotted around the best fit lines. The existence of part of the tree's pith in the sound travelling path seems to affect ultrasound propagation velocity because of its different structure than the rest of the wood of a tree. Also, for archaeological wood presenting severe manifestation of Teredo tunnels, these might have an effect on ultrasound propagation velocity, given that data were received from only one such sample, and were either in accord with the ones from the calibration curves or 'outliers. Notably, the well agreement of the measurements through the maple sample with the calibration curve shows the latter's potential of being useful for determining the density of other wood species other than oak and pine. Also, given that maple's density falls towards the lower end of the density range, use of ultrasound can here support the assumption that as the wood becomes more degraded, structural differences between species tend to eliminate, leading to homogeneity of wood as a material.

To increase the significance of the calibration curves, the data received from the on-axis, R and T, insonifications of the 'real' archaeological material, were added to the data received from the on-axis, R and T, insonification of the artificially degraded wood from which the curves were derived. Increasing the number of observations to 589 for each axis, statistical analysis showed that the new calibration curves retain their strength in predicting wood's density, independent of the existence of a tree's pith, or Teredo tunnels, and in general the nature of the archaeological material.

On a further search to increase the number of observations from the 'real' archaeological material, a new classification of the archaeological samples was defined, as can be applied

on planks from a real case, that of Kyrenia's hull. This time the classification was based on the angle between the wide surface of the sample and the direction tangent to wood's growth rings, at the position of the ultrasound insonification: flat-sawn, with angles between 0-30°, rift-sawn with angles between 30-60°, and quarter-sawn, with angles between 60-90°. Next step, based on statistical analysis, the data received from the archaeological samples presenting nominal angles between 0-30° were grouped with the Radial insonifications, and data received from the archaeological samples on nominal angles between 60-90° were grouped with the Tangential insonifications. Hence, the number of observation from the archaeological material increased to 23 for the first grouping and to 29 for the second, with new totals of 599 and 605 observations per insonification axis. These final groupings led to the establishment of two strong and significant linear regressions which are capable of predicting the density of flat sawn and quarter sawn boards, or else when the insonification angle between the insonification axis and the direction tangent to the ring is between 0-30° (flat sawn) ($y = 1404.9x + 1357.2$, $r^2 = 0.765$) and 60-90° (quarter sawn) ($y = 1077.3x + 1344.4$, $r^2 = 0.897$). Furthermore, these groupings reinforced earlier observations, about the ability of the calibration curves / regressions to predict wood's density irrespective of wood species and degradation type occurrence. The new grouping included insonification through the spruce sample, which showed good agreement with the rest of the data, while data from more samples presenting different attacks by organisms, especially by gribbles and micro-activity (Table 5-2, see for RT), were now included.

These results lead to a re-evaluation of the potential use of ultrasound *in situ,* as initially drawn in section 6.1.3. Here, results from the two last groupings show that quantitative results can be still possible *in situ* in cases where the position of the wooden member on the seabed is such that the insonification axis meets the direction tangent to the rings at an angle between 0-30° or/and 60-90°. It was not possible to include angles between 30-60° (or rift sawn boards), because lack of calibration data from test-pieces with nominal angles of 45° to the insonification axis (section 4.2.2.2).

6.1.5 In –situ potential of non-destructive ultrasound

In Chapter 2 three prototype shipwrecks, the 4th century BC merchant Kyrenia, the 16th century warship Mary Rose and the 17th century warship Vasa were presented, aiming to visualise familiar wreck sceneries under the eyes of the non-destructive ultrasound for assessing the preservation state of their wooden members. A reflection on these prototypes, together with useful information retrieved from the summary list of shipwrecks in Table 2-1, is here used to summarise the new knowledge acquired from the present research.

Using similar techniques to those used for remote sensing of marine sediments have been suggested as capable for application to wood (Quinn et al., 1997) and have been used in the past (Plets et al., 2008). They have been also proposed as a means of determining wood's physical properties that alter with the degree of degradation (Arnott et al., 2005). Based on geophysical theory, wood either exposed in the water column or buried under layers of amphorae and sediments, can be detected remotely using marine geo-acoustic techniques, due to the contrast in density and sound velocity which the wood emits between itself and the surrounding environment:

$$K_R = \frac{(z_2 - z_1)}{(z_2 + z_1)} \qquad (6.1)$$

Where K_R is the reflection coefficient and z is the acoustic impedance of the two media involved, that is z_1 is the acoustic impedance of the overlying medium (i.e. sediment or sea water) and z_2 that of the target (i.e. waterlogged wood). The acoustic impedance is simply the product of the density ρ and the speed of sound c.

$$z = c\,\rho \qquad (6.2)$$

Hence, all three shipwrecks have a potential of being detected. The ultimate accomplishment of the present research is the acquisition of the necessary data, c and ρ, for waterlogged wood which will enable conservators and archaeologists to estimate their preservation state based on the residual density. These data derive from the established relationships between wood's density and ultrasound propagation velocity (Figures 5-17 and 5-18).

Considering their positioning on the seafloor, ultrasound could have good potential to be informative, after the inclusion of insonification angles between 0-30° and 60-90° in the relationships. Another interesting aspect can be also considered here which could enhance this potential. It is based on two facts, first that shipwrecks on the majority of times, settle in an angle with the seafloor, and second that contemporary geophysical tools send sound from a towed vehicle on the surface of the sea above the shipwreck. For example, Kyrenia was found with a heel of about 15 degrees on her port bottom, the Mary Rose with a heel of 60 degrees on her starboard side, and the Vasa 'upright'. It can be concluded that after accounting for timber conversion techniques of hull's components and the degrees of heel of the hull with the seafloor, a new readjusted angle, representative of the final insonification angle between the insonification axis and the direction tangent to the wood's

growth rings, occurs. This can be in favour of insonification positions where no calibration data exist insofar, and hence, expand the use of the tool *in situ*.

The present work derived evidence that density readings can be possible irrespective of wood species, thus all three shipwrecks could possibly be assessed. Consideration has to be given to issues related with the complexity of shipwrecks as structures. Even if not the entire ship is discovered, as the upper works will have been perished leaving *in situ* mainly components as planks, frames and keel, still the surviving hull remains a multi-part body. Taking under consideration the stage of the research, where ultrasound has been tested against one simple layer of wood, this draws the attention to the interpretation of the readings when ultrasound meets multi-layered surfaces. For example, Figure 2-3 pictures the shipbuilding transition theory based on the evolution of planking edge-fastening. A gradual increase of the distance between the mortise-and-tenon joinery can be detected, until their elimination. The practical implication of this structural element is that, with the current knowledge derived from the present study, ultrasound has more chances to give an accurate reading through the planks of the 1st millennia Serçe Limani than the Kyrenia, where the space between mortise-and-tenon joints is as close as 12 cm. Similar thoughts can be made considering the complexity of the structures of the warships Mary Rose and Vasa, where spacing between frames are tighter than in the shell-first constructions as in Kyrenia, which means that there are more chances of ultrasound to 'read' a multi-layered area, where wood axes from different hull components cross each other in different directions. A last example can be seen in shipwrecks with double planking, which may also be of different wood species as the 1st BC Madrague de Giens (Table 2-1).

With this in mind, the reflection coefficients for waterlogged wood exposed to the water column or buried in three typical marine sediments as suggested by Arnott et al. (2005) were calculated and the regressions between the two studies are here compared. Table 6-1 gives the velocities and densities used for the calculation of the reflection coefficient as retrieved from Arnott et al. (2005).

Table 6-1 Velocities and densities for three typical marine sediments and seawater used in reflection coefficient calculations (From Arnott et al., 2005).

Material	Velocity (m/s)	Density (kg/m^3)
Sand	1734	2100
Sand - silt-clay	1575	1740
Clay	1496	1450
Water	1522	1025

Results are given in Figures 6-1 and 6-2. For plotting Arnott et al. (2005) regressions, the equations given in the paper were used to calculate the reflection coefficient, after substituting for basic density (ρ_c) the density ranges for oak and pine respectively, also provided in the paper; for oak it is between 580 kg/m^3 to 280 kg/m^3 and for pine it is 525 kg/m^3 to 165 kg/m^3. One of the chief differences between the present study and Arnott et al. (2005), is that the latter derive different equations for oak and pine, whereas the present study was able to derive one ultimate, irrespective of wood species. This is useful given that wood species identification might be not possible whilst *in situ*. Hence, reflection coefficient regressions from the present study are compared to those by Arnott et al. (2005) for oak in Figure 6-1, and those for pine in Figure 6-2. The type of regression driven by the present study follows that of Arnott et al. for comparison reasons. Additionally, both figures include a linear regression for the reflection coefficient of wood exposed in the seawater as calculated for the present study only, as no equations are given in Arnott et al. (2005) for this case to compare. Moreover, Arnott et al., note that the reflection coefficient cannot distinguish any variation in orientation (radial vs. tangential) within each wood species. Hence, they provide only one equation to represent each burial condition, irrespective of the wood's structural orientation (R and T) to the insonification angle. Similar result can be derived from the present study as seen in Figure 6-3. It seems that reflection coefficients from insonifications of flat sawn boards (0-30^o) and quarter sawn boards (60-90^o) do not differentiate consistently for all types of burial simulations. This may fulfil one of the aims of the present research, that the positioning of the wood whilst *in situ* may be overcome for remote sensing with the current geophysical survey equipment. Given this, in Figures 6-1 and 6-2, only the equations derived using the density and ultrasound propagation velocities from insonification angles between 0-30^o, are used to compare with those from Arnott et al. (2005).

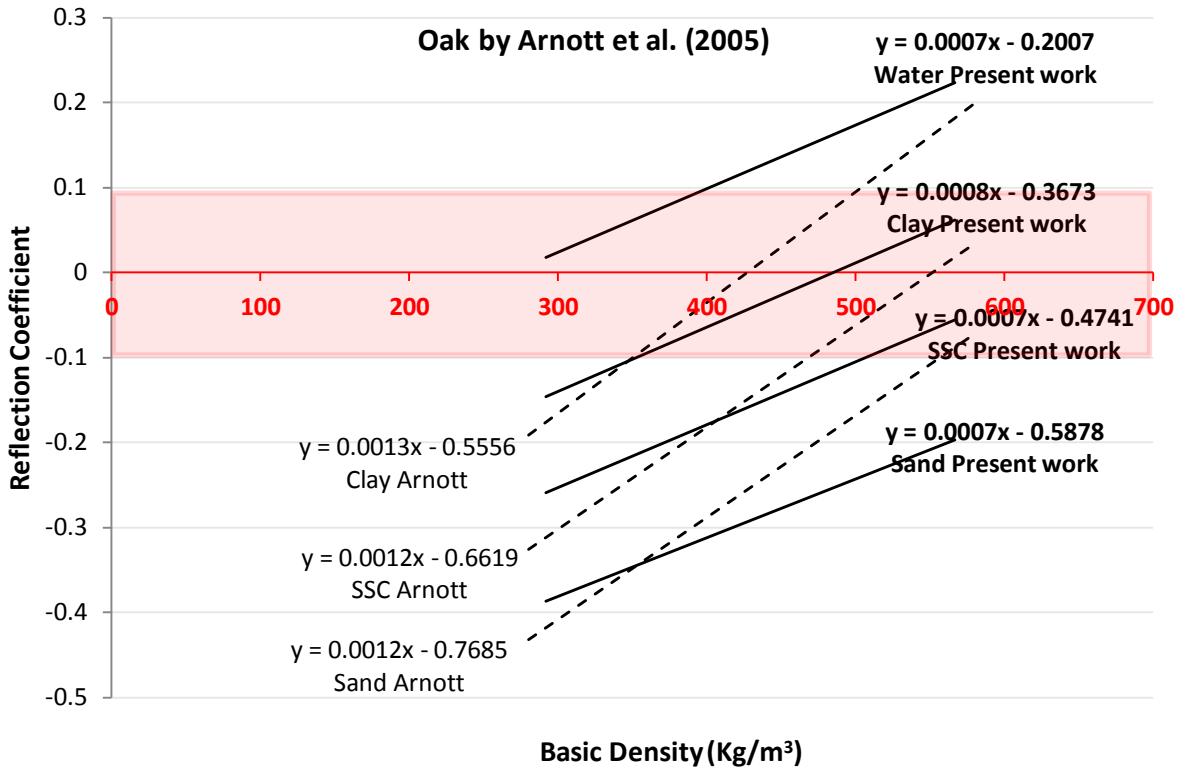

Figure 6-1 Reflection coefficient comparison between Arnott et al. (2005) and the present study for Oak wood in water, or buried in clay, sand-silt-clay and sand. Solid lines is present study, dashed lines is Arnott et al.

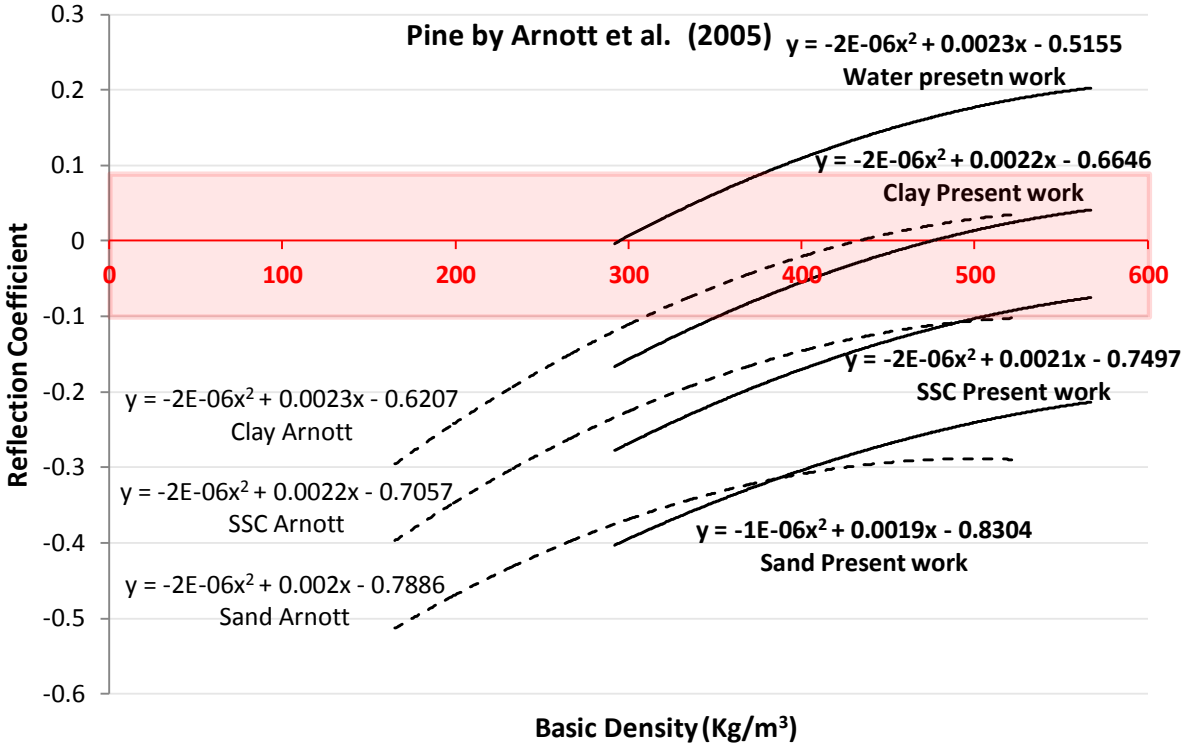

Figure 6-2 Reflection coefficient comparison between Arnott et al. (2005) and the present study for Pine wood in water, or buried in clay, sand-silt-clay and sand. Solid lines is present study, dashed lines is Arnott et al.

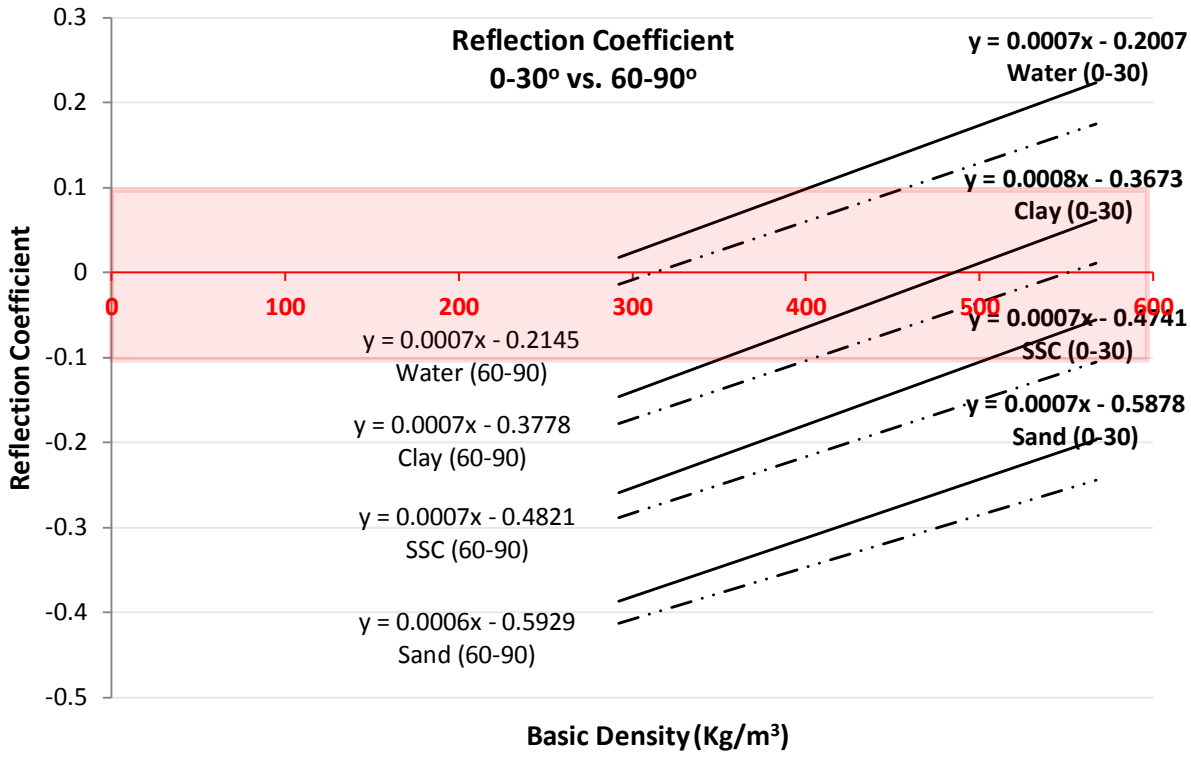

Figure 6-3 Reflection coefficients received from insonification angles between 0-30° (solid lines) and between 60-90° (dashed lines), for wood in water, or buried in clay, sand-silt-clay and sand.

Given that reflection coefficients between -0.1 to 0.1 are typical of geological features, designated by the red area in Figures 6-1 to 6-3, this leaves the rest of the area representative of typical reflection coefficients of waterlogged wood in various marine burial environments. The present study has improved our knowledge and reliability on these reflection coefficients. After the inclusion of 599 measurements, and for a density range between 0.567 g/cm³ to 0.292 g/cm³, the study gives strong linear relationships with wood's basic density with regression relationship of (Figure 6-3):

$K_R = 0.0007\rho_b - 0.2007$ for wood exposed in water with $r^2 = 0.82$

$K_R = 0.0008\rho_b - 0.3673$ for wood buried in clay with $r^2 = 0.83$

$K_R = 0.0007\rho_b - 0.4741$ for wood buried in sand-silt-clay with $r^2 = 0.83$

$K_R = 0.0007\rho_b - 0.5878$ for wood buried in sand-silt-clay with $r^2 = 0.83$

Where K_R is the reflection coefficient and ρ_b is the basic density here in kg/m³. Coefficient of determination might appear lower than those from Arnott et al. (2005), but this can be expected since the regression is derived from a total of 599 measurements as opposed to

Arnott et al., deriving up to a maximum of twenty measurements while number of observations is not similar for all regressions.

General conclusions from the calculation of the reflection coefficient by the present study, shown in Figure 6-3, are as follows:

1) Wood in a good preservation condition with a density of 0.567 g/cm^3 to 0.465 g/cm^3 will be detectable in the water column.
2) Wood with a moderate to degraded preservation condition with a density of 0.357 g/cm^3 to 0.292 g/cm^3 is detectable in clay, but won't be detectable until that point.
3) Wood with a density between 0.527 g/cm^3 to 0.292 g/cm^3, that is good to degraded preservation condition, is detectable in sand-silt-clay.
4) Wood with a density range between 0.567 g/cm^3 to 0.292 g/cm^3, that is good to degraded preservation condition, is detectable throughout the sand.
5) Orientation of the wood, flat-sawn (0-30^o) or quarter sawn (60-90^o), does not seem to influence the reflection coefficient.

6.2 Conclusions

The present study has significantly contributed to new knowledge on the use of ultrasound by conservators and archaeologists in the field of Maritime Archaeology. This work has established reliable empirical relationships between wood density and ultrasound propagation velocity, for a range of degradation, as encountered in the marine burial environment.

On-going research and ultrasound testing of more waterlogged archaeological wood samples will refine the calibration curves currently established in this thesis. The technique would be invaluable for conservators working in the laboratory for assessing the state of preservation of small wooden mobile artefacts and waterlogged timbers.

Even if limitations on the application of ultrasound *in situ* seem to rise for cases like the remains of a wooden hull, they can be used to draw further research to explore the subject. This research could lead to the development of a handheld ultrasound device that would greatly improve the assessment of waterlogged archaeological wood whilst *in situ*. Applications on archaeological underwater sites other than shipwrecks can also benefit from the use of ultrasound, as for example wooden beams featured in foundations of underwater settlements and ancient harbours.

The technique is going to be deployed in November on an ancient harbour in Greece. It is hoped that results from this will support the correlation between the laboratorial results and the real world.

Bibliography

Adams, J. (2007). Alchemy or science? Compromising archaeology in the deep sea. Journal of Maritime Archaeology, 2, 48–56.

Adams, J. (2013). A Maritime Archaeology of Ships. Oxford, UK: Oxbow Books.

Aicher, S., Höfflin, L., & Dill-Langer, G. (2001). Damage evolution and acoustic emission of wood at tension perpendicular to fiber. Holz Als Roh- Und Werkstoff, 59, 104–116.

AKUT. (2015). Handheld Wood Density Profiler - Type WP4UW-1, Product Brief.

Albion, R. (1926). Forests and sea power: The timber problem of the Royal Navy, 1652 - 1862. Cambridge: Harvard University Press.

Al-Hamdani, Z., Appelqvist, C., Björdal, C. G., Strætkvern, K., & Opdebeeck, J. (2011). Guidelines for Protection of Submerged Wooden Cultural Heritage. (M. R. Manders, Ed.). Wreck Protect.

Arnott, S., Dix, J. K., Best, A. I., & Gregory, D. (2002). Acoustic propagation in waterlogged wood. Acta Acustica United with Acustica, 88, 699–702.

Arnott, S. H. L. (2004). Ultrasonic evaluation of the degradation state of marine archaeological wood. Southampton: Ph.D dissertation, School of Humanities, University of Southampton.

Arnott, S.H.L., Dix, J.K., Best, A.I., & Gregory, D. (2005). Imaging of Buried Archaeological Materials: The Reflection Properties of Archaeological Wood. Marine Geophysical Researches, 26(2-4), 135–144.

Astley, A., Dix, J. K., Thompson, C. E., & Sturt, F. (2014). A seventeen year, near-annual, bathymetric time-series of a marine structure (SS Richard Montgomery). In S. and A. H. Cheng, Liang, Draper (Ed.), Scour and Erosion: Proceedings of the 7th International Conference on Scour and Erosion. International Conference on Scour and Erosion (pp. 715–724). Taylor & Francis.

Babiński, L., Izdebska-Mucha, D., & Waliszewska, B. (2014). Evaluation of the state of preservation of waterlogged archaeological wood based on its physical properties: Basic density vs. wood substance density. Journal of Archaeological Science, 46, 372–383.

Bader, T. K., de Borst, K., Fackler, K., Ters, T., & Braovac, S. (2013). A nano to macroscale

study on structure-mechanics relationships of archaeological oak. Journal of Cultural Heritage, 14(5), 377–388.

Barbour, J. R. (1990). Treatments for waterlogged and dry archaeological wood. In R. M. Rowell & J. R. Barbour (Eds.), Archaeological Wood: Properties, Chemistry and Preservation (pp. 177–192). Advances in Chemistry Series, vol.225, American Chemical Society, Washington, DC.

Barkas, W. W. (1941). Wood water relationship, VI. The influence of ray cells on the shrinkage of wood. Trans Faraday Society, 37, 535–547.

Beall, F. (2002). Overview of the use of ultrasonic technologies in research on wood properties. Wood Science and Technology, 36(2002), 197–212.

Bednar, H., & Fengel, D. (1974). Physikalische, chemische und strukturelle Eigenschaften von rezentem und subfossilem Eichenholz. Holz Als Roh- Und Werkstoff, 32, S. 99–107.

Bell, L. S., Lee Thorp, J. A., & Elkerton, A. (2009). The sinking of the Mary Rose warship: a medieval mystery solved? Journal of Archaeological Science, 36(2009), 166–173.

Berndt, H., Schniewind, A. P., & Johnson, G. C. (1999). High-resolution ultrasonic imaging of wood. Wood Science and Technology, 33, 185–198.

Best, A.,(1992). The prediction of the reservoir properties of sedimentary rocks from seismic measurements. PhD Thesis. University of Reading.

Björdal, C. (2012). Microbial degradation of waterlogged archaeological wood. Journal of Cultural Heritage, 13(3), S118–S122.

Björdal, C. G., Daniel, G., & Nilsson, T. (2000). Depth of burial, an important factor in controlling bacterial decay of waterlogged archaeological poles. International Biodeterioration & Biodegradation, 45, 15–26.

Björdal, C. G., Gregory, D., Manders, M., Al-Hamdani, Z., Appelqvist, C., Haverhand, J., & Dencker, J. (2012). Strategies for protection of Wooden Underwater Cultural Heritage in the Baltic Sea Against Marine borers: the EU Project “WreckProtect.” Conservation and Management of Archaeological Sites, 14(1-4), 201–214.

Björdal, C., & Nilsson, T. (2008). Reburial of shipwrecks in marine sediments: a long-term study on wood degradation. Journal of Archaeological Science, 35(4), 862–872.

Bjurhager, I. (2011). Effects of cell wall structure on tensile properties of hardwood. Ph.D. dissertation, KTH School of Chemistry, Stockholm, Sweden.

Blanchette, R. (2000). A review of microbial deterioration found in archaeological wood from different environments. International Biodeterioration & Biodegradation, 46, 189–204.

Blanchette, R. A., Cease, K. R., Abad, A. R., Koestler, R. J., Simpson, E., & Sams, G. K. (1991). An evaluation of different forms of deterioration found in archaeological wood. International Biodeterioration, 28, 3–22.

Blanchette, R. A., Haight, J. E., Koestler, R. J., Hatchfield, P. B., & Arnold, D. (1994). Assessment of Deteriotation in Archaeological Wood from Ancient Egypt. Journal of the American Institute for Conservation, 33(1), 55–70.

Blitz, J., & Simpson, G. (1996). Ultrasonic Methods of Non-destructive Testing. London: Chapman & Hall.

Bonde, N., & Christensen, A. E. (1993). Dendrochronological dating of the Viking Age ship burials at Oseberg, Gokstad and Tune, Norway. Antiquity, 67(256), 575–583.

Borgin, K., Parameswaran, N., & Liese, W. (1975). The effect of aging on the ultrastructure of wood. Wood Science and Technology, 9, 87–98.

Borst, K., Bader, T. K., & Wikete, C. (2012). Microstructure-stiffness relationships of ten European and tropical hardwood species. Journal of Structural Biology, 177, 532–542. Bray, D. E., & Stanley, R. K. (1997). Nondestructive Evaluation: A Tool in Design, Manufacturing and Service. CRC Press.

Brennan, M. L. (2011). Quantification of trawl damage to premodern shipwreck sites : Case studies from the Aegean and Black Seas. In UNESCO Scientific Colloquium on Factors Impacting the Underwater Cultural Heritage, 10th Anniversary of the Convention on the Protection of the Underwater Cultural Heritage. Brussels, Belgium: UNESCO.

Brillouin, L. (1960). Wave propagation and group velocity. London: Academic Press Inc.

Bruno, F., Lagudi, A., Gallo, A., Muzzupappa, M., Davidde Petriaggi, B., & Passaro, S. (2015). 3D Documentation of Archeological Remains in the Underwater Park of Baiae. ISPRS - International Archives of the Photogrammetry, Remote Sensing and Spatial Information Sciences, XL-5/W5(April), 41–46.

Buckingham, M. J. (2000). Wave propagation, stress relaxation, and grain-to-grain shearing in saturated, unconsolidated marine sediments. The Journal of the Acoustical Society of America, 108(6), 2796–2815.

Bucur, V. (1988). Wood Structural Anisotropy Estimated by Acoustic Invariants. IAWA Bulletin N.special, 9(1), 67–74.

Bucur, V. (1995). Acoustics of wood. Boca Raton: CRC Press.

Bucur, V. (2006). Acoustics of Wood. Springer-Verlag Berlin Heidelberg.

Bucur, V. (Ed.). (2011). Delamination in wood, wood products and wood-based composites (1st Ed.). Netherlands: Springer.

Bucur, V., & Declercq, N. F. (2006). The anisotropy of biological composites studied with ultrasonic technique. Ultrasonics, 44, 829–831.

Bucur, V., & Feeney, F. (1992). Attenuation of Ultrasound in Solid Wood. Ultrasonics, 30(2), 76–81.

Bucur, V., & Kazemi-Najafi, S. (2011). Delamination Detection in Wood: Based Composites Panel Products Using Ultrasonic Techniques. In V. Bucur (Ed.), Delamination in Wood, Wood Products and Wood-Based Composites. Springer. pp. 307-352.

Bucur, V., Lanceleur, P., & Roge, B. (2002). Acoustic properties of wood in tridimensional representation of slowness surfaces. Ultrasonics, 40, 537–541.

Bull, J. M., Gutowski, M., Dix, J. K., Henstock, T. J., Hogarth, P., Leighton, T.G., & White, P.R. (2005). 3D chirp sub-bottom imaging system: design and first 3D volume. In Proceedings of the International Conference "Underwater Acoustic Measurements: Technologies & Results", In J.S. Papadakis & L.Bjorno (Eds.) Heraklion, Crete, Greece. 777-782.

Bureau of Ships - Department of the Navy. (1983). Wood: A Manual For Its Use as a Shipbuilding Material. Kingston: Teaparty Books.

Bushberg, J.T., Seibert, J.A., Leidholt, Jr., Edwin, M., & Boone, J.M. (2012). The Essential Physics of Medical Imaging. Philadelphia: Lippincott Williams & Wilkins.

Calegari, L., Gatto, D. & Strangerlin, D. (2011). Influence of moisture content specific gravity and specimen geometry on the ultrasonic pulse velocity in eucalyptus grandis hill ex maiden wood. Braz. J. Wood Sci., 2(2), 64–74.

Casson, L. (1994). Ships and seafaring in ancient times. London: British Museum Press.

Caston, G. F. (1979). Wreck marks: Indicators of net sand transport. Marine Geology, 33, 193–204.

Castro, M., & Roig., F. (2007). Wood ultrastructure of ancient buried logs of Fitzroya Cupressoides. IAWA Journal, 28, 125-137.

Cederlund, C. O. (2004). Monitoring, Safeguarding and Visualising North-European Shipwreck Sites, MoSS Final Report. (C. O. Cederlund, Ed.). Helsinki, Finland: The National Board of Antiquities.

Chippendale, C. (1983). Conserving the Mary Rose. New Scientist, 99(1367), 281–284.

Choong, E.T., & Tesoro, F.O. (1989). Relationship of capillary pressure and water saturation. Wood Science and Technology, 23, 139-150.

Christensen, B. B. (1970). The conservation of waterlogged wood in the National Museum of Denmark. (T. N. M. of Denmark, Ed.). Copenhagen.

Clarke, D. L. (1968). Analytical Archaeology. Methuen young books.

Clarke, R., Dean, M., Hutchinson, G., McGrail, S., & Squirrell, J. (1993). Recent work on the R. Hamble wreck near Bursledon, Hampshire. The International Journal of Nautical Archaeology, 22(1), 21–44.

Clarke, R. W., & Squirrel, J. P. (1985). The Pilodyn - An instrument for assessing the condition of waterlogged wooden objects. Studies in Conservation, 30, 177–183.

Coggins, J. (2002). Ships and Seaman of the American Revolution. Dover Publications, Inc.

Colombini, M. P., Lucejko, J. J., Modugno, F., Orlandi, M., Tolppa, E.-L., & Zoia, L. (2009). A multi-analytical study of degradation of lignin in archaeological waterlogged wood. Talanta, 80, 61–70.

Comstock, G. L., & Côté, W. A. (1968). Factors affecting permeability and pit aspiration in coniferous sapwood. Wood Science and Technology, 2, 279–291.

Coppens, F., & Mari, J. L. (1995). Application of the intercept time method to full wave form acoustic data. First Break, 13(I), 11–20.

Creasman, P. P. (2010). Extracting Cultural Information from Ship Timber. PhD Thesis. Texas: Anthropology/ Nautical Archaeology, Texas A&M University.

Creasman, P. P., & Doyle, N. (2010). Overland boat transportation during the Pharaonic period: Archaeology and Iconography. Journal of Ancient Egyptian Interconnections, 2(3), 14–30.

Cremer, L., Heckl, M. ., & translated and revised by Ungar, E. E. (1973). Structure-borne Sound: Structural Vibrations and Sound Radiation at Audio Frequencies (2nd ed.). Berlin: Springer-Verlag.

Crumlin-Pedersen, O. (1997). Viking-age ships and shipbuilding in Hedeby/Haithabu and Schleswig. Ships and Boats of the North. Volume 2. Odense: Viking Ship Museum, Roskilde.

Crumlin-Pedersen, O. (2000). To be or not to be a cog: the Bremen Cog in perspective. International Journal of Nautical Archaeology, 29(2), 230–246.

Crumlin-Pedersen, O. (2004). Nordic Clinker Construction. In F. M. Hocker & C. Ward (Eds.), The Philosophy of Shipbuilding. Conceptual Approaches to the Study of Wooden Ships (pp. 37–64). Texas.

Dahl, K. B. (2009). Mechanical properties of clear wood from Norway spruce. Doctoral Thesis, Norwegian University of Science and Technology.

Dancey, C. P., & Reidy, J. (2004). Statistics Without Maths for Psychology. Pearson Education.

de Jong, J. (1977). Conservation Techniques for old archaeological wood from shipwrecks found in the Netherlands. In A. Walters (Ed.), Biodeterioration Investigation Techniques (pp. 295–338). London: Applied Science Publishers.

Dinwoodie, J. M. (2000). Timber: Its nature and behaviour (2nd ed.). London: E & FN Spon.

Dix, J.K., Arnott, S., Best, A.I. & Gregory, D. (2001). The acoustic characteristics of marine archaeological wood. In T. G. Leighton, G. J. Heald, & G. Griffiths (Eds.), Proceedings of the Institute of Acoustics Conference on Acoustical Oceanography, Southampton, 9-12 April 2001, Institute of Acoustics (pp. 299–306). Bath.

Dumas, F. (1972). Ancient wrecks. In Underwater archaeology: a nascent discipline (pp. 27–34). Paris: United Nations, UNESCO.

Dundar, T., Wang, X., As, N., & Avci, E. (2013). Assessing the Dimensional Stability of Two Hardwood Species Grown in Turkey with Acoustic Measurements. In Proceedings of

the 18th International Nondestructive Testing and Evaluation of Wood Symposium (pp. 459–468). Madison, WI.

Ehanti, E, Alvik, R & Tikkanen, S. (2009). Vrouw Maria Workshop. Helsinki, Suomenlinna: Maritime Archaeology Unit, National Board of Antiquities.

European Commission. (2014). Selected projects in marine research. Funded by the Seventh Framework Programme: Theme 6 – Environment (including climate change) and Ocean of Tomorrow calls. Directorate – General for Research and Innovation. Luxemburg: Publication Office of the European Union.

Feeney, B., & Chivers, R. (2001). Macroscopic Considerations of Ultrasonic Propagation in wood - Attenuation. Molecular and Quantum Acoustics, 22, 45–56.

Feeney, B., Chivers, R., & Barnard, G. (2001). Meso-Structural Considerations of Ultrasonic Propagation in Wood. Molecular and Quantum Acoustics, 22, 57–68.

Feeney, F. E., Chivers, R. C., Evertsen, J. A., & Keating, J. (1998). The influence of inhomogeneity on the propagation of ultrasound in wood. Ultrasonics, 36, 449–453.

Fengel, D. (1991). Aging and fossilization of wood and its components. Wood Science and Technology, 23, 153–177.

Fengel, D., & Wegener, G. (1989). Wood: Chemistry, Ultrastructure, Reactions. Walter de Gruyter.

Ferrari, B., & Adams, J. (1990). Biogenic modifications of marine sediments and their influence on archaeological material. The International Journal of Nautical Archaeology, 19(2), 139–151.

Fitzgerald, M. D. (1995). A Roman wreck at Caeserea maritima, Israel: A comparative study of its hull and equipment. Ph.D. dissertation, Texas A&M University, College Station.

Florian, M. (1990). Scope and history of archaeological wood. In R. M. Rowell & J. R. Barbour (Eds.), Archaeological Wood: Properties, Chemistry and Preservation (pp. 3–32). Advances in Chemistry Series, vol.225, American Chemical Society, Washington, DC.

Florian, M.-L. E. (1987). The Underwater Environment. In C. Pearson (Ed.), Conservation of Marine Archaeological Objects (pp. 1–20).

Forest Products Laboratory. (2010). Wood Handbook: Wood as an engineering material.

General Technical Report FPL-GTR-190. Madison, WI: U.S. Department of Agriculture, Forest Service, Forest Products Laboratory, p.508.

Fors, Y. (2005). Sulfur Speciation and Distribution in the Vasa's Wood. Thesis, Structural Chemistry, Stockholm University.

Fors, Y., Jalilehvand, F., & Sandström, M. (2011). Analytical aspects of waterlogged wood in historical shipwrecks. Analytical Sciences : The International Journal of the Japan Society for Analytical Chemistry, 27(8), 785–92.

Fors, Y., Nilsson, T., Risberg, E. D., Sandstrom, M., & Torssander, P. (2008). Sulfur accumulation in pinewood (Pinus sylvestris) induced by bacteria in a simulated seabed environment: Implications for marine archaeological wood and fossil fuels. International Biodeterioration and Biodegradation, 62(4), 336–347.

Freese, F. (1964). Linear Regression Methods for Forest Research. FPL 17, Forest Products Laboratory, Forest Service, U.S. Department of Agriculture, Madison. Wis.

Frost, H. (1962). Submarine Archaeology and Mediterranean Wreck Formations. The Mariner's Mirror, 48(2), 82–89.

Frost, H. (1963). Under the Mediterranean: Marine Antiquities. Prentice-Hall

Garab, J., Keunecke, D., Hering, S., Szalai, J., & Niemz, P. (2010). Measurement of standard and off-axis elastic moduli and Poisson's ratios of spruce and yew wood in the transverse plane. Wood Science and Technology, 44, 451–464.

General Electric. (2014). Pipe Crawling Underwater X-Ray Machines Find Leaks Before They Happen. Retrieved from http://gizmodo.com/pipe-crawling-underwater-x-ray-machines-find-leaks-befo-1532502471

Giachi, G., Capretti, C., Donato, I. D., Macchioni, N., & Pizzo, B. (2011). New trials in the consolidation of waterlogged archaeological wood with different acetone-carried products. Journal of Archaeological Science, 38(11), 2957–2967. doi:10.1016/j.jas.2011.06.012

Giachi, G., Lazzeri, S., Lippi, M. M., Macchioni, N., & Paci, S. (2003). The wood of "C" and "F" Roman ships found in the ancient harbour of Pisa (Tuscany, Italy): The utilisation of different timbers and the probable geographical area which supplied them. Journal of Cultural Heritage, 4(2003), 269–283.

Gonçalves, R., Trinca, A. J., & dos Ferreira, G. C. S. (2011). Effect of coupling media on velocity and attenuation of ultrasonic waves in Brazilian wood. Journal of Wood Science, 57(4), 282–287.

Goodburn, D. M. (1997). Reused Medieval ship planks from Westminster, England, possibly derived from a vessel built in the cog style. The International Journal of Nautical Archaeology, 26(1), 26–38.

Grattan, D. W., & Clarke, R. W. (1987). Conservation of waterlogged wood. In C. Pearson (Ed.), Conservation of Marine Objects (pp. 164–206). London: Butterworths.

Green, J. N., Hall, E. T., & Katzev, M. L. (1967). Survey of a Greek Shipwreck off Kyrenia, Cyprus. Archaeometry, 10, 47–56.

Greenawald, E. C., Draper, C., Chow, J., Levenberry, L., Poranski, C. F., & Ham, Y. S. (1996). Underwater X-ray Tomography Using Compton Backscatter Imaging. Review of Progress in Quantitative Nondestructive Evaluation, 15.

Greenhill, B. (1976). Archaeology of the Boat. A. & C.Black Limited.

Gregory, D. (1995). Experiments into the deterioration characteristics of materials on the Duart Point wreck-site: an interim report. International Journal of Nautical Archaeology, 24(1), 61–65.

Gregory, D. (1998). Re-burial of timbers in the marine environment as a means of their long-term storage: experimental studies in Lynaes Sands, Denmark. The International Journal of Nautical Archaeology, 27(4), 343–358.

Gregory, D. J., Eriksen, A. M., Pedersen, R., Jensen, P., Andersen, M. H., Davidde, B., Manders, M., Coenen, T., Dencker, J., Björdal, C.G., & Smith, B. (2014). Development of Tools and Techniques to Survey, Assess, Stabilise, Monitor and Preserve Underwater Archaeological Sites: Sasmap, a European research project. In ICOM-CC, 17th Triennial Conference. Melbourne.

Gregory, D. J., Jensen, P., Matthiessen, H., & Straetkvern, K. (2007). The Correlation between Bulk Density and Shock Resistance of Waterlogged Archaeological Wood using the Pilodyn. Studies in Conservation, 52, 289–298.

Gregory, D., & Jensen, P. (2006). The Importance of Analysing Waterlogged Wooden Artefacts and the Environmental Conditions when Considering their In Situ Preservation. In Journal of Wetland Archaeology (Vol. 6, pp. 65–81). Oxbow Books.

Gregory, D., Jensen, P., & Strætkvern, K. (2012). Conservation and in situ preservation of wooden shipwrecks from marine environments. Journal of Cultural Heritage, 13(3), S139–S148.

Gregory, D., Jensen, P., Straetkvern, K., Lenaerts, T., & Pieters, M. (2011). A preliminary assessment of the state of preservation of the wreck of the Belgica. Relicta 7, 145–162.

Grenier, R. (1998). The basque whaling ship from Red Bay, Labrador: a treasure trove of data on Iberian atlantic shipbuilding design and techniques in the mid-16th century. In International Symposium on Archaeology of Medieval and Modern Ships of Iberian-Atlantic Tradition (pp. 269–293). Lisbon, Portugal.

Guibal, F., & Pomey, P. (2003). Timber supply and Ancient Naval architecture. In C. Beltrame (Ed.), Boats, Ships, and Shipyards, Proceedings of the 9th Symposium on Boat and Ship Archaeology , Ile Tahitou (pp. 35–41). Oxford: Oxbow Books.

Håfors, B. (2001). Conservation of swedish warship Vasa from 1628. Stockholm VasaMuseet - Vasastudier (Vol. 18). Sweden: Vasa Museum, Stockholm.

Haneca, K., & Daly, A. (2014). Tree-Rings, Timbers and Trees: A dendrochronological survey of the 14th-century cog, Doel 1. International Journal of Nautical Archaeology, 43(1), 87–102.

Harris, D. C. (2003). Quantitative Chemical Analysis, Sixth Edition. W. H. Freeman.

Hasenstab, A., & Ostreloh, K. (2009). Defects in wood non destructive locating with low frequency ultrasonic echo technique. In NDTCE'09 Non Destructive Testing in Civil Engineering. Nantes, France.

Hedges, J. I. (1990). The chemistry of archaeological wood. In R. M. Rowell & J. R. Barbour (Eds.), Archaeological Wood: Properties, Chemistry and Preservation (pp. 111–140). Advances in Chemistry Series, vol.225, American Chemical Society, Washington, DC.

Hedges, J. I., Cowie, G. L., Ertel, J. R., James Barbour, R., & Hatcher, P. G. (1985). Degradation of carbohydrates and lignins in buried woods. Geochimica et Cosmochimica Acta, 49, 701–711.

Hedgpeth, J. W. (1957). Classification of Marine Environments. In Treatise On Marine Ecology And Paleoecology (pp. 17–28). The Geological Society of America.

Heise, E. A., Raymond, A., Parsons-Hubbard, K., Walker, S. E., Staff, G., Powell, E. A., Brett,

C., & Ashton-Alcox, K. A. (2011). Wood taphonomy in a tropical marine carbonate environment: Experimental results from Lee Stocking Island, Bahamas. Palaeogeography, Palaeoclimatology, Palaeoecology, 312(2011), 363–379.

Hocker, F. M. (2006). Vasa I: The Archaeology of a Swedish Warship of 1628. (F. M. Hocker, Ed.). National Maritime Museums of Sweden.

Hocker, E. (2010). Maintaining a Stable Environment: Vasa's New Climate-Control System. Journal of Preservation Technology, 41(2-3), 3–9.

Hocker, E., Almkvist, G., & Sahlstedt, M. (2012). The Vasa experience with polyethylene glycol: A conservator's perspective. Journal of Cultural Heritage, 13S, S175–S182.

Hoffmann, P. (1981). Chemical wood analysis as a means of characterising archaeological wood. In E. D.W. Grattan (Ed.), In Proceedings of ICOM Waterlogged Wood Working Group. Ottawa. pp.78-83.

Hoffmann, P. (1986). On the stabilization of waterlogged oakwood with PEG. II. Designing a two-step treatment for multiquality timbers. Studies in Conservation, 31(3), 103–113.

Hoffmann, P. (2013). Conservation of Archaeological Ships and Boats: Personal experiences. London: Archetype Publications.

Hoffmann, P., & Jones, M. A. (1990). Structure and degradation process for waterlogged archaeological wood. In R. M. Rowell & and R. J. Barbour (Eds.), Archaeological Wood: Properties, Chemistry and Preservation (pp. 35–66). Advances in Chemistry Series, vol.225, American Chemical Society, Washington, DC.

Huang, C.-L., Lindstrom, H., Nakada, R., & Ralston, J. (2003). Cell wall structure and wood properties determined by acoustics - a selective review. Holz Als Roh- Und Werkstoff, 61(5), 321–335.

Humphrey, J. W., Oleson, J. P., & Sherwood, A. N. (1998). Greek and Roman technology: A sourcebook. Routledge.

ICOMOS. (2006). Heritage at Risk Special Edition, Underwater Cultural Heritage at Risk: Managing Natural and Human Impacts. (R. Grenier, D. Nutley, & I. Cochran, Eds.). Biedermann Offsetdruck, München.

Imazu, S., & Morgos, A. (1997). Conservation of waterlogged wood using sugar alcohol and comparison the effectiveness of lactitol, sucrose and PEG 4000 treatment. In P.

Hoffmann, T. Grant, J. A. Spriggs, & T. Daley (Eds.), Proceedings of the 6th ICOM Group on Wet Organic Archaeological Materials Conference (pp. 235–255). York.

Jagels, R., Seifert, B., Shottafter, J. E., Wolfhagen, J. L., & Carlisle, J. D. (1988). Analysis of wet-site archaeological wood samples. Forest Products Journal, 38(5), 33–38.

Jenkins, S. A., Inman, D. L., Richardson, M. D., Wever, T. F., & Wasyl, J. (2007). Scour and burial mechanics of objects in the nearshore. IEEE Journal of Oceanic Engineering, 32(1), 78–90.

Jensen, P., & Gregory, D. J. (2006). Selected physical parameters to characterize the state of preservation of waterlogged archaeological wood: a practical guide for their determination. Journal of Archaeological Science, 33, 551–559.

Jones, M. A. (2003). For Future Generations: Conservation of a Tudor Maritime Collection. Portsmouth: The Mary Rose Trust Ltd.

Jordan, B. A. (2001). Site Characteristics Impacting Historic Waterlogged Wood : A Review. International Biodeterioration & Biodegradation, 47(2001), 47–54.

Jordan, B. A. (2003). Analysis of environmental conditions and types of biodeterioration affecting the preservation of archaeological wood at the Kolding shipwreck site. Ph.D. dissertation, University of Minnesota.

Jordan, R., Feeney, F., Nesbitt, N., & Evertsen, J. A. (1998). Classification of wood species by neural network analysis of ultrasonic signals. Ultrasonics, 36, 219–222.

Jurgens, J. A., Blanchette, R. A., & Filley, T. R. (2009). Fungal diversity and deterioration in mummified woods from the ad Astra Ice Cap region in the Canadian High Arctic. Polar Biology, 32, 751–758.

Kabir, M. F. (2001). Prediction of ultrasonic properties from grain angle. Journal of the Institute of Wood Science, 15(89), 235–246.

Kabir, M. F., Schmoldt, D. L., & Schafer, M. E. (2002). Time domain ultrasonic signal characterization for defects in thin unsurfaced hardwood lumber. Wood and Fiber Science, 34(1), 165–182.

Kabir, M. F., Sidek, H. A. A., Daud, W. M., & Khalid, K. (1997). Effect of Moisture Content and Grain Angle on the Ultrasonic Properties of Rubber Wood. Holzforschung, 51(3), 263–267.

Kahanov, Y. (1997). Wood conservation of the Ma'agan Mikhael shipwreck. The International Journal of Nautical Archaeology, 26(4), 316–329.

Kahanov, Y. (1998). The Ma'agan Mikhael ship (Israël). Archaeonautica, 14, 155–160.

Kahanov, Y., & Mor, H. (2014). The Dor 2001/1 Byzantine Shipwreck, Israel: Final report. International Journal of Nautical Archaeology, 43(1), 41–65.

Kahle, E., & Woodhouse, J. (1994). The influence of cell geometry on the elasticity of softwood. Journal of Materials Science, 29, 1250-1259.

Karsulovic, J. . T., Leon, L. A., & Gaete, L. (2000). Ultrasonic detection of knots and annual ring orientation in Pinus radiata lumber. Wood and Fiber Science, 32(3), 278–286.

Kassio, K. A. (1982). Dendrochronology: a useful technique for studying the ecology of the past (by Kuniholm, P.J., introduction and translation into Greek by Kassio, K.A.). Journal of the Greek Forestry Service, 25, 85–93.

Katzev, M. (1981). The Reconstruction of the Kyrenia Ship , 1972-1975. National Geographic Society Research Peports, 13, 315–328.

Katzev, M. L. (1970). Kyrenia, 1969; a Greek ship is raised. Expedition, 12(4), 6–14.

Katzev, M. L. (1980). Conservation of the Kyrenia Ship 1971-72'. National Geographic Society Research Peports, 12, 417–426.

Katzev, S. W. (2005). Resurrecting an Ancient Greek Ship: Kyrenia, Cyprus. In G. F. Bass (Ed.), Beneath the Seven Seas: Adventure with the Institute of Nautical Archaeology (pp. 72–79). Thames and Hudson Ltd; First edition.

Kavvouras, P. (2004). Identification of the wood of Greek forest species based on cross-section macroscopic features. Retrieved from http://www.fria.gr/EngPage/tools.html

Kavvouras, P. K., & Fotopoulou, M. (2006). A note on a simple device for measuring wooden artefact volume. Studies in Conservation, 51(4), 291–296.

Kavvouras, P. K., Kostarelou, C., Zisi, A., Petrou, M., & Moraitou, G. (2009). Use of Silanol-Terminated Polydimethylsiloxane in the Conservation of Waterlogged Archaeological Wood. Studies in Conservation, 54(2), 65–76.

Kawamoto, S., & Williams, R. (2002). Acoustic Emission and Acousto-Ultrasonic Techniques for Wood and Wood-Based Composites A review. General Technical Report FPL-GTR-

134. Madison, WI: U.S. Department of Agriculture, Forest Service, Forest Products Laboratory, p.16.

Kaye, G.W.C., & Laby, T.H. (1986). Tables of Physical and Chemical Constants. (15th Ed.). Longman.

Kazemi-Najafi, S., Shalbafan, A., & Ebrahimi, G. (2009). Internal decay assessment in standing beech trees using ultrasonic velocity measurement. European Journal of Forest Research, 128(4), 345–350.

Kearey, P., & Brooks, M. (1991). An Introduction to Geophysical Exploration (2nd ed.). Oxford: Blackwell Scientific Publications.

Keeney, C. A., & Pollio, S. E. (1984). Evaluation of Nondestructive Underwater Timber Inspection Techniques. Technical Note, Naval Facilities Engineering Command, Naval Civil Engineering Laboratory, Port Hueneme, California.

Kim, Y., & Singh, A. (2000). Micromorphological characteristics of wood biodegradation in wet environments: A review. IAWA Journal, 21(2), 135–155.

Kollmann, F.F.P. (1968). Physics of Wood. In Principles of Wood Science and Technology. Kollmann, F.F.P., & Côte, W.A. (Eds.). (pp.160-291). New York: Springer Berlin Heidelberg.

Kretschmann, D. E. (2010). Mechanical Properties of Wood. In Wood handbook (pp. 5–46). General Technical Report FPL-GTR-190. Madison, WI: U.S. Department of Agriculture, Forest Service, Forest Products Laboratory, p.508.

Kretschmar, E. I., Gelbrich, J., Militz, H., & Lamersdorf, N. (2008). Studying bacterial wood decay under low oxygen conditions—results of microcosm experiments. International Biodeterioration & Biodegradation, 61, 69–84.

Kruglowa, T. (2012). In-situ assessment of density and material properties in timber structures by non-destructive and semi-destructive testing. Thesis, Chalmers University of Technology, Gothenburg, Sweden.

Kruglowa, T., Sandin, Y., & Kliger, I. R. (2010). Density Calibration using X-ray Equipment for In-situ Assessment of Tomber Structures. In Proceedings of the 11th World Conference on Timber Engineering. Riva Del Garda, Italy. p.81-89.

Kuniholm, P. I. (2001). Dendrochronology and other applications of tree-ring studies in

archaeology. In D. R. Brothwell & A. M. Pollard (Eds.), Handbook of Archaeological Sciences (pp. 1–11). London: John Wiley & Sons, Ltd.

Lane, F. (1965). Navires et constructeurs à Venise pendant la Renaissance (S.E.V.P.E.). Paris.

Laugier, P. (2004). An overview of bone sonometry. International Congress Series, 1274, 23–32.

Lechner, T. (2013). In-situ assessment of timber structures: Assessment methods and case studies. Thesis, Chalmers University of Technology, Gothenburg, Sweden.

Lechner, T., Bjurhager, I., & Kliger, R. I. (2013). Strategy for developing a future support system for the Vasa warship and evaluating its mechanical properties. Heritage Science, 1(35), 1–11.

Leighton, T. G. (2007). What is ultrasound? Progress in Biophysics and Molecular Biology, 93, 3–83.

Liphschitz, N. (2012). Dendroarchaeological Studies of Shipwrecks Along the Mediterranean Coast of Israel. In R. Efe, M. Ozturk, & S. Ghazanfar (Eds.), Environment and Ecology in the Mediterranean Region (pp. 1–12). Cambridge Scholars Publishing.

Ljungdahl, J. (2006). Structure and properties of Vasa oak. Licentiate thesis, Roy. Inst. of Technology, Stockholm.

Loewen, B. (1998). The Red Bay vessel: an example of a 16th-century Biscayan ship. Itsas Memoria: Revista de Estudios Marítimos Del País Vasco, (2), 193–199.

Lopez-Anido, R., Michael, A. P., Goodell, B., & Sandford, C. (2004). Assessment of wood pile deterioration due to marine organisms. Journal of Waterway, Port, Coastal and Ocean Engineering, 130(April), 70–76.

Macchioni, N. (2003). Physical characteristics of the wood from the excavations of the ancient port of Pisa. Journal of Cultural Heritage, 4(2), 85–89.

Macchioni, N., Capretti, C., Sozzi, L., & Pizzo, B. (2013). Grading the decay of waterlogged archaeological wood according to anatomical characterisation. The case of the Fiave site (N-E Italy). International Biodeterioration and Biodegradation, 84, 54–64.

Manders, M. (2009). In Situ Preservation : " the preferred option ". Vol. 60, No.4. 2008. UNESCO Publishing and Blackwell Publishing Ltd.

Maragoudaki, E., & Kavvouras, P. K. (2012). Mycenaean shipwright tool kit: its reconstruction and evaluation. Archaeological and Anthropological Sciences, 4(3), 199–208.

Marsden, P. (2003). Sealed by Time: The Loss and Recovery of the Mary Rose. The Mary Rose Trust.

Martin, C. J. M. (1978). The Dartmouth, a British frigate wrecked off Mull, 1690. The International Journal of Nautical Archaeology, 7(1), 29–58.

Matsumura, J. Booker, R.E., Ridoutt, B.G., Donaldson, L.A., Mikajiri, N., Matsunaga, H., & Oda, K. (1999). Impregnation of radiata pine wood by vacuum treatment II: effect of pre-steaming on wood structure and resin content. Journal of Wood Science, 45, 456-462.

Matthiesen, H. (2015). Detecting and quantifying ongoing decay of organic archaeological remains: A discussion of different approaches. Quaternary International, 368, 43–50.

McConnachie, G., Eaton, R., & Jones, M. (2008). A re-evaluation of the use of maximum moisture content data for assessing the condition of waterlogged archaeological wood. E-Preservation Science, 5, 29–35.

McDonald, K. A. (1978). Lumber Defect Detection by Ultrasonics. Research paper FLP-311, Madison, WI: U.S. Department of Agriculture, Forest Service, Forest Products Laboratory.

McDonald, K. A., Cox, R. G., & Bulgrin, E. H. (1969). Locating lumber defects by ultrasonics. Research paper, FPL 120, Madison, WI: U.S.Department of Agriculture, Forest Service, Forest Products Laboratory.

McGrail, S. (1976). Further aspects of Viking Age boatbuilding. In B. Greenhill (Ed.), Archaeology of the Boat (pp. 234–349).

McGrail, S. (1993). The future of the Designated Wreck site in the R. Hamble. The International Journal of Nautical Archaeology, 22(1), 45–51.

McGrail, S. (1998). Ancient Boats in North-West Europe: The archaeology of Water Transport to AD 1500 (2nd ed.). Addison-Wesley Longman, Incorporated.

McGrail, S. (2001). Boats of the world: From the Stone Age to Medieval times. Oxford University Press.

McGrail, S. (2014). Early Ships and Seafaring: European Water Transport (2014th ed.). Pen & Sword Books Ltd.

McIntyre, M. E., & Woodhouse, J. (1984). On Measuring Wood Properties, Part 1. Journal of Catgut Acoustic Society, 42, 11–15.

McIntyre, M. E., & Woodhouse, J. (1986). On measuring wood properties, Part 3. J. Catgut Acoustical Society, 45, 14–23.

McKerrel, H., Roger, E., & Varsanyi, A. (1972). The aceton/rosin method for conservation of waterlogged wood. Studies in Conservation, 17(3), 111–125.

McNinch, J. E., Wells, J. T., & Trembanis, A. C. (2006). Predicting the fate of artefacts in energetic, shallow marine environments: An approach to site management. International Journal of Nautical Archaeology, 35(2), 290–309.

Medwin, H., & Clay, C.S. (1998). Fundamentals of Acoustical Oceanography. In Stern, R. & Levy, M. (Eds.). San Diego: Academic Press.

Meiggs, R. (1982). Trees and timber in the Ancient Mediterranean world. Oxford: Oxford University Press.

Millero, F. (2007). The marine inorganic carbon cycle. Chemical Reviews, 107, 308–341.

Millero, F. J. (2006). Chemical Oceanography (Third Edition). CRC Taylor & Francis, Boca Raton.

Mindell, D. A., & Bingham, B. (2001). A high-frequency, narrow-beam sub bottom profiler for archaeological applications. In Proceedings of OCEANS 2001, MTS/IEEE Conference and Exhibition (Vol. 4, pp. 2115–2123).

Mirahmadi, K., Kabir, M. M., Jeihanipour, A., Karimi, K., & Taherzadeh, M. J. (2010). Alkaline pretreatment of spruce and birch to improve bioethanol and biogas production. BioResources, 5(2), 928–938.

Molyneux, J. B., & Schmitt, D. R. (1999). First-break timing: Arrival onset times by direct correlation. Geophysics, 64(5), 1492–1501.

Mor, H., & Kahanov, Y. (2006). The Dor 2001/1 shipwreck, Israel - A summary of the excavation. International Journal of Nautical Archaeology, 35(2), 274–289.

Mouzouras, R., Jones, M. A., Jones, E. B. G., & Rule, M. (1990). Nondestructive evaluation of

hull and stored timbers from the Tudor ship Mary Rose. Studies in Conservation, 35, 173–188.

Muckelroy, K. (1977). Historic wreck sites in Britain and their environments. International Journal of Nautical Archaeology, 6(1), 47–57.

Muckelroy, K. (1978). Maritime Archaeology. Cambridge: Cambridge University Press.

Mueller, C., Woelz, S., & Kalmring, S. (2013). High-resolution 3D marine seismic investigation of Hedeby harbour, Germany. International Journal of Nautical Archaeology, 42(2), 326–336.

Nesteroff, W. D. (1972). Geological aspects of marine sites. In Underwater archaeology: a nascent discipline (pp. 175–183). Paris: United Nations, UNESCO.

Nicolotti, G., Socco, L., Martinis, R., Godio, A., & Sambuelli, L. (2003). Application and comparison of three tomographic techniques for detection of decay in trees. Journal Of Arboriculture, 29(2), 66–78.

O'Shea, J. M. (2002). The archaeology of scattered wreck-sites: formation processes and shallow water archaeology in western Lake Huron. The International Journal of Nautical Archaeology, 31(2), 211–227.

Oertling, T. J. (1989). The Molasses Reef wreck hull analysis: Final report. The International Journal of Nautical Archaeology and Underwater Exploration, 18(3), 129–243.

Oliveira, F. G. R. de, Campos, J. A. O. de, & Sales, A. (2002). Ultrasonic Measurements In Brazilian Hardwood. Materials Research, 5(1), 51–55.

Oliveira, F. G. R., Candian, M., Lucchette, F. F., Salgon, J. L., & Sales, A. (2005). Moisture Content Effect on Ultrasonic Velocity in Goupia Glabra. Materials Research, 8(1), 11–14.

Oliveira, F. G. R., & Sales, A. (2006). Relationship between density and ultrasonic velocity in Brazilian tropical woods. Bioresource Technology, 97(18), 2443–2446.

Olympus (2012). Ultrasonic Transducers Technical Notes. Retrieved from: http://www.olympus-ims.com/en/resources/white-papers/ultrasonic-transducer-technical-notes/

Olympus (2013). Olympus Material Sound Velocities. Retrieved from: http://www.olympus-ims.com/en/ndt-tutorials/thickness-gage/appendices-velocities/

Panthapulakkal, S., & Sain, M. (2013). Investigation of Structural Changes of Alkaline-extracted Wood Using X-ray Microtomography and X-ray Diffraction: A Comparison of Microwave versus Conventional Method of Extraction. Journal of Wood Chemistry and Technology, 33, 92–102.

Papatheodorou, G., Geraga, M., Christodoulou, D., Fakiris, E., Heath, S., & Baika, K. (2014). A Marine Geoarchaeological Survey , Cape Sounion, Greece: Preliminary Results. Mediterranean Archaeology and Archaeometry, 14(1), 357–371.

Papathoma, E., Kavvouras, P. K., & Moraitou, G. (2016). Diagnostic study methodology applied on the wooden finds from Brauron - Towards the development of an informed conservation protocol. Proceedings of the 12th ICOM-CC WOAM Conference Istanbul, *in press*.

Parameswaran, N. (1981). Micromorphology of Spruce Timber after Long-term Service in a Potash Store House. Holz Als Roh- Und Werkstoff, 39, 149–156.

Parker, A. J. (1981). Stratification and contamination in ancient Mediterranean shipwrecks. International Journal of Nautical Archaeology, 10(4), 309–335.

Parker, A. J. (1995). Maritime cultures and wreck assembages in the Graeco-Roman world. The International Journal of Nautical Archaeology, 24(2), 87–95.

Peacock, E. E. (1996). Biodegradation and characterization of water-degraded archaeological textiles created for conservation research. International Biodeterioration and Biodegradation, 38(1), 49–59

Pearson, C. (1987). Conservation of marine archaeological objects. Butterworth - Heinemann.

Peterson, C. E. (1990). New directions in the conservation of archaeological wood. American Chemical Society. Advances in Chemistry Series, vol.225, 433–449.

Phillips, E. W. J. (1933). Movement of the Pit Membrane in Coniferous Woods, with Special Reference to Preservative Treatment. Forestry, 7, 109–120.

Plets, R. M. K., Dix, J. K., Adams, J. R., Bull, J. M., Henstock, T. J., Gutowski, M., & Best, A. I. (2009). The use of a high-resolution 3D Chirp sub-bottom profiler for the reconstruction of the shallow water archaeological site of the Grace Dieu (1439), River Hamble, UK. Journal of Archaeological Science, 36(2), 408–418.

Plets, R. M. K., Dix, J. K., & Best, A. I. (2008). Mapping of the buried yarmouth roads wreck, \isle of Wight, UK, using a chirp sub-botton profiler. International Journal of Nautical Archaeology, 37(2), 360–373.

Plets, R., Quinn, R., Forsythe, W., Westley, K., Bell, T., Benetti, S., McGrath, F., & Robinson, R. (2011). Using Multibeam Echo-Sounder Data to Identify Shipwreck Sites: Archaeological assessment of the Joint Irish Bathymetric Survey data. International Journal of Nautical Archaeology, 40(1), 87–98.

Polzer, M. E. (2009). Hull Remains from the Pabuc Burnu Shipwreck and Early Transition in Archaic Greek Shipbuilding. MA dissertation, Texas A&M University.

Pomey, P. (2000). Reconstruction of the Marseilles 6th century BC Greek ships. In C. Beltrame (Ed.), Boats, Ships, and Shipyards. Ninth International Symposium on Boat and Ship Archaeology, Venice 2000 (pp. 57–65). Oxford.

Pomey, P. (2004). Principles and Methods of Construction in Ancient Naval Architecture. In F. M. Hocker & C. A. Ward (Eds.), The Philosophy of Shipbuilding. Conceptual approaches to the study of wooden ships (pp. 25–36). Texas A&M University Press.

Pomey, P., Kahanov, Y., & Rieth, E. (2012). Transition from Shell to Skeleton in Ancient Mediterranean Ship-Construction: Analysis, problems, and future research. International Journal of Nautical Archaeology, 41(2), 235–314.

Ponnamperuma, F. (1972). The chemistry of submerged soils (Reprinted.). Advances in Agronomy, Vol. 24, Academic Press.

Preston, J., Smith, A. D., Schofield, E. J., Chadwick, A. V., Jones, M. A., & Watts, J. E. M. (2014). The effects of Mary Rose conservation treatment on iron oxidation processes and microbial communities contributing to acid production in marine archaeological timbers. PLoS ONE, 9(2), 1–8

Price, A. T. (1929). A Mathematical Discussion on the Structure of Wood in Relation to Its Elastic Properties. Philosophical Transactions of the Royal SOciety of London. Series A, Containing Papers of a Mathematical or Physical Character, 228(1929), 1–62.

Pulak, C. (1998). The Uluburun shipwreck: an overview. The International Journal of Nautical Archaeology, 27(3), 188–224.

Pulak, C. (2008). The Uluburun Shipwreck and Late Bronze Age Trade. In J. Aruz, K. Benzel, & J. M. Evans (Eds.), Beyond Babylon. Art, Trade and Diplomacy in the Second

Millennium BC (pp. 289–310). New Haven and London.

Quinn, R. (2006). The role of scour in shipwreck site formation processes and the preservation of wreck-associated scour signatures in the sedimentary record – evidence from seabed and sub-surface data. Journal of Archaeological Science, 33(10), 1419–1432.

Quinn, R., Bull, J. M., & Dix, J. K. (1997). Imaging wooden artefacts using Chirp sources. Archaeological Prospection, 4(1), 25–35.

Rajeshwar, B., Bender, D. A., Bray, D. E., & McDonald, K. A. (1997). An Ultrasonic Technique for Predicting Tensile Strength of Southern Pine Lumber. American Society of Agricultural Engineers, 40(4), 1153–1159.

Richards, V., Godfrey, I., Blanchette, R., Held, B., Gregory, D., & Reed, E. (2009). In situ monitoring and stabilisation of the James Matthews site. In K. Strætkvern & H. D. J. Huisman (Eds.), Proceedings of the 10th ICOM Group on Wet Organic Archaeological Materials Conference (pp. 113–160). Amsterdam, 2007.

Rieu, R., Jestin, O., & Carraze, F. (1980). Mediterranean hull types compared 4: An unusual type of construction. The hull of wreck 1 at Bon Porte. International Journal of Nautical Archaeology, 9(1), 70–72.

Riggio, M., Sandak, J., Sandak, A., Pauliny, D., & Babin, L. (2014). Analysis and prediction of selected mechanical / dynamic properties of wood after short and long-term waterlogging. Construction and Building Materials, 68, 444–454.

Riley, J. (1988). The Watelrine Theory of Iron Ship Disintegration. In M. McCarthy (Ed.), Iron Ships and Steam Shipwrecks (pp. 191–197). Western Australian Museum, Perth.

Ringger, T., Höfflin, L., Dill-Langer, G., & Aicher, S. (2003). Measurement on the Acoustic Anisotropy of Soft and Hard Wood; Effects on Source Location. Otto-Graf-Journal. 14, 231-253.

Ross, R. J. (2015). Nondestructive evaluation of wood. In Nondestructive Evaluation of Wood: Second Edition. General Technical Report FPL-GTR-238. Madison, WI: U.S. Department of Agriculture, Forest Service, Forest Products Laboratory, 1–4.

Ross, R. J., Brashaw, B. K., & Pellerin, R. F. (1998). Nondestructive evaluation of wood. Forest Products Journal, 48(1), 14–19.

Ross, R. J., & Hunt, M. O. (2000). Stress wave timing nondestructive evaluation tools for

inspecting historic structures. General Technical Report FPL-GTR-119. Madison, WI: U.S. Department of Agriculture, Forest Service, Forest Products Laboratory.

Rowell, R.M. & Barbour, R. J. (Ed.). (1990). Archaeological Wood: Properties Chemistry and Preservation. Vol.225. American Chemical Society.

Rule, M. (1983). The Mary Rose: the excavation and raising of Henry VIII's flagship (2nd ed.). London : Conway Maritime Pr.

Sakai, H., Misamisawa, A., & Tagaki, K. (1990). Effect of moisture content on ultrasonic velocity and attenuation in wood. Ultrasonics, 28(6), 382–385.

Sakai, H., Takagi, K., & Minamisawa, A. (1987). Ultrasonic Properties in Woods. Japanese Journal of Applied Physics, S27-1, 55–57.

Salmi, A., Eskelinen, J., Peura, M., Haeggstrom, E., Steffen, K., & Montonen, L. (2009). Non-destructive evaluation of the 18 th century ship wreck Vrouw Maria. IEEE International Ultrasonics Symposium Proceedings, 1479–1482.

Sanabria, S. J., Neuenschwander, J., Furrer, R., Niemz, P., & Sennhauser, U. (2014). Bonding Defect Imaging in Glulam with Novel Air-Coupled Ultrasound Testing. In A. Aguilera & J. P. Davim (Eds.), Research developments in wood engineering and technology (pp. 221–246). IGI Global, Hershey, PA, USA.

Sandoz, J.-L. (1989). Grading of construction timber by ultrasound. Wood Science and Technology, 23, 95–108.

Sandström, M., Jalilehvand, F., Persson, I., Gelius, U., & Frank, P. (2002). Acidity and salt precipitation on the Vasa: the sulphur problem. In P. Hoffmann, J. A. Spriggs, T. Grant, C. Cook, & A. Recht (Eds.), Proceedings of the 8th ICOM-CC WOAM Conference Stockholm (2001) (pp. 67–89).

Santhakumaran, L. (1970). Preliminary observations on the natural resistance of sixty-nine species of Indian timber to marine borer attack from Bombay. Journal of the Bombay Natural History Society, 67(3), 430–442.

Schafer, M. E. (2000). Ultrasound for defect detection and grading in wood and lumber. In Proceedings IEEE Ultrasonics Symposium (Vol. 1, pp. 771–778). San Juan, Puerto Rico: IEEE.

Schniewind, A. (1990). Physical and mechanical properties of archaeological wood. In R. M.

Rowell & J. R. Barbour (Eds.), Archaeological Wood: Properties, Chemistry and Preservation (pp. 87–109). Advances in Chemistry Series, vol.225, American Chemical Society, Washington, DC.

Schock, S. (2008). Synthetic aperture 3D buried object imaging. Underwater Technology: The International Journal of the Society for Underwater, 27(4), 185–193.

Sebastian, C., Pescatore, C., & Niemz, P. (2014). Anisotropic elastic properties of common ash (Fraxinus excelsior L.). Holzforschung, 68(8), 941–949.

Secco, C. B., Gonçalves, R., Cerri, D. G. P., Vasques, E. C., & Batista, F. A. F. (2012). Behavior of Ultrasonic Waves in Wood With Presence of Holes. Cerne, Larvas, 18(3), 507–514.

Senalik, C. A., Schueneman, G., & Ross, R. J. (2014). Ultrasonic-Based Nondestructive Evaluation Methods for Wood A Primer and Historical Review. General Technical Report FPL-GTR-235, Madison, WI: U.S.Department of Agriculture, Forest Service, Forest Products Laboratory.

Senalik, C. A., Schueneman, G., & Ross, R. J. (2015). Ultrasonic-Based Nondestructive Evaluation Methods for Wood. In R. J. Ross (Ed.), Nondestructive Evaluation of Wood: second edition (pp. 21–51). General Technical Report, Forest Products Laboratory.

Shukla, A., & Prakash, V. (1990). Wave Propagation in Porous Media as a Function of Fluid Saturation. Experimental Mechanics, 47(1), 80–87.

Singh, H., Adams, J, Mindell, D & Foley, B. (2000). Imaging underwater for archaeology. Journal of Field Archaeology, 27, 319–328.

Smith, D. M. (1954). Maximum moisture content method for determining specific gravity of small wood samples. Forest Products Laboratory, Forest Service, USDA.

Spycher, M., Schwarze, F. W. M. R., & Steiger, R. (2008). Assessment of resonance wood quality by comparing its physical and histological properties. Wood Science and Technology, 42(4), 325–342.

Squirrel, J. P., & Clarke, R. W. (1987). An investigation into the condition and conservation of the hull of the Mary Rose: Part 1: Assessment of the hull timbers. Studies in Conservation, 32, 153–162.

Steffy, J. (1994). Wooden ship building and the interpretation of shipwrecks. London: Texas A&M University Press.

Steffy, J. R. (1985). The Kyrenia Ship: An Interim Report on Its Hull Construction. American Journal of Archaeology, 89(1), 71–101.

Steinmayer, A.G. & MacIntosh Turfa, J. (1996). Effects of shipworm on the performance of ancient Mediterranean warships. The International Journal of Nautical Archaeology, 25(2), 104–121.

Stewart, J., Murdock, L.D. & Waddell, P. (1995). Reburial of the Red Bay Wreck as a form of preservation and protection of the historic resource. In MRS Proceedings (pp. 791–805).

Stößel, R. (2004). Air-coupled ultrasound inspection as a new non-destructive testing tool for quality assurance. Ph.D. dissertation, Institut für Kunststofftechnik und Kunststoffkunde, Universität Stuttgart.

Tanasoiu, V., Miclea, C., & Tanasoiu, C. (2002). Nondestructive testing techniques and piezoelectric ultrasonics transducers for wood and built in wooden structures. Journal of Optoelectronics and Advanced Materials, 4(4), 949–957.

Tchernia, A. (1987). The Madrague de Giens wreck. The Courier, UNESCO, 11.

Tomalin, D. J., Simpson, P., & Bingeman, J. M. (2000). Excavation versus sustainability : a conclusion on 25 years of archaeological investigations at Goose Rock, a designated historic wreck-site at the Needles, Isle of Wight, England. The International Journal of Nautical Archaeology, 29(1), 3–42.

Tsoumis, G. (1968). Wood as raw material. Exeter: Pergamon Press Inc.

UNESCO. (2001). Convention on the protection of the underwater cultural heritage. UNESCO.

UNESCO. (2012). World Heritage Nomination for the Red Bay Basque Whaling Station. Newfoundland and Labrador, Canada: UNESCO.

Unger, A., Schniewind, A. P., & Unger, W. (2001). Diagnosis of Wood Condition. In Conservation of Wood Artifacts: A Handbook (pp. 143–164). Springer-Verlag Berlin Heidelberg.

Van de Noort, R., Cumby, B., Blue, L., Harding, A., Hurcombe, L., Hansen, T. M., Wetherelt, A., Wittamore, J., & Wyke, A. (2014). Morgawr: An experimental Bronze Age-type sewn-plank craft based on the Ferriby boats. International Journal of Nautical

Archaeology, 43(2), 292–313.

van Doorninck, F. H. (1981). Maritime Archaeology by Keith Muckelroy, Review by: Frederick H. van Doorninck, Jr. Society for American Archaeology, 46(1), 226–228.

Vardy, M. E. (2015). Deriving shallow-water sediment properties using post-stack acoustic impedance inversion. Near Surface Geophysics, 13(2061), 143–154.

Vardy, M. E., Bull, J. M., Dix, J. K., Henstock, T. J., Plets, R. M. K., Gutowski, M., & Hogarth, P. (2011). The geological "Hubble": A reappraisal for shallow water. The Leading Edge, (2), 154–159.

Vardy, M. E., Dix, J. K., & Henstock, T. J. (2008). Decimeter-resolution 3D seismic volume in shallow water: A case study in small-object detection. Geophysics, 73(2).

Vermeersch, J., & Haneca, K. (2015). Construction features of doel 1, a 14th-century cog found in Flanders. International Journal of Nautical Archaeology, 44(1), 111–131.

Veth, P., Philippou, C., Richards, V., Staniforth, M., Rodrigues, J., Khan, A., Creagh, D., Viduka, A., Barham, A., Macleod, I. & Harvey, P. (2013). The Australian Historic Shipwreck Preservation Project 2012 : First report on the background , reburial and in-situ preservation at the Clarence (1841 – 50). Bulletin of the Australian Institute for Maritime Archaeology, 37, 1–19.

Wang, S.-Y., & Chuang, S.-T. (2000). Experimental Data Correction of the Dynamic Elastic Moduli, Velocity and Density of Solid Wood as a Function of Moisture Content above the Fiber Saturation Point. Holzforschung, 54(2000), 309–314.

Wang, X., Divos, F., Pilon, C., Brashaw, B. K., Ross, R. J., & Pellerin, R. F. (2004). Assessment of decay in standing timber using stress wave timing nondestructive evaluation tools: A Guide for Use and Interpretation. General Technical Report FPL-GTR-147. Madison, WI: U.S. Department of Agriculture, Forest Service, Forest Products Laboratory.

Wangaard, F. F. (1966). Resistance of wood to chemical degradation. Forest Products Journal, 16(2), 53–64.

Ward, C. (2000). Sacred and Secular: Ancient Egyptian Ships and Boats. Archaeological Institute of America Monographs 5. Philadelphia: University of Pennsylvania Museum.

Ward, I., Larcombe, P., & Veth, P. (1999). A new process-based model for wreck site formation. Journal of Archaeological Science, 26, 561–570.

Wheeler, A. J. (2002). Environmental Controls on Shipwreck Preservation: The Irish Context. Journal of Archaeological Science, 29, 1149–1159.

White, B. Y. J. (1998). Estimating the Age of Large and Veteran Trees in Britain. Forestry Practice, 1–8.

Whitehouse, R. (1998). Scour at marine structures: A manual for practical applications. Thomas Telford.

Whitewright, J. (2011). Identification and History of the Flower of Ugie. In J. Whitewright & J. Satchell (Eds.), The Archaeology and History of the Flower of Ugie, Wrecked 1852 in the Eastern Solent (pp. 43–62). The Hampshire and Wight Trust for Maritime Archaeology HWTMA Monograph Series No.1.

Wilcox, W. W. (1988). Detection of Early Stages of Wood Decay with Ultrasonic Pulse Velocity. Forest Products Journal, 38(5), 68–73.

Wilhelm, E., Battino, R., & Wilcock, J. (1977). Low-pressure solubility of gases in liquid water. Chemical Reviews, 77(2), 219-262.

Wilkens, R. H., & Richardson, M. D. (2007). Special Issue Peer-Reviewed Technical Communication Mine Burial Prediction : A Short History and Introduction. IEEE Journal of Oceanic Engineering, 32(1), 3–9.

Wunderlich, J., Wendt, G., & Müller, S. (2005). High-resolution echo-sounding and detection of embedded archaeological objects with nonlinear sub-bottom profilers. Marine Geophysical Researches, 26(2-4), 123–133.

Zimmermann, T., Thommen, V., Reimann, P., & Hug, H.J. (2005). Ultrastructural appearance of embedded and polished wood cell walls as revealed by Atomic Force Microscopy. Journal of Structural Biology, 156, 363-369.